

9613

NATIONAL LIBRARY
OTTAWA



BIBLIOTHÈQUE NATIONALE
OTTAWA

NAME OF AUTHOR. *DONALD EDWARD Mc GREGOR*.....
TITLE OF THESIS. *RATE STUDIES OF THE CATALYTIC*.....
REACTION OF H₂S WITH SO₂: I. KINETIC.....
MEASUREMENTS. II. ONLINE DATA ACQUISITION AND PROCESSING.
UNIVERSITY.... *UNIVERSITY OF ALBERTA*.....
DEGREE FOR WHICH THESIS WAS PRESENTED... *PhD.*.....
YEAR THIS DEGREE GRANTED..... *1971*.....

Permission is hereby granted to THE NATIONAL LIBRARY
OF CANADA to microfilm this thesis and to lend or sell copies
of the film.

The author reserves other publication rights, and
neither the thesis nor extensive extracts from it may be
printed or otherwise reproduced without the author's
written permission.

(Signed) *Donald E. McGregor*

PERMANENT ADDRESS:

1305 Severin Drive,...
SARNIA, Ontario.....
.....

DATED. *July 19*.....19*71*

THE UNIVERSITY OF ALBERTA

RATE STUDIES OF THE CATALYTIC

REACTION OF H_2S WITH SO_2 :

I. KINETIC MEASUREMENTS

II. ONLINE DATA ACQUISITION AND PROCESSING

BY

(C) DONALD EDWARD MCGREGOR

A THESIS

SUBMITTED TO THE FACULTY OF GRADUATE STUDIES
IN PARTIAL FULFILMENT OF THE REQUIREMENTS FOR THE DEGREE
OF DOCTOR OF PHILOSOPHY

DEPARTMENT OF CHEMICAL AND PETROLEUM ENGINEERING

EDMONTON, ALBERTA

FALL, 1971

UNIVERSITY OF ALBERTA
FACULTY OF GRADUATE STUDIES

The undersigned certify that they have read, and recommend to the Faculty of Graduate Studies for acceptance, a thesis entitled "RATE STUDIES OF THE CATALYTIC REACTION OF H_2S WITH SO_2 " submitted by DONALD EDWARD MCGREGOR in partial fulfilment of the requirements for the degree of Doctor of Philosophy.

.....*James D. O'Leary*.....
Supervisor
Chairman, Examining Committee

.....*H.B. Dunford*.....

.....*Laurence E. Carter*.....

.....*Henry W. Hargood*.....

.....*W. H. Clark*.....

.....*J. A. Seyer*.....

Date *June 29/71*

PART I

ABSTRACT

An experimental investigation of the reaction of H_2S with SO_2 in the presence of a commercial bauxite catalyst (Porocel) was conducted in a stainless steel recycle reactor operated at steady-state flow and thermal conditions. Reactor feed and product compositions, measured by a process gas chromatograph, and the total volumetric feed rate enabled the calculation of a reactor material balance from which the isothermal reaction rate could be determined.

A series of 80 experiments, performed at four different temperatures between 208 and 287°C and at varying partial pressures of H_2S , SO_2 and H_2O , was conducted to provide data in the region of industrial interest. Mechanistic rate equations fitted the data well, although no attempt was made to discriminate between rival models.

Several characteristics of the reaction were revealed. The activation energy for the forward reaction was 7589 ± 451 calories and the order was 0.828 ± 0.0952 and 0.467 ± 0.111 with respect to H_2S and SO_2 , respectively. The error terms represent the 95% confidence limits of the estimates. The reaction takes place predominantly on the outer surface of the catalyst. Film diffusion did not limit the reaction rate in the experimental equipment and theoretical calculations suggested that the same is true for most commercial sulfur plant reactors. Water vapor displayed a barely perceivable autocatalytic effect on the re-

action at very low partial pressures and a marked retardation effect at high partial pressures. This effect, the magnitude of the activation energy, and the goodness of fit of a Freundlich-based rate expression supports the view of others that the reacting species were hydrogen bonded to surface hydroxyl groups.

Commercial sulfur recovery processes were reviewed and the thermodynamics of several sulfur plant reactions were analyzed using the free energy minimization technique. A different sulfur recovery strategy which incorporates the features of the Modified Claus and Townsend processes has been recommended for improved sulfur recovery.

PART II

Following Part I of this thesis, the research equipment used to study the kinetics of the reaction of H_2S with SO_2 was interfaced to an IBM Data Acquisition and Control System. Part II of this thesis describes the interface between the laboratory reactor and the computer, and the programs and operating procedures which were developed for on-line data acquisition and reduction.

As a rule, the research equipment was not operated in the on-line mode for the kinetic study primarily because reliable gas chromatograph monitoring software for the computer had not been fully developed by the time the kinetic study was completed. However, a fully documented example of an online kinetic run is presented which made use of a temporary G.C. monitoring scheme devised for this purpose, but which was intolerably

inaccurate for the procurement of precise kinetic data.

At the termination of this research program, the development of an improved gas chromatograph monitoring software system by the personnel of the Data Acquisition, Control and Simulation Centre was underway.

ACKNOWLEDGEMENTS

The author wishes to thank Dr. I.G. Dalla Lana for his supervision and valuable guidance throughout this program. The co-operation of the Instrument Shop under the supervision of Mr. D. Sutherland, of the Chemical Engineering Workshop under the supervision of Mr. G. Walsh, and particularly the perseverance of Mr. K. Faulder in constructing the recycle pump were sincerely appreciated. Others, with whom the author enjoyed many years of pleasant association, have contributed directly and their efforts relevant to this project are warmly acknowledged. Miss Helen Wozniuk, who typed the manuscript, is gratefully acknowledged.

Acknowledgements go to the University of Alberta for a Dissertation Fellowship, and to the National Research Council and the Canadian Natural Gas Processors Association for their contribution to the financial support of this project.

With gratitude, I acknowledge the unfailing patience and encouragement given to me by my wife, Yvonne.

TABLE OF CONTENTS

	<u>Page</u>
CHAPTER I INTRODUCTION	
1.1 Background	1
1.2 Previous Work on the Catalytic Reaction of H ₂ S with SO ₂	3
1.3 Approach and Extent of Present Work	3
CHAPTER II LITERATURE REVIEW AND THEORY	
2.1 Industrial Sulfur Plant Technology	7
2.1.1 Sulfur Recovery Processes	7
2.1.2 Claus Type Sulfur Plant Design and Operation	12
2.2 Fundamental Research Performed on Sulfur Plant Reactions	15
2.2.1 Carbon Disulfide and Carbonyl Sulfide Reactions	15
2.2.2 The Claus Reaction	19
2.2.3 Dissociation Reactions of Sulfur	26
2.2.4 Bauxite and Alumina Catalyst	28
2.2.5 Gas-Solid Studies Performed on Alumina and Bauxite	31
2.3 Adsorption, Surface Reaction and Related Laws	34
2.4 Mass Transfer in Heterogeneous Catalysis	36
2.4.1 Film Diffusion	38
2.4.2 Pore Diffusion	39
2.5 Recycle Reactors	43
CHAPTER III DETERMINATION OF EQUILIBRIUM COMPOSITIONS	
3.1 Background	49
3.2 Review of Free Energy Minimization Method	50

TABLE OF CONTENTS (continued)

	<u>Page</u>
CHAPTER III continued	
3.3 Applications of the Free Energy Minimization Method	54
3.3.1 Comparison with Gamson and Elkins' Data	54
3.3.2 Analysis of Miscellaneous Sulfur Plant Reactions	56
CHAPTER IV DESCRIPTION OF EXPERIMENTAL EQUIPMENT	
4.1 Feed Metering and Preparation System	60
4.2 Feed and Product Analysis	64
4.3 Fluidized Sand in Air Bath	71
4.4 Recycle Loop and Reactor	73
4.5 Recirculation Pump	77
4.6 Sulfur and Water Condensers	83
4.7 Process Measurements	87
4.8 Operation of Equipment and Experimental Procedures	90
4.8.1 Catalyst Treatment	90
4.8.2 Fluidized Bath Startup	91
4.8.3 Execution of Kinetic Measurements	91
4.8.4 Termination of Kinetic Measurements	93
4.8.5 Periodic Equipment Maintenance and Accuracy Tests	93
4.8.6 Catalyst Activity Test	94
4.9 Materials	94
CHAPTER V REDUCTION OF DATA	
5.1 Introduction	96
5.2 Ideal Gas Law Assumption	96

TABLE OF CONTENTS (continued)

	<u>Page</u>
CHAPTER V continued	
5.3 Reactor Material Balance	101
5.4 Partial Pressure of Reaction Species	104
CHAPTER VI PRESENTATION AND DISCUSSION OF EXPERIMENTAL RESULTS	
6.1 Experimental Program	106
6.2 Test for Homogeneous Reaction	109
6.3 Bulk Mass Transfer Test	109
6.4 Catalyst Activity Test Results	111
6.5 Initial Rate Data	114
6.6 Experimental Test for Porous Diffusion	117
6.7 Examination of the Effects of Specie Partial Pressures and Temperature on the Kinetics of the Claus Reaction	123
6.8 Correlation of Experimental Data to Rate Equations	130
6.8.1 Empirical Rate Expressions	132
6.8.2 Langmuir Hinshelwood Rate Models	139
6.8.3 Reaction Mechanism with Mutually Rate Controlling Catalytic Process Steps	144
6.9 Comparison of this Work with the Results of Other Investigators	147
CHAPTER VII CONCLUSIONS AND RECOMMENDATIONS	
7.1 Performance of Equipment	151
7.2 Evaluation of Measured Rate Data	152
7.3 Reaction Mechanism	154
7.4 Evaluation of the Catalyst	156

TABLE OF CONTENTS (continued)

	<u>Page</u>
CHAPTER VII continued	
7.5 Suggested Processing Scheme for Higher Sulfur Recovery	157
NOMENCLATURE	161
BIBLIOGRAPHY	165
APPENDIX A CALIBRATION OF EXPERIMENTAL EQUIPMENT	A1
APPENDIX B DOCUMENTATION OF FREE ENERGY MINIMIZATION METHOD PROGRAM	B1
APPENDIX C REDUCTION OF DATA AND ERROR ANALYSIS	C1
APPENDIX D ESTIMATION OF FILM AND PORE DIFFUSION RATES	D1
APPENDIX E DATA CORRELATION AND PARAMETER CONFIDENCE LIMITS	E1
APPENDIX F DEVELOPMENT OF A RATE EQUATION WITH MUTUALLY RATE CONTROLLING CATALYTIC PROCESS STEPS	F1

LIST OF TABLES

<u>Table</u>	<u>Page</u>
1.1 Comparison of Experimental Program with a Sulfur Plant	5
2.1 Sulfur Plant Selection Criteria	11
2.2 Space Velocity-Conversion Data of Gamson and Elkins	20
2.3 A Selection of Adsorption Isotherms	37
3.1 Thermodynamic Analysis of Sulfur Plant Reactions	58
4.1 Performance Data for Recycle Pump	86
5.1 Critical Constants and Reduced Properties of N_2 , H_2S , SO_2 and H_2O	99
5.2 Fugacity Coefficients at 533°K and 293°K and 1 Atmosphere	99
5.3 Molecular Volumes	100
6.1 Experimental Program	108
6.2 Chromatograms for Film Diffusion Test	111
6.3 Initial Rate Data Determined from Fitting a Hyperbolic Tangent Function	120
6.4 Porous Diffusion Test Results	121
6.5 Data Banks for Correlation	132
6.6 Rate Expression Parameter Estimates	134
6.7 Langmuir Hinshelwood Kinetic Models	140
6.8 Comparison of This Work with Other Results	148

LIST OF TABLES (continued)

Table

- | | |
|------|---|
| A.1 | Summary of Correlation Coefficients for Instrument Calibration |
| A.2 | Range and Resolution of Calibration Thermometers for Thermocouples |
| A.3 | Thermocouple Calibration Data |
| A.4 | Stem-Corrected Thermocouple Calibration Data |
| A.5 | Least Squares Fit of Standard Iron - Constantan Thermocouple Data |
| A.6 | Comparison of Thermocouple Calibration Data with Standard Data |
| A.7 | Calibration Coefficients for Thermocouples |
| A.8 | Feed Pressure Transmitter Calibration Data |
| A.9 | Least Squares Fit of Feed Absolute Pressure Transducer Data |
| A.10 | Reaction Pressure Transmitter Calibration Data |
| A.11 | Least Squares Fit of Reactor Absolute Pressure Transducer |
| A.12 | Calibration Data for Dry Test Meter |
| A.13 | Experimental Results for D/P Cell Calibration |
| A.14 | Calculated Results for D/P Cell Calibration |
| A.15 | Least Squares Fit of Feed D/P Cell Data |
| A.16 | Physical Properties of Pure Nitrogen and a Reactor Feed Mixture (1 atm, 60°F) |

LIST OF TABLES (continued)

Table

- | | |
|------|---|
| A.17 | Variation of Orifice Coefficient with NR_e |
| A.18 | Volume of Geometric Irregularities in Gas Chromatograph Calibration Equipment |
| A.19 | Gas Chromatograph Calibration Results |
| A.20 | Least Squares Fit of Gas Chromatograph Calibration Data |
| B.1 | Equilibrium Data for the Claus Reaction |
| B.2 | Equilibrium Data for Sulfur Specie Split |
| B.3 | Equilibrium Data for the COS/SO_2 Reaction |
| B.4 | Equilibrium Data for the CS_2/SO_2 Reaction |
| B.5 | Equilibrium Data for the $\text{COS}/\text{H}_2\text{O}$ Reaction |
| B.6 | Equilibrium Data for the $\text{CS}_2/\text{H}_2\text{O}$ Reaction |
| B.7 | Equilibrium Data for the $\text{H}_2\text{S}/\text{CO}_2$ Reaction |
| B.8 | Equilibrium Data for the CH_4/S_x Reaction |
| B.9 | Equilibrium Data for the $\text{COS}/\text{H}_2\text{S}$ Reaction |
| B.10 | Equilibrium Data for the COS/O_2 Reaction |
| B.11 | Equilibrium Data for the CO/S_x Reaction |
| | |
| C.1 | Error Analysis of H_2S Conversion |
| C.2 | Experimental Finite Rate Data |
| C.3 | Experimental Catalytic Activity Tests |
| C.4 | Experimental Initial Rate Data |
| | |
| D.1 | Physical Properties of N_2 , H_2S and SO_2 at 500°F , 1 atm |
| D.2 | Calculation Results for Estimation of Mass Transfer Coefficients for H_2S and SO_2 |

LIST OF FIGURES

<u>Figure</u>		<u>Page</u>
2.1	Dry Bed Catalytic Conversion Sulfur Plants	10
2.2	Computer Model of a Dehydroxylated Alumina Surface	30
2.3	Sketch of a Recycle Reactor	45
3.1	Chemical Equilibrium Between Sulfur Species at One Atmosphere	55
3.2	Claus Reaction Equilibrium Conversion versus Temperature	57
4.1	Feed Metering and Preparation System	61
4.2	Constant Differential Type Flow Controller	63
4.3	Mixing Venturi	63
4.4	Stream Selector Valve	65
4.5	Gas Chromatograph Oven	67
4.6	Gas Chromatograph Control Cam System	67
4.7	Sample Chromatogram	69
4.8	Repeatability of Chromatogram Area Measurement	70
4.9	Schematic Layout of Fluidized Bath	72
4.10	Photograph of Recycle Reactor	74
4.11	Reactor Assembly	76
4.12	Recirculation Pump Body and End Plate	79
4.13	Section A-A of Pump Assembly	80
4.14	Water Cooled Shaft Seal	82
4.15	Peripheral Accessories for Crane Seal	84

LIST OF FIGURES (continued)

<u>Figure</u>		<u>Page</u>
4.16	Performance Curves for Recirculation Pump	85
4.17	Sulfur and Water Condenser	88
6.1	Catalyst Activity Tests	113
6.2	Conversion versus Space Time Plots	118
6.3	Porous Diffusion Test	119
6.4	Rate of H_2S Oxidation as a Function of H_2S Partial Pressure with SO_2 Partial Pressure as a Parameter	125
6.5	Rate of H_2S Oxidation as a Function of H_2S Partial Pressure with Temperature as a Parameter	126
6.6	Effect of Water Partial Pressure on the Reaction Rate of H_2S	127
6.7	Isorate Lines Plotted on Equilibrium Diagram of Claus System	129
7.1	Modified Claus Townsend Process	158
A.1	Thermocouple Calibration Equipment	
A.2	Dry Test Meter Calibration Factor Variation with Apparent Flow Rate	
A.3	Schematic Diagram of Gas Chromatograph Calibration Equipment	
A.4	Gas Chromatograph Calibration for H_2S	
A.5	Gas Chromatograph Calibration for SO_2	

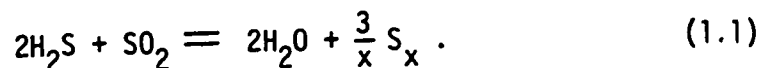
PART I
KINETIC MEASUREMENTS

CHAPTER I

INTRODUCTION

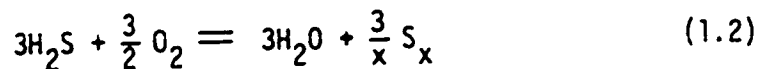
1.1 Background

For more than a century it has been known that H_2S reacts with SO_2 according to the equation



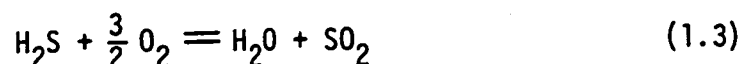
This work describes a study of the kinetics of this reaction over a commercial bauxite catalyst known as Porocel. The reaction has become of great importance for the recovery of sulfur from refinery and sour gases and it is surprising how little fundamental work has been published about the nature of the reaction.

A major source of sulfur in Canada is hydrogen sulfide which occurs in abundance in natural gas in Alberta and in acid-gas streams found in many petroleum refineries. Numerous recovery schemes exist and are described in the literature review but the modified Claus process, which involves reacting H_2S with SO_2 over bauxite catalyst, is most commonly used. The overall reaction which takes place in the recovery of elemental sulfur from H_2S is



Since the reaction is highly exothermic ($\Delta H = -145$ to -173 kcal), the modified Claus process is designed to cope with it in two stages to reduce reactor costs and increase conversion [47]. These stages are

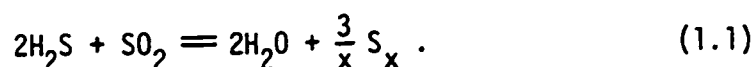
(i) free flame combustion:



$$\Delta H = -124.3 \text{ kcal}, T = 250^\circ\text{C}, P = 1 \text{ atm}$$

and,

(ii) catalytic oxidation:



$$\Delta H = -14.7 \text{ kcal}, T = 250^\circ\text{C}, P = 1 \text{ atm}.$$

Over 80% of the total heat release occurs in the first stage. The second stage occurs in catalytic converters which are vital to obtaining high yields of sulfur.

In view of the need for increased natural gas sweetening facilities, for improved air pollution control in refineries, and the growing world demand for sulfur, an investigation of the oxidation of H_2S with SO_2 over commercial bauxite catalyst was initiated at the University of Alberta in 1964 by Cormode [15].

1.2 Previous Work on the Catalytic Reaction of H_2S with SO_2

A detailed review of earlier investigations of the catalytic reaction, hereafter referred to as the Claus reaction, is given in Section 2.2.2 of the literature survey. Many investigators have studied the Claus reaction more or less qualitatively, but their results were misleading because they permitted water to condense in the reaction system. The reaction of H_2S and SO_2 in the presence of water was commonly used as a lecture-room demonstration as early as 1812 [101].

The Claus reaction kinetic data which Cormode [15] measured in a recycle flow reactor packed with Porocel catalyst have been compared to the results of the work reported herein in Chapter VI. Other results which are discussed include those of Gamson and Elkins [35] who have obtained a limited amount of space time vs. conversion data for one feed composition which was fed to a fixed bed integral reactor. Gamson and Elkins also studied the thermodynamics of the reaction. Hammar [44] also studied the Claus reaction in an integral fixed-bed reactor over a cobalt-molybdenum-alumina catalyst, in a 1:1:10 ratio, respectively.

The surface chemistry of γ -alumina, the catalytically active constituent of bauxite for the Claus reaction [22], has also been discussed in the literature review.

1.3 Approach and Extent of Present Work

Rate studies on the reaction of H_2S and SO_2 over a bauxite catalyst were performed in a recycle flow reactor in preference to dif-

ferential or integral flow reactors. The use of a differential bed flow reactor requires very precise feed and product stream analyses to obtain reliable rate measurements since only a small change in composition occurs across the differential bed. Difficulties in formulating synthetic feed mixtures containing sulfur vapor would be anticipated. A differential reactor offers the advantage that nearly isothermal rate data can be obtained since only a small temperature rise takes place across the catalyst bed for exothermic reactions. The use of an integral reactor avoids the synthetic feed mixture problem and thus the requirement of high analytical precision however, the experimental rate data so obtained are unlikely to be isothermal for a reaction as highly exothermic as the Claus reaction. The recycle reactor consists of a catalyst bed through which a large portion of the product stream is recycled after mixing with the incoming fresh feed. Because of the considerably reduced conversion obtained per pass, the performance of the recycle reactor approximates that of a differential reactor and isothermal data can be more easily measured. Because of the large number of passes (recycle to feed flow ratio is roughly 20:1), the overall conversion across the reactor provides large changes between the composition of the feed and that of the product stream.

The experimental program described in Section 6.1 was designed to reflect the operating conditions encountered in the catalytic stage of commercial modified Claus sulfur plants. The region of H_2S , SO_2 and H_2O partial pressures and the temperature range which were investigated

are compared to plant conditions in Table 1.1. A sulfur plant with 100% H_2S acid gas composition and 50% conversion of H_2S to sulfur in the waste heat boiler was used as a basis for comparison. The temperature range for commercial plants is shown in Figure 3.2, an equilibrium plot of percent conversion of H_2S to sulfur vapor versus temperature, on which Gamson and Elkins [35] indicate the region for the catalytic reaction.

Table 1.1

Comparison of Experimental Program with a Sulfur Plant

	<u>Experimental Program</u>	<u>Commercial Sulfur Plant (1atm) 1st Converter</u>	<u>95% Conversion</u>
H_2S pressure (mmHg)	12-62	83	8.8
SO_2 pressure (mmHg)	10-45	41.5	4.4
H_2O pressure (mmHg)	nil-120	116.	250.
Temperature ($^{\circ}\text{K}$)	481-560	460-600	

The range of operating conditions in the experimental program represents the plant operation well except for the water vapor partial pressures. A higher water vapor pressure was not studied because it was anticipated that high steam content would damage the recycle pump, a sliding-vane compressor which depended upon the lubricating quality of graphite for smooth operation. Considerable "vane-chatter" prevailed when the water vapor pressure was raised to 150 mm Hg.

Film and pore diffusion effects have been considered both in

theory and experimentally in this program. A brief discussion of the theory in Section 2.4 and application of it in Appendix D suggests that the reaction is not limited by bulk mass transfer and that the Claus reaction takes place predominantly on the external surface of the bauxite catalyst.

Since the incentive for carrying out this research project has been to contribute information which will improve sulfur plant reactor design and operations, and thus help to reduce SO_2 emissions to the atmosphere from sulfur plants, the other reactions which can take place in modified Claus plants have also been reviewed. This review emphasizes the scope of chemical technology which must be examined to upgrade sulfur plant design and operation.

CHAPTER II

LITERATURE REVIEW AND THEORY

2.1 Industrial Sulfur Plant Technology

2.1.1 Sulfur Recovery Processes

A number of processes exist for recovery of sulfur from manufactured or natural gases containing hydrogen sulfide. The majority of these schemes fall in one of four categories:

- (i) dry bed-catalytic conversion
- (ii) dry bed adsorption-catalytic conversion
- (iii) liquid media absorption-air oxidation, and
- (iv) liquid media absorption-direct conversion.

Dry bed adsorption-catalytic conversion is used in the Haines process [42]. Hydrogen sulfide from a sour gas is adsorbed on a bed of zeolites until the bed is saturated with H_2S . The bed is then regenerated with hot sulfur dioxide, obtained from burning part of the sulfur product in air, which reacts with adsorbed hydrogen sulfide to produce sulfur vapor. The effluent vapor is condensed and stored as liquid sulfur.

Liquid media absorption-air oxidation is usually best suited for gases containing 1-1000 grains of H_2S per 100 standard cubic feet of gas [92]. The Thylox and Perox processes [57] are typical examples of this recovery scheme. Absorption of H_2S occurs in a slightly alkaline solution containing oxygen carriers which oxidize the H_2S to sulfur. The solution is generated with air which also acts as a flotation agent

for suspended sulfur in the liquid. Arsenic-activated potassium carbonate, sodium arsenate or thioarsenate, and aqueous ammonia in hydroquinone are commonly used liquid media.

The Townsend process [103] is an example of the liquid media absorption-direct conversion category. Here, an aqueous SO_2 -rich organic solvent such as triethylene glycol contacts the sour gas and simultaneously sweetens and dehydrates the gas and converts the absorbed H_2S to sulfur. Sulfur product is burned to SO_2 which is absorbed by the glycol prior to contacting H_2S . It is theorized that the water present in the glycol catalyzes the reaction.

Dry bed catalytic conversion, the principal concern of this thesis, first became a commercial process for the recovery of sulfur from H_2S produced in coke ovens between 1883 and 1887 [12]. In the 1940's large-scale processing of sour gas and effective sulfur recovery commenced with the operation of the gas processing units at McKamie, Arkansas by the Arkansas Fuel Oil Company [28].

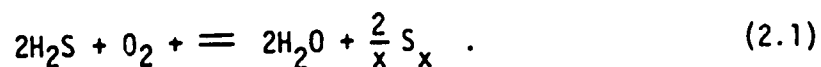
In gas processing terminology, sour is a term which is used to describe gases containing appreciable quantities of H_2S and/or CO_2 . For natural gas, strict residue gas specifications require that H_2S and CO_2 be almost completely removed. Two absorbents are commonly used in industrial practice: monoethanolamine (MEA) and diethanolamine (DEA). A correctly designed MEA system will produce a residue gas containing less than 0.1 grain of H_2S per 100 cu. ft. High molecular weight hydrocarbons also tend to absorb into MEA and for refinery gases containing high percentages of these heavy hydrocarbons, DEA was found to be an

effective H_2S absorbent [28]. Dimethyl formamide is another successful absorbent used for removing H_2S from light hydrocarbon streams.

The two gaseous offstreams from the absorption unit are called the sweet gas stream, which exits from the absorber, and the acid gas stream, which leaves the absorbent regenerator. The latter stream flows to the sulfur recovery unit and may contain from two to one hundred percent H_2S if the plant is based on the Claus process.

When designing a dry bed catalytic conversion type of sulfur recovery unit, three distinctly different types of processes are available: the once-through process, the split-stream process and the direct oxidation unit. Figure 2.1 schematically describes the flow in each type of plant. There are many variations of flow schemes within each type of plant however, they will not be dealt with here.

The straight-through and split-flow processes both involve burning one-third of the acid gas stream with air to produce the SO_2 necessary for the Claus reaction. The free flame combustion and catalytic conversion stages of the modified Claus process were described in the Introduction. The direct oxidation process involves reacting the H_2S with the oxygen in air over catalyst, as indicated by the following reaction,



No burning of H_2S takes place in this type of plant.

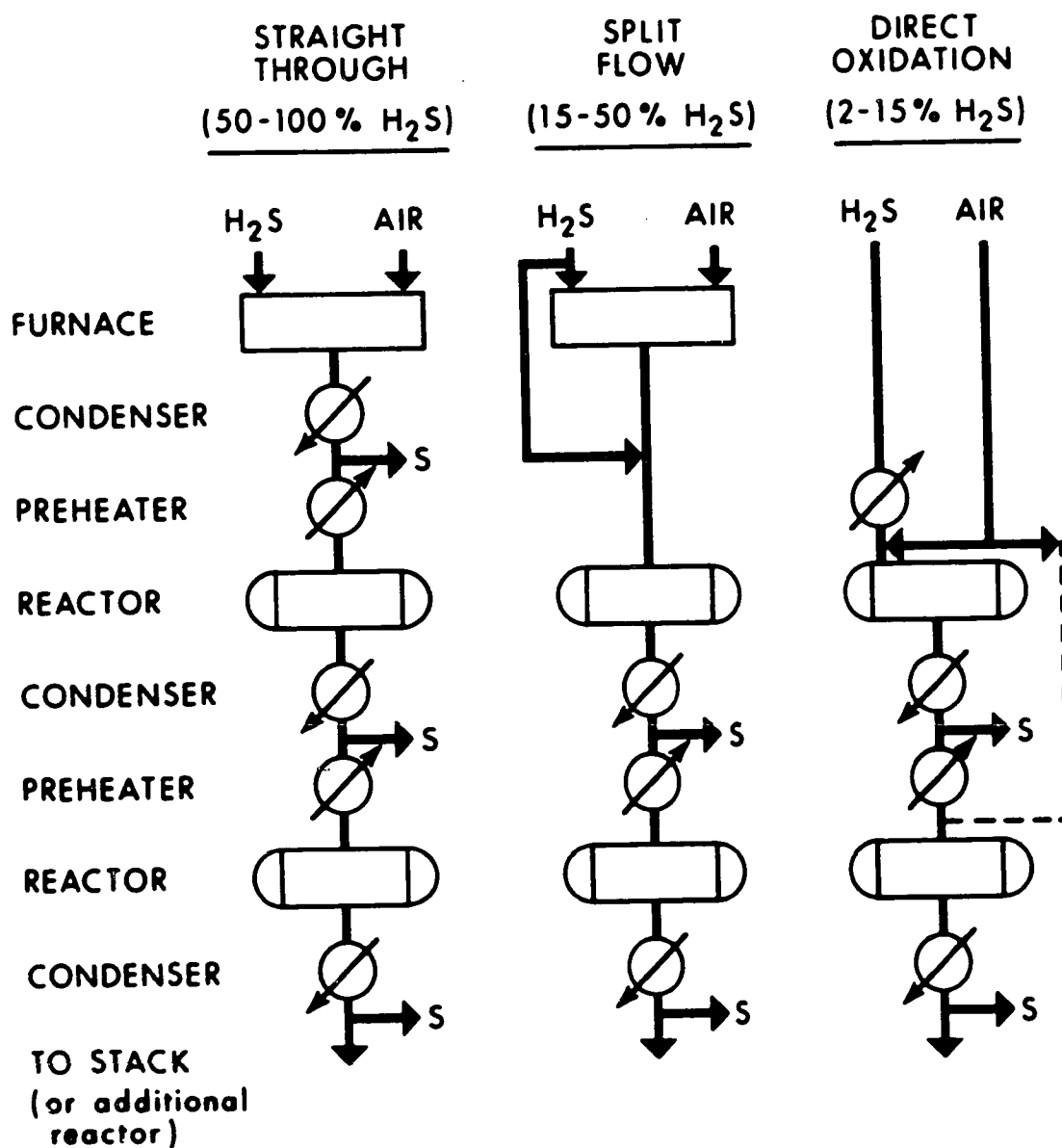


FIGURE 2.1: DRY BED CATALYTIC CONVERSION SULFUR PLANTS(29)

Design of sulfur plants is discussed in numerous papers [35, 39,82,84,105] and the literature describing sulfur plant operations is also quite prolific [2,11,41,84,106]. Table 2.1 indicates the primary guidelines for selecting one of the three sulfur plant flow schemes depicted in Figure 2.1.

The level of H_2S content in the acid gas exerts the strongest influence on plant selection. Flame stability in these plants is affected by the H_2S concentration. At low levels of H_2S in the acid gas, it is not possible to maintain adiabatic H_2S combustion hence, the direct oxidation process is employed. The 2/3 by-pass or split flow is used at intermediate H_2S levels since only 1/3 of the acid gas is ever burned. Since there is no sensible heat loss to the remaining 2/3 of the stream, flame stability is enhanced. High concentration H_2S acid gas streams experience relatively few problems maintaining effective combustion.

Table 2.1

Sulfur Plant Selection Criteria

<u>Physical Constraint</u>	<u>Straight Through</u>	<u>Split Flow</u>	<u>Direct Oxidation</u>
Acid gas composition	50-100% H_2S	15-50% H_2S	2-15% H_2S
High HC content in acid gas	Least acceptable	Acceptable	Acceptable
Necessary efficiency of sulfur recovery	\geq 93-95%	\geq 87-93%	\geq 80-85%
Heat recovery efficiency	Highest	Moderate	Lowest

High acid gas hydrocarbon content, say 2 to 5%, causes the formation of COS and CS₂ in the burner zone of these plants [97]. Since they are very difficult to remove, it therefore is desirable to by-pass 2/3 of the acid gas to minimize the formation of these two compounds. Substantial amounts of soot are also formed in the burning process if hydrocarbons are present [10] which causes catalyst fouling. Pan-American [28,40,41] indicates that saturated hydrocarbons can be dealt with in their process, but unsaturated hydrocarbons adversely affect the direct oxidation process and only traces can be tolerated.

2.1.2 Claus Type Sulfur Plant Design and Operation

The conventional Claus type sulfur plant involves a series of conversion and condensation steps. In designing sulfur plants, industry attempts to reach an economic balance between capital investment and sulfur recovery subject to reasonable air pollution constraints.

A.R. Valdes has formulated the problem of how to design the waste heat boiler and used a computer program to solve it [106]. Although heat transfer mechanisms have been rigorously formulated and incorporated into the solution, Valdes assumes that gas composition is known and invariant from the burner end of the firetube to the outlet of the boiler. The equilibria between H₂S, SO₂, H₂O and the various sulfur species are highly temperature-dependent and the associated heats of reaction are considerable [35]. Therefore, it would be most desirable if this assumption could be eliminated by assuming that equilibrium composition exists at the temperatures encountered as the gases

pass through the boiler. The heat balance could then be adjusted as the equilibrium shifts.

Opekar and Goar [82] have proposed and developed a computer program which optimizes sulfur plant design. They assume that hydrocarbons are completely oxidized to CO_2 and water, which is not strictly true. Side reactions occur in waste heat boilers to produce appreciable quantities of COS and CS_2 from CO_2 and hydrocarbons. These constituents contribute roughly one third of the sulfur losses emitted from sulfur plants [10].

The literature appears to be generally scanty with regard to firetube boiler design, with the objective of minimizing COS, CS_2 and soot formation, indicating a lack of fundamental research on flame technology.

The literature on the actual design of catalytic converters is also sparse. Opekar and Goar [82] used the Gamson and Elkins method [35] for calculating adiabatic converter equilibrium conversions used in material and energy balance calculations. No information is given on how the converter size or geometry were selected.

Valdes [105] considers the optimum operating temperature for catalytic converters to be 475°F . Below this temperature, the rate of reaction of H_2S and SO_2 will limit conversion and above 475°F , the equilibria of the system will limit the conversion. No reference is made in his article to the source of the statement regarding kinetics however, at temperatures below 475°F , sulfur will condense, poisoning

the catalyst.

To maintain reasonably low reaction temperatures, Valdes suggests that two or more converter beds are much more efficient than one. Carbon deposition occurs primarily in the top layer of the initial catalyst bed (two to six inches from the top of the bed) thus carbon residue poisoning is not important if bed thicknesses exceed six inches by a sufficient margin.

Petrunic [90] has recently indicated that contemporary sulfur plants still experience operational difficulties. Bauxite catalyst of 2/4 mesh size proved to be lacking in mechanical strength in Canadian Fina's Wildcat Hills sulfur plant. Resultant disintegration during service caused the formation of excessive catalyst fines which created intolerable converter pressure drop. Regeneration produced more fines from catalyst deterioration and they were generally dissatisfied with bauxite catalyst which varied physically and chemically from shipment to shipment. This problem was solved when they used a new catalyst which was called activated alumina, K-201. The K-201 activated alumina was in the form of hard, spherical particles with diameter 1/8 to 1/4 in.

The Wildcat Hills plant also encountered problems in poor sulfur separation in the sulfur condensers. This can be attributed to sulfur fog formation which can be predicted [52]. Inline separators installed after the catalyst beds removed virtually all of the entrained sulfur.

2.2 Fundamental Research Performed on Sulfur Plant Reactions

Although the primary focus of the work reported herein concerns the Claus reaction, this section will also deal with other reactions which conceivably take place in sulfur plants and which are increasingly more important from the standpoint of air pollution abatement.

The major source of sulfur compound air pollution emitted from different plants vary with the type of installation, however, it is generally conceded that the major contributors include:

- (i) unreacted H_2S and SO_2 ,
- (ii) CS_2 and COS , and
- (iii) entrained sulfur vapor.

Therefore, the remainder of this section will deal with published research related to these problems.

2.2.1 Carbon Disulfide and Carbonyl Sulfide Reactions

Most commercial H_2S streams contain appreciable quantities of CO_2 and light hydrocarbons. It has been established [10] that the high temperature combustion of such a gas results in the conversion of part of these carbon compounds to COS and CS_2 . Thus, the free flame combustion zone of a sulfur plant is one source of these two pollutants.

Merryman and Levy [67,68,69,70] have investigated the kinetics and mechanism of the combustion of H_2S -air mixtures and COS -air mixtures using a mass spectrometric flame sampling technique.

For COS combustion, the depletion rate of COS was found to be [67]

$$-\frac{d[\text{COS}]}{dt} = -r_{\text{COS}} = k_5 [\text{COS}] [\text{O}_2] \quad (2.1)$$

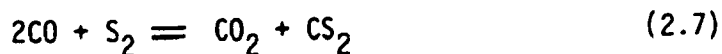
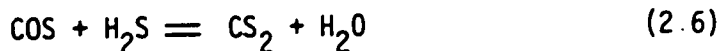
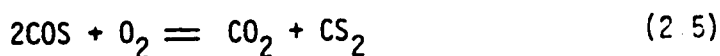
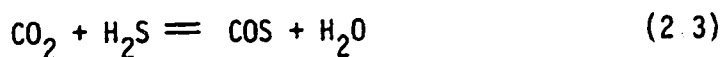
where, $k_5 = 8.24 \times 10^{14} \exp\left[-\frac{29,100}{RT}\right] \text{ CC mole}^{-1} \text{ sec}^{-1}$.

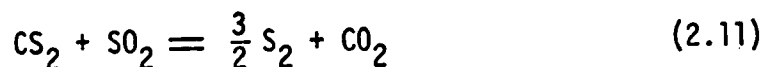
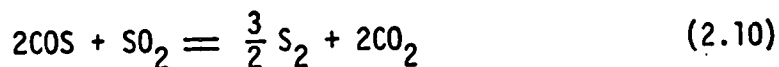
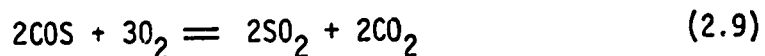
For H_2S combustion the overall rate expression is not so simple, but the overall reaction rate is predicted by [68]

$$-\frac{d[\text{H}_2\text{S}]}{dt} = -r_{\text{H}_2\text{S}} = k_6 [\text{H}_2\text{S}] [\text{O}] \quad (2.2)$$

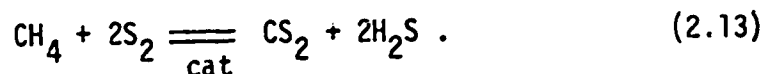
where, $k_6 = 1.45 \times 10^{15} \exp\left[-\frac{6,600}{RT}\right] \text{ CC mole}^{-1} \text{ sec}^{-1}$.

Aside from the work of Levy and Merryman, very little fundamental research results are available on the burning process in sulfur plants. Opekar and Goar [82] have suggested that some of the following overall reactions may occur:



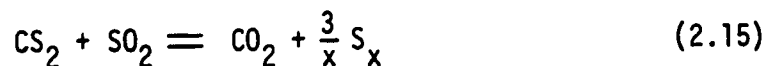
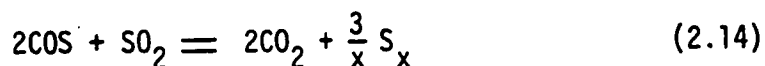


Smith [30,31,80] has studied the following heterogeneous reaction over a silica catalyst,



This suggests that it may be possible that CS_2 could be formed in the catalytic converters of sulfur plants however, plant data have not been released which could substantiate the possibility that alumina is also catalytically active for this reaction. Furthermore, kinetic considerations indicate [30,31,80] that this reaction occurs very slowly even on silica gel at Claus converter temperatures.

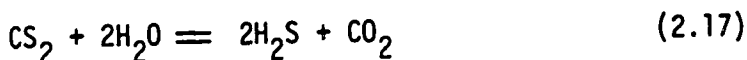
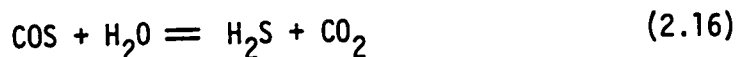
On the other hand, the literature [14,34] suggests that bauxite is an effective catalyst for converting CS_2 and COS with SO_2 to sulfur in the following reactions:



Gamson and Elkins [35] studied reaction (2.14) using bauxite catalyst and found that with a gas stream composition of 5.5% COS, 2.75% SO₂ and 91.75% N₂ (volumetric basis) yields of 90% or better were attainable between 250°C and 300°C at a space velocity of 200 std cu.ft./(cu.ft. catalyst)(hr). A typical sulfur plant space velocity falls between 650 and 900 std cu.ft./(cu.ft. catalyst)(hr) [16] and so, conversions for reaction (2.14) may be limited in commercial bauxite converters by the short contact time.

From available Claus sulfur plant data [95], the amount of COS and CS₂ which is removed, even in three converter units, is very marginal. In view of this fact and the reported efficiency of bauxite catalyst for catalyzing reactions (2.14) and (2.15), it is possible that the H₂S and SO₂ may be poisoning the catalyst for these reactions. This could result from H₂S or SO₂ having a much higher affinity for the same active centre required by the COS and CS₂ for their catalytic reaction.

Cameron and Beavon [10] suggest another means of CS₂ and COS removal, which involves hydrolysis to hydrogen sulfide by reaction with water,



Ample water is released by the Claus reaction to provide the necessary reactant for the COS and CS₂ and the equilibrium is very favourable for completion of these reactions. However, reaction rates are very slow over bauxite catalyst even at temperatures as high as 650°F. The authors claim to have found another catalyst with much higher activity than bauxite for the reactions. They indicated that these organic sulfur compounds contribute one-third or more to the total losses of sulfur to plant stack gases.

2.2.2 The Claus Reaction

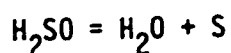
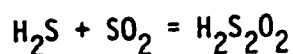
Gamson and Elkins [35] studied the Claus reaction in an integral reactor (18 in. long by 1.5 in. diameter) packed with 4/8 mesh Porocel catalyst. A hypothetical sulfur plant acid gas stream containing 100% H₂S which had undergone 69.4% conversion in a waste heat boiler formed the basis for selecting the reactor feed composition of 6.78% H₂S, 3.39% SO₂, 63.00% N₂ and 26.83% H₂O by volume. The integral reactor was operated at four space velocities (240, 480, 960 and 1920 (scf gas)/cu.ft. catalyst)/(hr) and three temperatures (230, 260 and 300°C). At these twelve operating conditions, the overall conversion of the H₂S was measured and the results were plotted on a conversion vs. space time diagram. The article [35] states that in a typical experiment,

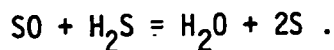
Table 2.2
Space Velocity - Conversion Data of
Gamson and Elkins [35]

<u>Space Velocity</u> <u>SCF/(cu.ft. catalyst)(hr)</u>	<u>Temperature</u> <u>(°C)</u>	<u>Total</u> <u>Conversion</u> <u>(%)</u>
240	230	97.9
240	260	96.7
240	300	94.8
480	230	96.9
480	260	95.8
480	300	94.4
960	230	96.0
960	260	95.2
960	300	94.0
1920	230	93.8
1920	260	93.4
1920	300	92.9

the catalyst was charged and brought to temperature. After passing reactants through the reactor for fifteen minutes, the fractional conversion was measured using wet chemical techniques. This implies that no time was allowed for conditioning the catalyst. Also, nothing is stated about catalyst bed temperature rise. The data which were obtained in the Gamson and Elkins study are presented in Table 2.2. These data provide a basis from which a reactor could be sized, but only for the feed composition which they used and only between 230 and 300°C. However, these authors cautioned that their kinetic data was inconsistent with their thermodynamic analysis of the Claus reaction because they measured conversions which were higher than thermodynamic equilibrium conversions for the same temperature and pressure.

Murthy and Rao [79], using a batch recycle reactor, studied metallic sulfides as catalysts for the Claus reaction and found that at 25°C the reaction would not proceed with any of their catalysts unless water was present. In fact water exhibited an autocatalytic effect with silver sulfide. They also studied the reaction over cobalt thiomolybdate, cobalt sulfide, and molybdenum sulfide. They postulated that the reaction took place in the following sequence:





The first step was considered to be rate-controlling, but this mechanism could not be tested against their data since they permitted sulfur to condense on the catalyst during their runs. Sulfur deposition would likely foul the catalyst, which meant that accurate, steady-state rate data were not measured.

Pyrex glass surfaces were studied as catalysts for the Claus reaction by Taylor and Wesley [101]. Their results can be summarized by the following rate equation which includes a term to account for the area of the glass surface,

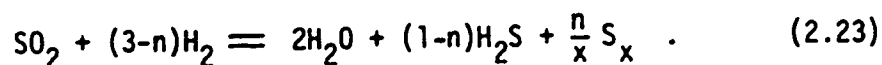
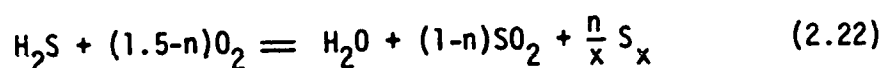
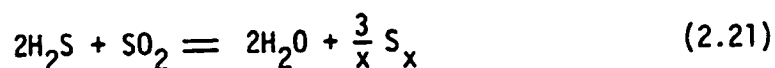
$$-r_{\text{H}_2\text{S}} = k \cdot A_E \cdot P_{\text{H}_2\text{S}}^{1.5} P_{\text{SO}_2} \quad (2.19)$$

where A_E is the area of the glass surface. In the course of their investigation they found that no measurable homogeneous reaction took place at 580°C and that water vapor would not react with liquid sulfur in their sulfur condenser. As indicated by the above equation, they noted that overall reaction rates were proportional to the glass surface area, thus revealing the heterogeneous nature of the reaction.

Udintseva and Chufarov [104] also noted that H_2S and SO_2 would not react homogeneously between 250°C and 350°C. Glass, aluminium and aluminium oxide were reported to be effective catalysts for the Claus reaction while iron and iron oxide exerted only a weak catalytic effect.

In an activation study of bauxite catalyst, Landau and Molyneux [62] concluded that the Claus reaction was a diffusion-controlled process. This conclusion was based on the fact that catalytic activity increased with smaller particle sizes. These authors did not state whether it was film or pore diffusion which was controlling the reaction rate. Since they provided no equipment description or catalyst charge sizes it was not possible to examine what type of diffusion, if any, prevailed. Therefore the usefulness of this conclusion was rather limited.

Hammar [44] has made a substantial contribution to the information available on the kinetics and mechanism of some of the sulfur plant reactions. He studied the following reactions primarily over cobalt-molybdenum-alumina catalyst mixtures,



Hammar used glass differential flow reactors for obtaining rate measurements. In his study of reaction (2.20) he concluded that sulfur reacted in the adsorbed form but that the interior surface of the catalyst was

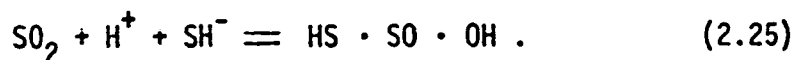
not available for reaction due to capillary condensation of the sulfur. This conclusion was based on the observation that above a critical sulfur concentration the reaction rate very abruptly decreased. His glass equipment catalyzed the Claus reaction, (2.21), but only an insignificant amount compared to that from the catalyst. Before his product analytical train, Hammar condensed the sulfur vapor on glass wool and water was removed and gravimetrically determined by adsorption on Dehydrite. It was observed that the Dehydrite catalyzed the reaction only when it became visibly moistened and therefore it was renewed after each run. This author attempted this same approach for water determination and found that even if the Dehydrite was not visibly moistened, sulfur would form on the dessicant at room temperature. Furthermore, it was found that Dehydrite can adsorb and retain small amounts of H_2S . Therefore, the method was discarded and it is suggested that the water determinations of Hammar which were used directly for calculating fractional conversions were systematically high since more than just the weight of water on the Dehydrite was being measured.

Hammar concluded that the reaction rate decreased as the partial pressure of sulfur vapor was increased. However, he did not prepare synthetic feed mixtures which contained sulfur. This conclusion was based on the fact as the fractional conversion of H_2S increased, the reaction rate decreased more, than it should have for the decreased H_2S and SO_2 partial pressures which accompanied the higher

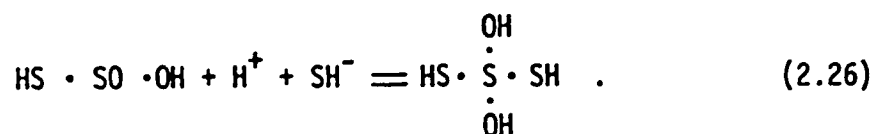
conversion. On the basis of this observation he can not say that it is sulfur vapor and not water vapor or, for that matter, either product species which retard the reaction. With regard to sulfur vapor, he noted no sudden decrease of reaction rate at conditions where sulfur vapor capillary condensation was likely to take place and he concluded therefore that the Claus reaction takes place predominantly on the external surface of the catalyst. Hammar used the Kelvin equation given below to predict the occurrence of capillary condensation in pores,

$$\ln\left(\frac{p_i^0}{p_i^s}\right) = \frac{(2\bar{v})(\sigma)(\cos\phi)}{(r_k)(RT)} \quad (2.24)$$

The following mechanism for the Claus reaction was postulated by Hammar. Both H_2S and SO_2 are adsorbed on adjacent active centres and H_2S dissociates. This gives a primary reaction of,

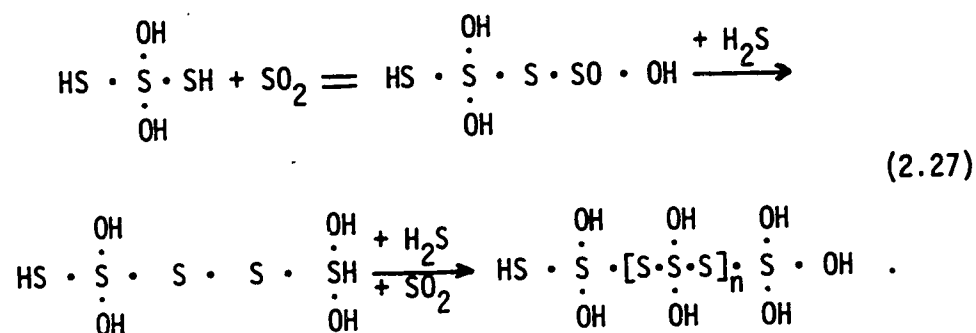


He could not suggest how the intermediate reacted further but offered two possibilities. One case involved,



This product permits water to split off and sulfur, in the form of S_3 , adsorbs on the catalyst. The S_3 formed initially combines with other

S_3 adsorbed on adjacent sites and the desorption occurs from a network of adsorbed sulfur. The other case involved a propagation reaction whereby,



Water is split off from all of the intermediates at different rates and the sulfur formed will be distributed according to some probability function.

Cormode [15] studied the Claus reaction over commercial porocel catalyst using a recycle flow reactor. He suggested that H_2S , itself, was decomposing to a very limited extent in his apparatus however, the accuracy of the analytical procedure used did not permit him to make a firm conclusion on this matter. A quantitative comparison of the kinetic data measured by Cormode and the work reported herein is given in Section 6.9.

2.2.3 Dissociation Reactions of Sulfur

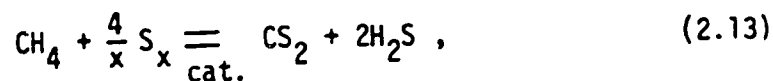
Sulfur vapor shows an apparently variable molecular weight dependent upon the temperature and pressure at which it exists. Kelly [55] has taken the data of Preuner and Schupp [91] and derived equations for the calculation of equilibrium constants at any temperature for the

following reactions,



Braune, Peter and Neveling [8] found that their experimental data required the presence of S_4 as well as S_2 , S_6 and S_8 for adequate explanation. Both Preuner and Braune performed vapor density measurements. Berkowitz and Marquhart [5], using a mass spectrometric technique, confirmed the presence of S_2 , S_3 , S_4 , S_5 , S_6 , S_7 , and S_8 and negligible amounts of S_9 and S_{10} around 400°K.

No direct measurements of the rates of dissociation and association of sulfur species seem to be available. The question is raised because it is necessary to know whether equilibrium is attained when calculating the average molecular weight (or vapor density) of sulfur vapor to determine its partial pressure. Hammar [44] assumed sulfur species equilibrium throughout his work. Smith [70,30,31], in his study of the previously discussed catalytic reaction,



determined a rate expression which treated sulfur vapor pressure as that which would be exerted by a sulfur specie with the average molecular weight of the vapor. That is, he assumed that the sulfur vapor

dissociation reactions were very rapid. Since the rate constant strictly followed the Arrhenius law, this was taken to be evidence that this assumption was correct.

The equilibrium distribution of sulfur species between 100 and 800°C and at 1 atm pressure is shown in Figure 3.1. Chapter III deals with the calculation of equilibrium compositions using the free energy minimization method. In this work it was also assumed that the sulfur vapor was a mixture of the species S_2 , S_6 and S_8 at chemical equilibrium.

2.2.4 Bauxite and Alumina Catalyst

It is clear that all reactions involving two phases must involve an interfacial reaction before the bulk process can occur. This is true of heterogeneous catalytic reactions and it is of interest to consider the fundamental aspects of gas-solid interfacial phenomena as they apply to the Claus reaction.

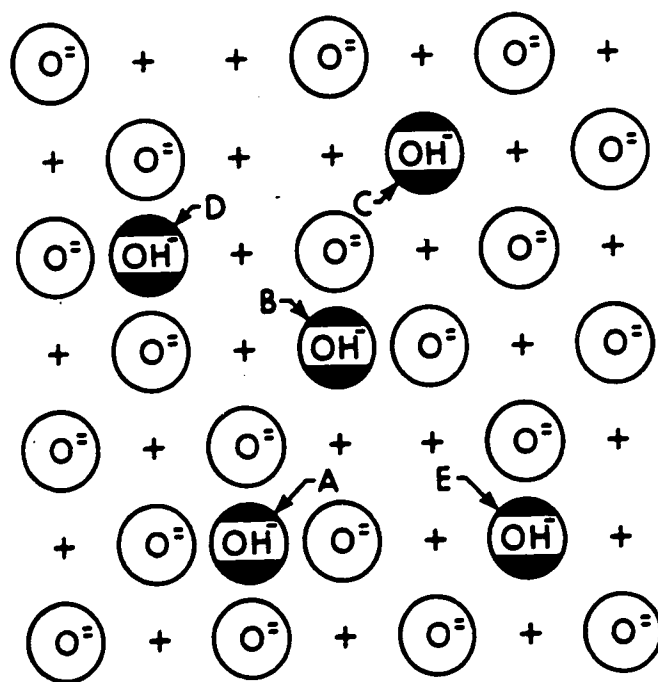
The regularity of atomic species arrangement associated with the structure of a crystalline material ends at the surface of the material. At this surface, irregular bonds occur and the surface atoms are subject to an asymmetric distribution of forces. This state of strain can be reduced either by rearrangement of surface atoms or by adsorption. In the latter process, molecules of a foreign substance are added to the surface thus relieving the strain and causing a decrease in free energy at the surface.

Catalytic aluminas are transition intermediates which occur

in the process of dehydrating the α - and β -aluminium trihydrates to the stable crystalline material, corundum. The three aluminas of catalytic interest are α -, γ - and η - Al_2O_3 . Their different structures are their most distinguishing feature and they are dependent on environmental conditions such as temperature, pressure and ambient moisture.

Boehmite, which has been suggested by Landau [62] to be the catalytically active phase of bauxite for the Claus reaction, can be written as $\gamma\text{-Al}_2\text{O}_3 \cdot \text{H}_2\text{O}$. The structure is made up of double sheets of oxygen octahedra with aluminium ions at their centres. Hydrogens are asymmetrically placed between the hydrogen bonded pairs of oxygen. Deer [22] suggests that it is a metastable material which decomposes at around 300°C yielding the nearly anhydrous γ -alumina.

Peri [85] has proposed a statistical model of a dehydroxylated alumina surface which is useful for describing the different types of surface sites. He suggests that five different types of surface hydroxyl groups exist and that they are distinguished by the number and orientation of neighbouring O^{2-} and Al^{+3} ions. These other ions offer two other possible surface sites. The square lattice depicted in Figure 2.2 indicates the surface situation which Peri's model predicts. The five unique surface OH sites have been verified using infrared techniques, and they are labelled as A, B, C, D and E in Figure 2.2 [43].



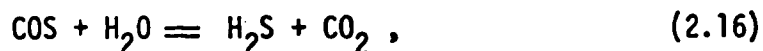
+ DENOTES Al^{3+} IN LOWER LAYER

FIGURE 2.2: COMPUTER MODEL OF A DEHYDROXYLATED ALUMINA SURFACE (85).

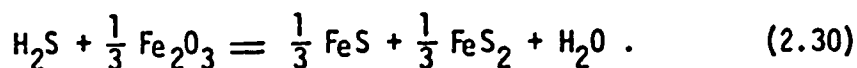
2.2.5 Gas-Solid Studies Performed on Alumina and Bauxites

Landau et al [62], have considered the activation and deactivation of bauxite catalyst and the effect of water on the Claus reaction. They found that the high catalytic activity of bauxite or alumina catalysts coincided with good dessicant properties of the solid and, that on bauxite catalysts, iron sulfate formed after only a few hours of operation. Their observations led them to believe that iron sulfate in bauxite tended to promote the formation of aluminium sulfate. Catalyst deactivation was directly attributed to the aluminium sulfate. Water was found to retard the reaction at high partial pressures.

In a kinetic study of the reactions of H_2S with bauxite and COS with bauxite, Korobeinichev [58] concluded that COS , undergoing the hydrolysis reaction,



on bauxite accelerates the reaction of H_2S with ferric oxide in the bauxite according to the following reaction,



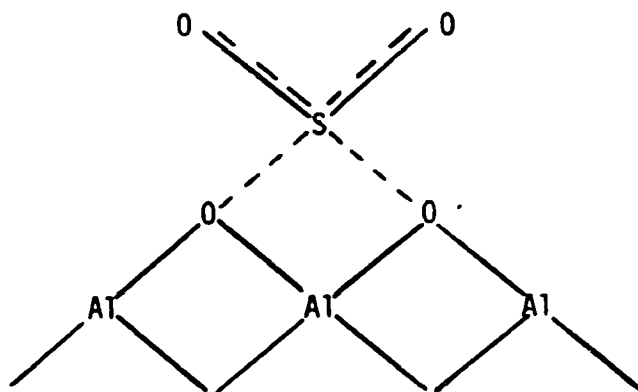
The author stated that this interaction of reactions can be accomplished with the aid of some active intermediate product which he did not specify.

Analagous effects were also observed in the system CS_2 - H_2S - bauxite.

Deo, Dalla Lana and Habgood [24] have studied the adsorption and surface reactions of H_2S and SO_2 on four catalysts, including γ -alumina, using an infrared technique. They concluded that,

- (i) both H_2S and SO_2 are physically adsorbed to γ -alumina,
- (ii) strong hydrogen bonding exists between both H_2S or SO_2 and surface hydroxyl groups of type D in Figure 2.2,
- (iii) a chemisorbed form of SO_2 exists on γ -alumina which reacts with H_2S according to the Claus reaction and,
- (iv) the function of the catalyst is to primarily bring the reactants together in a suitable orientation, most probably through hydrogen bonding.

The chemisorbed form of SO_2 was explained as a sulfate-like structure shown below.



MacIver, Tobin and Barth [74] studied the surface properties of well characterized samples of η - and γ -alumina. They found that after removal of physically adsorbed water, γ -alumina contained 7% by

weight water and η -alumina contained 4.5%. This "excess" 2.5% water on γ -alumina could be desorbed below 300°C and could originate from three sources which are:

- (i) condensation of surface hydroxyl groups,
- (ii) molecular water bound to the surface, and
- (iii) chemically bound water incorporated into the lattice as internal hydroxyl groups.

Based on their rather extensive literature survey of work in this field and their own experience, MacIver et al concluded that the excess water corresponded to a monolayer of molecular water, hydrogen bonded to surface hydroxyl groups and that the remaining 4.5% water could be accounted for by condensation of surface hydroxyl groups.

DeRosset and associates [25] determined the isotherms of H_2S adsorbed on $\gamma-Al_2O_3$ from H_2S/H_2 mixtures over the temperature range of 260°C to 560°C. Isosteric heats of adsorption ranged from 25-38 k.cal/mole of H_2S depending on the degree of predrying of the alumina. They found the adsorption to be ideal based on entropy calculations. The number and strengths of the adsorption sites indicated to DeRosset et al that they were Lewis-acid sites formed by stripping oxygen anions from a spinel surface exposing incompletely coordinated aluminium cations. The H_2S , like water and ammonia, reacts as a base at these sites and forms an Al-S bond.

According to the electrical measurements of Heldt and Hasse [46], alumina is essentially an insulator with an activation energy of 2.38

to 2.50 e.v. for conduction.

This review of bauxite and alumina is very limited considering the available published material describing work in this field. Additional references are recommended for more comprehensive information available on these catalysts [22,43,72].

2.3 Adsorption, Surface Reaction and Related Rate Laws

In heterogeneous kinetic studies, one observes the reactants and products in the gas phase rather than in the actual surface phase in which reaction occurs. This leads to the distinction between the true rate law expressed in terms of surface concentrations and the apparent rate law dependent upon the various gas pressures. The true and apparent rate laws for a system are related by the adsorption equilibrium since this connects the surface with gas phase concentrations.

To discuss all of the adsorption isotherms which describe adsorption equilibrium would add unduly to the bulk of this literature review however, to omit them would limit the interpretation of the kinetic data which has been measured in this program.

Laidler [61] points out that there are three important features of chemisorption related to the kinetics of surface reactions. The first is that after a surface has become covered with a single layer of adsorbed molecules it is essentially saturated preventing further chemisorption. This is the unimolecular layer and has been emphasized by Langmuir [63] in his work.

The second feature is that chemisorption may have an appreci-

able activation energy and hence may be a slow process. It is generally agreed that chemisorption on oxides involves appreciable activation energy.

Thirdly, there is frequently a considerable variation in the adsorptive capacities of the various surface sites. This is called surface heterogeneity and the concept has led to the belief that chemical reaction occurs on active centres on catalysts which correspond to lattice defects on the surface. These active centres have been envisaged by Boudart [6] as constantly being created and destroyed with the movement of excited electrons in the lattice.

Although numerous adsorption isotherms have been successfully fitted to adsorption data and have some theoretical basis, in adsorption theory, the Langmuir isotherm is of great importance equivalent to that of the ideal gas law [61]. The Langmuir expression for the fraction, θ_i , of a surface covered by a gas at adsorption equilibrium is

$$\theta_i = \frac{K p_i}{1 + K p_i} \quad (2.31)$$

where p_i is the partial pressure of the gas and K is the equilibrium constant. Zeldowich [109], in trying to derive an isotherm which incorporated the concept of surface heterogeneity and the Langmuir adsorption isotherm, arrived at an isotherm which was synonymous with the Freundlich equation, which had been regarded as an empirical equation. The Freundlich equation may be written in the form,

$$\theta_i = K p_i^{1/n}, \quad (n > 1) \quad (2.32)$$

and, as Thomas [102] points out, it should no longer be criticised for predicting progressively increasing surface coverage with increasing pressure because according to the derivation of Zeldowich [109], which is available in a simplified version due to Laidler [61], the isotherm is expected to be valid only at low coverages [102]. In several systems involving the chemisorption of gases on metals and oxides, the Freundlich equation has been found to be strictly applicable and Thomas [102] suggests the following references to be consulted to see examples [32,102].

A selection of isotherm equations and their applicability is given in Table 2.3 which was compiled by Thomas and Thomas [102]. The Langmuir and Freundlich equations have been invoked to provide a basis for arguments which attempt to justify the use of Freundlich-based rate equations for data correlation which are discussed in Chapter VI.

2.4 Mass Transfer in Heterogeneous Catalysis

The investigation of catalytic reactions is complicated by the fact that the process frequently involves diffusion as well as chemical phenomena. The overall rate of a catalytic reaction is liable to be determined by one of the following steps:

- (i) diffusion of the reactant molecules to the catalyst surface,
- (ii) adsorption of the reactants on the surface,
- (iii) reaction in the adsorbed layer,
- (iv) desorption of the product molecules, and

- (v) diffusion of the product molecules away from the vicinity of the catalyst surface.

Table 2.3

A Selection of Adsorption Isotherms

<u>Name</u>	<u>Isotherm Equation</u>	<u>Applicability</u>
Langmuir	$\theta_i = \frac{K p_i}{1 + K p_i}$	Chemisorption and physical adsorption
Freundlich	$\theta_i = K p_i^{1/n}, (n>1)$	Chemisorption and physical adsorption
Henry	$v_a = K p_i$	Chemisorption and physical adsorption
Temkin	$\theta = \frac{1}{K} \ln C_0 p_i$	Chemisorption
Brunauer-Emmett-Teller (BET)	$\frac{p_i}{v_a(p_i^0 - p_i)} = \frac{1}{K v_m} + \frac{(K-1)}{v_m K} \frac{p_i}{p_i^0}$	Multilayer physical adsorption

In kinetic studies it is desirable to eliminate steps (i) and (v) as rate controlling steps, however film diffusion is often encountered industrially. Pore diffusion also can exert a profound effect on the observed kinetics of a reaction and consequently, confuse the interpretation of the rate data. Therefore, the theory of mass transfer and its effect on reaction rate measurements is reviewed in this section.

2.4.1 Film Diffusion

Gas passing over a catalyst surface develops a boundary layer through which reactants and products are transported at rates which depend mainly on the nature of the bulk stream flow [96]. This is generally referred to as boundary layer or film diffusion.

Data on mass transfer from gas to solid are commonly expressed in terms of a mass transfer coefficient, k_G , defined by,

$$N_i = k_G (p_i - p_i^s) . \quad (2.33)$$

The flux and pressures refer to the i^{th} constituent in the chemical system.

Dimensional considerations [96] lead to the following basis for mass transfer data correlation:

$$\frac{k_G d_p}{D_{12}} = f(N_{Re}, N_{Sc}) . \quad (2.34)$$

A graphical correlation of j_D versus N_{Re} is available [96] which is very useful for obtaining k_G from the following equation,

$$j_D = \frac{k_G P}{G_M} N_{Sc}^{2/3} . \quad (2.35)$$

In the absence of diffusivity data, the Lennard-Jones expression [49] has been suggested [96] as a reasonable theoretical ap-

proach to estimating diffusivities,

$$D_{12} = \frac{0.001858 T^3 [(M_1 + M_2)/M_1 M_2]^{1/2}}{P \sigma_{12}^2 \Omega_D} \quad (2.36)$$

From estimates of mass transfer coefficients, it is possible to evaluate the molecular diffusion rates of constituents to and from the catalyst surface. When applied to a catalyst bed, the overall rates can be determined. The above equations were applied in Appendix D in order to estimate whether or not film diffusion is a rate-limiting feature of the Claus reaction for flow conditions in the experimental equipment and in modified Claus sulfur plants.

2.4.2 Pore Diffusion

After reaching the external surface, constituents can enter or leave catalyst pores by one or a combination of three mechanisms, involving ordinary diffusion. According to Sherwood [96], surface diffusion has not been studied extensively and available data [54,38] indicate that it contributes very little to the overall transport processes through a porous mass.

Ordinary gas diffusion occurs in pores if gas-gas molecular collisions predominate. The effective diffusivity, $D_{12,eff}$, may be employed to relate the mass flux to the total cross-section of the porous solid, where

$$D_{12, eff} = \frac{D_{12} \theta}{\tau} \quad (2.37)$$

The tortuosity factor, τ , is roughly 1.5 to 2.0 for unconsolidated particles, but may be considerably larger for consolidated porous media such as typical solid catalysts.

If the gas density is low, or if the pores are very small, or both, the molecules collide with the pore wall much more frequently than with each other. Under these conditions, Knudsen diffusion predominates and the criterion for Knudsen diffusion is that the pore diameter be approximately ten times smaller than the mean free path of the gas at the temperature and pressure of interest. Satterfield and Sherwood [96] give the Knudsen diffusion coefficient as

$$D_{K \text{ eff}} = 19,400 \frac{\theta^2}{(\tau)(S)(\rho_p)} \sqrt{\frac{T}{M}} \quad (2.38)$$

From a practical point of view, one would like to have a criterion which used measured values of reaction rate, effective diffusivity, reaction order and so forth which could then be used to discern whether a reaction is operating near the pore-diffusion controlled regime. As Peterson points out [89], it is important to know whether measured rate data represent catalytic kinetics or interaction between catalytic kinetic and mass transport phenomena. Weisz and Prater [107] developed a criterion for power law kinetics however, Peterson [88] showed that it was much too liberal when applied to reactions which possessed strong product inhibition. Peterson [87] offered a criterion which resulted from an asymptotic solution of the partial differential equations which describe the conservation of mass

and energy for the reaction system. However, the derivation for a specific case is rather complex. Hudgins [50] developed a solution to this problem by a method similar to that of Anderson [1].

The development of the criterion for absence of diffusion control which Hudgins suggested is now described. The Taylor expansion for the rate about an external concentration of reactant is,

$$r(C) = r(C_0) + (C-C_0)r'(C_0) + (C-C_0)^2 \frac{r''(C_0)}{2!} + \dots \quad (2.39)$$

in which he ignored second order and higher terms. He then assumed that the concentration profile inside the catalyst particle could be approximated by

$$C - C_0 = r(x^2 - 1) \quad (2.40)$$

where $x = C/C_0$. Substituting Equation (2.40) into (2.39) and integrating over the sphere he obtained,

$$\frac{4}{3} \pi \bar{r} = r_0 \int_0^1 \left[1 + r(x-1) \frac{r'(C_0)}{r(C_0)} \right] 4\pi x^2 dx, \quad (2.41)$$

which after rearrangement led to,

$$\frac{\bar{r}}{r_0} = 1 - \frac{2}{5} r \left[\frac{r'(C_0)}{r(C_0)} \right] \quad (2.42)$$

where \bar{r} is the overall rate and r_0 is the rate corresponding to C_0 .

In order to have the overall rate, \bar{r} , approximately equal to the rate obtained if the particle were completely accessible to C_0 , the final term of Equation (2.42) must be small, and Hudgins suggested 0.05 for its maximum value. Therefore,

$$\frac{2}{5} \Gamma \left[\frac{r'(C_0)}{r(C_0)} \right] < 0.05 . \quad (2.43)$$

A steady state mass balance on the sphere gave,

$$\bar{r}V = S D \left. \frac{dC}{dr} \right|_{r=r_0} . \quad (2.44)$$

The concentration gradient at the surface was evaluated from Equation (2.40) and, since $S/V = 3/r_0$ for a sphere,

$$\frac{\bar{r} r_0^2}{D} = 6\Gamma . \quad (2.45)$$

The Γ from Equation (2.45) was substituted into (2.43) to give,

$$\frac{\bar{r} r_0^2}{D} < 0.75 \frac{r(C_0)}{r'(C_0)} , \quad (2.46)$$

which was cleared of the fraction by changing 0.75 to 1. On this basis, the criterion for absence of diffusion control was taken as

$$\bar{r} \frac{1}{C_0} \frac{r_0^2}{D} < \frac{1}{C_0} \cdot \frac{r(C_0)}{r'(C_0)} \quad (2.47)$$

which Hudgins indicated was a simple generalization of the Weisz-Prater criterion.

Hudgins' criterion has been used in Appendix D to establish whether or not diffusion is significant in the Claus reaction catalyzed by bauxite.

2.5 Recycle Reactors

In Section 1.3, reasons were given for using a recycle reactor to study the Claus reaction. Perkins and Rase [86] have discussed the advantages and disadvantages of using recycle reactors for kinetic research and they are now reviewed. Advantages:

- (i) Near isothermal conditions exist in the catalyst bed. Recycle rates ten times larger than fresh feed rates, for instance, would give one tenth of the temperature rise which would occur in an adiabatic differential reactor operating with the same overall conversion.
- (ii) High recirculation rates permit high gas velocities past the catalyst without the use of excessive quantities of reactants. Theoretically, mass transfer could be enhanced until even for very rapid reactions the bulk mass transfer rate would no longer influence the rate of reaction.
- (iii) Low conversions per pass of reactant through the catalyst bed can be accomplished without limiting the total conversion to very low values, which would introduce errors through analysis.

Disadvantages:

- (i) An excessive time period may be required for such a system to reach steady state if the recycle system is large.
- (ii) Pressure drop may be higher than those observed in ordinary differential reactors.
- (iii) One should use a continuous method of analysis for such a reactor. In addition to these disadvantages, this author comments that it may in some cases be difficult to obtain a reliable, inert recycle pump.

In this program, at least six months were spent developing and building the recycle blower which is described later. Another advantage is that it is possible to obtain direct measurement of reaction rates at finite levels of conversion and, as previously indicated, at near isothermal conditions.

Although the concept of the recycle reactor was first proposed by Dohse [26] in 1930, its application has been relatively sparse in kinetic studies until recent years. However, users of this technique [9,20,65,86,100] have expressed enthusiasm for it as a research tool. The recycle reactor and its behaviour will now be reviewed.

Consider the recirculation reactor in Figure 2.3 where a reactant stream of fixed composition and flow rate is fed to the reactor loop. Let the conversion of the selected reactant A be zero at the reactor inlet, x_{A1} just before the catalyst bed and x_{Af} just after the catalyst bed. Also, assume that the rate of reaction is the same

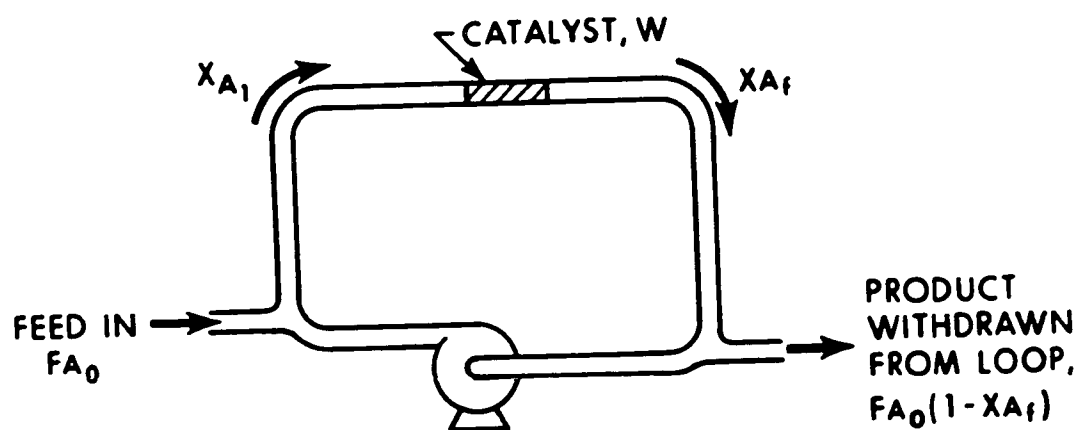


FIGURE 2.3: SKETCH OF A RECYCLE REACTOR

at all points in the catalyst bed for a specific run.

With no recycle, $x_{A1} = 0.$, and a steady state material balance gives,

$$(-r_A)_{av} = \frac{x_{Af}}{W/F_{A0}} \quad (2.48)$$

where $(-r_A)_{av}$ is measured at some average conversion, i.e. at average reactant concentration values, of the streams entering and leaving the catalytic bed. Thus $x_{Af} > x_{AV} > x_{A1}$. Since $(x_{Af} - x_{A1})$ may be large, choosing to use an average rate may lead to serious error.

Now suppose that a part of the product stream is recycled. As the recycle rate increases, the incoming feed is mixed with more product stream causing x_{A1} to approach x_{Af} . Thus the error in the assumption of a constant rate decreases accordingly. So at high recycle ratios,

$$(-r_A)_{av} = (-r_A)_f = \frac{x_{Af}}{W/F_{A0}} \quad (2.49)$$

where the rate is measured at the exit stream conditions. At high recycle rates, this type of reactor may properly be considered to be a perfectly mixed backmix reactor.

The validity of the assumption that a recycle reactor is in fact a perfectly mixed backmix reactor can be assessed by considering its residence time distribution. Rippin [93] has developed the RTD for a recycle reactor in the following way. The time for a

single passage through the recycle reactor is:

$$\frac{V_R}{(1+R')Q} = \frac{\theta'}{1+R'} \quad (2.50)$$

where V_R = reactor volume
 R' = recycle flow to feed flow ratio
 Q = volumetric flow rate of feed
 θ' = mean residence time, V_R/Q

An amount $Q\Delta t$ of material entering the system between time $t = 0$ and Δt will reach the reactor exit at time $\theta'/1+R'$. But a fraction, $R'/1+R'$, is returned in the recycle so that the amount leaving the system with age $\theta'/1+R'$ is $Q\Delta t/1+R'$ and the fraction of material in the outlet with this age is $1/1+R'$. An amount of recycle material, $Q\Delta t R'/1+R'$, passes through the reactor again, and, on reaching the reactor exit for the second time, its age is $2\theta'/1+R'$. The fraction of the original material in the outlet stream is now $1/1+R'(R'/1+R')$. After i passes through the reactor, the age is $i\theta'/1+R'$ and the fraction of the original material in the exit stream is $1/1+R'(R'/1+R')^{i-1}$. The RTD will thus consist of an infinite series of impulses or delta functions spaced at intervals of $\theta'/1+R'$ and whose magnitude decreases as a geometric series.

$$f(t) = \sum_{i=1}^{\infty} \frac{1}{1+R'} \left(\frac{R'}{1+R'}\right)^{i-1} \delta\left(t - \frac{i\theta'}{1+R'}\right) \quad (2.51)$$

Rippin then points out that for large R' , the RTD reduces to

that for a CSTR: $1/\theta' \exp(-t/\theta')$.

Perkins and Rase [86] confirm that a recycle reactor behaves as a backmix reactor when R' is greater than 10. Zwietering [111], points out, however, that a knowledge of the RTD of a continuous flow system is not sufficient for the description of the state of mixing. He introduced the concept of "maximum mixedness" which is most easily understood by regarding the state of maximum mixedness for a system as that state for which the mixing model reduces to the nonsegregated condition. Danckwerts [19] degree of segregation, J , is the ratio of the variance of ages between points to the total variance of ages in the reactor.

Rippin found the degree of segregation for a recycle reactor to be:

$$J = \frac{1}{12 R' (1+R') + 1} \quad (2.52)$$

For a plug flow reactor, $R'=0$ and $J=1$ the reactor is completely segregated. For the recycle reactor with R' very large, J approaches zero implying complete molecular mixing. Gillespie and Carberry [68] indicate that the mixing state of the recycle reactor reduces to the nonsegregated, micro-mixedness condition as R' is increased to values above 20.

CHAPTER III

DETERMINATION OF EQUILIBRIUM COMPOSITIONS3.1 Background

When a chemical reaction is being studied, it is desirable to know the distribution of products that will exist at thermodynamic equilibrium. The classical approach to solving this problem uses the equilibrium constant method however, this procedure becomes unwieldy when many chemical reactions occur simultaneously. Gamson and Elkins have used this method for calculating equilibrium compositions for the Claus Reaction [35]. Several techniques for determining the equilibrium composition of complex system reaction systems have been reviewed by Zeleznik and Gordon [110].

In 1958, White et al [108] devised a method for calculating equilibrium composition by minimizing the system free energy using a steepest descent technique. The free energy minimization method was extended by Kubert and Stephanov [59] to include not only gaseous but also condensed phases. In 1962, Oliver et al [83] demonstrated the method applied to a methane-water reaction system. Since the free energy minimization method has been used in this study, the mathematics of the procedure will now be reviewed.

3.2 Review of the Free Energy Minimization Method

For the determination of equilibrium composition, the only specie property needed is the molal standard (Gibbs) free energy function, F/RT . The basic assumption of the method requires that the gases behave ideally.

The total free energy of a mixture of N gaseous components is expressed as

$$F(X) = \sum_{i=1}^N f_i . \quad (3.1)$$

The free energy contributed by a gaseous specie is given by

$$f_i = x_i (C_i + \ln x_i / \bar{x}) , \quad (3.2)$$

where,
$$C_i = \left(\frac{F}{RT} \right)_i + \ln P . \quad (3.3)$$

The determination of the equilibrium composition requires finding a non-negative set of mole numbers, X , which will minimize the total free energy of the system, $F(X)$. This set of mole numbers must also satisfy mass balance considerations so that

$$\sum a_{ij} x_i = b_j \quad (j = 1, 2, \dots, M) . \quad (3.4)$$

Let $Y = (y_1, y_2, \dots, y_N)$ be an initial guess for the mole numbers of the gaseous species (x_1, x_2, \dots, x_N) . Choose Y such that it

is a positive set and satisfies the mass balance constraints. The free energy is

$$F(Y) = \sum_{i=1}^N y_i (c_i + \ln y_i / \bar{y}) \quad (3.5)$$

where
$$\bar{y} = \sum_{i=1}^N y_i \quad (3.6)$$

Let
$$\Delta_i = x_i - y_i ; \Delta' = \bar{x} - \bar{y} \quad .$$

An expression, $Q(X)$, is obtained as an approximation for $F(X)$, the minimum free energy, by using a Taylor expansion about the initial guess, Y . Using this expansion technique, and substituting in values of the partial derivatives $\partial F / \partial x_i$, the following expression can be obtained

$$Q(X) = F(Y) = \sum_{i=1}^N (c_i + \ln y_i / \bar{y}) \Delta_i + \frac{1}{2} \sum_{i=1}^N y_i \left[\frac{\Delta_i}{y_i} - \frac{\Delta'}{\bar{y}} \right]^2. \quad (3.7)$$

In order to find a better approximation to the desired solution, $Q(X)$ is minimized subject to the mass balance constraints, Equation (3.4). First it is necessary to define $G(X)$ in the manner

$$G(X) = Q(X) + \sum_{j=1}^M \pi_j (b_j - \sum_{i=1}^N a_{ij} x_i) \quad (3.8)$$

where the π_j are Lagrange multipliers. Then set

$$\frac{\partial (X)}{\partial x_i} = 0, \quad i = 1, 2, \dots, N$$

The change in free energy with a change in the moles of the gaseous species becomes

$$\frac{\partial (X)}{\partial x_i} = [c_i + \ln \left(\frac{y_i}{y} \right) + \left[\frac{x_i}{y_i} - \frac{\bar{x}}{y} \right] - \sum_{j=1}^M \pi_j a_{ij}] = 0. \quad (3.9)$$

Now, solve for x_i in Equation (3.9)

$$x_i = -y_i \left(c_i + \ln \frac{y_i}{y} \right) + y_i \left(\frac{\bar{x}}{y} \right) + \sum_{j=1}^M (\pi_j a_{ij}) y_i. \quad (3.10)$$

Summing over i in this equation gives

$$\sum_{j=1}^M \pi_j \sum_{i=1}^N a_{ij} y_i = \sum_{i=1}^N y_i \left[c_i + \ln \frac{y_i}{y} \right]. \quad (3.11)$$

Let
$$r_{jk} = r_{kj} = \sum_{i=1}^N (a_{ij} a_{ik}) y_i \quad j, k = 1, 2, \dots, M. \quad (3.12)$$

Substitute Equation (3.10) into Equation (3.4). This gives M equations which together with Equation (3.11) give $M+1$ linear equations in the unknowns $\pi_1, \pi_2, \pi_3, \dots, \pi_M$ and \bar{x}/y as follows:

$$\alpha_1 \left(\frac{\bar{x}}{y} \right) + r_{11} \pi_1 + r_{12} \pi_2 + \dots + r_{1M} \pi_M = b_1 + \sum_{i=1}^N a_{i1} f_i$$

$$\alpha_2 \left(\frac{\bar{x}}{y} \right) + r_{21}\pi_1 + r_{22}\pi_2 + \dots + r_{2M}\pi_M = b_2 + \sum a_{i2}f_i \quad (3.13)$$

$$\alpha_M \left(\frac{\bar{x}}{y} \right) + r_{M1}\pi_1 + r_{M2}\pi_2 + \dots + r_{MM}\pi_M = b_M + \sum a_{iM}f_i$$

$$\alpha_1\pi_1 + \alpha_2\pi_2 + \dots + \alpha_M\pi_M = \sum f_i$$

where

$$\alpha_j = \sum_{i=1}^N a_{ij}y_i$$

To find the new values of the x_i 's, it is necessary to substitute the values of the α_j 's, \bar{x}/y and y_i 's into Equation (2.10). The procedure is repeated until the differences between subsequent iterations are small enough to satisfy some arbitrary convergence criterion.

If the computed set of new mole numbers x_i include negative numbers, the computed values of mole numbers are not used in the next approximation. It is desirable that the species not be negative or zero. The method of eliminating negative species is arbitrary within the limitation that the mass balance must be adhered to. One such way is to choose λ so that

$$y_i' = y_i + \lambda(x_i - y_i) \quad (3.14)$$

is not negative or zero. For y_i' being zero, λ becomes

$$\lambda' = \frac{-y_i}{x_i - y_i} \quad (3.15)$$

Therefore λ is set to some fraction (usually .99) of λ' . As it was previously mentioned, all of the mole numbers must be greater than zero for this method to work.

3.3 Applications of the Free Energy Minimization Method

3.3.1 Comparison with Gamson and Elkins Data

A computer program was written to carry out the free energy minimization calculations. Good agreement was noted between the results from this method and those from Gamson and Elkins [35] for the equilibrium between molecular species of sulfur at various temperatures using the same free energy data [55]. A graph indicating the distribution between the various sulfur species S_2 , S_6 and S_8 at one atmosphere pressure is shown in Figure 3.1, and the program output from which the points for the graph were obtained is in Appendix B. Since the agreement was good, the method was used for determining the average molecular weight of sulfur vapor in the recycle reactor which, in turn, was used to calculate the mole fraction of sulfur in the reactor.

The free energy minimization method was also used for calculating the equilibrium conversion of H_2S and SO_2 to sulfur according to the following definition of conversion:

$$\text{Fractional conversion} = \frac{S + 2S_2 + 6S_6 + 8S_8}{H_2S + SO_2 + S + 2S_2 + 6S_6 + 8S_8}$$

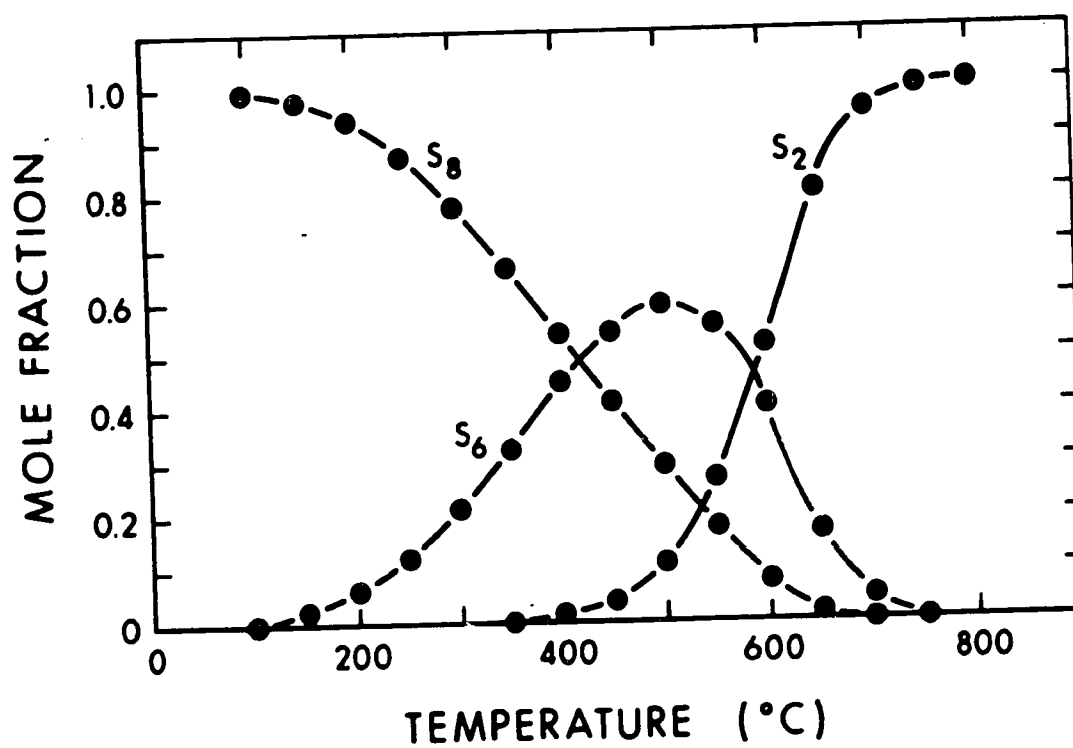


FIGURE 3.1: CHEMICAL EQUILIBRIUM BETWEEN SULFUR SPECIES AT ONE ATMOSPHERE.

where the molecular formulae refer to the mole fraction of each specie at equilibrium. A slight discrepancy may be seen between this work and that of Gamson and Elkins when equilibrium conversion was plotted against temperature as seen in Figure 3.2. The difference arises from the source of free energy data. Gamson used the data of Kelley [55] while that of McBride et al [112] was used in this work.

The program output for Figure 3.2 is given in Table B.1, Appendix B. It should be noted in this table that only very minute quantities of hydrogen could be formed at the experimental conditions employed by Cormode [15] in his kinetic study and so, the observation that hydrogen sulfide may form both hydrogen and sulfur is thermodynamically unlikely.

3.3.2 Analysis of Miscellaneous Sulfur Plant Reactions

The literature survey indicated that a large number of reactions are taking place in sulfur plants. Some of these reactions have been analysed for thermodynamic equilibrium conditions and the results of the analysis are presented in Table 3.1. All of the studies were conducted at a total pressure of one atmosphere and stoichiometric ratios of reactants diluted with nitrogen. The computer output for the four temperatures shown in Table 3.1 as well as the results for intermediate temperatures is given in Appendix B in Tables B-3 to B-11.

The results shown in Table 3.1 indicate that it is possible to remove almost all of the COS and CS₂ from sulfur plant tail gas streams according to the first four reactions. Table 3.1 also shows

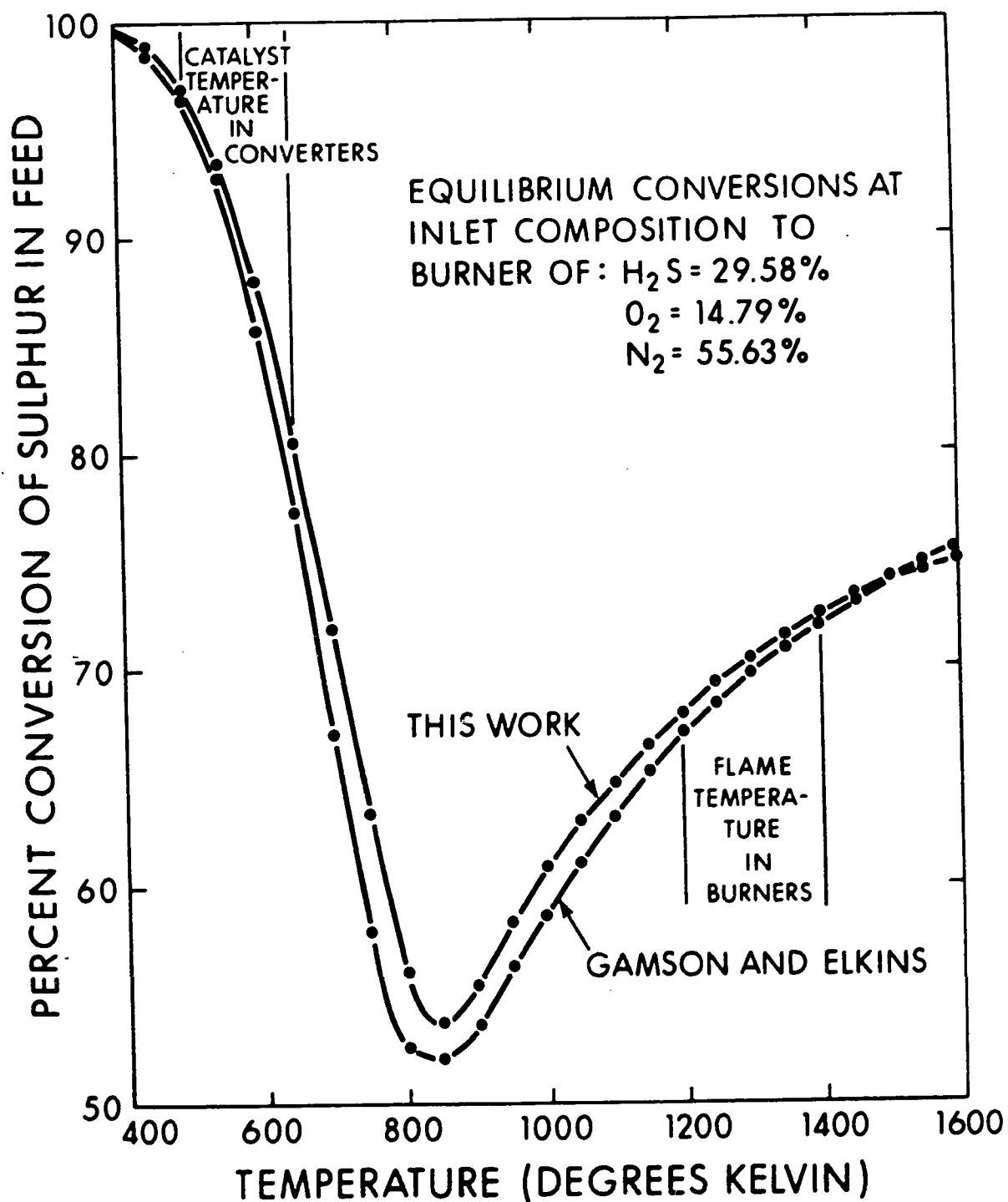


FIGURE 3.2: CLAUS REACTION EQUILIBRIUM CONVERSION VERSUS TEMPERATURE

Reaction				Initial Mole Percent		Equilibrium Percent Conversion		
A	B	C	D	A	B N ₂	500°K	1000°K	1500°K 2000°K
2COS	+ SO ₂	= 2CO ₂	+ $\frac{3}{x}$ S _x	6	3 91	99.99	97.29	96.25 95.57
CS ₂	+ SO ₂	= CO ₂	+ $\frac{3}{x}$ S _x	5	5 90	99.99	99.71	99.55 99.37
COS	+ H ₂ O	= CO ₂	+ H ₂ S	5	5 90	98.34	87.69	78.06 72.02
CS ₂	+ 2H ₂ O	= CO ₂	+ 2H ₂ S	3	6 91	99.67	95.31	89.31 84.07
H ₂ S	+ CO ₂	= COS	+ H ₂ O	5	5 90	1.65	12.30	21.94 27.98
CH ₄	+ $\frac{4}{x}$ S _x	= CS ₂	+ 2H ₂ S	2	$\frac{8}{x}$ 94	99.75	99.15	96.82 93.44
COS	+ H ₂ S	= CS ₂	+ H ₂ O	5	5 90	1.04	7.03	12.48 16.90
2COS	+ 3O ₂	= 2SO ₂	+ 2CO ₂	4	6 90	99.99	99.99	99.99 99.99
CO	+ $\frac{1}{x}$ S _x	= COS		5	$\frac{5}{x}$ 92.5	99.99	54.11	4.33 0.79

Table 3.1

Thermodynamic Analysis of Sulfur Plant Reactions.

the reactions through which COS and CS₂ can be formed. Since COS and CS₂ emission from sulfur plants accounts for approximately one-third of the sulfur loss, and since it is thermodynamically possible to remove 98-100% of the COS and CS₂, it is suggested that a search for an effective catalyst for any of the first four reactions in Table 3.1 would have considerable merit. It is further suggested that bauxite catalyst does not promote any of the first four reactions to the extent required for effectively removing COS or CS₂.

CHAPTER IV

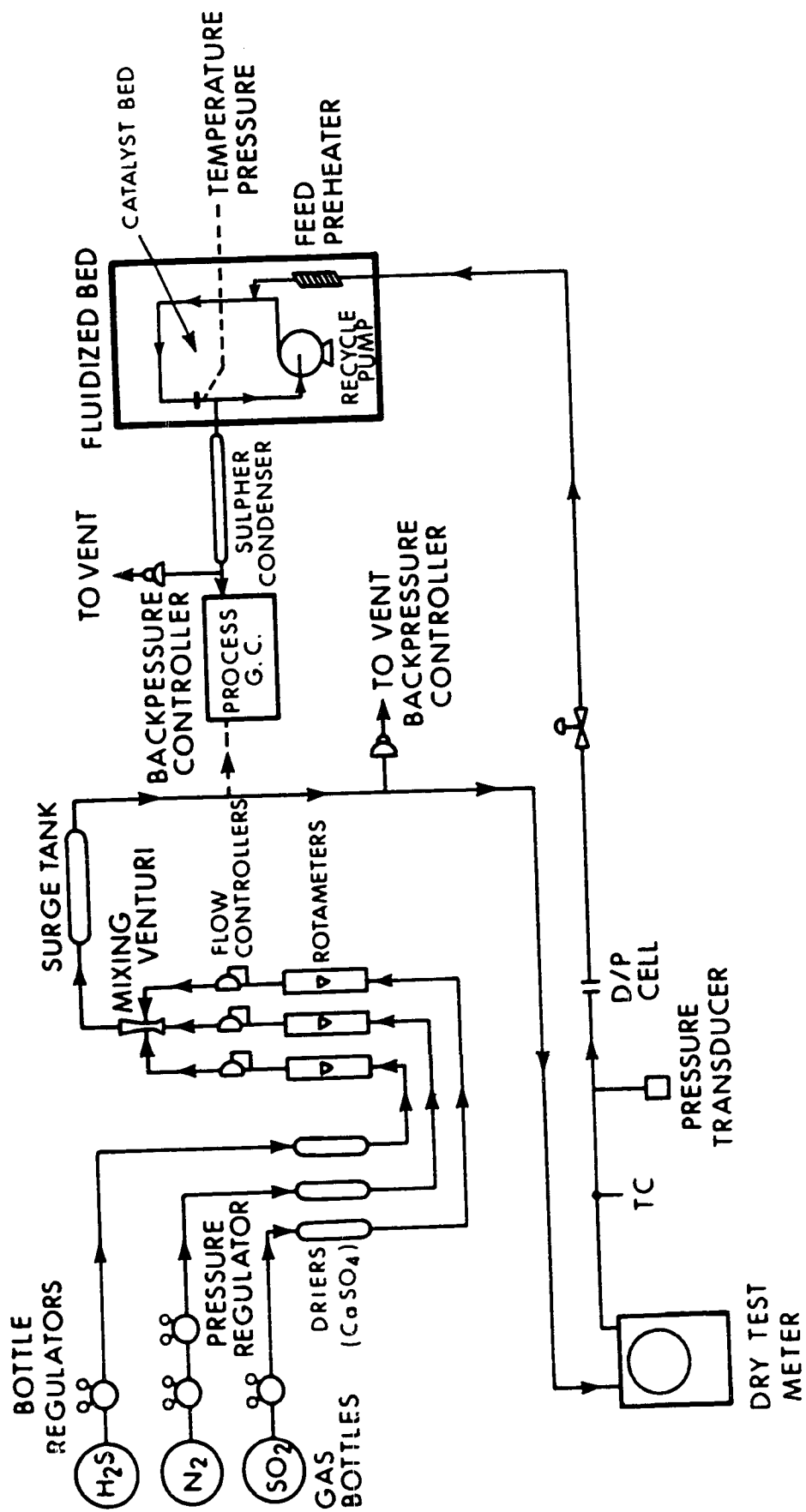
DESCRIPTION OF EXPERIMENTAL EQUIPMENT4.1 Feed Preparation and Metering System

The feed system was designed so that it would be possible to supply the reactor with a gas stream of constant flow rate and composition over long periods of time. Also it was considered desirable to be able to change the feedstream flow rate to the reactor and still have the composition remain constant. These primary objectives exerted considerable influence on the selection and configuration of equipment shown in Figure 4.1.

Each gas bottle was equipped with its own pressure regulator, and, in the case of nitrogen, a second regulator was placed in series with the first. This was done to improve the control of nitrogen pressure upstream of the flow controller, since, as the bottle contents depleted, the bottle pressure dropped.

Calcium sulfate, packed in 500 cu cm stainless steel cylinders, was used as a drying agent for N_2 and H_2S . Silica gel was used for drying SO_2 . This was done to prevent reaction in the feed system since H_2S and SO_2 readily react with one another in the presence of water.

Glass rotameters with stainless steel balls were used to measure the magnitude of each gas stream flow rate. The flow rate of each gas stream was set manually and controlled by the diaphragm flow



SCHEMATIC FLOW DIAGRAM OF RESEARCH REACTOR

FIGURE 4.1: FEED METERING AND PREPARATION SYSTEM

controllers depicted in Figure 4.2. All of the process lines were stainless steel 316.

The particular constant differential-type flow-controller which was used required that the upstream pressure remain constant. A constant flow of gas is maintained through the external needle valve by maintaining a constant pressure drop across it. The differential applied to the valve is determined by the spring loaded diaphragm in the controller. This diaphragm determines the action of valve plunger to automatically control the flow of gas through the needle valve at the required rate. A feedback line connected from the upstream side of the needle valve to the top of the controller holds the differential pressure across the valve and diaphragm at the same value. Since the differential across the diaphragm is maintained constant by the loading spring, it follows that the differential across the needle valve is constant. This needle valve required sixteen turns from closed to full open.

The mixing of different gases is not generally considered a difficult operation, and a simple mixing venturi was designed and fabricated for blending the three constituents of the feedstream. This is shown in Figure 4.3.

A small portion (approximately 20 cu cm per minute) of the feedstream is continuously vented to the gas chromatograph for analysis. Also another fraction of the feedstream is vented through the back pressure controller. The size of this fraction depends on the required amount of the feedstream being sent to the reactor. The equipment is

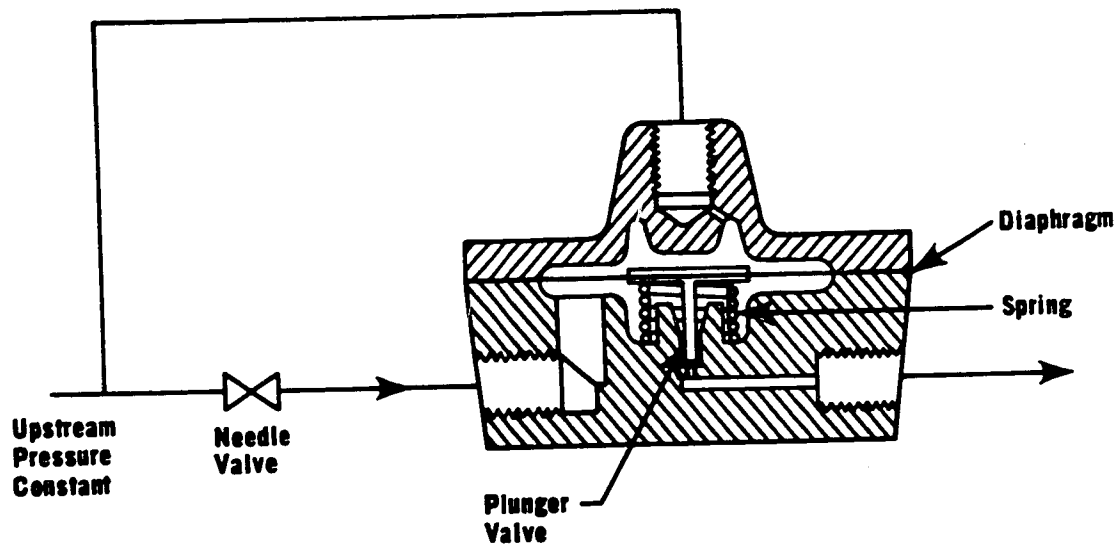


FIGURE 4.2: CONSTANT DIFFERENTIAL TYPE FLOW CONTROLLER

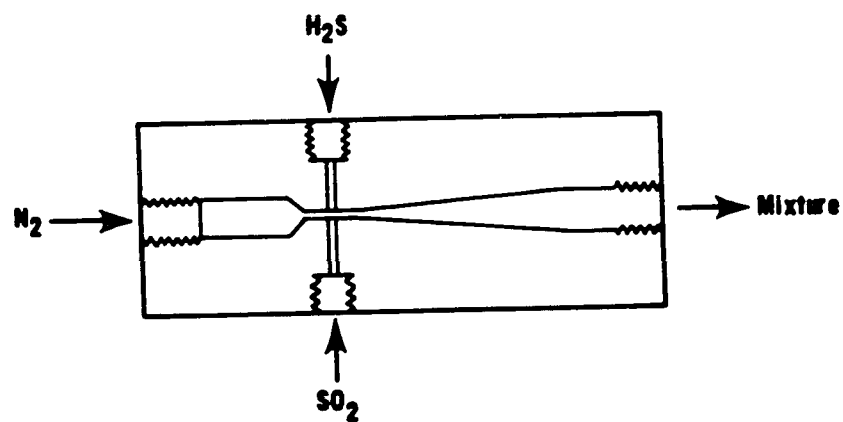


FIGURE 4.3: MIXING VENTURI

operated so that the sum of the two flow rates is held constant over a series of runs in which the flow-rate of the feedstream is varied.

The feedrate was calculated from the measurements of temperature and pressure taken from the thermocouple, absolute pressure transducer and differential pressure cell shown in Figure 4.1. The flow rate was controlled by the Foxboro control valve. A 500 cu cm surge tank was inserted between the control valve and the D/P cell to provide some capacitance in the control loop.

4.2 Feed and Product Analysis

Both the feed and the product streams of the reactor were analysed using a process gas chromatograph. A small fraction of both streams was continuously fed to a stream selector valve located inside the chromatograph's heated compartment. Peripheral valving could be adjusted so that no back pressure change would take place in either stream when the selector valve position was changed. The stream selector valve flow configuration is shown in Figure 4.4. Valve A which may be called the feed sample throttling valve can be adjusted to match the pressure drop which the flowing stream undergoes across the reactor and the sulphur condenser. Hence when the selector valve position is changed, the pressure of the sample in the sample loop remains the same. Valves B and C are set to match the pressure drop between the stream selector valve and the discharge of the sample loop in the sampling valve. This discharge passes through a valve (for sample pressure control) and into the vent manifold. Thus by setting B and C to cause

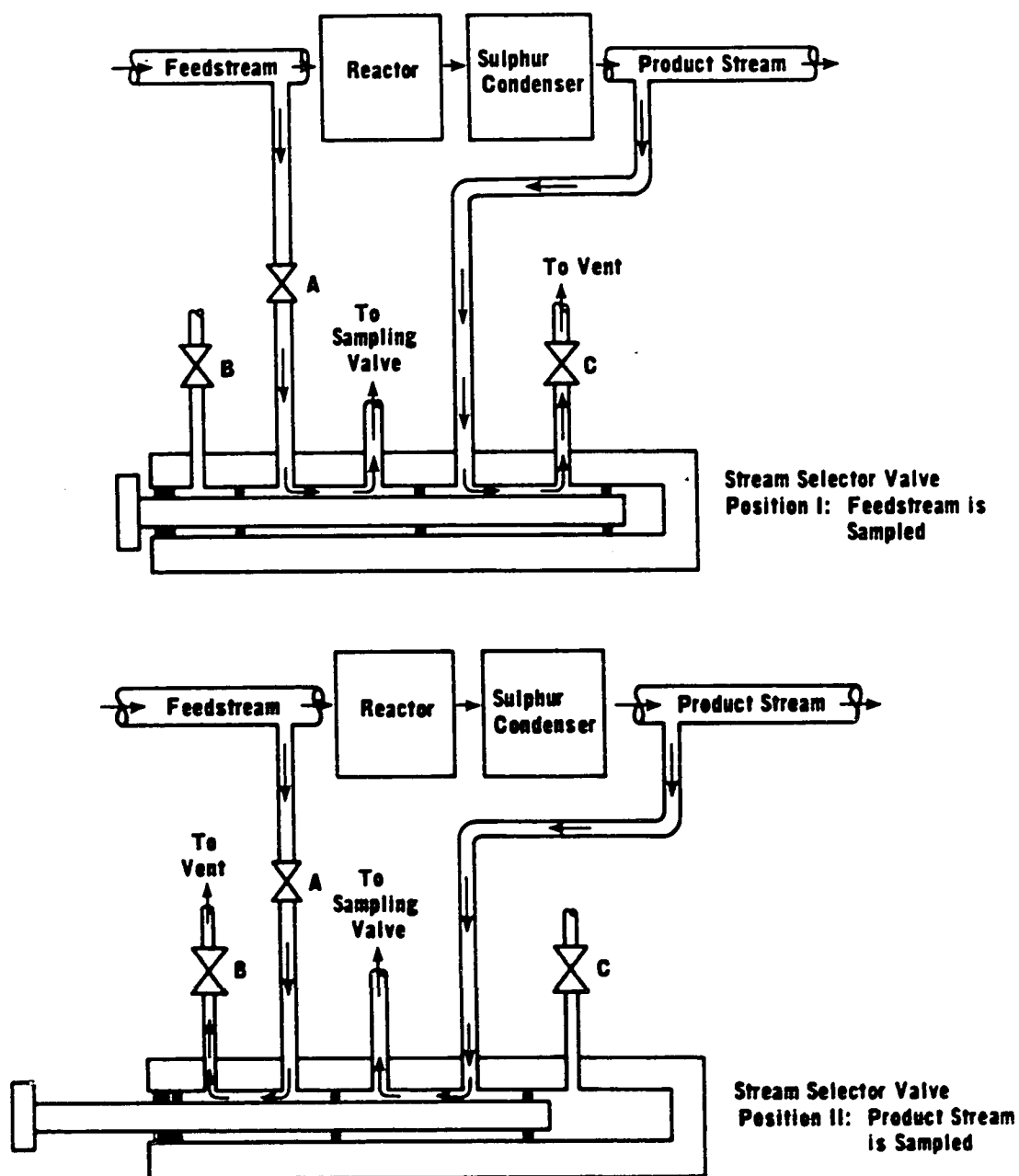


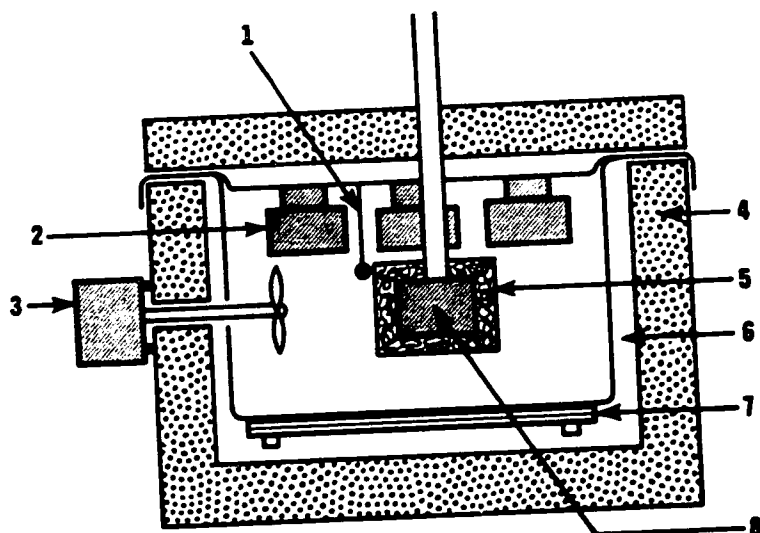
FIGURE 4.4: STREAM SELECTOR VALVE

the appropriate pressure drop, the stream selector valve position can be changed without upsetting steady state flow conditions in either the feedstream or the product stream. The setting of these valves is arrived at experimentally.

An oven, shown in Figure 4.5, was fabricated to house the sampling valve, backflush valve, stream selector valve and thermal conductivity detector of the gas chromatograph. Heated air inside this compartment was circulated by means of a four inch diameter fan and its temperature was controlled by a Honeywell R7161 proportional plus reset temperature controller.

A Beckman model 320 process chromatograph programmer supplied the four-filament thermal conductivity detector with power and controlled the operations of the chromatograph: sampling, backflushing and change of output signal attenuation. The control of these operations is implemented by means of a cam and microswitch system depicted in Figure 4.6. When a micro switch falls into the slot on its cam, its position is changed (open or closed) and its control action is carried out. The output signal of the detector was usually monitored by a Sargent model SR millivolt recorder.

A dual column arrangement was provided whereby the first column could be backflushed while forward flow was maintained in the second column. This arrangement was necessary so that water, a reaction product, could be trapped in the first column and subsequently removed during an analysis cycle. The columns which were used and the operating



LEGEND:

- 1 Thermocouple
- 2 Six Port Valve
- 3 Fan Motor
- 4 Asbestos Insulation
- 5 Fibreglass Insulation
- 6 Dead Air Space
- 7 Strip Heaters
- 8 Thermal conductivity cell

FIGURE 4.5: GAS CHROMATOGRAPH OVEN

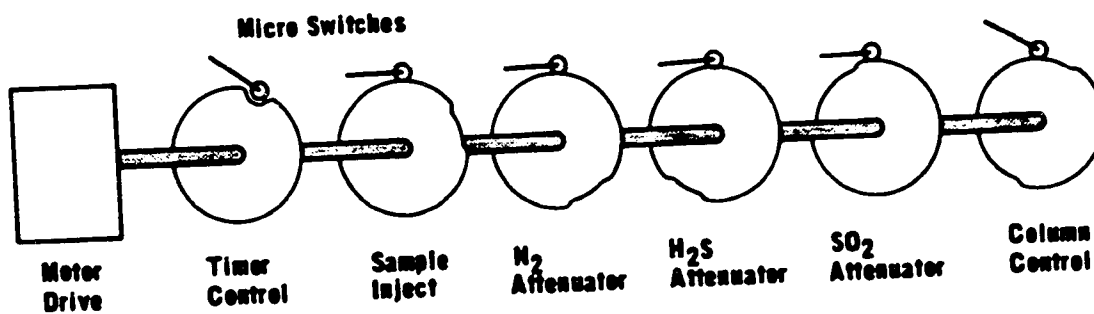


FIGURE 4.6: GAS CHROMATOGRAPH CONTROL CAM SYSTEM

conditions of the chromatograph are given in Figure 4.7, a sample chromatogram. It is notable in this diagram that the areas of the component peaks are obtained by the number of deflections made by the arm of the disk integrator. The repeatability of this device is demonstrated on four nitrogen peaks in a row shown in Figure 4.8. Sample size was held constant and, as indicated, the area remained constant at 99 counts.

A number of ways have been suggested in the literature for analyzing for hydrogen sulfide and sulfur dioxide mixtures using gas chromatography. A complete separation of air, H_2S , SO_2 and A has been reported by Obermiller [81] using Poropak Q in a novel dual column arrangement. A similar separation has been shown [4] to be possible using two columns; one four foot column packed with 15% Ucon on 40/60 mesh Teflon T-6 and the second a composite column of 5 feet of Chromosorb P followed by 7 feet of molecular sieve 13X. Beckman recommends the use of polyethylene glycol 15% by weight on acid washed chromosorb G in a 20 foot column. Silica gel [33] has also been successfully used for the separation of air, CO_2 , COS , H_2S , CS_2 and SO_2 mixtures.

All of the above methods appear satisfactory in the figures depicted in the respective articles. The polyethylene glycol-chromasorb G column combined with a silica gel column used in this work provided chromatograms with much less tailing on the SO_2 peak than the method recommended by Beckmann.

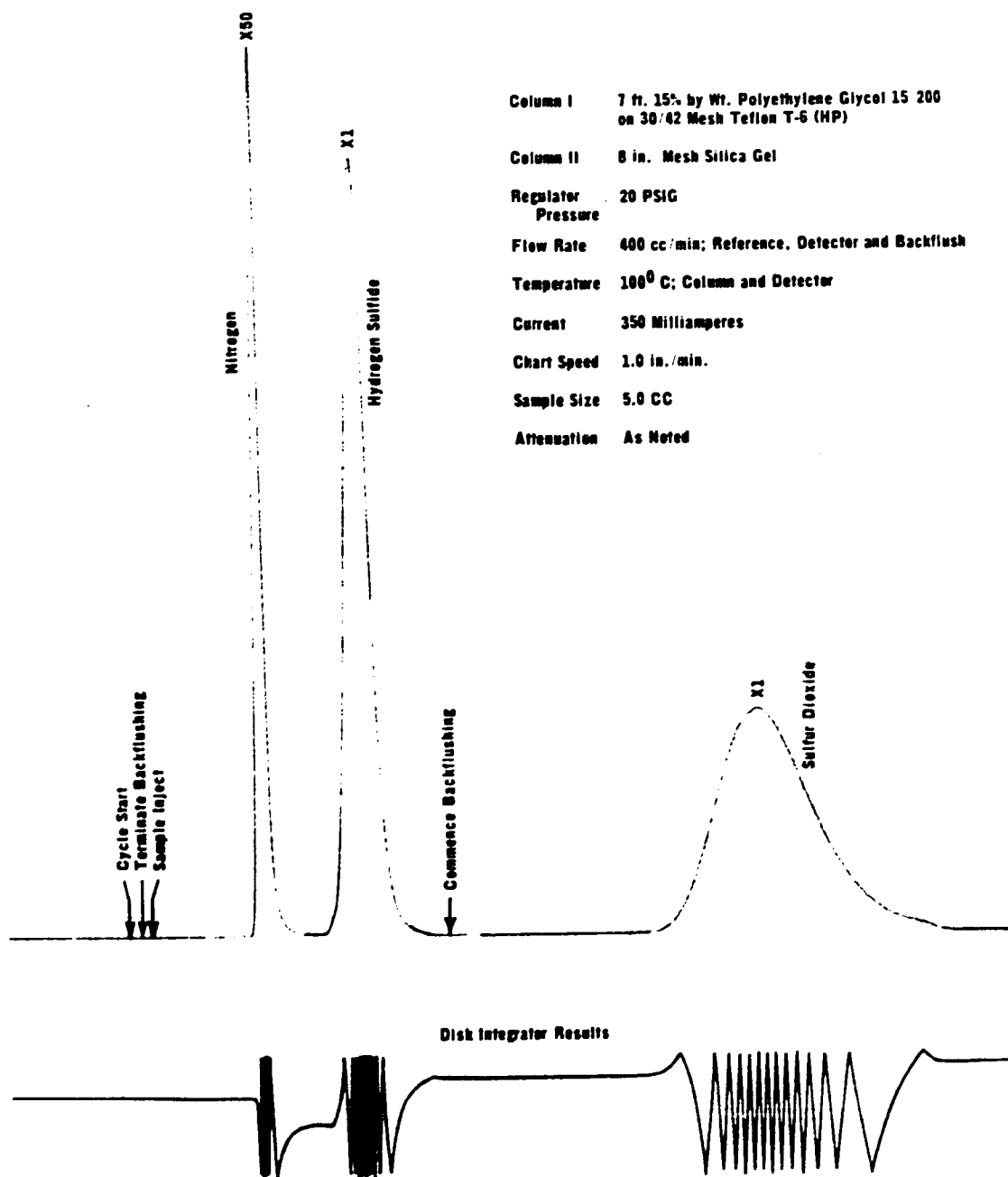


FIGURE 4.7: SAMPLE CHROMATOGRAM

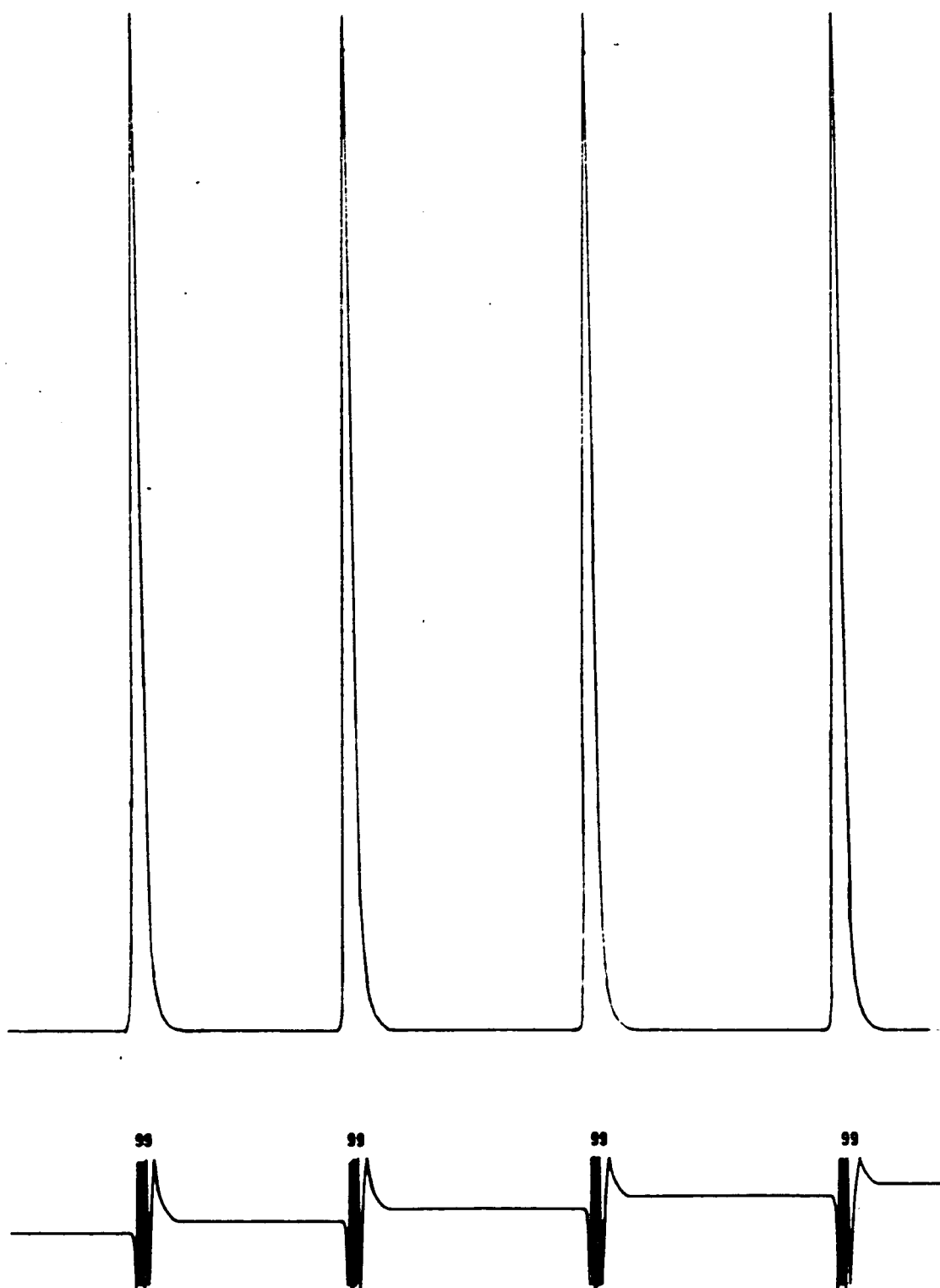


FIGURE 4.8: REPEATABILITY OF CHROMATOGRAM AREA MEASUREMENT

4.3 Fluidized Sand in Air Bath

After passing the air through a Webster Auto Drain air filter to remove water and oil, it was heated in both 6 kilowatt and 3 kilowatt Chromalox immersion heaters. The first heater was equipped with a Chromalox AR-5514 on/off thermostat and the air temperature leaving the second heater was controlled by a Honeywell type R7161 proportional plus reset temperature controller. This preheated air was admitted to the fluidized bath through a porous bronze disk located below the base of the recycle pump.

The fluidized bath, depicted in Figure 4.9, contained the recycle pump, recycle loop, reactor and the temperature and pressure measuring elements necessary for taking data. It was made from 10 inch schedule 40 pipe and flange mounted to the reactor stand. The top section could be raised and lowered using an American Power Pull hand winch. The overall height of the bath was 18 inches and the top section was 15 inches.

As a final heat source, 12 cross section curving strip heaters were bolted longitudinally to the top section of the bath. This 1.5 kilowatt energy source provided even heating around the circumference of the bed and was controlled by a Foxboro 625M temperature controller with proportional, reset and derivative action.

An easily removeable 2 inch thick asbestos sheath enclosed the fluidized bath. Conductive heat losses from the base of the bath were reduced by drilling 1/2 inch diameter holes through the reactor

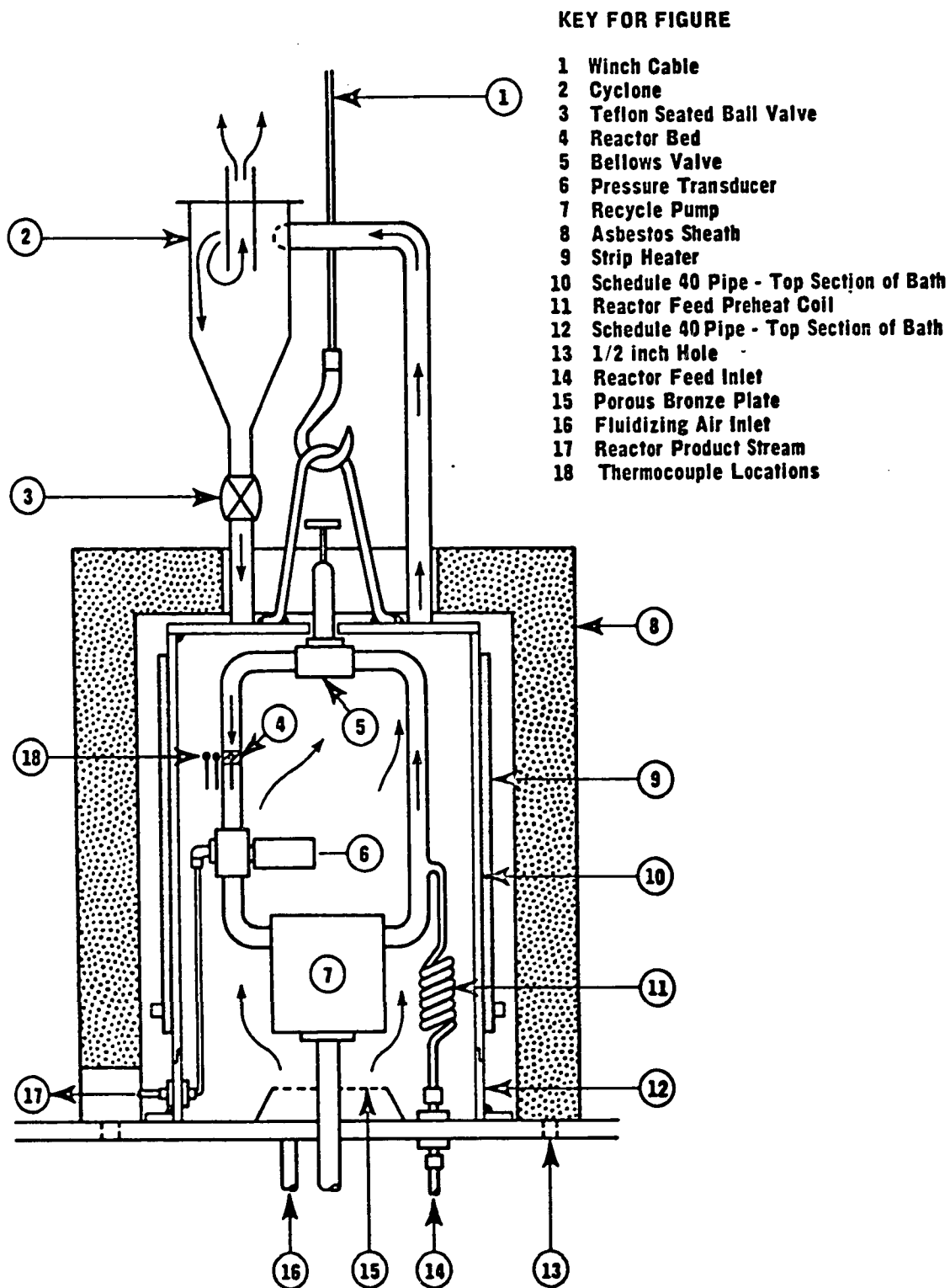


FIGURE 4.9: SCHEMATIC LAYOUT OF FLUIDIZED BATH

stand around the circumference of the fluidized bath.

Air left the fluidized bath through a cyclone which was designed to knock out entrained sand and return it to the bath. Flow was restricted between the bottom of the cyclone and the bath by a 1 inch teflon seated Crane ball valve.

To permit the addition of water vapor to the reactor feedstream, a "T" was installed just after the feed preheat coil as shown in Figure 4.9. Distilled water was supplied at accurately measured and constant rates by a 100 cu cm syringe microfeeder driven by a synchronous motor. This apparatus was fabricated in the department shop and is described elsewhere [51]. The liquid water was passed through an 18 in. long coil which was situated in the fluidized bath and connected to the above-mentioned "T". This coil vaporized the water so that steam was mixed with the reactor feedstream.

4.4 Recycle Loop and Reactor

A colour photograph of the recycle reactor is shown in Figure 4.10 where it is apparent that the recycle loop is 1/2 inch diameter stainless steel 316 tube. All of the Swagelok fittings were lubricated with an antiseizing compound called "Silver Goop" manufactured by the Crawford Fitting Company. This antiseizing compound reduced the "welding action" of fittings while they were exposed to high temperatures for extended periods of time.

At the top of the recycle loop is a bellows valve constructed entirely from stainless steel 316. This Nupro valve was included in the

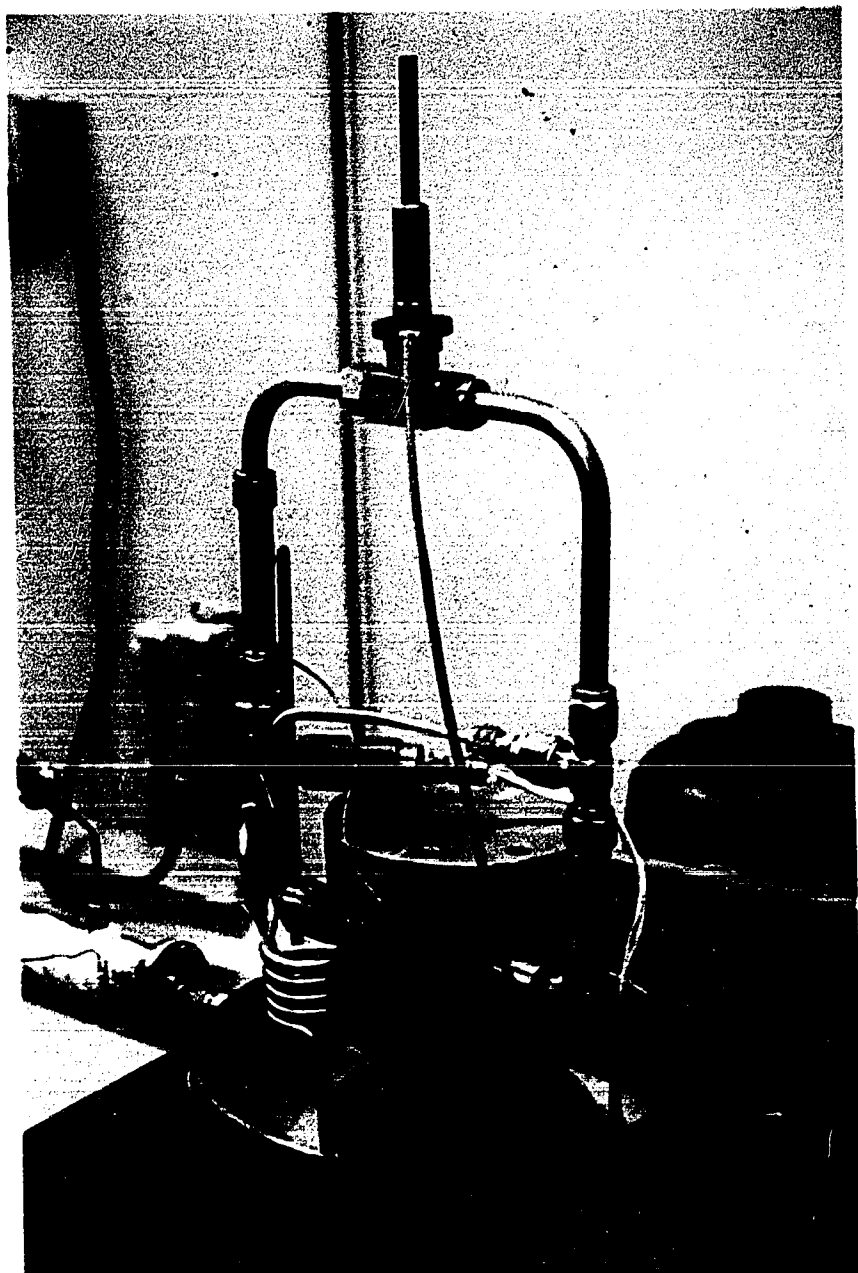


FIGURE 4.10: PHOTOGRAPH OF RECYCLE REACTOR

loop to provide some load for the sliding vane compressor. While obtaining the performance curve for the recycle pump, it was found that considerable "chatter" of the vanes would result with the unloaded pump in the recycle mode.

The reactor assembly, depicted in Figure 4.11, was also fabricated from stainless steel 316. The 4.5 inch long reactor tube was threaded at each end to accommodate Swagelok nuts and ferrules. At the top, the inside diameter was bored so that a 1/2 inch tube could slide into it for two inches. The reactor "basket" slides into this area and is secured in place by the 1/2 inch tubing which is attached to the reactor tube using a Swagelok nut and ferrules.

This basket is easily removeable for changing catalyst. It is 3/4 of an inch long and at the bottom a thermocouple guide has been press-fitted into the walls of the basket. The guide holds the thermocouple in the centre of the catalyst bed and also supports the 200 mesh stainless steel screening.

When a catalyst charge is made, a mixture of 1/16 inch and 1/64 inch diameter stainless steel balls are placed on top of the screen to such a depth that the end of the thermocouple will be in the centre of the catalyst bed. The catalyst is then poured in and then a 3/16 inch layer of these balls is placed above the catalyst bed. The purpose of these balls is to enhance heat transfer from the catalyst bed.

A thick-walled section of stainless steel, located below the reactor tube, was fabricated to secure the pressure transducer and

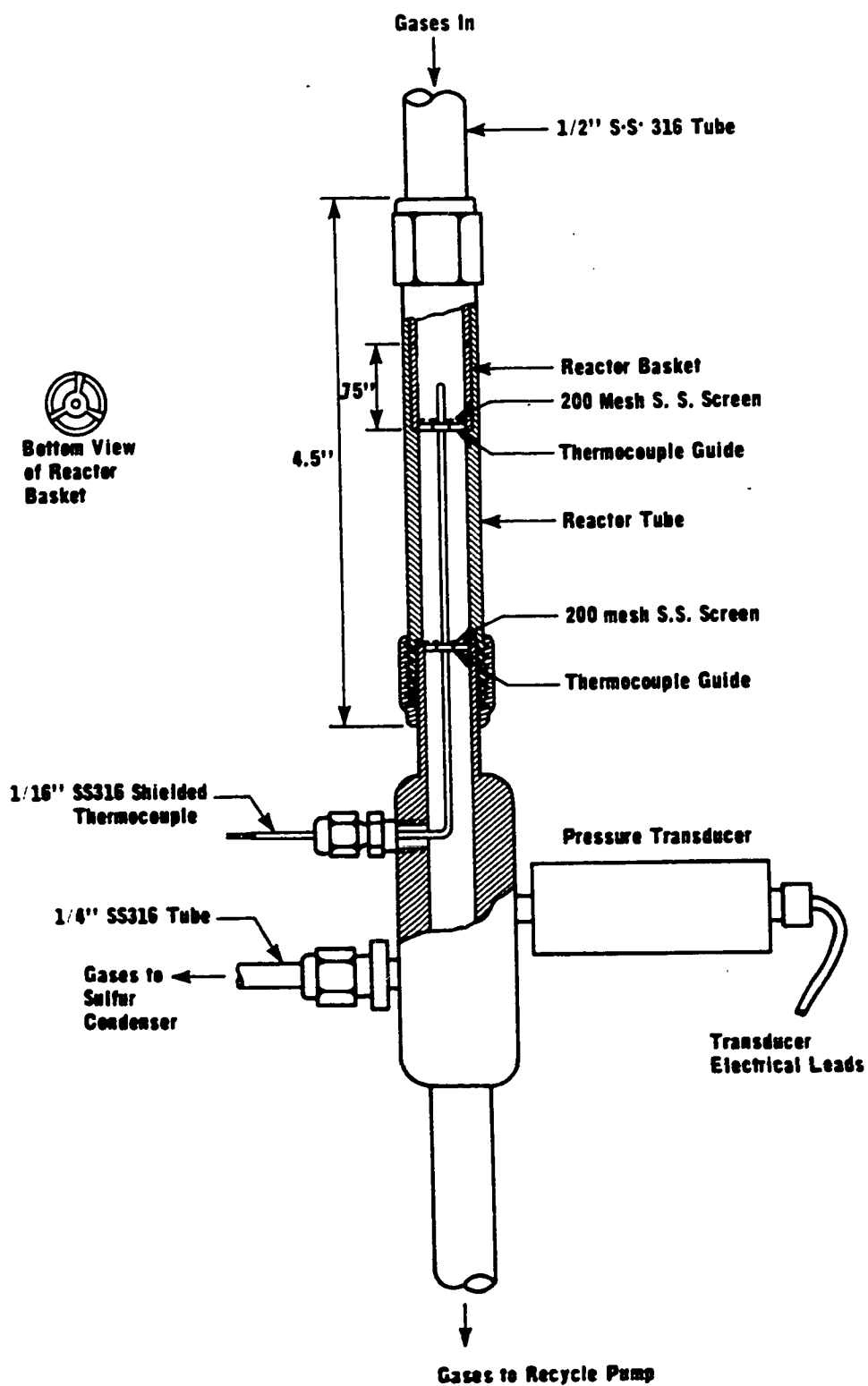


FIGURE 4.11: REACTOR ASSEMBLY

Swagelok fittings to the recycle loop. As indicated in Figure 4.11, the fittings seal the reactor bed thermocouple and the reactor product line. The inside diameter of this unit is the same as that for 1/2 inch tubing, and at the top the outside diameter is the same as well. Hence it could be fitted to the reactor tube using the conventional nut and ferrules. Another thermocouple guide was press fitted into the top of this device and stainless steel screening was secured to this guide. This was done to prevent catalyst pellets from falling into the recycle loop when the catalyst bed was changed. There was a possibility that a pellet could fall through the hole for the thermocouple when a charged reaction tube was removed from the loop.

4.5 Recirculation Pump

A sliding vane compressor was built in the department for use as the recycle pump. Stainless steel 316 and graphite are the only materials of construction exposed to the process stream. Completely oil and grease free, this unit was designed to operate at temperatures as high as 800 degrees Fahrenheit.

The rotor, sliding vanes and shaft are the only moving parts in the pump body. Centrifugal force holds the vanes tightly against the housing for a uniform efficient seal as shown in Figure 4.12. The direction of rotation of the rotor is indicated by the curved arrow drawn in the pump cavity.

When the compressor is operating, gas is drawn in through the suction port and passes through the suction channel. This channel

was milled into the end plate and tapers from a depth of 0.000 inches at the shallow end to 0.375 inches at the deep end. The straight line drawn across the suction channel marks the end of the taper at a depth of 0.375 inches. The discharge channel was milled uniformly also to a depth of 0.375 inches into the 0.500 inch thick end plate.

As depicted in Figure 4.12, sliding vanes A and B are drawing gas in through the suction channel. Vane C has just terminated drawing gas into the pump cavity (14) and the leading edge of vane B will start to compress this gas as it approaches the discharge channel. The leading edge of vane C is forcing gas out of the discharge port while vane D is providing a seal to prevent gas leakage from the discharge side through to the suction side of the compressor.

When assembled, the clearance between the rotor and the end plates is 0.005 inches. The rotor was tightly secured to the drive shaft by two set screws and a key inserted into keyways on the rotor and shaft. By using the two ball bearings below the water cooled seal (Figure 4.13) as thrust bearings, the vertical position of the shaft was held steady.

Although not apparent in Figure 4.13, the compressor body is mounted on the reactor stand in the centre of the fluidized bath near the bottom. Preheated air is admitted to the bath from below the reactor stand and up through the sintered bronze ring located below the pump body. This arrangement was chosen in order that the recycle pump be close to the main heat source of the bath. It is

KEY FOR FIGURE

- 1 End Plate
- 2 Pump Discharge Channel
- 3 Graphite Bearing Housing
- 4 Bolt Hole
- 5 Pump Section Channel (deep end)
- 6 Pump Section
- 7 Pump Section Port
- 8 Rotor
- 9 Vane Slot
- 10 Drive Shaft
- 11 Pump Discharge
- 12 Sliding Vane (A)
- 13 Pump Body
- 14 Pump Cavity

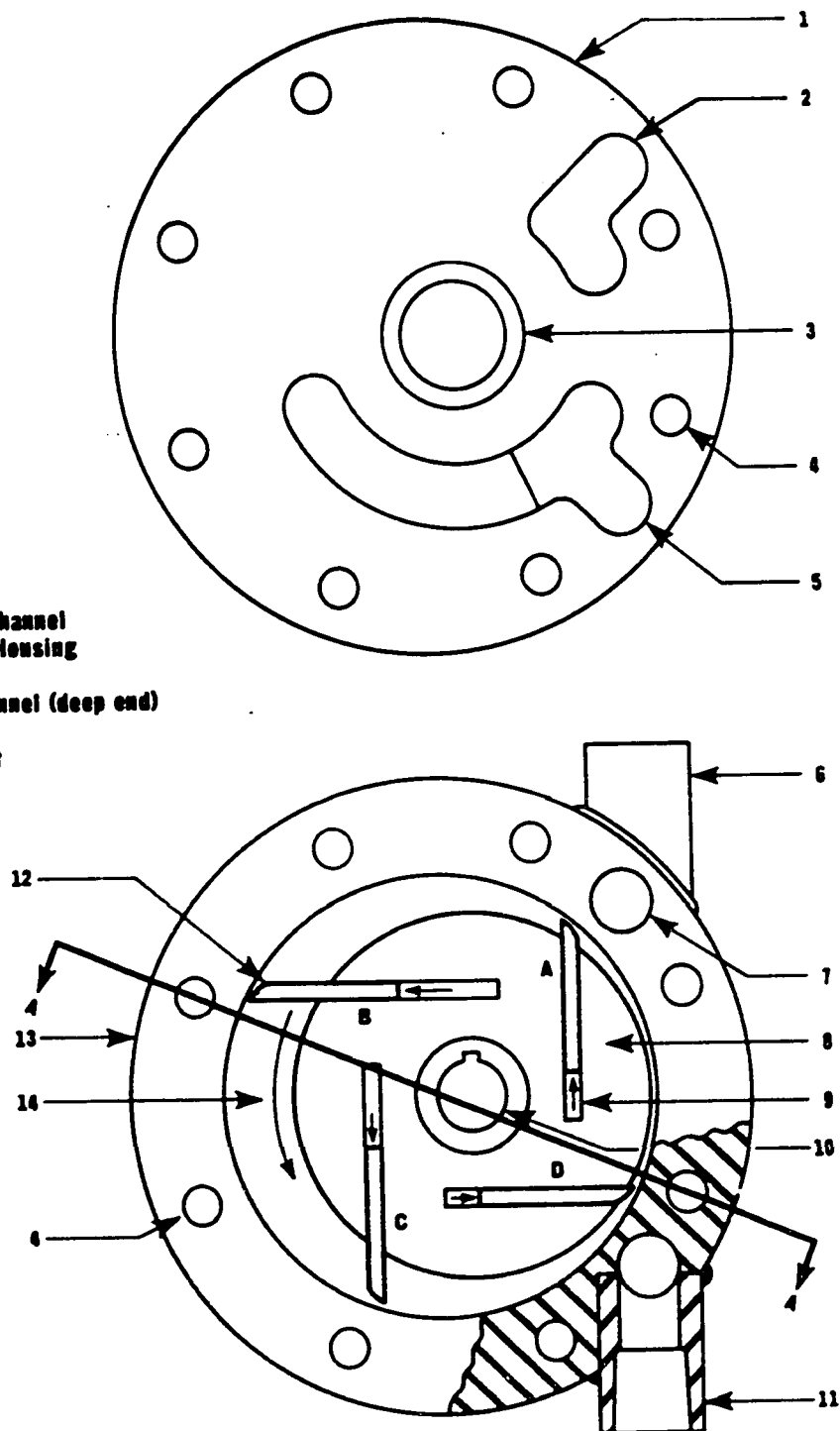


FIGURE 4.12: RECYCLE PUMP BODY AND END PLATE

KEY FOR FIGURE

- 1 Allen Nut
- 2 Graphite Bearing
- 3 Pump Rotor
- 4 Pump End Plate
- 5 Pump Body
- 6 Aluminium Wedge Ring
- 7 Shaft Housing
- 8 Pump Shaft
- 9 Porous Bronze Plate
- 10 Preheated Air Inlet
- 11 Reactor Stand
- 12 Asbestos Gasket
- 13 Water Cooled Shaft Seal
- 14 Bearing Housing
- 15 Thrust Bearing
- 16 V-Belt Pulley
- 17 Thrust Ring
- 18 Tie Bar
- 19 Sleeve Ring
- 20 Vane Slot

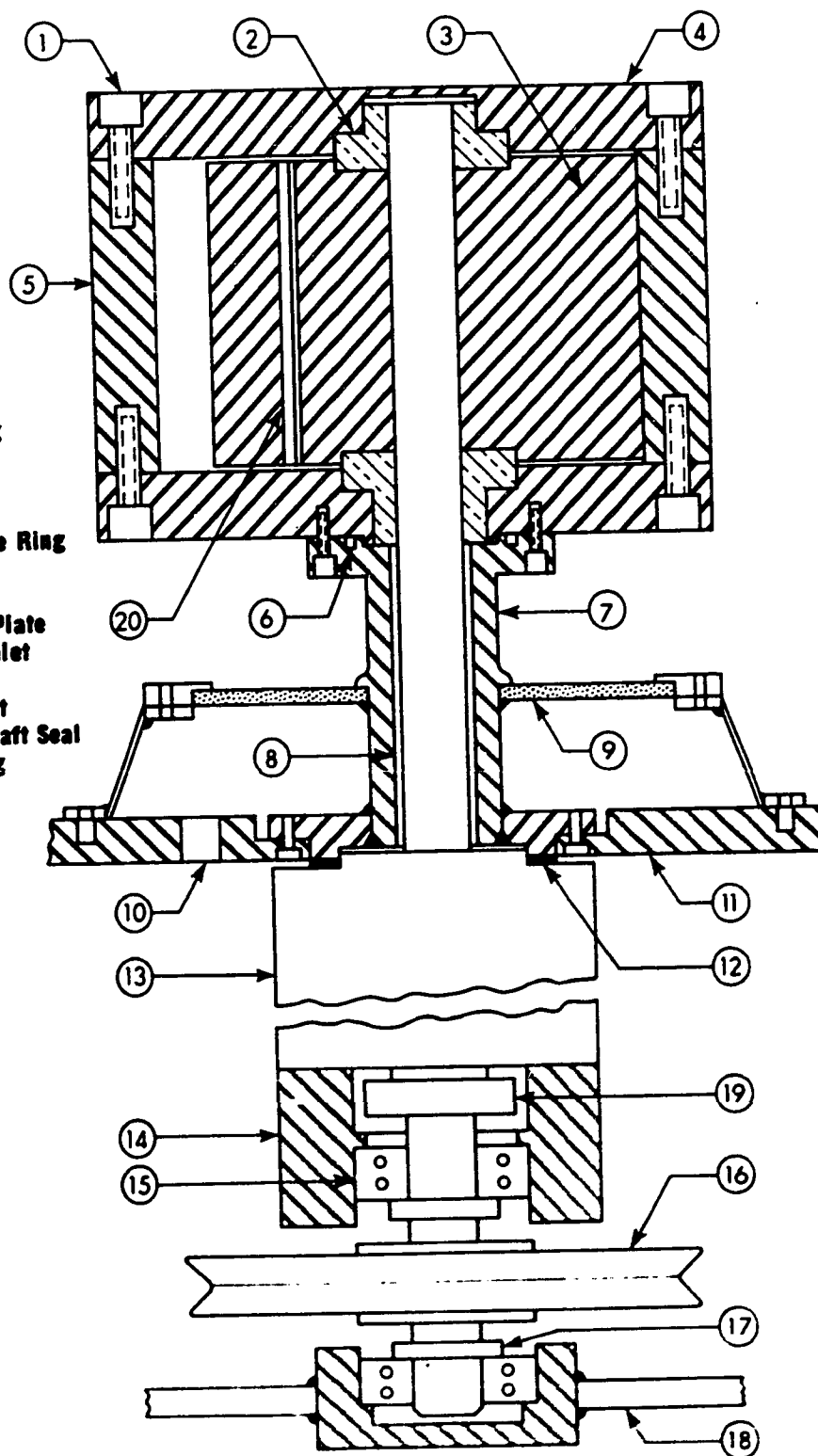


FIGURE 4.13: SECTION A-A OF PUMP ASSEMBLY

important that sulfur not condense in the compressor while operating, otherwise considerable damage would result to the vanes and pump body surfaces.

This design eliminated the leakage problem. The pump body and end plates were ground to an optically smooth condition at the contact faces and eight uniformly tightened allen nuts provided sufficient interfacial pressure to form a good seal. Possible leaks between the shaft housing and the bottom end plate of the pump were prevented by using an aluminium wedge gasket. Since aluminium has a higher thermal coefficient of cubical expansion than stainless steel, the seal became tighter as the pump assembly was heated up. A John Crane type 8B1 water-cooled mechanical seal averted gas leakage around the drive shaft. An asbestos gasket was used to avoid leakage between the base of the shaft housing and the Crane seal.

The Crane seal, shown in Figure 4.14, performed very well throughout the program. Cooling water was filtered by a Nupro 4FR inline filter, and temperature and pressure indicators were installed on the drain line. Water flow rate was set manually by adjusting valves before and after the mechanical seal. The exit water flow rate was maintained at roughly 70 degrees Fahrenheit and the water pressure held to a level slightly below the reactor pressure. A Honeywell pressuretrol type L404B adjustable pressure switch was added to the cooling water inlet line to cut power from the pump motor if the filter plugged or the water stopped flowing to the seal. The configu-

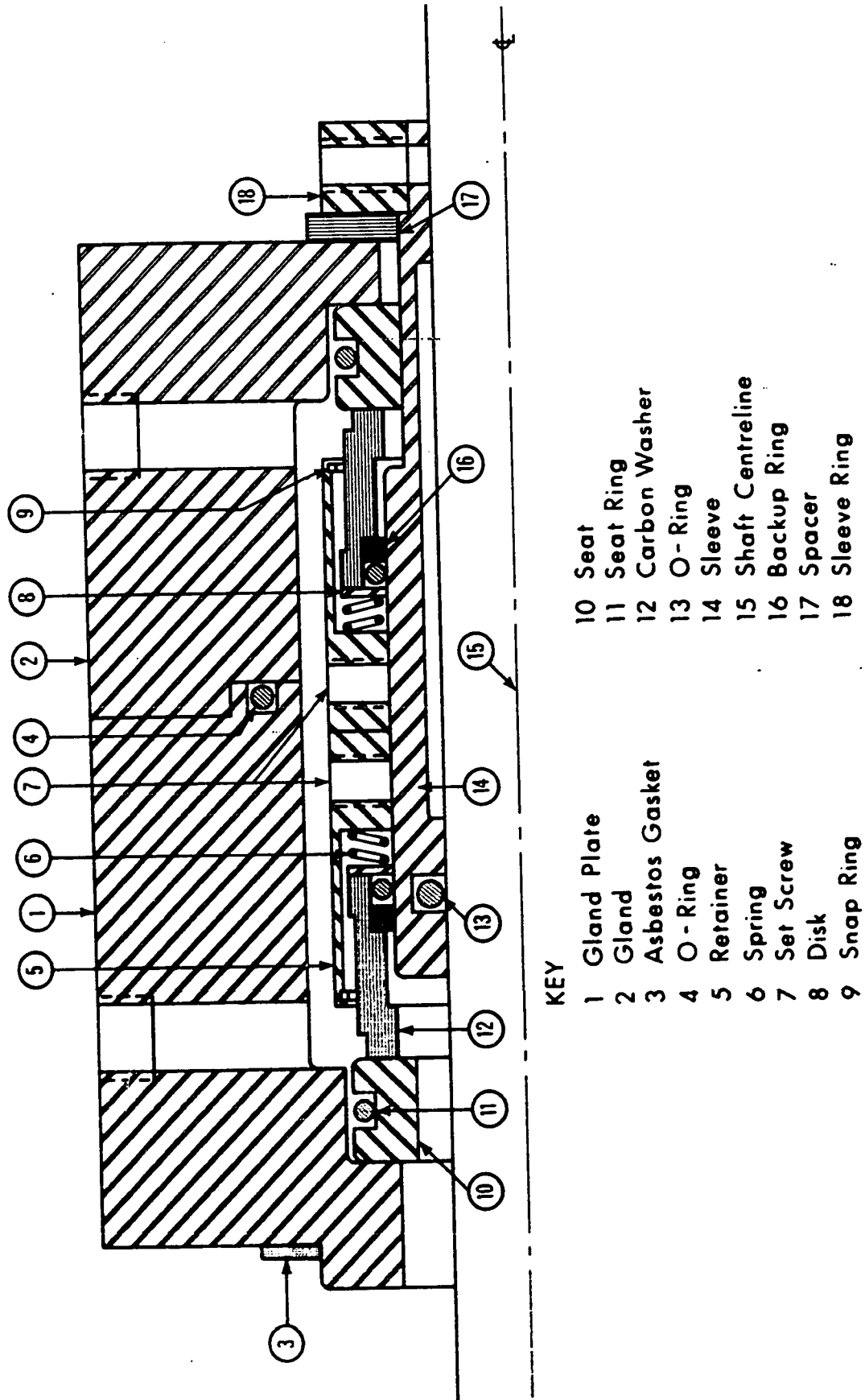


FIGURE 4.14: WATER COOLED SHAFT SEAL

ration of these protective devices is shown in Figure 4.15.

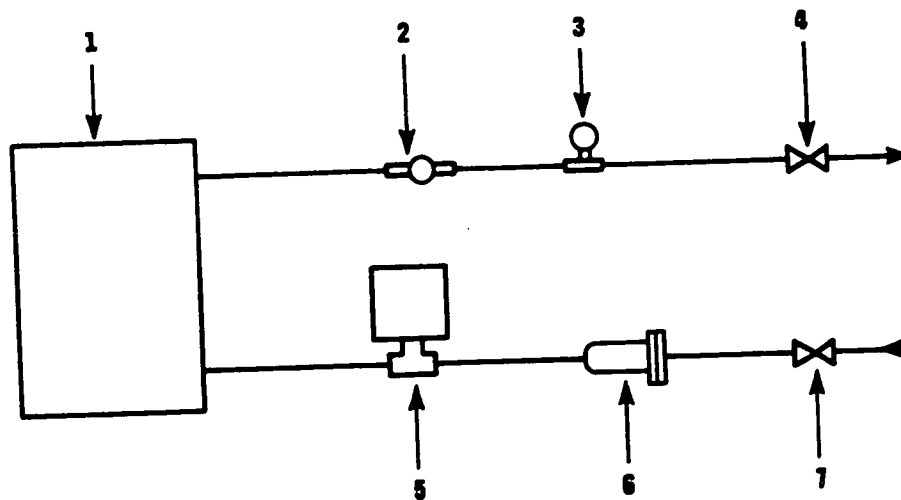
A one horsepower variable speed motor (Reliance type DM) was used to drive the pump. Power was transmitted between the motor and the pump by means of a V-belt. Circuit breakers were located in the motor starting switch and in the variable speed drive unit to prevent damage which could be caused by electrically overloading the system.

Performance curves were obtained for the recycle pump both in the recycle mode and with the discharge vented to the atmosphere. A dry test meter, manometer, stopwatch and thermometer provided the necessary data to determine flow rate corrected to standard cubic feet per minute. The performance data is tabulated in Table 4.1 and the curves are depicted in Figure 4.16. The pressure on the pump discharge was not varied since it was felt that the reactor recycle loop including the catalyst bed would offer less resistance to flow than the dry test meter which was used in this test.

4.6 Sulfur and Water Condensers

The product stream from the reactor passes through the stainless steel 316 sulfur condenser shown in Figure 4.17. This device was wound with nichrome wire which provided the heat source to maintain the condenser temperature above the dew point of water and below that of sulfur. To prevent carryover of sulfur into the gas chromatograph or into the vent line, twenty stainless steel baffles were added to the condenser as indicated.

Since stainless steel tends to lose the alloy properties which



- KEY:**
- 1 Crane Seal
 - 2 Dial Thermometer
 - 3 Pressure Gauge
 - 4 Outlet Valve
 - 5 Pressure Switch
 - 6 Nupro Filter
 - 7 Cooling Water Inlet Valve

FIGURE 4.15: PERIPHERAL ACCESSORIES FOR CRANE SEAL

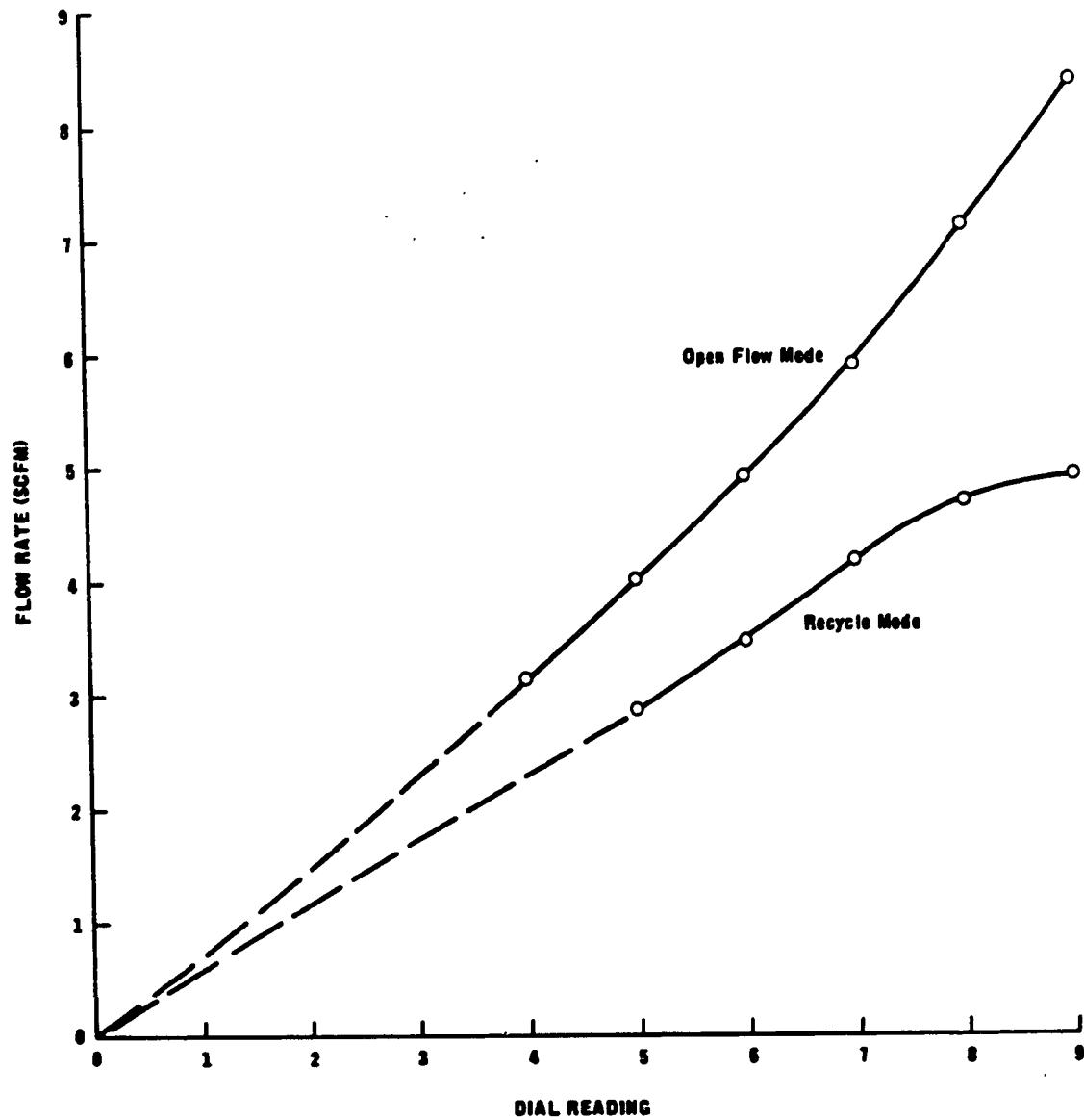


FIGURE 4.16: PERFORMANCE CURVES FOR RECIRCULATION PUMP

Table 4.1
Performance Data for Recycle Pump

<u>Dial Reading</u>	<u>Open Flow Mode</u>			<u>Recycle Flow Mode</u>		
	<u>Time</u>	<u>Head</u>	<u>Flow Rate</u>	<u>Time</u>	<u>Head</u>	<u>Flow Rate</u>
4.0	1.167	0.8	3.14			
5.0	0.919	1.2	4.02	1.292	1.8	2.88
6.0	0.750	1.7	4.95	1.073	2.0	3.48
7.0	0.632	2.3	5.92	0.894	2.4	4.20
8.0	0.533	3.5	7.15	0.800	3.1	4.73
9.0	0.463	5.4	8.43	0.770	3.7	4.96

Atmospheric Pressure 706.2 millimeters of mercury

Atmospheric Temperature 72.0 degrees Fahrenheit

Time - number of minutes elapsed for the flow of four cubic feet of air through the dry test meter.

Head - static pressure in centimeters of mercury at the entrance of the dry test meter.

Flow Rate - standard cubic feet per minute.

prevent corrosion where it has been welded, the baffle plates were not welded to the central spacer bar, but secured as shown in Figure 4.17. Similarly, the flange plates at the ends of the condenser were welded from the outside. This precaution was taken with all of the fabricated pieces of the equipment.

It has been pointed out [13] that H_2S and SO_2 react together in the presence of liquid water, and thus it was necessary to maintain the sulfur condenser above the water dew-point. To avoid sulfur plugging problems in the condenser vent line which would result from this reaction, a glass water condenser was included as depicted in Figure 4.17. Here, the water reaction product was condensed on glass wool prior to venting the product stream.

4.7 Process Measurements

All temperatures were measured by stainless steel shielded iron constantan thermocouples. The seven thermocouples which were monitored were situated in the following areas; catalyst bed, reactor wall, fluidized bath, two in the sulfur condenser, gas chromatograph and the reactor feed line. Figures 4.1, 4.8 and 4.10 clearly indicate their location.

The millivolt signal from the thermocouples was adjusted by an Acromag model 323 electronic $0^\circ C$ reference and then measured by a Honeywell 24 point Electronik 16 millivolt recorder. The recorder was equipped with an integral solid state calibrator, chart span selector (5 millivolts to 5000 millivolt span) and a millivolt suppression unit

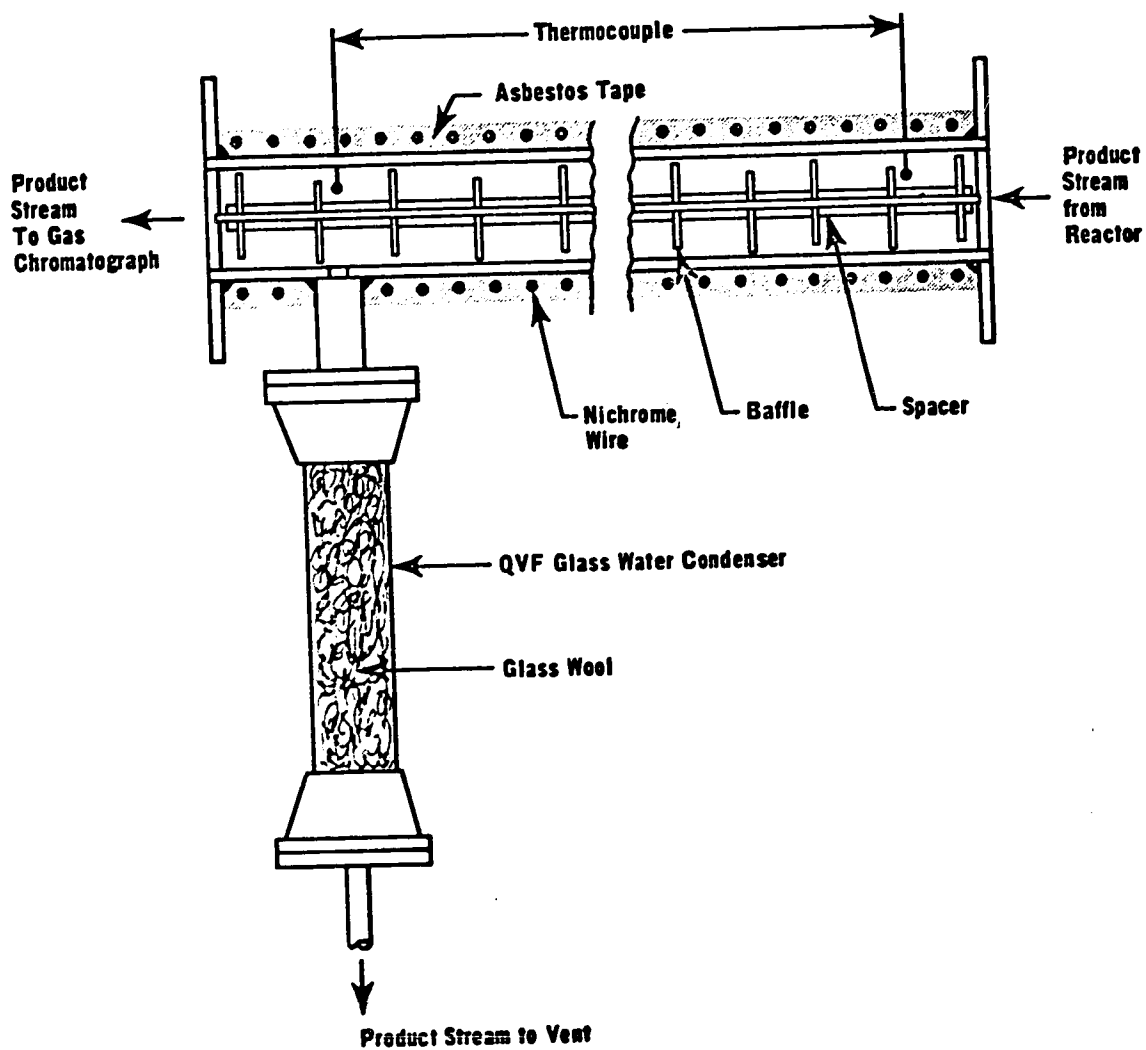


FIGURE 4.17: SULFUR AND WATER CONDENSER

with a range of 0 to 10,000 millivolts.

The accuracy of the recorder, which was usually run with a 5 millivolt span, was regularly checked with the integral calibrator and a Leeds and Northrup model 8686 millivolt potentiometer. The integral calibrator proved to be a very reliable facility. Also the electronic zero reference unit was occasionally checked against an ice bath and it proved to be very accurate needing no adjustment throughout the investigation.

A Foxboro 6430 HF electronic consotrol three-pen recorder monitored the 10 to 50 milliamper signals sent to it by the two absolute pressure transducers and differential pressure cell in the system. A Foxboro 610 AR power supply was necessary for both the feed pressure transducer and the d/p cell. The reactor pressure transducer was powered by a Kepco KG-25-0.2 power supply unit and interfaced to the recorder through a Foxboro 693 AR EMF to current converter.

The calibration of each of the absolute pressure transducers was checked at least weekly with the same procedure used for calibrating them. Frequently, slight adjustments had to be made to these devices to maintain the calibration, however, the chart reading error was never more than one percent.

The differential pressure cell was checked at the same time as the pressure transducers but not as frequently since it was fairly repeatable and rarely gave an error more than 0.5 percent of full scale. Again the normal calibration procedure was used for this verification.

4.8 Operation of Equipment and Experimental Procedures

4.8.1 Catalyst Treatment

Porocel is a commercially-used catalyst and was selected for this study. Since it was a commercial catalyst which had been activated by the manufacturer, the pretreatment only included steps to ensure constant catalyst activity in the day-to-day operation of the equipment.

After loading a fresh batch of catalyst, the reactor temperature was raised to 500°F and held there for 24 hours. A slow stream of dry nitrogen was passed through the catalyst bed during this period. This was done to remove combined water. The catalyst surface was then exposed to H_2S by adding H_2S to the nitrogen feed-stream to give an approximate molar composition of 95% N_2 and 5% H_2S . The H_2S reaction with the catalyst surface was manifested by a sharp rise in the catalyst bed temperature when it was added to the nitrogen. The completion of this interaction was marked by the existence of small and repeatable changes in the bed temperature when the H_2S was turned off and on. The exposure generally lasted for six hours.

SO_2 was then added to the slow N_2/H_2S stream going to the reactor and the Claus reaction was allowed to proceed for at least two hours before kinetic measurements were made. The catalytic activity was always highest with fresh catalyst and generally became stable after this two hour period.

4.8.2 Fluidized Bath Startup

The fluidizing air and cooling water to the recycle pump seal were always turned on before any heater to the fluidized bed was started. The gate valve which controlled the air flow rate was adjusted to give 8.0 psig on the line pressure gauge between the valve and the bath. This corresponded to about 50 scfm of air which adequately fluidized the sand bed. The water flow rate was adjusted so that the pressure switch on the pump's power supply was activated and no less than 1 gpm of water flowed. The pressure switch setting was maintained at approximately 1 psi below the operating pressure of the reactor. This practice was followed to prevent water leakage into the reactor in the event of a seal failure. The two air preheaters and the fluidized bath heater were then turned on at the appropriate settings.

Usually, the reactor would reach the desired operating temperature within 2-1/2 hours. The first air heater was always turned to a setting of 550°F but, since it was capacity limited and could not heat the air to this temperature, it was always on. The second heater's controller was generally set at 150°F above the desired operating temperature since there was a considerable heat loss around the base of the fluidized bed. This controller had proportional plus reset modes of temperature control. The fluidized bath temperature controller was usually set very close to the desired reaction temperature.

4.8.3 Execution of Kinetic Measurements

The sulfur condenser was turned on at least twenty minutes

before any kinetic run was made. The nichrome wire windings on this unit received energy from a rheostat which was manually set to maintain the temperature in the condenser above 100°C.

While the condenser warmed up, the flow rates of N_2 , H_2S and SO_2 were adjusted to provide what would be required for the maximum feed rate to the reactor and the desired feed composition as analysed by the gas chromatograph. While adjustments to the flow rates were being made, the gas was bled to vent through the feed-line back-pressure controller and no feed gas was permitted to reach the reactor. The feed back-pressure controller was set to give the desired feed pressure which was maintained constant throughout a set of runs with constant feed composition.

The recycle pump was started after the desired feed composition was attained and flow at the specified rate was started to the reactor. Fine adjustments to the fluidized bath temperature were then made and steady state temperatures were usually achieved within five minutes.

The desired reaction pressure was obtained and controlled by manually adjusting the product stream back-pressure controller and the GC product vent valve. These settings were very easy to make once experience had been obtained running the equipment.

For most runs, two product and at least one feed chromatograms were taken. The former were to verify the existence of steady-state reaction conditions and the latter to ensure that constant feed

composition was being maintained.

The measurements which were recorded for a steady-state run included the following: catalyst bed, reactor wall, and fluidized bath thermocouple readings, feed and reactor absolute pressure transducer readings, feed D/P cell reading and chromatogram component areas as measured by the disk integrator.

The sulfur condenser removed sulfur vapor from the product stream, but the sulfur merely accumulated at the bottom of this device. Periodically the sulfur had to be removed by disconnecting the water condenser, passing a slow nitrogen stream through the reactor and subsequently the condenser, and heating the condenser above the boiling point of sulfur. The sulfur vapor was discharged into the room air until the condenser was reasonably clean.

4.8.4 Termination of Kinetic Measurements

At the end of a series of runs, the fluidized bath was usually left hot and the H_2S and SO_2 gas streams were turned off. Nitrogen was purged through the entire system for at least fifteen minutes to avoid unnecessarily excessive time of contact between H_2S and SO_2 in the feed system, reactor and analytical equipment. This practice was followed to prevent the reaction of H_2S and SO_2 in the presence of water which could get into the equipment by diffusing back from the water condenser and being further propagated as a reaction product.

4.8.5 Periodic Equipment, Maintenance, and Accuracy Tests

As previously indicated in Section 4.7, the D/P cell and abso-

lute pressure transducers were checked against the calibration data at regular intervals using normal calibration procedures. The carrier gas flow-rates and filament current of the gas chromatograph were checked and adjusted to calibration settings every day that kinetic measurements were being made. Also, the calibration of the gas chromatograph was checked by making up an N_2 , H_2S and SO_2 mixture of known composition and running its chromatogram at least once a week during the more active periods of the research program.

The equipment did not require much in terms of preventative maintenance. The six-port diaphragm valves of the process GC were opened and inspected for wear and dirt, however, they were always clean and never leaked. The 1/2 litre of dessicant in the stream driers was changed every month to be certain that moisture did not enter the system.

4.8.6 Catalyst Activity Test

To determine if the catalyst activity was remaining constant throughout the course of a series of runs and between different catalyst batches, one feed composition and temperature were repeatedly analysed and compared on a space time conversion plot. The results of the activity tests are discussed in Chapter VI.

4.9 Materials

The Matheson Company [75] specified the following minimum purity limits on the gases supplied:

N ₂	99.996%	(prepurified grade)
SO ₂	99.98%	(anhydrous grade)
H ₂ S	99.5%	(C.P. grade)

Samples of the gases from their cylinders were analysed using a gas chromatograph and nitrogen impurity was present in the SO₂. The concentration of N₂ in the SO₂ was found to be 0.3%. Using a mass spectrometer, trace quantities of COS, CO₂, and CS₂ were found in the H₂S but were not measured quantitatively. These compounds were not detected using the gas chromatograph.

The catalyst used in this investigation was donated by Minerals and Chemicals Philipp Corporation of Menlo Park, New Jersey. The properties of the catalyst were given on a data sheet supplied by the company.

Porocel Sulfur Recovery Catalyst

Volatile material		6%
Chemical composition	Al ₂ O ₃	89.0%
(Volatile free basis)	Fe ₂ O ₃	5.0%
	TiO ₂	2.8%
	SiO ₂	2.6%
	Insoluble	0.6%
Surface area	215 m ² /gm	

CHAPTER V

REDUCTION OF DATA

5.1 Introduction

All of the process measurements which were read from laboratory recording devices were punched on computer cards and read into the nonprocess data processing program (NPRDP). A Fortran listing of NPRDP is shown in Appendix C and the input data and resulting output for each experiment follows the listing. A sample calculation and error analysis are also provided.

NPRDP was set up to calculate and print out the material balance across the reactor, the reaction temperature, and the reaction pressure. From the material balance calculations, the following information also was printed out: feed and product $\text{H}_2\text{S}/\text{SO}_2$ molar ratios, percent conversion of H_2S and SO_2 , reaction rate of H_2S and SO_2 , and the weight of the catalyst divided by the molar feed rate of H_2S .

5.2 Ideal Gas Law Assumption

The ideal gas law is inherent in the calculation procedure and the validity of its use will now be considered. After Gibbs developed the concept of chemical potential, Lewis [71] proposed a new variable called fugacity, f , which was related to chemical potential, μ , in the following way,

$$\mu = RT \ln f + \theta, \quad (5.1)$$

where θ is a function of temperature only and μ is based on one mole of material. Using the first and second laws of thermodynamics [99], the following relationship can be developed from Equation (5.1),

$$\frac{d(\ln f)}{dP} = \frac{v}{(R)(T)} \quad (5.2)$$

When the pressure to which Equation (5.2) is applied approaches zero, the behaviour of all substances approaches that of an ideal gas. Hence at very low pressures

$$d(\ln f) = d(\ln P) \quad (5.3)$$

If upon integration the constant of integration is chosen as zero, the fugacity is equal to the pressure, or

$$f^* = p^* \quad (5.4)$$

where the superscript symbolizes a pressure approaching zero where the fugacity is equal to the pressure.

One method of determining pure component fugacities employs the principle of corresponding states and uses generalized charts to arrive at the value of the fugacity coefficient, ϕ'

$$\phi' = \frac{f}{p} \quad . \quad (5.5)$$

This approach was used for determining ϕ' for the components of interest at the operating conditions of the experiments.

The critical constants and the reduced temperature and pressure for each component are given in Table 5.1 based upon data taken from The Matheson Gas Data Book [75]. In Table 5.2, the fugacity coefficients [103] are given for conditions in the recycle reactor as well as those which existed for calibration of the gas chromatograph and analysis of feed and product streams. It is apparent that at the conditions in the reactor (roughly 533°K and 1 atmosphere) the fugacity coefficients for all of the species would be very close to 1.000. Unfortunately, ϕ' data were only available down to reduced pressure of 0.10 however, the trend in the data indicates that the ideal gas law is applicable under these conditions. The same holds true for conditions of room temperature and pressure except possibly for SO₂. Haywood [45] indicates that SO₂ may be considered to be a perfect gas at normal atmospheric conditions.

The values which were used for the molecular volumes [75] of these compounds are given in Table 5.3.

Throughout this work, including calibration of the gas chromatograph, the equation of state for an ideal gas was employed,

$$Pv = RT \quad . \quad (5.6)$$

Table 5.1
Critical Constants and Reduced Properties
of N₂, H₂S, SO₂ and H₂O

Compound	Critical Constants			Reduced Pressure (1 atm.)	Reduced Temperature	
	T _c , °K	P _c , atm	Z _c		(533°K)	(293°K)
N ₂	126.0	33.5	0.291	0.0299	4.24	2.32
H ₂ S	373.6	88.9	0.284	0.0112	1.43	0.784
SO ₂	430.7	77.8	0.269	0.0129	1.24	0.680
H ₂ O	647.4	218.3	0.230	0.0046	0.825	--

Table 5.2
Fugacity Coefficients at 533°K and
293°K and One Atmosphere

Reduced Pressure	φ' at 533°K and 1 atm.				φ' at 293°K and 1 atm.		
	N ₂	H ₂ S	SO ₂	H ₂ O	N ₂	H ₂ S	SO ₂
0.4	1.000	0.967	0.939	0.363	0.993	0.551	0.168
0.3	1.000	0.977	0.958	0.482	0.995	0.730	0.220
0.2	1.000	0.986	0.974	0.719	0.997	0.900	0.325
0.1	1.000	0.995	0.991	0.906	0.999	0.966	0.640

Table 5.3
Molecular Volumes

Compound	Molecular Volume (liter)
N_2	22.40360
H_2S	22.14424
SO_2	21.88930

The number of moles of a component has been calculated by

$$n_i = \frac{V_{is}}{v_i}, \quad (5.7)$$

and the volume at measured temperature and pressure was converted to standard conditions using

$$\frac{P_1 V_{i1}}{T_1} = \frac{P_s V_{is}}{T_s} . \quad (5.8)$$

For a mixture of ideal gases, the mole fraction, volume fraction and partial pressure as a fraction of the total pressure are all equal [99] and this useful fact has also been employed.

5.3 Reactor Material Balance

Using the readings of the D/P cell, absolute pressure transducer, and the gas chromatograph, it is possible to carry out a material balance calculation for the reactor. The total volumetric feed rate to the reactor at standard conditions of 0°C and 1 atm is called FF_0 . Then the molar flow rate of any component, FF_i , can be calculated,

$$FF_i = (FF_0)(y_i)/(\sum y_i v_i) \quad (5.9)$$

The denominator of the above expression represents the average molar volume of the gas mixture at standard conditions.

It is assumed that nitrogen passes through the reactor as an inert component, so the product flow rate of N_2 equals that entering the reactor,

$$FP_{N_2} = FF_{N_2} \quad (5.10)$$

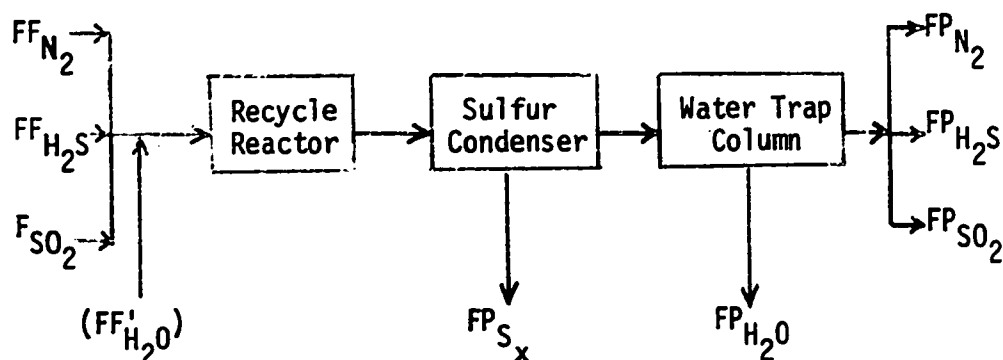
Therefore the product flow rate of H_2S and SO_2 can be expressed as

$$\begin{aligned} FP_i &= (FP_{N_2})(y_i^*)/(y_{N_2}^*) \\ &= (FF_{N_2})(y_i^*)/(y_{N_2}^*) \end{aligned} \quad (5.11)$$

The asterisk was added to the above y_i^* because the symbol does not re-

present the mole fraction of the component in the bulk product stream. The y_i^* is the mole fraction of component i in the product stream after the sulfur and water vapor have been removed.

From the equations (5.10) and (5.11) all of the streams depicted in the following figure are known except for FP_{S_x} and FP_{H_2O} .



Assuming that all of the sulfur contained in the H_2S and SO_2 which reacted formed sulfur product, then

$$FP_{S_x} = (FF_{H_2S} + FF_{SO_2} - FP_{H_2S} - FP_{SO_2})/X \quad (5.12)$$

The water could be calculated in two ways,

$$FP_{H_2O} = 2(FF_{SO_2} - FP_{SO_2}) \quad (5.13)$$

or

$$FP_{H_2O} = FF_{H_2S} - FP_{H_2S}$$

The two answers should be the same if the GC analysis of the feed and products streams were perfect but since this was not the case, the average of the two results was taken.

$$FP_{H_2O} = (2(F_{SO_2} - F_{SO_2}) + F_{H_2S} - F_{H_2S})/2 . \quad (5.14)$$

An indication of the accuracy of the balance was obtained by performing a hydrogen balance,

$$F_{H_2} = F_{H_2S} - F_{H_2S} - F_{H_2O} . \quad (5.15)$$

This term, of course, should be zero. For experiments which involved the addition of water, F'_{H_2O} , to the reactor feedstream, Equation (5.14) was modified by adding to it the molar feed rate of water.

The rate of reaction of H_2S and SO_2 were obtained directly from the reactor material balance by subtracting their product flow rates from their reactor feed rates and dividing the result by the weight of catalyst in the reactor. Such kinetic data are referred to as finite rate data in this thesis and are calculated as shown in Equation (5.16),

$$-r_{H_2S} = (F_{H_2S} - F_{H_2S})/W . \quad (5.16)$$

This equation is mathematically the same as Equation (2.49), which

states

$$-r_{H_2S} = (X_{H_2S})(FF_{H_2S})/W \quad (2.49)$$

More than 80% of the kinetic data presented in this thesis are finite rate data. To augment these data, the conversion and space-time data which were also measured with each run were correlated to provide initial rate data. This approach is discussed in Section 6.5.

5.4 Partial Pressure of Reaction Species

The composition of the effluent from the reactor is very close to that of the reacting mixture since at high circulation rates the recycle reactor behaviour is the same as for the perfectly mixed backmix flow reactor. Thus, the partial pressures of the reacting species may be determined from the composition of the product stream. In turn, the composition of the product stream was calculated from the material balance,

$$y_i = \frac{(FP_i)(v_i)}{\sum [(FP_i)(v_i)]} \quad (5.17)$$

It was not possible to use FP_s in Equation (5.17) since sulfur vapor exists as a mixture of S_8 , S_6 and S_2 molecules. The relative amounts of each sulfur species present at equilibrium are dependent on the temperature and pressure of the sulfur vapor system.

The average molecular weight of sulfur in the vapor was determined by using the free energy minimization method which was discussed in Chapter III. The FP_S was replaced in the material balance by FP_{S_x} where,

$$FP_{S_x} = FP_S / X \quad (5.18)$$

where X is the average number of sulfur atoms in the sulfur vapor molecule.

Since the reaction mixture behaves like an ideal gas mixture, then the partial pressures could be calculated as follows,

$$P_i = (y_i)(P) . \quad (5.19)$$

CHAPTER VI

PRESENTATION AND DISCUSSION OF EXPERIMENTAL RESULTS6.1 Experimental Program

The kinetics measurements for the Claus reaction were obtained with the following objectives: the data should permit correlation of and discrimination between mechanistic kinetic models for the system. It should also yield an empirical rate equation adequate for plant design if sufficient confidence could not be expressed for any of the mechanistic type models.

In modified Claus type sulfur plants, H_2S and SO_2 mole fractions rarely exceed 0.10 in the catalytic converters where the Claus reaction takes place. Accordingly, in this investigation the upper concentration levels of H_2S and SO_2 were set for 0.10 mole fraction. Existing sulfur recovery plants operate only slightly above atmospheric pressure and, so, in the research program, the reaction pressure was held to slightly above one atmosphere.

The temperature range decided upon was also consistent with plant operating conditions, the lowest possible temperature above the sulfur dew point. Minimum and maximum temperatures were 208°C and 287°C respectively.

It was also recognized that substantial water vapor partial pressures existed in sulfur plant converters, so facilities were pro-

vided to study the effect of excess water vapor on the reaction rate.

It was therefore felt that the state variables for this reaction could be studied within the range of industrial interest and yet with sufficient scope to allow correlation of a useful rate expression and inferences to be made on the reaction mechanism.

Table 6.1 summarizes the experimental program. Each run has been assigned an alphanumeric number which consists of two letters and an integer. The first letter refers to the temperature level at which the run took place. The second letter designates the feed composition for the run. The integer assigned to each run number differentiates between the feed flow rates to the reactor. Generally, the lowest number corresponds to the slowest feed rate.

Four exceptions were made to this numbering convention. Runs which have been labelled CAT1, CAT2, ... are catalyst activity tests which took place at experimental conditions corresponding to CB. The number refers to the batch number of the catalyst charge. Runs with X as the second letter have been carried out under feed composition conditions which correspond to the letter A, and the intent of the run has been to operate at high conversions of H_2S . FMS denotes runs which were executed using a finer mesh sized catalyst than that used for the rest of the experimental program. Finally, HW applies to runs which took place at high water partial pressures by adding water to the reactor feed stream.

Tables in Appendix C contain the kinetic data which were ob-

Table 6.1
Experimental Program

Letter	1st Letter-Temperature (Degrees Kelvin)	2nd Letter-Composition (Mole Percent)		
		N ₂	H ₂ S	SO ₂
A	559	88.39	7.93	3.68
B	541	92.50	3.82	3.68
C	515	94.37	1.95	3.68
D	481	87.11	7.51	5.38
E	-	90.73	7.63	1.64
F	-	92.66	1.94	5.40
G	-	96.23	2.05	1.70
H	-	90.43	3.84	5.73
K	-	94.36	3.89	1.75
X	-	88.39	7.93	3.68

FMS Activity Test on fine mesh catalyst

HW Kinetic data taken at high water levels

CAT Catalyst Activity Test

tained in this investigation. The data have been presented in three groups; directly measured finite rate data, catalyst activity test data, and initial rate data which were determined from plots of H_2S fractional conversion versus reactor space time for H_2S .

6.2 Test for Homogeneous Reaction

The first experiment performed on the equipment was one which tested for the existence of homogeneous reaction. With no catalyst in the reactor, a feed stream with a composition of approximately 88% N_2 , 8% H_2S and 4% SO_2 was used. The reactor temperature approximated $500^\circ K$ and the recycle pump was running at a dial setting of 9 throughout this test. It was found that chromatograms for both feed and product streams were the same within the limits of experimental error and so it was concluded that homogeneous reaction was not occurring to any significant extent in the reactor. The experimental error is discussed in Appendix C.

6.3 Bulk Mass Transfer Test

The recycle reactor is ideally suited for determining whether bulk mass transfer (film diffusion) is the rate-controlling step in heterogeneous catalytic reactions. By simply holding all of the state variables (feed composition, feed flow rate, temperature and pressure) for the reactor constant and changing the rate of recirculation, it is possible to determine whether mass transfer is rate controlling.

In the film diffusion test which was performed, the variable speed drive on the recycle pump was set at dial readings of 4., 6., 8. and 10. which corresponded to recirculation rates of approximately 2.3, 3.5, 4.75, 5.0 scfm. At each dial setting, a product chromatogram was taken and, in each case, they were identical within the limits of experimental error (indicated in Appendix C).

It was concluded that film diffusion was not significant and that the reactor was behaving as a perfectly mixed backmix reactor. Unfortunately, the recycle pump could not be run slowly enough to demonstrate departure from these ideal conditions. This was due to the nature of the pump drive, powered by a direct current motor which would not turn over at dial settings below 3.5.

The data for this series of runs is tabulated under run CB-2 in Appendix C and the chromatograms are given in Table 6.2. In Appendix D, theoretical calculations indicated that at a dial reading of 5.0 on the recycle pump the bulk diffusion rate of H_2S to the catalyst surface could be more than 250 times as rapid as the rate required to sustain the surface reaction at 500°F and 30.4 and 15.2 mm Hg pressure for H_2S and SO_2 , respectively. For similar temperature and pressure conditions, calculations indicated that the film diffusion rate for modern sulfur plants could be 7.5 times as fast as that necessary to sustain the surface reaction. When the partial pressures of H_2S and SO_2 are increased, this ratio of 7.5 would decrease.

Table 6.2
Chromatograms for Film Diffusion Test

Stream Sampled	Pump Dial Reading	Recirculation Rate (scfm)	Component Areas		
			N ₂	H ₂ S	SO ₂
Feed			90.5	219.5	259.0
			90.5	220.0	258.0
Product	4.	2.30	90.2	190.0	242.0
Product	6.	3.50	90.2	191.5	243.0
Product	8.	4.75	90.2	192.0	242.5
Product	10.	5.00	90.1	190.0	240.0
Product	7.5	3.90	90.2	190.0	242.0
Product	7.5	3.90	90.1	192.0	242.0

For the ensuing experimental program, the pump dial reading was maintained at 7.5 which corresponded to a flow rate of 3.90 scfm through the catalyst bed. This flow provided recycle ratios which averaged at 25 for the rate measurements. This is better than two times the recycle ratio of 10, above which, a recycle reactor behaves like a backmix reactor.

6.4 Catalyst Activity Test Results

As indicated in Section 5.1, the catalytic activity was relatively higher for freshly loaded catalyst, and a procedure was followed which avoided taking kinetic measurements under these conditions. To ensure that constant catalytic activity was prevailing, runs at the feed composition and experimental conditions which corresponded to CB

were made periodically and the results were compared on a fractional conversion (XA) of H_2S versus space time (WFA) plot. This not only served to check the catalytic activity, but also demonstrated the repeatability of the experiments.

The catalytic activity appeared constant within the limits of experimental error for all cases. In Figure 6.1, the results of all of the activity tests are plotted as well as those for run series CB. The dotted lines on either side of the solid line indicate the limits of experimental accuracy as determined in Appendix C.

Catalyst activity tests were performed at the discretion of the experimentalist. Generally, activity tests were carried out before and after long series of runs and in particular, if the equipment had been cooled down and then reheated because of a necessary repair or new catalyst charge. Normally, the fluidized bath temperature was maintained at all times between runs, for days at a time.

The results of the activity tests and run series CB are given in Table C-3 in Appendix C. Three batches of Porocel catalyst 28/35 mesh were used for the runs. Activity tests denoted ACT1 were performed on catalyst batch number 1 which weighed 0.4995 grams. This batch was used extensively for kinetic measurements. Catalyst batch number 2 weighed 1.5141 grams and was used for the high conversion run series. Catalyst batch 3 weighed 1.1530 grams and was used for the runs made at high levels of water partial pressure.

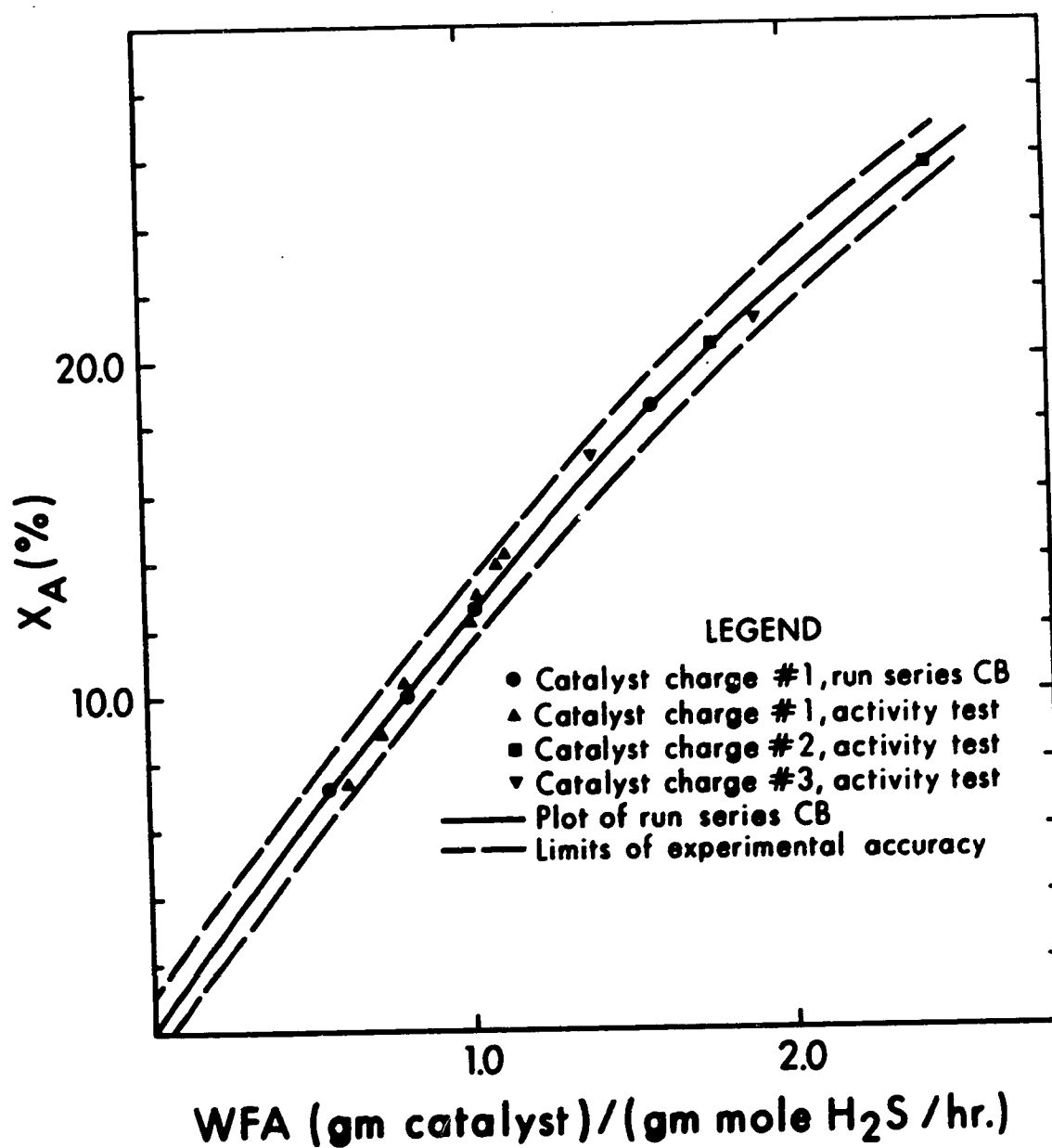


FIGURE 6.1: CATALYST ACTIVITY TESTS

6.5 Initial Rate Data

From plots of fractional conversion of H_2S and reactor space time with respect to the H_2S feed rate, it is possible to determine the rate of reaction at zero percent conversion of H_2S by taking the slope of such a plot at the origin. Since this is not as immediately clear for a recycle reactor as it is for a differential reactor, the mathematics of obtaining rates from such plots will now be reviewed.

Consider the sketch of a recycle reactor shown in Figure 2.3. The following material balance equation describes the differential change in fractional conversion of component A with a differential change in weight of catalyst in the reactor.

$$F_{A0} (1+R') dX'_A = r_A dW \quad (6.1)$$

This equation is being applied in the "differential reactor sense" since the total flow of component A past the catalyst at zero conversion is used. The prime is used on X'_A because it refers to the conversion across the catalyst bed and not across the recycle reactor as a whole, X_A . These two conversions are related by the following equation.

$$X'_A = X_A / (1+R') \quad (6.2)$$

Differentiating Equation (6.2) and substituting into Equation (6.1), the following result is obtained.

$$F_{A0} dX_A = r_A dW \quad (6.3)$$

Equation (6.3) may be integrated and rearranged to give:

$$\int_0^{X_A} \frac{dX_A}{r_A} = \frac{W}{F_{A0}} = WFA \quad (6.4)$$

which is valid at low values of X_A .

Holding the catalyst weight constant and permitting the feed rate of component A, F_{A0} , to vary when the above equation is differentiated, corresponds to finding the reaction rate taken from derivatives taken at the origin on conversion versus space-time plots. Differentiating, Equation (6.4) becomes

$$\frac{dX_A}{r_A} = d(WFA) \quad (6.5)$$

or

$$r_A = \frac{dX_A}{d(WFA)} \quad (6.6)$$

The initial reaction rates were obtained by fitting the conversion-space time data to the function

$$X_A = A \tanh[B(WFA)] \quad (6.7)$$

and analytically differentiating at the origin. The curve fitting was carried out using Rosenbrock's method which is described in Appendix E.

The derivative of the above function with respect to WFA is

$$\begin{aligned}\frac{dx_A}{d(WFA)} &= (A)(B)(\operatorname{sech}^2[B(WFA)]) \\ &= \frac{4AB}{(e^{(WFA)B} + e^{-(WFA)B})^2}\end{aligned}\tag{6.8}$$

At WFA = 0, which corresponds to the initial rate of reaction, the above derivative reduces to

$$\frac{dx_A}{d(WFA)} = (A)(B) .\tag{6.9}$$

This method was proposed and applied by Mezaki and Kittrell [77] on space time-conversion data taken by Johnson [53] on the vapor-phase dehydration of secondary butyl alcohol over a commercial silica-alumina cracking catalyst.

Table 6.3 summarizes the results of fitting the conversion-space time data and also indicates the calculated initial rates. Using the fitted hyperbolic tangent functions, the space-time conversion data were calculated at thirty five points for each of the eighteen sets of data. These calculated points were used for plotting the

curves shown in Figure 6.2, which also shows the experimentally measured space time-conversion data.

The ideal gas law was used in conjunction with the average feed composition and reaction pressure for each of the sets of runs for determining the partial pressure of reactants which would exist for each initial rate. These initial rate data are shown in Table C.4.

6.6 Experimental Test for Pore Diffusion

Porocel catalyst, 28/35 mesh, was used throughout the experimental program for measuring kinetic data. To test if pore diffusion was limiting the reaction rate, a finer mesh-sized catalyst (48/65 mesh) was subjected to the normal pretreatment procedure and then kinetic measurements were taken at experimental conditions similar to those for run series CA.

After one run it was very clear that this finer mesh catalyst was much more active than the 28/35 mesh material, so the pretreatment time span was tripled. The results from the three ensuing kinetic measurements are shown on a conversion-space time plot in Figure 6.3 along with those of run series CA.

The activity of the smaller catalyst particles was obviously much higher than that of the catalyst particle size used in the majority of the experiments. The initial rates of reaction which were obtained by the previously described hyperbolic tangent fitting procedure are shown in Table 6.4 as well as the external areas of the

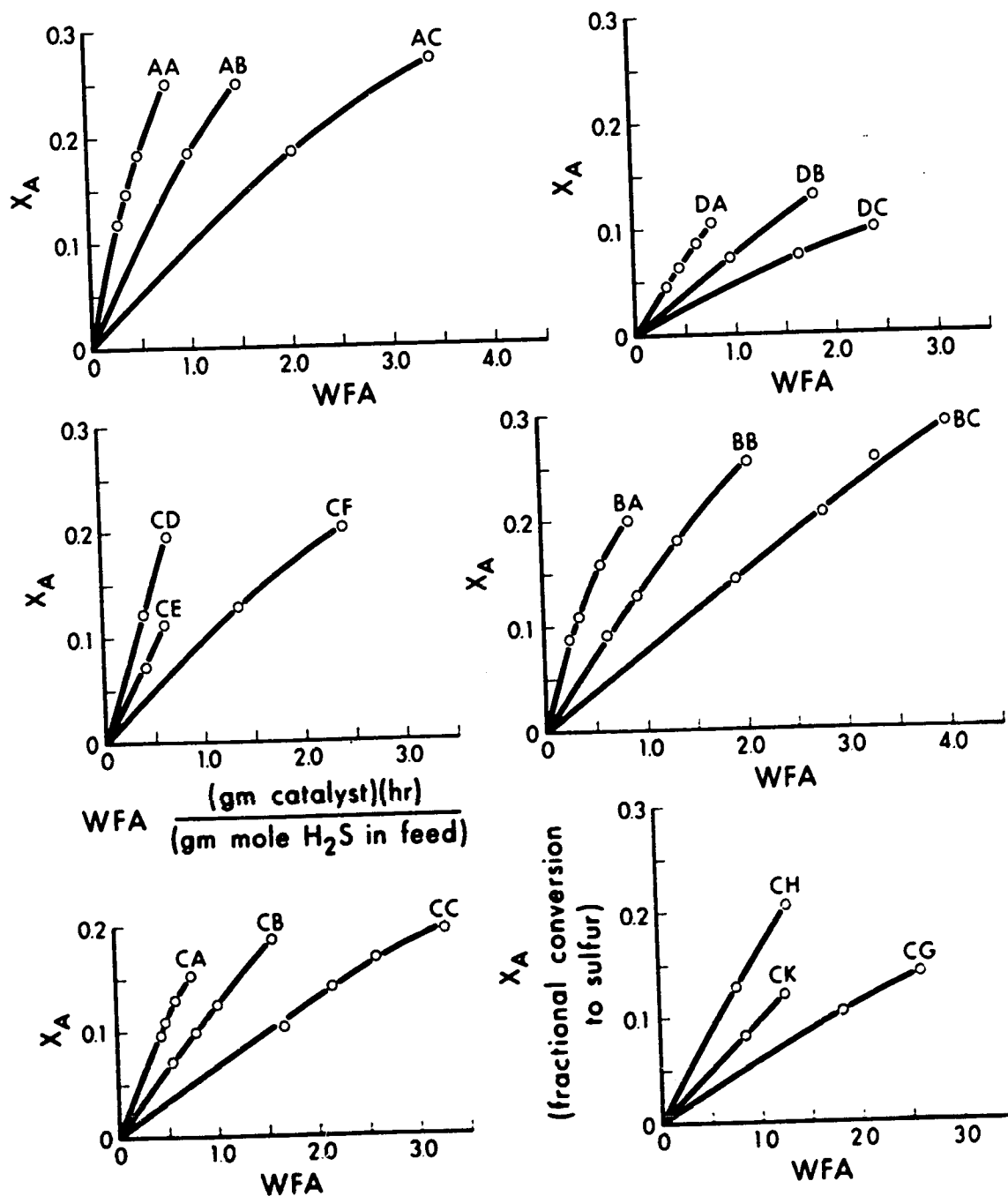


FIGURE 6.2: CONVERSION VS SPACE TIME PLOTS

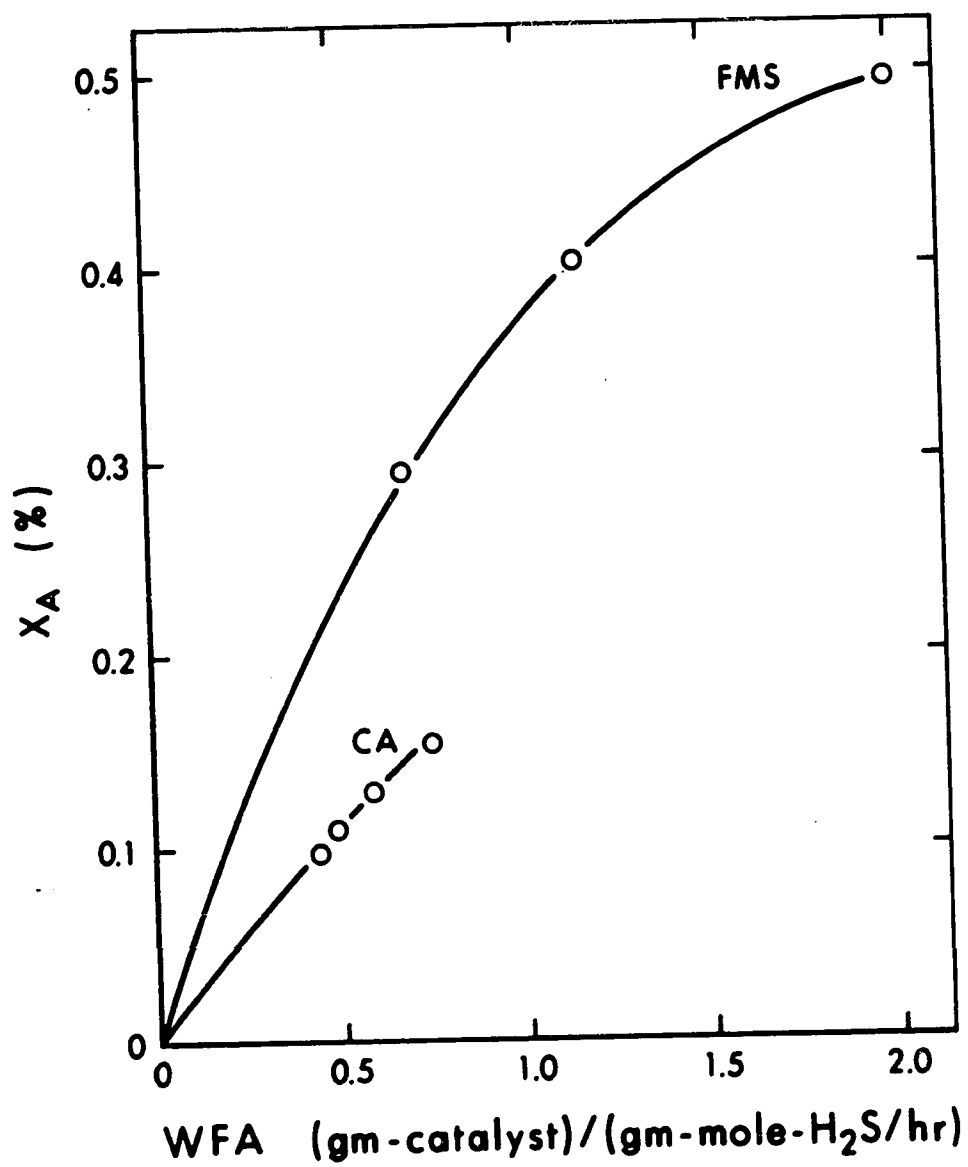


FIGURE 6.3: PORE DIFFUSION TEST

Table 6.3
Initial Rate Data Determined From
Fitting a Hyperbolic Tangent Function

Curve No.	Parameter Values		Fit Variance	Initial Rate
	A	B		
AA	32.7480	1.26700	0.0485	0.4149
AB	37.2910	0.54262	0.0000	0.2023
AC	38.3180	0.25993	0.0000	0.0995
BA	23.5153	1.44195	0.0000	0.3390
BB	41.3226	0.35167	0.0289	0.1453
BC	72.0617	0.10762	0.3362	0.0775
CA	24.1780	0.99983	0.0632	0.2417
CB	41.8180	0.30316	0.0127	0.1267
CC	34.9180	0.19497	0.2344	0.0680
CD	196.3460	0.14900	0.0003	0.2925
CE	132.8240	0.13472	0.0645	0.1789
CF	31.2100	0.32707	0.0000	0.1020
CG	25.8230	0.23634	0.0000	0.0610
CH	51.4540	0.32945	0.0000	0.1695
CK	197.3260	0.04899	0.0002	0.0966
DA	38.9446	0.36094	0.0001	0.1405
DB	51.5323	0.14600	0.0000	0.0752
DC	15.9675	0.31023	0.0000	0.0495
FMS	51.6322	0.92734	0.3923	0.4788

two different sized catalyst particles. In both cases, the same reactor feed composition and reaction temperature were used.

Table 6.4

Pore Diffusion Test Results

Catalyst Mesh Size (Tyler Std)	Particle Diameter			External Specific Surface Area (cm ² /gm)	Initial Rate of Reaction (g.mol./hr.g.cat.)
	Max (cm)	Min (cm)	Avg (cm)		
28/35	0.0595	0.0420	0.051	46.2	0.242
48/65	0.0297	0.0210	0.025	94.1	0.479

From the results shown in Table 6.4 it is clear that the catalyst activity is almost proportional to the external area of catalyst. The external area of the catalyst was estimated using the average particle diameter shown above, a specific gravity of 3.3 for bauxite and assuming a cubical particle shape. The area ratio of the 28/35 mesh catalyst to the 48/65 mesh catalyst is 1:2.08 and the ratio of the initial reaction rates is 1:1.98. It is therefore concluded that only the external area of the catalyst was actively catalyzing the reaction in this kinetic study.

A third catalyst of smaller particle size was not tested since it was anticipated it would be too fine for use in the reactor. It could cause a very high pressure drop in the recycle loop with the added danger that it could have been blown through the catalyst support

screen and into the pump.

The absence of pore diffusion effects is analogous to what Hammar [44] observed with his cobalt, molybdenum and alumina catalyst. He observed that when the level of sulfur vapor partial pressure was increased beyond the region where sulfur capillary condensation should have taken place, no sudden decrease in the reaction rate occurred. On this basis, he concluded that the reaction was taking place predominantly on the outer surface of the catalyst.

Calculation of effective diffusivity and subsequent testing of a reaction rate diffusion control criterion [50] as shown in Appendix D, led to the conclusion that the Claus reaction would be limited by pore diffusion if the pores were not plugged. The criterion requires that [50] for the absence of pore diffusion control of a reaction the following inequality must be satisfied,

$$\left(\bar{r}\right)\left(\frac{1}{C_0}\right)\left(\frac{d_p^2}{D_{eff}}\right) < \left(\frac{1}{C_0}\right)\left(r(C_0)/r'(C_0)\right).$$

The value of the left hand side of this inequality was found to be 0.16 sec versus a value of 0.011 for the right hand side. This means that the pore diffusion interaction with reaction phenomenon could have been observed if the surfaces were available for reaction.

It is most probable that sulfur vapor, which is primarily S_8 at 260°C, is slow in diffusing out of the catalyst pore and is forming

a monolayer or more on the internal surface. The high activity of fresh catalyst could result from initial internal area utilization which later diminishes because of sulfur buildup on the surface.

Sulfur buildup on internal surfaces is visualized as follows: when a monolayer or more of sulfur forms on the capillary walls, the effective diameter is so reduced that reactants cannot diffuse in and more likely, S_8 , which may have been formed within the pore, cannot diffuse out. Sulfur thus remains permanently inside the catalyst.

This hypothesis is supported by tests which were performed on fresh and used catalyst by Mr. M. de Germiny [23]. Using BET- N_2 adsorption measurements, fresh catalyst surface area measured at $148 \text{ m}^2/\text{gm}$ and used catalyst from the same batch at $56 \text{ m}^2/\text{gm}$. The surface area reduction can be attributed to reduction of the pore diameter. Subsequent differential thermal analysis of the used catalyst failed to detect the presence of sulfur in the material. It was felt that the measurement device was not sensitive enough to detect the sulfur which likely formed less than 1% of the mass of the sample. On the other hand, electron probe measurements indicated the absence of sulfur from fresh catalyst but approximately 10% sulfur content uniformly dispersed within used catalyst.

6.7 Examination of the Effects of Species Partial Pressures and Temperature on the Kinetics of the Claus Reactions

The outline of the experimental program describes the ranges of feed compositions and temperature which were used in this study.

Figures 6.4 to 6.6 graphically show how the reaction rate was affected by the state variables. Each point on the plots is an experimentally measured piece of kinetic data. Excluding initial rate data, the measured rate data were recorded at varying levels of H_2S and SO_2 conversion. Fortunately, the conversion range was small enough that corresponding changes in S_x and H_2O pressure did not cause excessive scatter in the data on plots which do not take these changes into account.

Figure 6.4 shows how the reaction rate varies with H_2S partial pressure with SO_2 as a parameter. It is apparent that the order of the reaction with respect to H_2S pressure remains constant with varying levels of SO_2 . The reaction order with respect to H_2S calculates at 0.84 using the slopes of the lines shown in Figure 6.4. A cross plot of Figure 6.4 would provide a graphical estimate of 0.50 for the order of the reaction with respect to SO_2 . As will be seen later these estimates of the reaction order agree with those obtained from correlating the kinetic data to an empirical rate expression.

It is also notable in Figure 6.4 that in general the initial rate data points (open symbols) were lower than the finite rate points (dark symbols). At first it was felt that there was some form of systematic error in reducing the data, since the high water activity experiments, discussed later, indicated that water retards the reaction. However, no error could be found.

What has been observed is possibly a very unique effect. At low levels of water content, the presence of water enhances the number of hydroxyl groups on the catalyst surface which in turn provides more

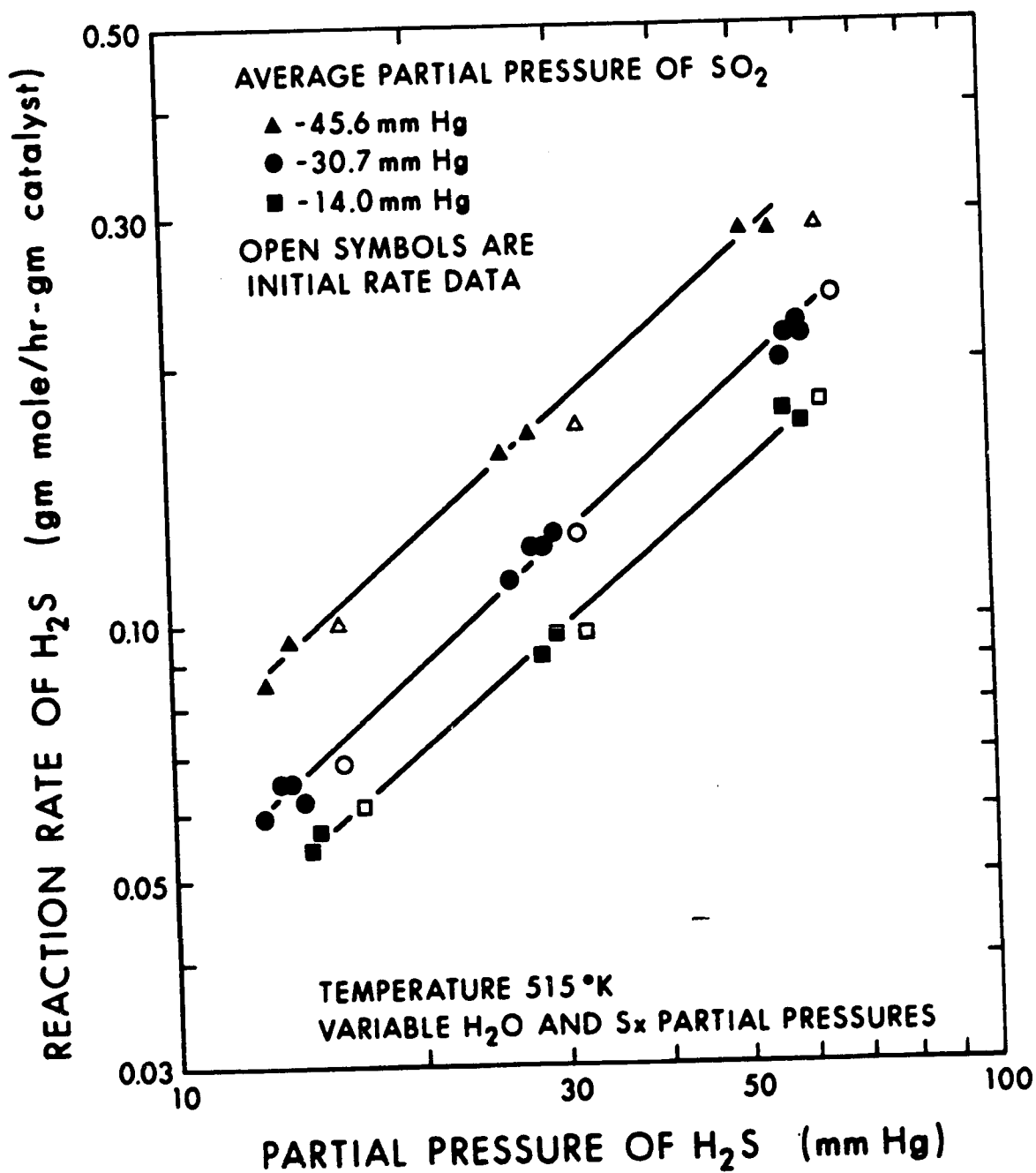


FIGURE 6.4: RATE OF H_2S OXIDATION AS A FUNCTION OF H_2S PARTIAL PRESSURE WITH SO_2 PARTIAL PRESSURE AS A PARAMETER.

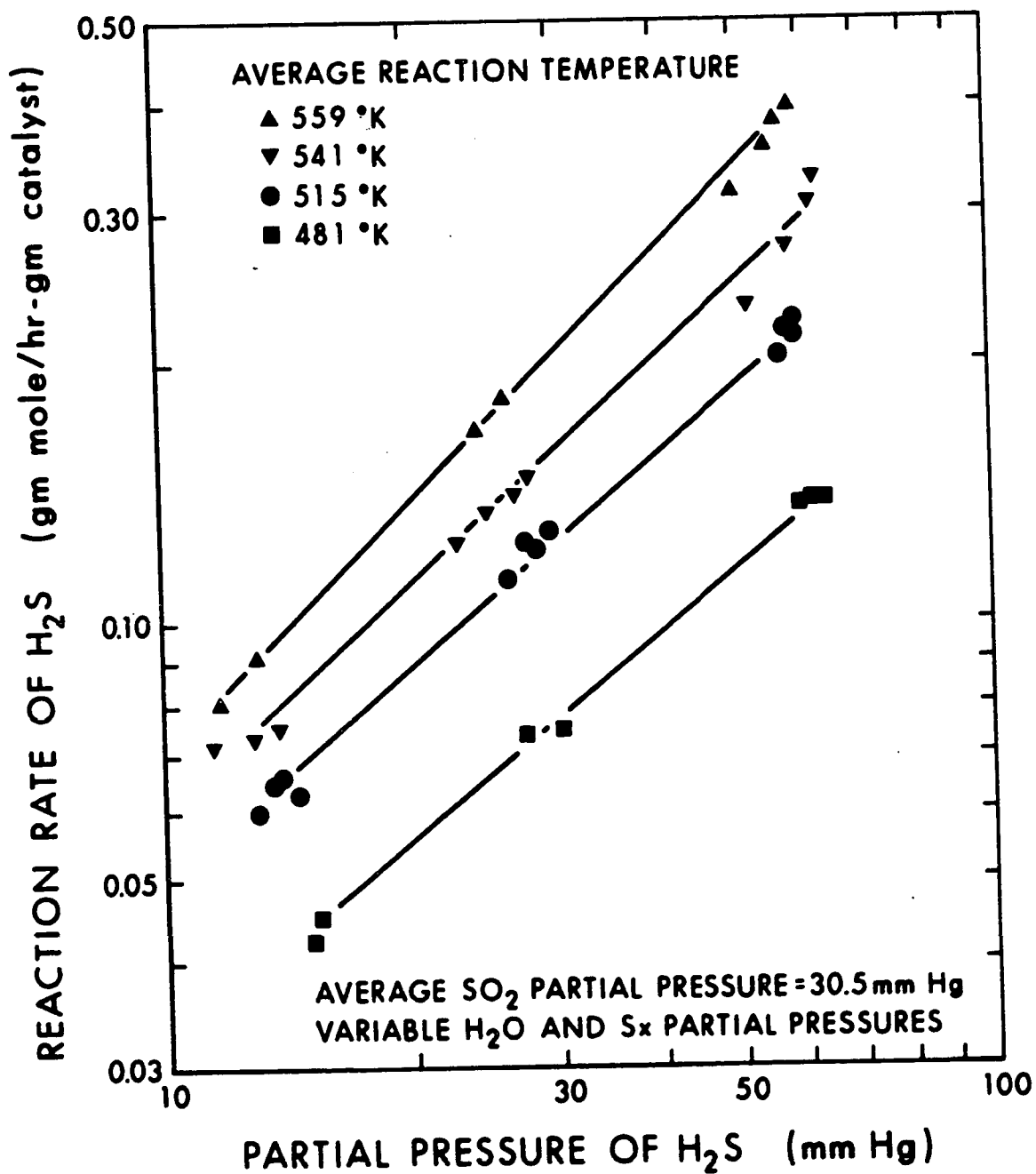


FIGURE 6.5: RATE OF H_2S OXIDATION AS A FUNCTION OF H_2S PARTIAL PRESSURE WITH TEMPERATURE AS A PARAMETER.

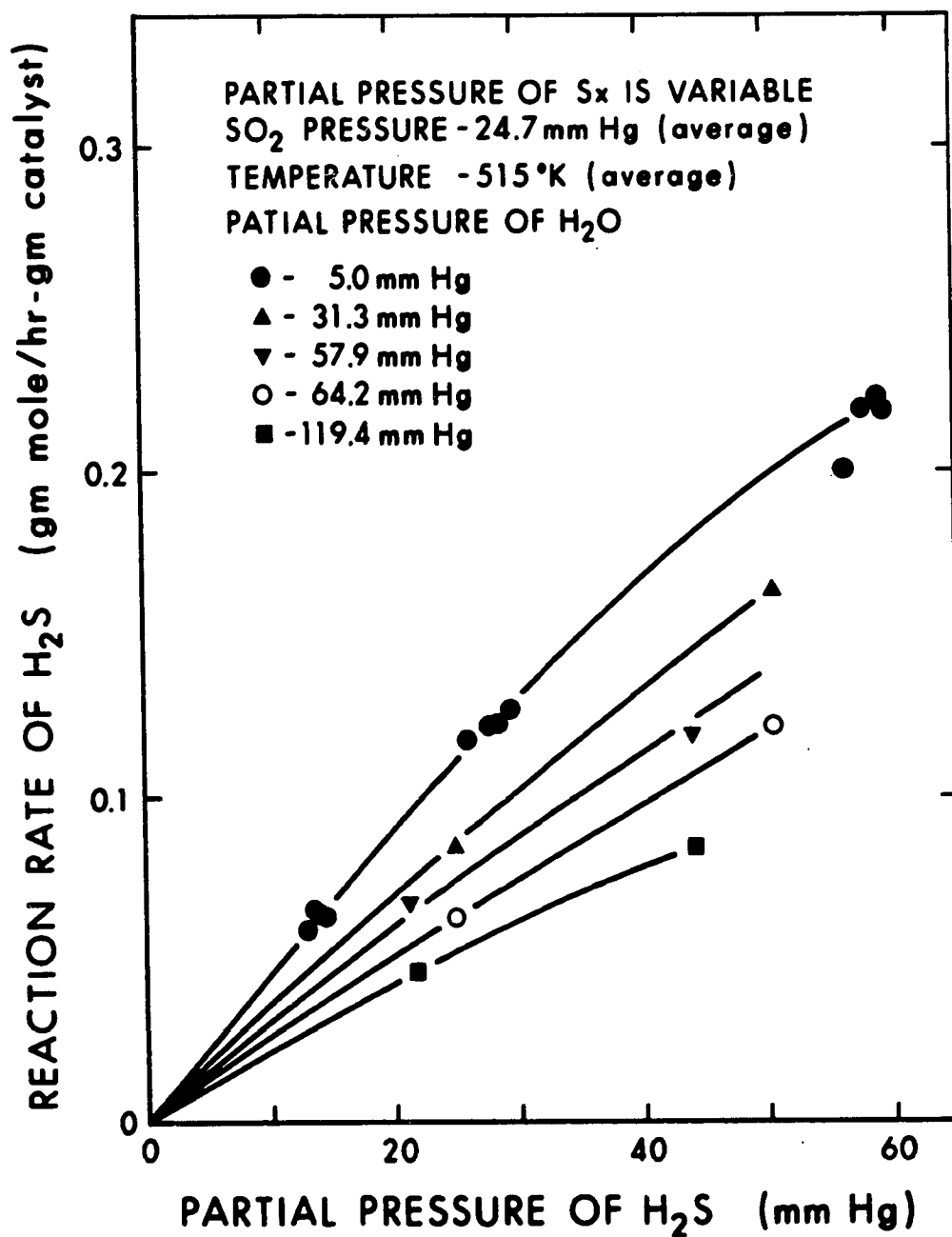


FIGURE 6.6: EFFECT OF WATER PARTIAL PRESSURE ON THE REACTION RATE OF H_2S

sites for H_2S and SO_2 adsorption. At higher levels of water content, after all of the possible hydroxyl groups were formed, the water competes with the reactants for these adsorption sites.

Figure 6.5 displays how the temperature affects the kinetics of the reaction and again it is seen that the reaction order with respect to H_2S remains fairly constant at different temperature levels. The initial rate points were not included here to avoid cluttering the plot, but the same trend would be observed as with Figure 6.4 if they were included. From cross plots of the data in Figure 6.5, the activation energy for the reaction calculates at 7530 calories. Again this comes close to the estimate arrived at by curve fitting.

From Figure 6.6 it can be seen that as the partial pressure of water increases, the forward rate of the Claus reaction decreases. An increase in the velocity of the reverse reaction most probably causes the observed reduced forward rate at higher water vapor pressures.

Figure 6.7 shows isorate lines drawn on a graph with percent conversion of H_2S and SO_2 to sulfur and temperature as coordinates. The data points were obtained from plots of the high conversion data (series A,B,C and DX) with reaction rate plotted against percent conversion. Unfortunately the equipment was not designed for operating at high conversion levels and therefore very little confidence could be expressed in these data. To obtain high conversions, it was necessary to operate at very low feed flow rates and it is felt that the associated flow rate measurement error could lead to errors of 100% in the measured reaction rate.

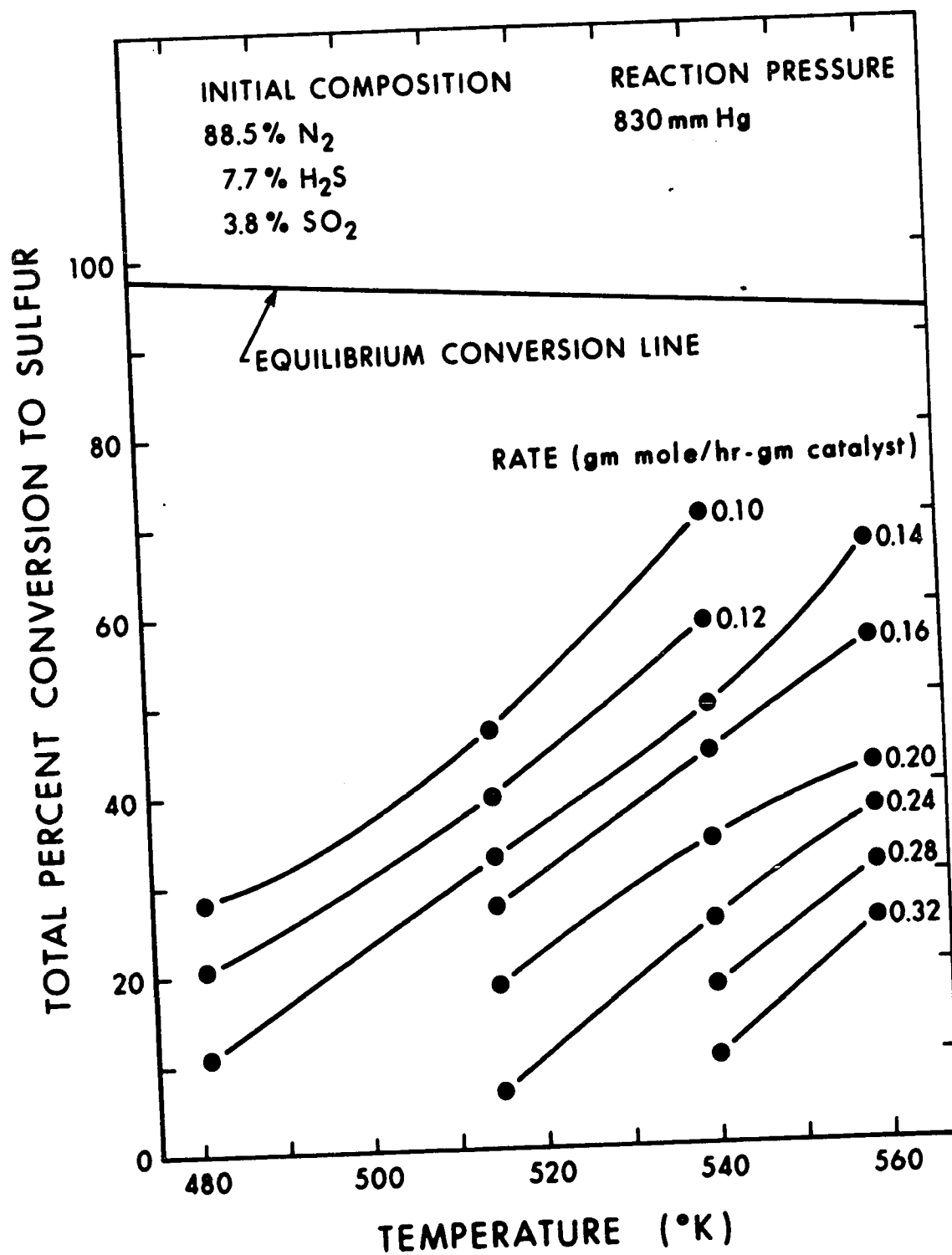


FIGURE 6.7: ISORATE LINES PLOTTED ON EQUILIBRIUM DIAGRAM OF CLAUSS SYSTEM

The objective of the high conversion series was to provide directly measured data in the form presented by Kubota [60] which would facilitate sulfur plant reactor design and staging according to a method recently applied to Claus reactors by Dalla Lana [17].

6.8 Correlation of Experimental Data by Rate Equations

An objective of the research program was to determine the parameters of empirical rate expressions fitted to the experimental kinetic data. Also, the data would be tested with mechanistic models which would be selected on the basis of previously described characteristics of the heterogeneous reaction of H_2S with SO_2 . Finally, an attempt should also be made to fit the rate data to a more comprehensive mechanistic model with the mutually rate-controlling steps of reaction adsorption and subsequent bimolecular surface reaction.

The Rosenbrock method of rotating coordinates [94] satisfactorily minimized the error variance of the fitted rate expressions. A Fortran listing of this computer program and documentation of the algorithm are given in Appendix E.

Rosenbrock's method was originally intended to provide parameter estimates for an initial guess for a nonlinear least squares program however, the latter approach did not reduce the sum of residual mean squares of the errors of the correlation below that achieved using Rosenbrock's method so it was deleted from the fitting process.

Experimental data were divided into 11 groups of results, each group being obtained at a characteristic set of reaction conditions.

The reason for doing this was to avoid confusing the correlation results. For example, if a rate expression without a temperature term was correlated to find the reaction order with respect to H_2S and SO_2 , only data taken at one temperature level should be used and not all of the available data. These data banks are listed in Table 6.5. Isothermal data refers to kinetic measurements taken at approximately 242°C and at H_2S and SO_2 partial pressures which range from 12 to 60 mm Hg and 10 to 45 mm of Hg, respectively. The total pressure of the reactor was held constant at 840 mm Hg. These data were presented in Figure 6.4 along with the initial rate data for the experiments. Non-isothermal data depicts the results obtained at 515°K and the three other temperatures which were studied as well. Figure 6.5 exhibits all of the non isothermal data points. Initial rate data were calculated by the procedure discussed in Section 6.6, and the results from high water composition tests were obtained from experiments in which water was injected into the reactor feed stream using the microfeeder.

After a bank of data had been correlated to a rate expression, the covariance matrix was calculated to obtain a measure of the reliability of the parameter estimates. In the covariance matrix the diagonal elements are the variances, and their square roots are the standard deviations of the parameter estimates [64]. Off diagonal elements indicate the interdependence of the estimates of the various parameters. The 95% confidence intervals for parameters were obtained by multiplying the standard deviations by two. This is often referred

Table 6.5
Data Banks for Correlation

<u>Bank Number</u>	<u>Bank Description</u>	<u>Number of Data Points</u>
1	Isothermal	24
2	Isothermal Initial Rate	9
3	1 + 2	33
4	Nonisothermal	40
5	Nonisothermal Initial Rate	12
6	4 + 5	52
7	3 + 6	85
8	2 + 5	21
9	1 + 4	52
10	High water + 1	32
11	10 + 4	60

to as two sigma intervals [64]. An explanation of how the covariance matrix was constructed and a listing of the Fortran program which was used is given in Appendix E.

6.8.1 Empirical Rate Expressions

Several empirical rate equations were fitted to the kinetic data. Initially they were simple and became more complex as more information was gained about the reaction order with respect to specie

partial pressures and about the reaction activation energy. This approach reduced the tendency of the correlation program to converge on unreasonable parameter estimates, since initial guesses for some parameter values, which were required by the Rosenbrock program, could be made fairly accurately. The more complex empirical expressions were not unimodal in the parameter space and several initial guesses were attempted before correlation coefficients were finally accepted. Table 6.6 summarizes the results which were obtained for the empirical rate expression parameter estimates.

The first rate equation in Table 6.6 was fitted to isothermal data measured at 515°K for obtaining the order of the forward rate expression with respect to H_2S and SO_2 at one temperature. The orders were found to be 0.832 ± 0.0745 and 0.437 ± 0.0834 respectively. The third rate expression which includes an activation energy term, was fitted to nonisothermal kinetic data measured at 481, 515, 541 and 559°K. The reaction orders with respect to H_2S and SO_2 were 0.963 ± 0.0448 and 0.359 ± 0.135 . Since the nonisothermal data were measured at a higher average temperature than the isothermal data, it is possible that the reaction order increases with respect to H_2S and decreases with respect to SO_2 as the temperature increases. However, the 95% confidence limits for the order estimates indicate that they could both be the same for the two sets of results and so, the data do not permit us to conclude that the order changes with temperature.

The apparent activation energy of 7589 ± 451 calories per

Table 6.6

Rate Expression Parameter Estimates

<u>Rate Equation</u>	<u>Equation Number</u>	<u>k₁</u>	<u>E₁</u>	<u>m</u>	<u>n</u>	<u>k₋₁</u>	<u>p</u>	<u>Data Bank</u>	<u>Fit Variance</u>
$r = k_1 P_A^m P_B^n$	(6.10)	0.00184 (0.000716)		0.832 (0.0745)	0.437 (0.0834)			3	2.57×10^{-4}
$r = k_1 P_A^m P_B^n - k_{-1} P_C^p$	(6.11)	0.00180 (0.00108)		0.828 (0.0952)	0.467 (0.111)	0.00215 (0.00636)	0.757 (0.607)	10	2.81×10^{-4}
$r = k_1 \text{EXPFI} P_A^m P_B^n$	(6.12)	2.198 (0.564)	7589. (451.)	0.963 (0.0448)	0.359 (0.135)			6	1.47×10^{-4}
$r = k_1 \text{EXPFI} (P_A^m P_B^n - k_{-1} P_C^p)$	(6.13)	1.292 (0.885)	7100 (625.)	0.904 (0.069)	0.474 (0.134)	0.504 (1.925)	0.982 (0.825)	11	3.21×10^{-4}

Note: P_A = partial pressure of H_2S (mm Hg)

P_B = partial pressure of SO_2 (mm Hg)

P_C = partial pressure of H_2O (mm H_2O)

r = reaction rate of H_2S , (gm mole/hr-gm-catalyst)

$\text{EXPFI} = \exp(-E_1/RT)$

$R = 1.98 \text{ cal}/(\text{gm mole} \cdot ^\circ K)$

T = temperature ($^\circ K$)

Sigma intervals enclosed by brackets below parameter estimates

mole may be lower than the true activation energy for the reaction. Under strong pore diffusional resistance the observed activation energy may be as low as one-half of the true activation energy [102]. Since it was previously concluded that virtually none of the catalyst interior was being used, it is more likely that the measured energy of activation is representative of the diffusion free value.

Another problem involved with the credibility of this activation energy is whether or not the empirical rate expression is representative of the mechanism of the reaction. This type of rate equation corresponds to the Freundlich adsorption isotherms for H_2S and SO_2 and suggests that a surface reaction between chemisorbed species is rate limiting. This isotherm is expected to be valid only at low surface coverages [102].

The empirical rate expressions do correlate the kinetic data as well as the mechanistic equations which are discussed later. A Freundlich-based rate equation is reasonable for summarizing the kinetic data. The work of Deo et al [24] suggested that the function of alumina catalyst is to orient the physically-absorbed reacting molecules. Since it is probable that only a small fraction of these molecules are properly oriented for reaction, the reactive adsorbed molecules would correspond to a sparsely covered surface to which the Freundlich adsorption isotherm may be applied.

The magnitude of the activation energy, 7589 cal/l gm mole, suggests that the chemical reaction is an easily activated process since activation energies for most chemical reactions are commonly in

the range 10,000 to 50,000 calories per gram mole [18]. For the formation of hydrogen bonds, activation energies range from 4,000 to 7,000 calories per mole. Therefore the activation energy of the Claus reaction suggests that hydrogen bonded molecules may be involved. Evidence has been given [24] for the existence of physically adsorbed, hydrogen-bonded and chemisorbed H_2S and SO_2 on alumina.

The remaining rate expressions in Table 6.6 were correlated in an attempt to take into account the effect of water which definitely retards the chemical reaction at high partial pressures. Before discussing the rate equations, it is important to consider this water effect in conjunction with the postulated mechanism.

The previously cited work of MacIver et al [74] indicated that on γ -alumina water would form hydroxyl groups with dehydroxylated aluminium ions and, subsequently, it would hydrogen bond to surface hydroxyl groups after all of the aluminium ions were hydroxylated. In this work, initial rate data tended to measure lower than finite rate data and it has previously been suggested that water reaction product autocatalyzes the Claus reaction at low values of reactant fractional conversion. The water injection experiments unrefutably showed that high water partial pressures retard the reaction. These observed phenomena are the final pieces of information which support the hydrogen-bonded reactant theory, and they are explained with the help of the MacIver work. At low levels of conversion, the water product of reaction forms surface hydroxyl groups which serve as sites for hydrogen bonding

H₂S and SO₂. At high conversion and correspondingly high water partial pressures, the water competes with H₂S and SO₂ for surface hydroxyl groups since the water also hydrogen bonds to them. Thus, water retards the reaction by imposing this competition for surface hydroxyl groups. As was previously stated, it is most probable that the reverse Claus reaction rate is increased as the water partial pressure increases. Therefore it is the combination of site competition and reverse reaction which causes the lowered apparent forward rate at higher water partial pressures.

The rate expressions shown in Table 6.6 which take into account the effect of water have considerably larger confidence limits on the reverse reaction rate constant and order than those found for the forward reaction. This reflects the relative amounts of kinetic data available for correlating the forward and reverse reaction rates. Only eight runs were carried out at conditions of high water partial pressures where the reverse reaction would be substantial whereas for data bank 10, of the 32 data points, 24 observations were made for the forward reaction rate with negligible reverse reaction.

The most comprehensive rate expression which could be fitted to the data is at the bottom of Table 6.6. It has the following form:

$$r = k_1 \exp(-E_1/RT) (P_A^m P_B^n - k_{-1} P_C^p) \quad (6.13)$$

Again, the confidence limits on k_{-1} and p are large and more experi-

mentation would be necessary to reduce them.

This expression is indeed empirical and implies that the activation energy for the forward and reverse reaction rates are equal. This of course is unlikely. It is also implied by this rate equation that sulfur product does not play a role in the reverse reaction which again is unknown. Nevertheless, the data were too few to permit estimation of the reverse reaction activation energy or the effect of sulfur on the reverse reaction. More experimentation would be necessary for studying these parameters.

The usefulness of the above rate equation should not be overlooked because it should give reasonable estimates of reaction rate for reactor design. Most Claus type sulfur plants incorporate sulfur condensers between catalytic converters so sulfur vapor partial pressures are generally low.

Since it has been shown that only the external surface of the catalyst is accelerating the reaction, the form of the rate expression should be altered so that the external surface area of plant-sized catalyst may be incorporated into the equation. A suitable form of equation (6.13) would be

$$r = \left(\frac{A_{EP}}{A_{EE}} \right) (k_1 \exp(-E_1/RT) (p_A^m p_B^n - k^{-1} p_C^D)) \quad (6.14)$$

where A_{EP} is the specific external area of catalyst used in the plant and A_{EE} is that for the catalyst used in this study.

6.8.2 Mechanistic Rate Models

Several different rate expressions which were derived by using the Langmuir adsorption isotherm were correlated to the isothermal data using the Rosenbrock program. As was previously mentioned, no rate expression was derived which could correlate the data better than the empirical rate expressions.

Since the adsorption equilibrium constants for the first two rate expressions shown in Table 6.7 are negative, it is concluded that adsorption of either reactant to the catalyst surface is not rate-limiting.

The three rate expressions, which Hammar [44] found to correlate his Claus reaction kinetic data best, also fitted the rate data of this study reasonably well. These included 2nd and 3rd order reaction between adsorbed H_2S and adsorbed SO_2 and the third expression was the reaction between adsorbed SO_2 and both fragments of a dissociated H_2S molecule adsorbed on the surface. All three of these mechanisms could be equally well fitted by a Freundlich-isotherm-based rate expression if the surface coverages were low.

No attempt has been made to discriminate between the models listed in Table 6.7, however, as one reads the list, at least ten of the rate expressions correlate the data better than the rest as indicated by the variance of the fit.

Table 6.7

Langmuir Hinshelwood Kinetic Models

<u>Rate Expression</u>	<u>Rate Controlling Step</u>	<u>Fit Variance</u>	<u>Comment</u>
$r = k_0 P_A / (1 + k_1 P_B)$	Adsorption of H_2S	2.62×10^{-4}	- ve/ k_1
$r = k_0 P_B / (1 + k_1 P_A)$	Adsorption of SO_2	1.89×10^{-3}	- ve/ k_1
$r = k_0 P_A P_B / (1 + k_1 P_A^{0.5})^2$	Reaction between adsorbed dissociated H_2S and gaseous SO_2 . Both dissociation fragments react.	1.23×10^{-3}	
$r = k_0 P_A P_B / (1 + k_1 P_A + k_2 P_B)^2$	Second order reaction between adsorbed bed molecules.	3.82×10^{-4}	Hammar's Best
$r = k_0 P_A^2 P_B / (1 + k_1 P_A + k_2 P_B)^2$	Third order reaction between adsorbed bed molecules.	4.38×10^{-4}	Hammar's Best
$r = k_0 P_A P_B / (1 + k_1 P_A)$	Reaction between adsorbed H_2S and gaseous SO_2 .	1.23×10^{-3}	
$r = k_0 P_A P_B / (1 + k_1 P_B)$	Reaction between adsorbed SO_2 and gaseous H_2S .	1.25×10^{-3}	
$r = k_0 P_A P_B / (1 + k_1 P_A^{0.5} + k_2 P_B)^3$	Reaction between adsorbed dissociated H_2S and adsorbed SO_2 . Both dissociation fragments react.	3.77×10^{-3}	Hammar's Best

Table 6.7 (continued)

<u>Rate Expression</u>	<u>Rate Controlling Step</u>	<u>Fit Variance</u>	<u>Comment</u>
$r = k_0 P_A^2 P_B / (1 + k_1 P_A)^2$	Third order reaction between adsorbed H ₂ S and gaseous SO ₂ .	1.23×10^{-3}	
$r = k_0 P_A^2 P_B / (1 + k_1 P_A + k_2 P_B)^2$	Third order reaction between adsorbed H ₂ S and adsorbed SO ₂ .	4.56×10^{-4}	
$r = k_0 P_A P_B / (1 + k_1 P_A + k_2 P_B)$	Reaction between adsorbed H ₂ S and gaseous SO ₂ , but SO ₂ adsorbs also.	3.30×10^{-4}	
$r = k_0 P_A^2 P_B / (1 + k_1 P_A)$	Reaction between adsorbed H ₂ S, gaseous SO ₂ and gaseous H ₂ S.	1.26×10^{-3}	
$r = k_0 P_A^2 P_B / (1 + k_1 P_A + k_2 P_B)$	Reaction between adsorbed H ₂ S and gaseous SO ₂ and gaseous H ₂ S, but SO ₂ adsorbs as well.	1.22×10^{-3}	
$r = k_0 P_A P_B / (1 + k_1 P_A^{1/2} + k_2 P_B)^2$	Reaction between adsorbed dissociated H ₂ S and gaseous SO ₂ . Both dissociation fragments react and SO ₂ adsorbs as well.	3.91×10^{-4}	
$r = k_0 P_A^{1/2} P_B / (1 + k_1 P_A^{1/2})$	Reaction between one fragment of adsorbed dissociated H ₂ S and gaseous SO ₂ .	1.30×10^{-3}	- ve/k ₁
$r = k_0 P_A^2 P_B / (1 + k_1 P_A^2 + k_2 P_B)$	Reaction between an adsorbed dissociated H ₂ S fragment and gaseous SO ₂ , but SO ₂ adsorbs as well.	4.16×10^{-4}	- ve/k ₁

Table 6.7 (continued)

<u>Rate Expression</u>	<u>Rate Controlling Step</u>	<u>Fit Variance</u>	<u>Comment</u>
$r = k_0 P_A^{1.5} P_B / (1. + k_1 P_A^{1/2})$	Reaction between an adsorbed dissociated H ₂ S fragment, gaseous H ₂ S and gaseous SO ₂ .	1.27 x 10 ⁻³	
$r = k_0 P_A^{1.5} P_B / (1. + k_1 P_A^2 + k_2 P_B)$	Reaction between an adsorbed dissociated H ₂ S fragment, gaseous H ₂ S and gaseous SO ₂ but SO ₂ adsorbs as well.	9.55 x 10 ⁻⁴	
$r = k_0 P_A P_B / (1. + k_1 P_A) (1. + k_2 P_B)$	Reaction between adsorbed molecules on different site types.	3.18 x 10 ⁻⁴	
$r = k_0 P_A^2 P_B / (1. + k_1 P_A^2) (1. + k_2 P_B)$	Reaction between an adsorbed dissociated H ₂ S fragment and adsorbed SO ₂ / adsorption on different site types.	8.75 x 10 ⁻⁴	- ve/k ₁
$r = k_0 P_A P_B / (1. + k_1 P_A^2)^2 (1. + k_2 P_B)$	Reaction between two adsorbed dissociated H ₂ S fragments and adsorbed SO ₂ ; adsorption on different site types.	3.26 x 10 ⁻⁴	
$r = k_0 P_A P_B / (1. + k_1 P_A + k_2 P_B + k_3 P_C)^2$	Surface reaction between adsorbed H ₂ S and SO ₂ retarded by H ₂ O.	1.39 x 10 ⁻³	
$r = k_0 P_A P_B / (1. + k_1 P_A^2 + k_2 P_B + k_3 P_C)^2$	Surface reaction between two adsorbed dissociated H ₂ S fragments and gaseous SO ₂ retarded by H ₂ O, but SO ₂ adsorbs as well.	4.85 x 10 ⁻⁴	

Table 6.7 (continued)

<u>Rate Expression</u>	<u>Rate Controlling Step</u>	<u>Fit Variance</u>	<u>Comment</u>
$r = \frac{k_0 P_A P_B}{(1 + k_2 P_B)(1 + k_1 P_A + k_3 P_C)}$	Reaction between adsorbed H ₂ S and adsorbed SO ₂ on a different site type. H ₂ O inhibits the reaction by competing with H ₂ S for surface sites.	8.89 x 10 ⁻⁴	
$r = \frac{k_0 P_A P_B}{(1 + k_2 P_B + k_3 P_C)(1 + k_1 P_A)}$	Reaction between adsorbed H ₂ S and adsorbed SO ₂ on a different site type. H ₂ O retards the reaction by competing with SO ₂ for surface sites.	7.27 x 10 ⁻⁴	
$r = \frac{k_0 P_A P_B}{(1 + k_2 P_B + k_3 P_C)(1 + k_1 P_A^{1/2})^2}$	Reaction between two adsorbed dissociated H ₂ S fragments and adsorbed SO ₂ on a different site type. H ₂ O retards the reaction by competing with SO ₂ for surface sites.	7.94 x 10 ⁻⁴	- ve/k ₁
$r = \frac{k_0 P_A P_B}{(1 + k_2 P_B)(1 + k_1 P_A^{1/2} + k_3 P_C)^2}$	Reaction between two adsorbed dissociated H ₂ S fragments and adsorbed SO ₂ on a different site type. H ₂ O retards the reaction by competing with H ₂ S for surface sites.	2.07 x 10 ⁻³	

6.8.3 Reaction Mechanisms with Mutually Rate-Controlling Catalytic Process Steps

Bradshaw and Davidson [7] successfully correlated an eight-parameter expression to ethanol dehydrogenation kinetic data obtained by Franckaerts and Froment. Their approach was to assume that the steps of reactant adsorption, reversible surface reaction, and product desorption were all taking place at the same rate without any single step assumed to be rate-controlling which, of course, reflects the true situation more closely. Their generalized rate expression is obtained by simultaneous solution of the nonlinear algebraic equations which describe the rate processes. The solution is given by

$$r = - \frac{B \pm \sqrt{B^2 - 4AC}}{2A} .$$

The details of what A, B and C represent will be described later.

One of the problems which arise, in using the above expression as a rate equation, lies in deciding which sign to use for $\pm \sqrt{B^2 - 4AC}$. It was not possible for Bradshaw and Davidson to prove that one sign is invariably correct for all conceivable parameter values. However, by invoking Descartes' rule of signs in conjunction with the macro terms A, B and C, they found that to obtain positive roots for r the negative sign worked in 80% of the cases when a solution was possible.

A model which corresponds to surface reaction between adsorbed H_2S and SO_2 with no product inhibition has been developed in

Appendix F. It has the following form,

$$r = \frac{-B - \sqrt{B^2 - 4AC}}{2A}$$

where,

$$A = \left(\frac{1}{k_A k_B} - \frac{P_B^M}{k_A^I D} - \frac{P_A^M}{k_B^I D} + \frac{P_A P_B M^2}{D^2} \right)$$

$$B = \left(-\frac{1}{k_0} - \frac{P_B^L}{k_A^I D} - \frac{P_A^L}{k_B^I D} + \frac{2P_A P_B M^L}{D^2} \right)$$

$$C = \left(\frac{P_A P_B L^2}{D^2} \right)$$

$$D = 1. + K_A P_A + K_B P_B$$

$$M = \frac{K_A}{k_A^I} + \frac{K_B}{k_B^I}$$

For more insight into the constants of the above rate expression, the reader should consult Appendix E of the thesis. For the rate equation, six parameters were necessary and had to be estimated by the data correlation program.

It was very difficult to estimate these parameters since the term enclosed by the square root bracket would often go negative regardless of the sign which preceded it and consequently the computer program would stop due to this error condition. When the square root

term did not go negative, the correlation routine would converge after only a few axes rotations on a set of parameter estimates which did not provide a very low fit variance. This was attributed to the highly nonunimodal nature of the error in parameter space. A typical set of results is given below:

$$k'_A = 0.228$$

$$k'_B = 0.346$$

$$K_A = 0.101$$

$$K_B = 0.0952$$

$$k_0 = 0.161$$

$$L = 0.161$$

$$\text{Fit variance} = 2.08 \times 10^{-3}.$$

This expression does not fit the data as well as a three parameter empirical expression which fits the same data with a variance of 2.57×10^{-4} . Of course the overall rate expression with the correct parameter estimates could likely do a better correlation job than the empirical equation, but the above set of parameters and variance represent the best fit which could be obtained after several different sets of initial guesses for the parameters.

It is concluded that overall rate expression correlations should not be attempted without some knowledge of the order of magnitude of the parameters. Even then, the overall expression for the rate involves numerous constants and as suggested by Smith [98] could become very unwieldy.

6.9 Comparison of this Work with the Results of Other Investigators

Cormode [15] carried out thirteen rate measurements on the Claus reaction at 507°K and 1 atm pressure. The feedstream to his recycle reactor contained H_2S concentrations varying from 2.2 to 6.3 mole percent and the ratio of H_2S to SO_2 was maintained at 2:1 in all runs. Conversions of H_2S ranged from 0.5 to 2.0%. He used Porocel catalyst which had an average particle diameter of 0.068 cm compared to the particle diameter of 0.051 cm which was used in this work.

The rate expression, described by Equation (6.12) and correlated to the kinetic data obtained in this study, provided rate estimates for the Claus reaction at the experimental conditions in Cormode's work. These rate estimates and the measured rates of Cormode are given in Table 6.8 along with the experimental conditions which prevailed while Cormode noted the reaction rates.

In eleven of the thirteen cases, Cormode has measured a higher reaction rate than what the empirical rate expression of this thesis predicted. This suggests that either his catalyst was more active than the one used in this study or one of the two programs had a systematic error in measuring the reaction rate. Another possibility is that the ratio of catalyst particle specific areas is not exactly equal to the inverse ratio of the diameters. This is how the A_{E1}/A_{EE} term in the rate expression was calculated. If A_{E1}/A_{EE} is taken as 1.0 the predicted values of reaction rate are higher than the measured rates.

Table 6.8

Comparison of this Work with Other Results

Reacting Mixture Composition (mole percent)					Observed and Predicted Reaction Rates Cormode Predicted Data Values ((gm moles)/(hr)/(gm catalyst))		Percent Deviation
N ₂	H ₂ S	SO ₂	H ₂ O	S _x			
95.10	2.99	1.50	0.34	0.07	0.0496	0.0428	- 13.7
96.40	2.20	1.10	0.25	0.05	0.0349	0.0279	- 20.0
95.21	2.71	1.39	0.57	0.12	0.0459	0.0369	- 19.6
93.95	3.43	1.70	0.76	0.16	0.0626	0.0503	- 19.6
93.27	3.87	1.96	0.75	0.16	0.0622	0.0605	- 2.7
92.20	4.23	2.10	0.80	0.17	0.0672	0.0684	+ 1.8
91.31	4.88	2.43	1.14	0.24	0.0975	0.0823	- 15.6
91.91	4.66	2.35	0.89	0.17	0.0760	0.0783	+ 3.0
91.29	4.89	2.44	1.14	0.24	0.0970	0.0827	- 14.7
90.53	5.38	2.68	1.17	0.24	0.1014	0.0946	- 6.7
89.07	5.95	2.92	1.71	0.35	0.1490	0.1068	- 28.3
88.34	6.33	3.11	1.84	0.38	0.1610	0.1165	- 27.6
89.37	5.75	2.87	1.37	0.28	0.1268	0.1035	- 18.4

In view of these uncertainties, it is concluded that agreement between the Cormode data and the empirical expression is satisfactory. The manufacturers of the catalyst indicate that it varies in composition according to the source of the bauxite. The sample which Cormode used was received from the manufacturer one year earlier than the sample which was used in this study.

Using a catalyst of cobalt, molybdenum and alumina in a 1:1:10 ratio, Hammar [44] investigated the kinetics of the Claus reaction. This catalyst had a surface area of $291 \text{ m}^2/\text{g}$, a pore radius of 20.7 \AA and a pore volume of 0.301 cc/g . The catalyst was prepared using a precipitated alumina-water slurry in which $\text{Co}(\text{NO}_3)_2 \cdot 6\text{H}_2\text{O}$ and $(\text{NH}_4)_6 \cdot \text{Mo}_7\text{O}_{24} \cdot 4\text{H}_2\text{O}$ salts were dissolved. After an unspecified period of vigorous mixing, the slurry was filtered and the filter cake was dried. Unfortunately, the grain size of the catalyst was not measured.

Since Hammar observed no severe reduction in the rate of the Claus reaction at conversions of H_2S high enough to cause capillary condensation in the catalyst pores, he concluded that the reaction takes place predominantly on the external surface. The same observation was also made in this investigation.

Without knowing the particle diameter of Hammar's catalyst it is virtually impossible to compare his results with this work in a quantitative way. This is because the units of the reaction rates which Hammar published were based on per unit mass of catalyst. If rate was given in terms of external area rather than mass, his data could be compared to this work. Nevertheless, it is notable that the

mechanistic rate equations which correlated the data of Hammar best also correlated our data better than most of the other proposed models.

CHAPTER VII

CONCLUSIONS AND RECOMMENDATIONS7.1 Performance of Equipment

The experimental apparatus used in the study of the Claus reaction functioned well in most respects. Reactor feed composition and flow rate control were excellent, and feed and product composition analyses were satisfactory since the reactor material balance could be closed to within 2%. The repeatability of experiments was good as was discussed in Section 6.4. Catalyst bed temperature could be maintained constant within $\pm 0.25^{\circ}\text{F}$ of the steady state average value. However it was difficult and time-consuming to operate the reactor at a prespecified temperature. Usually the bed temperature could be brought to within 2°F of the desired temperature and this margin decreased after more operating experience to 1.5°F .

The recycle pump proved to be very reliable after at least six months of construction and development time had been spent. High temperature gas-recycle reactors should be designed to avoid making use of heated gas-moving equipment. If possible the gas should be cooled before entering the pump and heated upon leaving so that the blower can operate at room temperature. In this project such an approach would have permitted the use of a commercially available blower and resulted in considerable saving of time and effort. Unfortunately,

this method could not be used since it was necessary that sulfur not condense at any point in the recycle reactor.

7.2 Evaluation of Measured Rate Data

The rate data measured on the Claus reaction were curve-fitted to four empirical rate equations. In the experimental program, forward reaction rates have been measured in the presence of H_2S and SO_2 partial pressures which vary from 12 mm Hg to 62 mm Hg and 10 mm Hg to 45 mm Hg respectively. This covers the range of industrial importance for modified Claus sulfur plants in which H_2S partial pressure rarely exceeds 70 mm Hg in the first catalytic converter.

It has been confirmed that the reverse Claus reaction is important since at high water partial pressure the measured reaction rate was substantially lower than rates measured under similar experimental conditions except for lower water partial pressure. This is in agreement with the work of Molyneux et al [62] which is discussed in Section 2.2.2. Hammar [44] has given a qualitative indication that increased sulfur vapor partial pressure severely retards the forward rate of the Claus reaction.

In sulfur plants, water vapor partial pressure approaches 250 mm Hg. The experimental water injection apparatus when operated at full capacity provided water vapor partial pressure of only 120 mm Hg. In view of the retarding effect of water, which is quantitatively apparent in the rate expressions described in Section 6.8.1 and Figure 6.6, and of sulfur vapor, the Claus reaction kinetic studies reported

herein cannot be regarded as being complete. More investigation is required to quantify the inhibition effects of water and sulfur vapor in a study which spans industrial conditions. Only then can a reliable rate expression be developed which is satisfactory for sulfur plant reactor design. Later in this chapter, a discussion is presented which advocates the use of a different catalyst for sulfur plant converters.

The Claus reaction kinetic data of Cormode [15] was the only previous work available with which one of the rate expressions developed in this study was quantitatively compared. The standard percent deviation between rates measured by Cormode and rates predicted by the rate expression was 16%. Generally, the data of Cormode measured higher than the predicted rate.

No direct comparison of rate data could be made with the results of Hammar [44] since it was proven in both studies that reaction was taking place predominantly on the external catalyst surface and no particle diameter data was published along with the kinetic data measured by Hammar. The Langmuir-Hinshelwood kinetic models which correlated his data best also fitted the kinetic data of this study better than many of the other attempted models.

Experimental reaction rate measurements were made between 481°K and 560°K which spans reported industrial converter operating temperatures. The activation energy for the forward reaction was 7600 calories per gram mole. This was determined by correlating the rate

measurements to the following rate expression,

$$r = k_1 \text{Exp}(-E_1/RT) p_A^m p_B^n .$$

There has been no nonisothermal Claus reaction rate data reported in the literature from which an activation energy could be calculated and compared to the value reported herein.

It is concluded that the empirical rate expressions, which summarize the kinetic data obtained in this project, provide reaction rate estimates for the Claus reaction which would fall within the standard deviation band reported for each rate expression. The basis for making this conclusion is that reaction rate values predicted by one of the expressions agreed with the rate measurements of Cormode within its standard deviation band.

7.3 Reaction Mechanism

Deo et al [24] propose that the function of the catalyst may be to bring the reactants together in a suitable orientation, most probably through hydrogen bonding. No inferences have been made from this work which would dispute this mechanism and some of the observations support it.

The data could be correlated to empirical rate expressions which have a theoretical basis in the Freundlich adsorption isotherm at low surface coverages. This is discussed in Section 2.3. Although there is most probably a high coverage of hydrogen bonded H_2S and SO_2

to surface hydroxyl groups, the fraction of these which assume the proper orientation for reaction would likely be very low. It is concluded that this surface situation simulates sparse surface coverage and validates the use of Freundlich adsorption isotherms for formulating rate equations.

The apparent activation energy of 7589 calories per mole is inside the range of hydrogen bond energies which span 2. to 10. kilocalories per mole [48]. This leads to the conclusion that the apparent activation energy could be close to the energy required for forming the hydrogen bonds which Deo et al [24] report and tends to support their hypothesis for the reaction mechanism.

At low partial pressures (<10mm Hg) water vapor appeared to be exerting a slight auto-catalytic effect on the reaction and at higher partial pressures (> 20 mm Hg) water vapor was retarding the Claus reaction. This phenomenon was discussed in Sections 2.2.5 and 6.7. Briefly, water forms surface hydroxyl groups on alumina (the principle constituent of bauxite) which is dehydroxylated and subsequently after no more groups can be formed on the surface [74] hydrogen bonds to them. The observed effect of water on the Claus reaction is explained as follows. At low partial pressures (and fractional conversions of H_2S) its presence is promoting the formation of surface hydroxyl groups which serve as reaction sites for H_2S and SO_2 . At high partial pressures, water competes with H_2S and SO_2 for these sites and thus retards the reaction.

7.4 Evaluation of the Catalyst

Activated bauxite catalyst is employed by a majority of modified Claus sulfur plants in their catalytic converters. The practical problems which have been experienced are attributable to low mechanical strength and high iron content [16, 62] which is characteristic of most commercial bauxite catalyst. The lack of mechanical strength permits catalyst fines to form while converter beds are filled and subsequently these fines plug process piping [16]. Bauxite does not stand up satisfactorily to regeneration because heating it to 1000°F at 1 atm, which is necessary for regeneration, causes further loss of mechanical strength and substantial particle disintegration [62]. The regeneration process is essentially a controlled sulfur burning process. The iron in bauxite will sulfate under sulfur plant operating conditions, and the iron sulfate causes the γ -alumina to sulfate resulting in a loss of activity [62]. It is therefore concluded that high iron content bauxite should not be used as Claus sulfur plant catalyst and that grades of bauxite which exhibit superior mechanical strength are preferable.

In Section 6.6 data were presented which showed that the Claus reaction was taking place predominately on the external surface of the catalyst. Hammar [44] concluded that the same situation prevailed on the cobalt-molybdenum-alumina catalyst which he used for studying the Claus reaction. In both cases, most of the pores had diameters between 20 Å and 30 Å. It is therefore concluded that the catalyst effectiveness factor was well below 1% for the bauxite

and that pore diameters far greater than 30 \AA^0 would be a necessary prerequisite for a catalyst to have significant usage of its total available active surface.

7.5 Suggested Processing Scheme for Higher Sulfur Recovery

In view of available process technology and some of the findings of this work, the author suggests that the processing scheme which is shown in Figure 7.1 would be more effective for increasing sulfur recovery above currently attainable levels of conversion. Higher conversions are possible because the reaction product, water, is removed before the final converter which enables the reaction equilibrium to shift further to the right.

The scheme involves the combustion of H_2S to form SO_2 as is typical of most sulfur plants. Either the split stream flow or 2/3 by-pass flow scheme can be employed. Furnace effluent is fed to a small converter which should contain a cheap catalyst such as bauxite. The function of this catalyst bed is not only to promote the Claus reaction, but also to guard against carbon deposition in the second converter by retaining carbonaceous combustion products from the burning process. This first reactor should have the following design features: easy access to the catalyst bed for changing charges and, thermowells which probe deep enough into the bed to sense reaction temperature. When this catalyst is completely deactivated as indicated by bed temperature rise measurements, it should be replaced.

The second catalyst bed should contain a high quality alumina

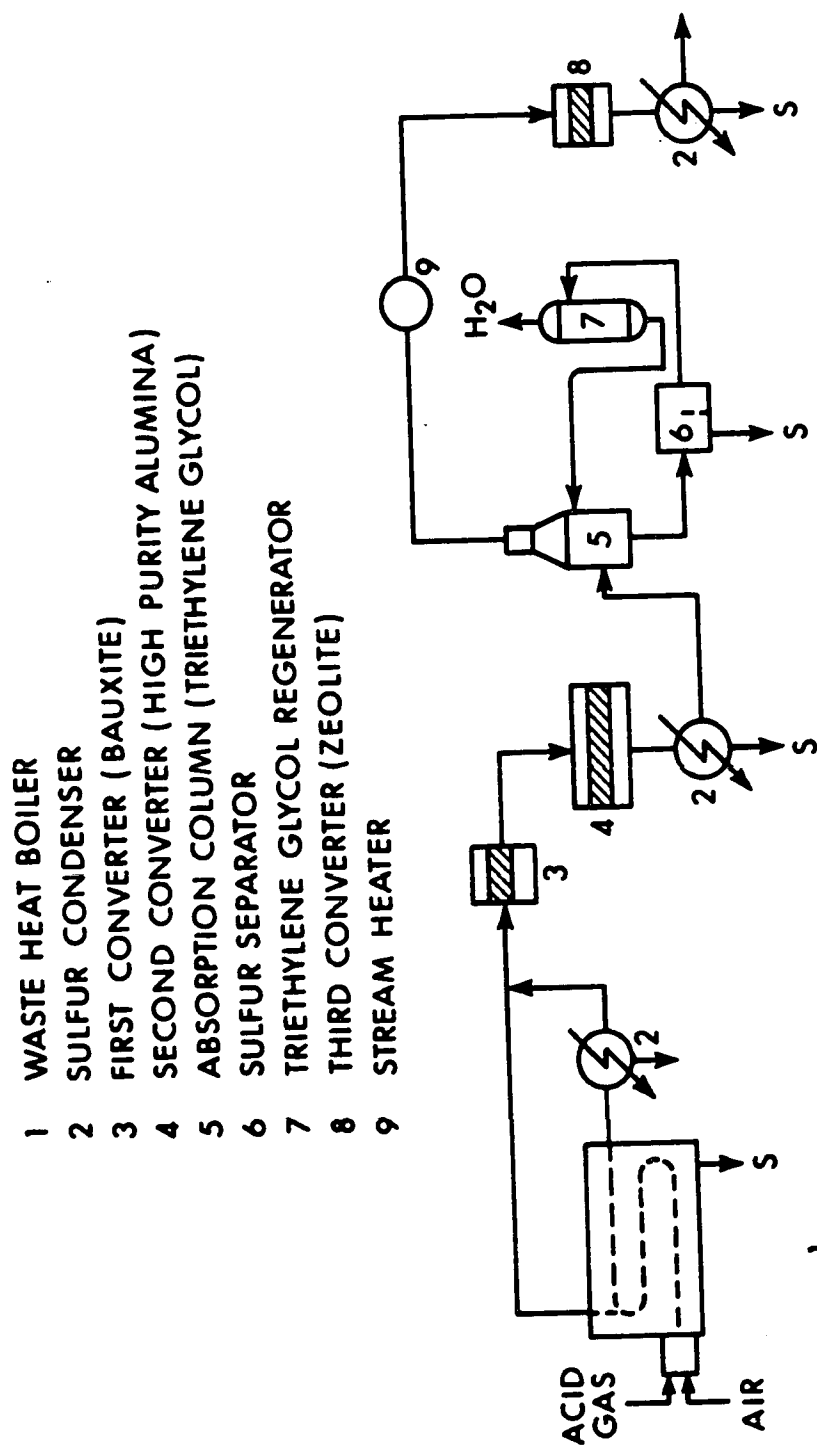


FIGURE 7.1: MODIFIED CLAUS-TOWNSEND PROCESS

catalyst such as the K-201 activated alumina recommended by Petrunic [90]. This should be a larger bed however, it would not tend to deactivate as rapidly as bauxite [90] most probably because of the lower iron content [62] which should be expected in a more expensive catalyst. From available process data [90], it appears that only the external surface of this catalyst is employed by the Claus reaction.

Water is next removed in the Townsend reactor which follows the second converter. This would be in the form of a sieve plate absorption column which would be designed for fouling service. Triethylene glycol would dehydrate the gas stream as it passed through the column and also promote the Claus reaction in the liquid phase. Steam produced in the waste heat boiler could be used for regenerating the triethylene glycol.

A final conversion unit on the plant would provide the final conversion step for the Claus reaction. A heater would be necessary to warm the reactants up before the final converter and it is suggested that an indirect-fired heater or a steam condenser be used for this service. In-line burners have been used in the past, but it is this author's opinion that they cause the formation of impurities such as CS_2 , COS and soot and water combustion products which unfavourably influence reaction kinetics, equilibrium and catalyst activity.

The catalyst in this final converter should be a large pore sized alumina (in excess of 150-200 Å) or perhaps a zeolite. It is anticipated that such a catalyst would be more than 100 times as active as bauxite since the internal surface area would be available for re-

action. It is not expected that severe heat transfer problems would develop because most of the H_2S would have been converted to sulfur in previous processing steps. Therefore a very dilute acid gas stream would be dealt with in this reactor.

Of course there are many unanswered questions about such a sulfur recovery scheme. The economics could make it prohibitive however it is anticipated that no stack or incinerator would be required for such a plant. In many cases, the stack accounts for 1/3 of the capital outlay for sulfur plants. Impurities such as COS, CO_2 or CS_2 could deactivate the triethylene glycol. Triethyleneglycol carry over into the zeolite catalyst bed could permanently poison it.

It is this approach that is necessary to significantly contribute to "high efficiency" (> 99.99%) sulfur recovery. Overall conversions of 95 and 96% are not sufficient for really large sulfur plants which produce 100 tons of sulfur per day. The unrecovered 4% of sulfur amounts to 8 tons per day of SO_2 emission and contemporary plant managers and ecologists are both agreeing that the solution to pollution is not dilution through the use of high, expensive stacks.

NOMENCLATURE

Symbol	Meaning
A	constant estimated by curve-fitting conversion-space time data
A_{EE}	external surface area of catalyst used in this experimental program (cm^2/gm)
A_{EP}	external surface area of catalyst to which rate expressions developed herein are applied (cm^2/gm)
a_{ij}	number of atoms of the jth kind in the ith specie
B	constant estimated by curve-fitting conversion-space time data
b_j	total number of atoms of the jth type
C	concentration (moles/ cm^3)
C_0	bulk stream concentration (moles/ cm^3)
D_{ij}	molecular diffusivity of component i in component j (cm^2/sec)
D_K	Knudsen diffusion coefficient (cm^2/sec)
d_p	particle diameter (cm)
E_1	activation energy (cal/gm mole)
F_{A0}	reactor feed rate of component A (gm mole/sec)
FF_i	reactor feed rate of component i (gm mole/sec)
FP_i	reactor product rate of component i (gm mole/sec)
$F(X)$	total system free energy (cal)

f	fugacity (mm Hg)
f_i	free energy of component i (cal)
G_M	molar velocity (gm mole/sec/cm ² of bed cross-section)
J	Danckwert's degree of segregation
K	adsorption equilibrium constant
k	constant
k_1	forward rate constant
k_{-1}	reverse rate constant
M_i	molecular weight of component i
m	order of reaction with respect to H ₂ S
N	diffusion flux (gm mole/sec/cm ²)
N_{Re}	Reynolds number
N_{Sc}	Schmidt number
n	order of reaction with respect to SO ₂
P	total pressure (mm Hg or atm)
P_i	partial pressure of component i (mm Hg or atm)
P_i^0	saturated vapor pressure of component i (mm Hg or atm)
P_i^s	vapor pressure of component i at solid surface (mm Hg or atm)
p	order of reaction with respect to H ₂ O
Q	total feed rate to reactor
R	gas constant (1.98 cal/gm mole/°K)
R'	recycle ratio (ratio of recirculation flow rate to reactor feed flow rate)
r	reaction rate (gm mole/hr/gm catalyst)
r_k	Kelvin radius (cm)

\bar{r}	measured reaction rate (gm mole/hr/gm catalyst)
S	total surface area of porous catalyst (cm^2/gm)
T	temperature ($^{\circ}\text{K}$)
t	time (sec or hr)
V_g	geometric volume of catalyst pellet (cm^3)
v_i	molar volume of component i (cm^3)
v_a	volume adsorbed (cm^3)
v_m	volume adsorbed to form a monolayer (cm^3)
W	weight of catalyst (gm)
X'	fractional conversion
X_{A1}	fractional conversion of component A before catalyst bed
X_{Af}	fractional conversion of component A after catalyst bed
x'	C/C_0
x_i, y_i	number of moles or mole fraction of component i (depending on application)
\bar{x}, \bar{y}	total number of moles
ΔH	heat of reaction (K cal/gm mole)
θ	porosity (void fraction)
θ'	recycle reactor residence time (sec)
θ_i	fraction of solid surface covered by component i
μ	chemical potential
ρ'	distance from centre of catalyst pellet (cm)
ρ_0	catalyst pellet radius (cm)
σ	surface tension (dyne/cm)

σ_{12}	Lennard Jones force constant
τ	tortuosity
Ω	collision integral for diffusion
\bar{v}	molar volume of liquid (cm ³ /g mole)

BIBLIOGRAPHY

1. Anderson, J.B., Chem. Eng. Sci., 18, 147, (1963).
2. Anon., Can. Pet., 7, No. 2, 37, (1966).
3. Anon., Hydro. Proc., 46, 225, (1967).
4. Anon., The Laboratory, 36 7, (1968).
5. Berkowitz, J., and Marquart, J.R., J. Chem. Phys., 39, 275, (1963).
6. Boudart, M., Ph.D. Thesis, Princeton University, Princeton, New Jersey, 1950.
7. Bradshaw, R.D., and Davidson, B., Chem. Eng. Sci., 24, 1519 (1969).
8. Braune, H., Peter, S., and Neveling, V., Z. Naturforsch, 6a, 32, (1951).
9. Butt, J.B., Bliss, H., and Walker, C.A., A.I.Ch.E.J., 8, 42, (1962).
10. Cameron, D.J., and Beavon, D.K., "Problems in the Design of High Efficiency Sulfur Plants", paper presented at the February, 1970 meeting of the Canadian Natural Gas Processing Association, Edmonton, Alberta.
11. Carmassi, M.J., and Zwilling, J.P., Hydro. Proc., 46, 117, (1967).
12. Claus, C.F., British Patent 5958, Dec. 31, 1883.
13. Cluzel, C., Ann. Chim. Phys., 84, 162, (1812).
14. Chowdhury, J.K., and Datta, R.M., J. Indian Chem. Soc., 20, 253, (1943).

15. Cormode, D.A., M.Sc. Thesis, Department of Chemical and Petroleum Engineering, University of Alberta, Edmonton, Alberta, 1965.
16. Cunliffe, R.S., "Optimizing Conversion of Hydrogen Sulfide to Sulfur", paper presented at the 19th Canadian Chemical Engineering Conference and Third Symposium on Catalysis, Edmonton, Alberta, October, 1969.
17. Dalla Lana, I.G., presentation at the February, 1969 Sulphur Symposium, Calgary, Alberta.
18. Daniels, F., and Alberty, R.A., "Physical Chemistry", 2nd Ed., Chapter 12, John Wiley and Sons, Inc., New York, N.Y., 1961.
19. Danckwerts, P.V., Chem. Eng. Sci., 8, 93, (1958).
20. Davidson, B., and Thodos, G., A.I.Ch.E.J., 10, 568, (1964).
21. Deal, C.H., Derr, E.L., Papadoupoulas, M.N., and Wilson, G.M., U.S. Pat. 3284162, 1966.
22. Deer, W.A., Howie, R.A., and Zussman, J., "Rock Forming Minerals", Chapter 3, William Clowes and Sons Ltd., London, 1962.
23. DeGerminy, M., private communication, May, 1970.
24. Deo, A.V., Dalla Lana, I.G., and Habgood, H.W., paper presented at the 19th Canadian Chemical Engineering Conference and Third Symposium on Catalysis, Edmonton, Alberta, October, 1969.
25. DeRosset, A.J., Finstrom, C.G., and Adams, C.J., J. of Catalysis, 1, 235, (1962).
26. Dohse, H., Z. Physik. Chem., Abt. B, 6, 343, (1930).

27. Doumani, T.F., Deery, R.F., and Bradley, W.E., Ind. Eng. Chem., 36, 329, (1944).
28. Estep, J.W., McBride, G.T., and West, J.R., "Advances in Petroleum Chemistry and Refining", Ed., McKetta, J.J., Chapter 7, Vol. 6, 1962.
29. Estep, J.W., and McBride, G.T., "Economics of the Sour Gas Industry", seminar presented at the University of Alberta, Edmonton, Alberta, 1967.
30. Fisher, R.A., and Smith, J.M., Ind. Eng. Chem., 42, 704, (1950).
31. Forney, R.C., and Smith, J.M., Ind. Eng. Chem., 43, 1841, (1951).
32. Frankenburg, W.G., J. Am. Chem. Soc., 66, 1827 (1944).
33. Freeport Sulfur Company, An. Chem., 37, 1065, (1965).
34. Gamson, B.W., U.S. Patent 2594 194, April, 1952.
35. Gamson, B.W., and Elkins, R.H., Chem. Eng. Prog., 49, 203, (1953).
36. Gibbs, J.W., "Collected Works", Vol. 1, 55, Longmans, Green and Company, Inc., New York, N.Y., 1931.
37. Gillespie, B.M., and Carberry, J.J., Ind. Eng. Chem. Fund., 5, 164, (1966).
38. Gilliland, E.R., Baddour, R.F., and Russell, J.L., A.I.Ch.E.J., 4, 90, (1958).
39. Goar, B.G., Hydro. Proc., 47, 248, (1968).
40. Greke?, H., Oil Gas J., 57, 76, (1959).
41. Grekel, H., Kunkel, L.V., and McGalliard, R., Chem. Eng. Prog., 61, 70, (1965).

42. Haines, H.W., VanWielingen, G.A., and Palmer, G.H., Hydro. Proc., 40, 123, (1961).
43. Hair, M.L., "Infrared Spectroscopy in Surface Chemistry", 141, Marcel Dekker, Inc., New York, N.Y., 1967.
44. Hammar, B.G.G., Doktorsavhandling, Chalmers Tek. Högskola, No. 14, 166, (1957).
45. Haywood, R.W., "Thermodynamics Tables in SI (metric) Units", 2, Cambridge University Press, 1968.
46. Heldt, K., and Haase, G.Z., Angew. Phys., 6, 157, (1954).
47. Herdon, L., Morningstar, E., Sawyer, E., and Hadner, R., Ind. Eng. Chem., 42, 1938, (1950).
48. Hildebrand, J.H., Scott, R.L., "The Solubility of Nonelectrolytes", 171, Dover Publications, Inc., New York, N.Y., 1964.
49. Hirschfelder, J.O., Curtiss, C.F., and Bird, R.B., "Molecular Theory of Gases and Liquids", John Wiley and Sons, New York, N.Y., 1954.
50. Hudgins, R.R., Chem. Eng. Sci., 20, 587, (1965).
51. Imai, T., M.Sc. Thesis, University of Alberta, Edmonton, Alberta, 1967.
52. Johnson, H.E., Kelley, M.D., and McKinley, D.L., Ind. Eng. Chem., 42, 2298, (1950).
53. Johnson, S.M., White, W.B., Dantzic, G.B., J. Chem. Phys. 28, 751 (1958).

54. Kammermeyer, K.A., and Rutz, C., Chem. Eng. Prog. Symposium Series, 55, 163, (1959).
55. Kelley, K., U.S. Bur. Mines, Bull. 406, (1937).
56. King, E.J., "Qualitative Analysis and Electrolytic Solutions", Chapter 1, Harcourt, Brace and Company, New York, N.Y., 1959.
57. Kohl, A.L., and Riesenfeld, F.C., Chem. Eng., 66, 151, (1959).
58. Korobeinichev, O.P., Kinetika i Kataliz, 8, 471, (1967).
59. Kubert, B.R., and Stephanou, S.E., "Kinetics Equilibria and Performance of High Temperature Systems", ed., Bahn, G.S., and Zukoski, E.E., Chapter 4, Butterworths, London, 1960.
60. Kubota, H., Akehata, T., and Shindo, M., Can. J. Chem. Eng., 39, 64, (1961).
61. Laidler, K.J., "Catalysis", ed., Emmett, P.H., Chapters 3, 4, and 5, Reinhold Publishing Corporation, New York, N.Y., 1954.
62. Landau, M., Molyneux, A., and Houghton, I. Chem. E., Symposium Series No. 27, (1968).
63. Langmuir, I., J. Am. Chem. Soc., 38, 221, (1916).
64. Lapidus, L., and Bard, Y., Cat. Rev., 2, 67, (1968).
65. Leinroth, J.P., and Sherwood, T.K., A.I.Ch.E.J., 8, 42, (1962).
66. Levenspiel, O., "Chemical Reaction Engineering", 452, John Wiley and Sons, Inc., New York, N.Y., 1964.
67. Levy, A., and Merryman, E.L., Comb. Flame, 9, 229, (1965).
68. Levy, A., and Merryman, E.L., J. Eng. Power, 87, 374, (1965).
69. Levy, A., and Merryman, E.L., J. Air Pollution Cont. Assoc., 17, 800, (1967).

70. Levy, A., and Merryman, E.L., Environ. Sci. and Tech., 3, 63, (1969).
71. Lewis, G.N., and Randall, M., "Thermodynamics and the Free Energy of Chemical Substances", McGraw-Hill Book Company, Inc., New York, N.Y., (1923).
72. Little, L.H., "Infrared Spectra of Adsorbed Species", 180, Academic Press, New York, 1966.
73. Lyderson, A.L., Greenkorn, R.A., and Hougen, O.A., University of Wisconsin, Eng. Expt. Station, Report 4, 1955.
74. MacIver, D.S., Tobin, H.H., and Barth, R.T., J. Catalysis, 2, 485, (1963).
75. Matheson Gas Data Book, 4th Edition, Herst Litho Inc., New York, N.Y., 1966.
76. Meissner, H.P., Kusik, C.L., and Dalzell, W.H., Ind. Eng. Chem. Fund., 8, 659, (1969).
77. Mezaki, R., Kittrell, J.R., Can. J. Chem. Eng., Oct., 285, (1966).
78. Mungen, R., and Grekel, H., "Pan American's Direct Oxidation Sulfur Recovery Process", paper presented at the Natural Gas Symposium of the Chemical Institute of Canada, June, 1966.
79. Murthy, A.R., and Rao, S.B., Proc. Ind. Acad. Sci., 34A, 283, (1951).
80. Nabor, G.W., and Smith, J.M., Ind. Eng. Chem., 45, 1272, (1953).
81. Obermiller, E.L., and Charlier, G.O., J. Gas Chrom., 6, 446, (1968).

82. Opekar, P.C., and Goar, B.G., Hydro. Proc., 45, 181, (1966).
83. Oliver, R.C., Stephanou, S.E., and Baier, R.W., Chem. Eng., 69, 121, (1962).
84. Patton, J.K., and Henderson, D.R., Oilweek, 17, No. 49, 48 (1967).
85. Paeri, J.B., J. Phys. Ech., 69, 220, (1965).
86. Perkins, T.K., and Rase, H.F., A.I.Ch.E.J., 4, 351, (1958).
87. Peterson, E.E., Chem. Eng. Sci., 17, 987, (1962).
88. Peterson, E.E., Chem. Eng. Sci., 20, 587, (1965).
89. Peterson, E.E., Chem. Eng. Sci., 23, 94, (1968).
90. Petrunic, A., Petroleum Society of the Canadian Institute of Mining, Paper No. 6803, 1968.
91. Preuner, G., and Schupp, W.Z., Physik. Chem., 68, 129, (1909).
92. Riesenfeld, F.C., and Blohm, C.L., Hydro. Proc., 41, 123, (1962).
93. Rippin, D.W.T., I & EC Fundamentals, 6, 488, (1967).
94. Rosenbrock, H.H., and Storey, C., "Computational Techniques for Chemical Engineers", 64, Pergamon Press, Toronto, 1966.
95. Ryan, J.T., private communication, 1970.
96. Satterfield, C.N., and Sherwood, T.K., "The Role of Diffusion in Catalysis", Addison-Wesley Publishing Company, Inc., Reading, Mass., 1963.
97. Sawyer, F.G., Hader, R.N., Herdon, L.K., and Morningstar, E., Ind. Eng. Chem., 42, 1938, (1950).
98. Smith, J.M., "Chemical Engineering Kinetics", 244, McGraw-Hill Book Company, Inc., New York, N.Y., (1956).

99. Smith, J.M., and Van Ness, H.C., "Introduction to Chemical Engineering Thermodynamics", McGraw-Hill Book Company, Inc., New York, N.Y., (1959).
100. Smith, S.B., Hiltgen, A.X., and Juhola, A.J., Chem. Eng. Prog. Symposium Series, 55, 25, (1959).
101. Taylor, H.A., and Wesley, W.A., J. Chem. Phys., 31, 216, (1927).
102. Thomas, J.M., and Thomas, W.J., "Introduction to the Principles of Heterogeneous Catalysis", Chapter 1, Academic Press, New York, N.Y., 1967.
103. Townsend, F.M., and Reid, L.S., Hydro. Proc., 37, 263, (1958).
104. Udintseva, V.S., and Chufarov, G.I., J. Chem. Ind., (USSR), 17, 24, (1940).
105. Valdes, A.R., Hydro. Proc., 43, 104, (1964).
106. Valdes, A.R., Hydro. Proc., 44, 223, (1965).
107. Weisz, P.B., and Prater, C., Adv. in Catalysis, 6, 143, (1954).
108. White, W.B., Johnson, S.M., and Pantzig, G.B., J. Chem. Phys., 28, 751, (1958).
109. Zeldowitch, J., Acta. Phys. Chim., URSS, 1, 961, (1935).
110. Zeleznik, F.J., and Gordon, S., Ind. Eng. Chem., 60, 27, (1968).
111. Zweitering, T.N., Chem. Eng. Sci., 11, 1, (1959).
112. McBride, B.J., Heimerl, S., Ehlers, J.G., and Gordon, S., "Thermodynamic Properties to 6000°K for 210 substances involving the first 18 Elements", NASA, 1963.

PART II

ONLINE DATA ACQUISITION AND PROCESSING

ACKNOWLEDGEMENT

The author again wishes to thank Dr. I.G. Dalla Lana for his patience and supervision which were necessary for this part of the program. The valuable assistance of the personnel of the Data Acquisition, Control and Simulation Centre under the supervision of Dr. D.G. Fisher and Mr. H. Ramstead is also gratefully acknowledged.

TABLE OF CONTENTS

	<u>Page</u>
CHAPTER I	INTRODUCTION
1.1	Data Acquisition and Control 173
1.2	Objectives and Approach of this Work 174
CHAPTER II	ONLINE DATA ACQUISITION FROM THE RECYCLE REACTOR
2.1	Communication Between the Computer and the Laboratory 176
2.2	Recycle Reactor-Computer Interface 178
2.3	Software Schemes 185
2.3.1	Software Implementation of Data Acquisition 185
2.3.1.1	Loop Records 185
2.3.2	Supervisory Software 186
2.3.3	Gas Chromatograph Monitoring Program 195
CHAPTER III	OPERATION OF THE RECYCLE REACTOR ONLINE 200
CHAPTER IV	PRESENTATION AND DISCUSSION OF RESULTS 203
CHAPTER V	CONCLUSIONS AND RECOMMENDATIONS 205
BIBLIOGRAPHY	206
APPENDIX	ONLINE DATA ACQUISITION AND REDUCTION PROGRAMS II-A1

LIST OF TABLES

<u>Table</u>		<u>Page</u>
2.1	Computer Interface Points	180
2.2	Data Acquisition Loop Records - Description	187
2.3	Data Acquisition Loop Records - Listing	189
2.4	Data Acquisition Loop Records - Description	190
2.5	Data Acquisition Loop Records - Listing	191
2.6	Loop Record Names and Purposes	192
2.7	Signal Derivative Behaviour with GC Peak Events	198

LIST OF FIGURES

<u>Figure</u>		<u>Page</u>
2.1	Flow of Information Between the Process and the Data Acquisition System	177
2.2	Thermocouple-Computer Interface	179
2.3	Foxboro Recorder-Computer Interface	179
2.4	Electrical Diagram of Computer-Button-Interface	182
2.5	Electrical Diagram of Computer-GC Programmer Interface	184
2.6	Relationship Between Chromatograph Peak and the Curve Derivatives	197

CHAPTER I

INTRODUCTION1.1 Data Acquisition and Control

The use of online digital computers for process monitoring and control in industrial and research applications is a very rapidly expanding field. Fortunately, even in its infancy, online computer technology is being described extensively in the literature.

Fehr (3) reported, in his M.Sc. thesis, numerous literature references concerned with practical problems that online computers pose such as online computer-process interfacing and data acquisition and control software. This thesis provides an excellent starting-point for an introduction to this subject.

In the realm of online computer applications in laboratory work, the analytical chemist is adapting and using this new tool with success and enthusiasm. A recently published monograph (4), "Computers in Analytical Chemistry", reports on laboratory computers and their use in the field of mass spectrometry, X-ray spectography, NMR spectrometry, gas chromatography and infrared spectrometry. A wealth of information is available from the articles and bibliographies which comprise this textbook.

A 1968 staff article in Chemical Processing reports that an Argus 400D computer has been successfully interfaced to a research reactor for studying the thermal cracking of carbon tetrachloride. The function of the computer was to bring the experimental equipment to pre-

specified operating conditions and maintain it there while measurements were being taken. Controlled variables included reaction temperature and pressure, individual feed rates to the reactor, and the operation program of a process gas chromatograph. Only the product stream composition was measured by the GC whose thermal conductivity signal was monitored three times per second.

1.2 Objectives and Approach of this Work

The objective of this study was to provide a process/computer interface and software scheme whereby kinetic data for the $\text{H}_2\text{S}/\text{SO}_2$ reaction systems could be obtained accurately, online and reduced to meaningful results within seconds of the completion of an experiment. Furthermore it was also hoped to demonstrate the operation of an online reactor and to provide a basis for evaluating the feasibility of using it extensively in future research endeavours.

The approach taken aimed at achieving these objectives as simply as possible. Communication from the research laboratory to the computer was made possible through the use of four coding buttons and a fifth one for interrupting the computer. Information from the computer was printed out on an IBM 1053 typewriter located in the laboratory.

The interface hardware involved terminal strips on the back of the main control module on the stand alone system connected by an appropriate cable to the back of the computer. The cable distance covered roughly 300 feet through two inch conduit.

The software for data reduction was almost the same as for

the offline data reduction programs and therefore only minor programming changes were necessary in adapting the latter to online needs. Additional programs were necessary for reading the coding buttons, queuing the appropriate data reduction program, storing raw and reduced data on disk files, file housekeeping, and providing information flow to the laboratory typewriter. An IBM-developed gas chromatograph monitoring package of programs was found to be unworkable after substantial effort by Mr. P. Coxhead, DACS centre personnel and this author. It was replaced by a more simple scheme originally devised by Mr. M.W. Berry (1) and modified for this application by the author.

CHAPTER II

ONLINE DATA ACQUISITION FROM THE RECYCLE REACTOR2.1 Communication Between the Computer and the Laboratory

A form of remote communication between the experimental apparatus and the IBM 1800 was essential since the two facilities were situated on different floors of the building. The nature of the experimental apparatus required the full-time presence of an operator if an experimental run was to be successful. It was also necessary to issue instructions to the computer during a run if online data acquisition and reduction was to be effective.

Four button switches for coding and a fifth one for interrupting the computer served as communication from the laboratory to the computer and provided the operator with fourteen different possible codings and associated programmeable commands. The backlight of the interrupt button would go on when the computer had begun to service the interrupt and would go out when the instruction coded on the other four button switches had been carried out.

An IBM 1053 typewriter was used primarily as a verification device which printed out messages in the laboratory. The printout from the 1053 indicated what instruction had been executed after an interrupt had been received by the computer from the laboratory. Also, the 1053 would print out a warning message if there had just been a computer failure of a severe nature. Figure 2.1 shows the flow of information between the process and the data acquisition system.

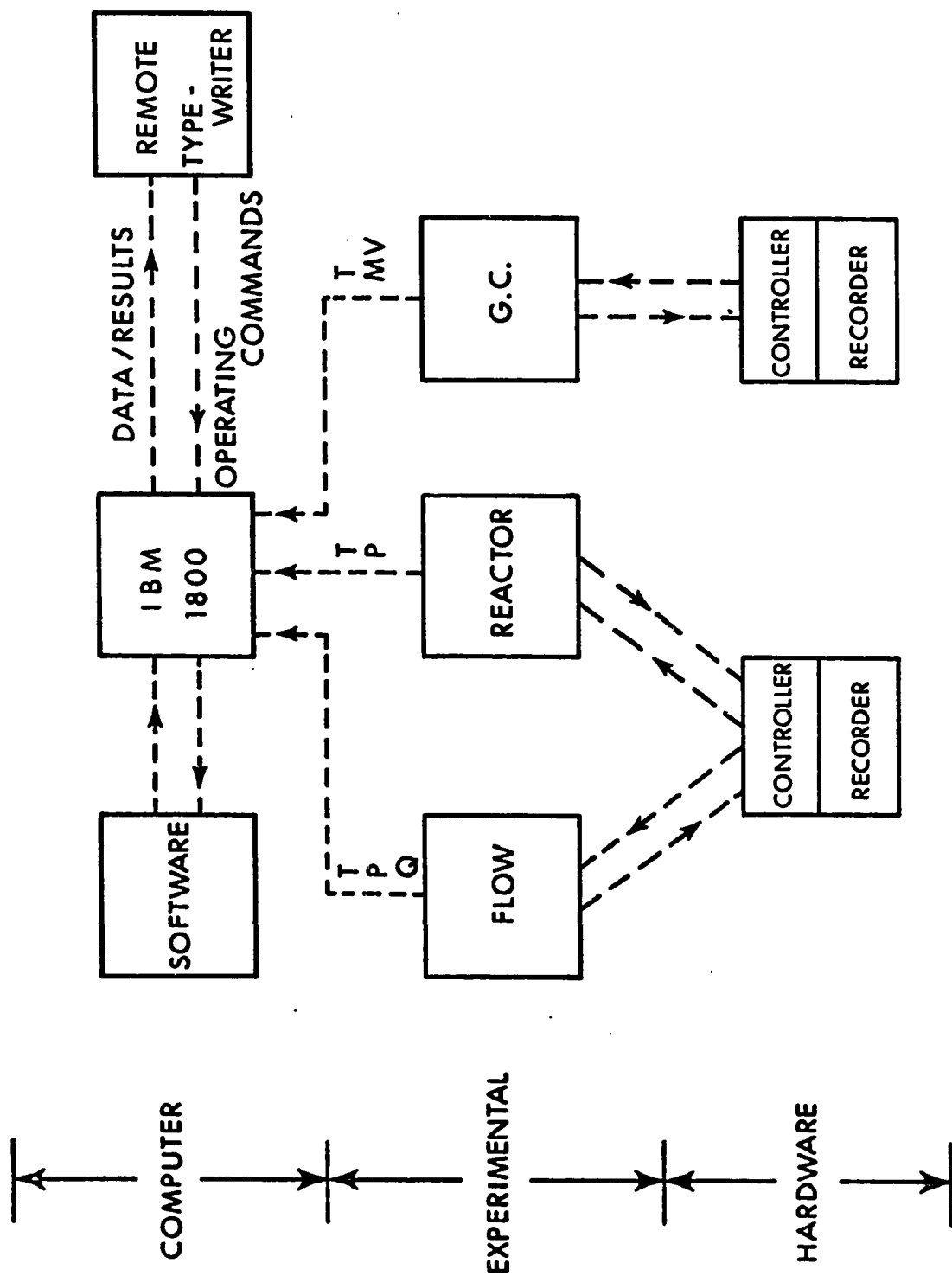


FIGURE 2.1: FLOW OF INFORMATION BETWEEN THE PROCESS AND THE DATA ACQUISITION SYSTEM

2.2 Recycle Reactor-Computer Interface

A nineteen individually twisted shielded-pair 22 gauge copper wire cable was run through two-inch conduit from the laboratory to the computer room, a distance of roughly 275 feet. A record of the connections which were made is given in Table 2.1.

Noise problems were not anticipated however, the following procedures were carried out to check if significant electrical interference did exist over the 300 feet between the two ends of the cable. Using a Leeds and Northrup model 8686 millivolt potentiometer, a one millivolt signal was placed on one of the pairs at the laboratory. In the computer room, another potentiometer was used to measure the signal. No fluctuations or drop in voltage of this signal was observed at the second potentiometer. Also in the computer room, this 1 millivolt dc signal was monitored by a high speed, high sensitivity Beckman model 6-D Dynograph for high frequency noise. Again, no electrical interference could be detected.

As indicated in Table 2.1, the process measurements to be monitored by the computer were millivolt signals in the 0-50 millivolt range and voltage signals in the 0-5 volt range. The millivolt channels were used for the iron-constantan thermocouple signals which were all zero referenced in the laboratory and sent up to the computer via copper wire. Figure 2.2 depicts the configuration of the thermocouple-computer interface. This approach was used instead of using the electronic zero referencing facility at the computer so that the use of thermocouple extension wire could be avoided. As a result, the cable could be used at a later date for any

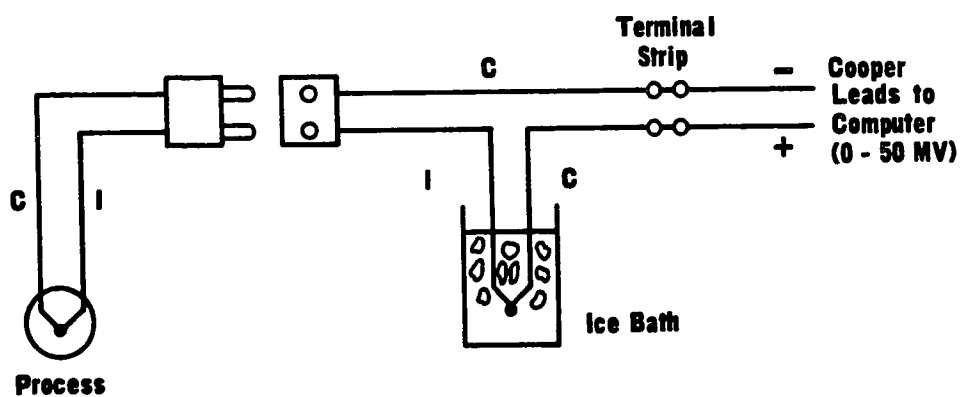


FIGURE 2.2: THERMOCOUPLE-COMPUTER INTERFACE

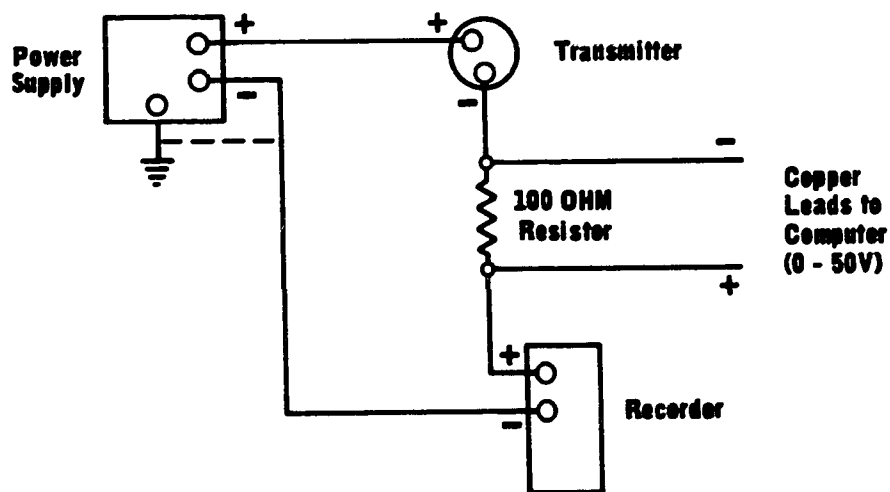


FIGURE 2.3: FOXBORO RECORDER-COMPUTER INTERFACE

Table 2.1
Computer Interface Points

<u>Computer Pin No.</u>	<u>Pin Description</u>	<u>Pin Address</u>	<u>Unit Serviced</u>	<u>Wire Colour</u>	
				<u>+ve</u>	<u>-ve</u>
02	0-20 MVAI	75	G.C. Detector	Red	Green
03	0-20 MVAI	67	Rctr. Bed Temp.	Blue	Black
05	0-20 MVAI	69	Rctr. Wall Temp.	Orange	Green
10	0-20 MVAI	74	Fl. Bath Temp.	Green	Black
60	0-50 MVAI	60	G.C. Temp.	Red	White
61	0-50 MVAI	61	Rctr. Feed Temp.	Blue	White
34	0-5 VAI	34	D/P Cell	Blue	Red
36	0-5 VAI	36	Abs. Press. Feed	Yellow	Red
37	0-5 VAI	37	Abs. Press. Rctr.	Yellow	Black
0	D3 (1801)	070	Code Button	Orange	Black
1	D3 (1801)	070	Code Button	Red	Brown
2	D3 (1801)	070	Code Button	Green	White
3	D3 (1801)	070	Code Button	Red	Orange
4	B3 (1826)	GP3ADP1	Interrupt Button	Brown	Black

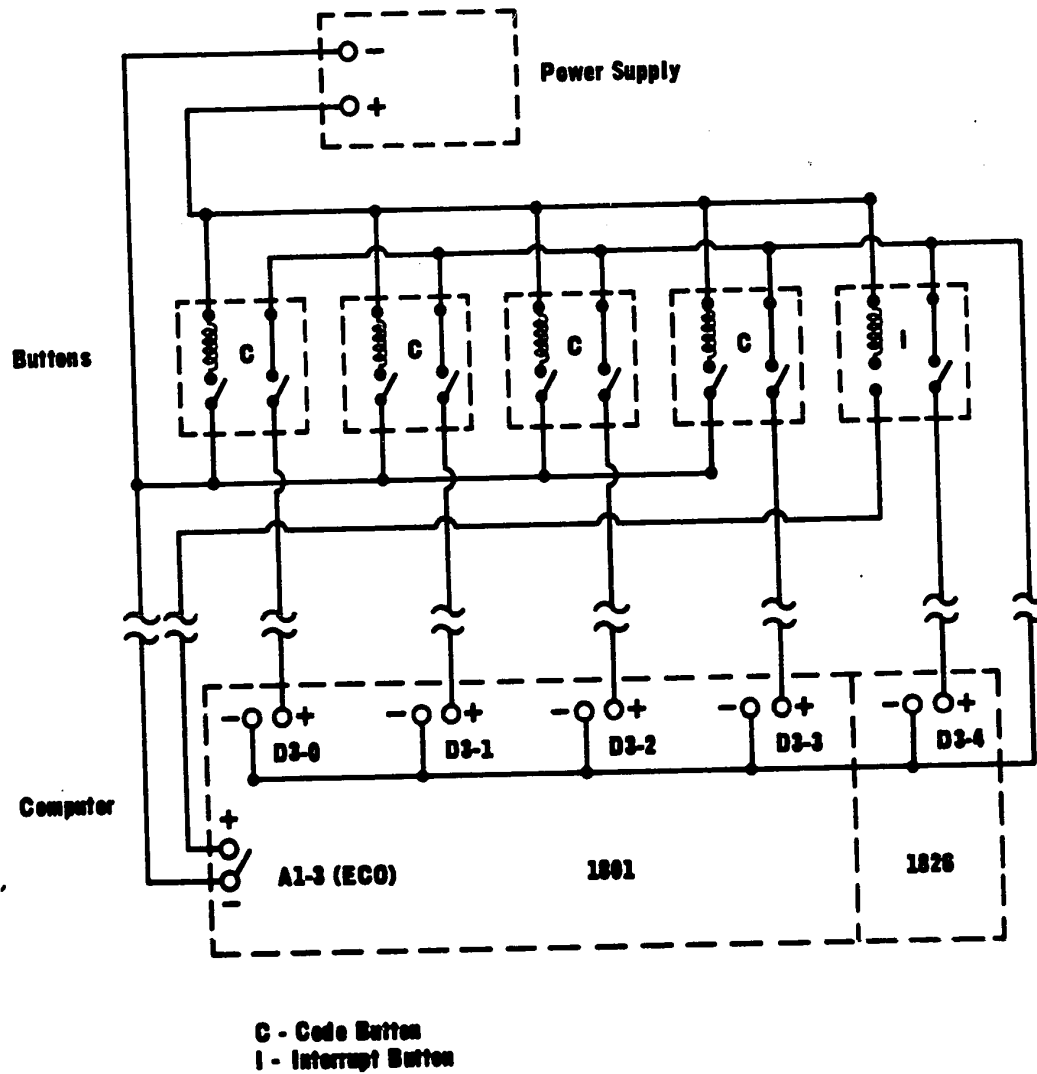


FIGURE 2.4: ELECTRICAL DIAGRAM OF COMPUTER-BUTTON INTERFACE

type of process measurement.

The 0-5 volt channels were used for monitoring the 10-50 milli-ampere signal which drives the Foxboro recorder pens. The procedure here was to place a 100 ohm resistor ($\pm 1\%$) in series with the signal and the voltage drop across the resistor (1-5 volts) was read by the computer. Figure 2.3 shows the configuration of this interface.

The five buttons which were used for communicating from the laboratory to the computer were interfaced to the computer as indicated in Figure 2.4. These were Honeywell 7A1CC alternate action two pole switches. The four coding buttons on the left in Figure 2.4 were wired so that the button back lights would illuminate when the button was depressed and the coding contact was made. The interrupt button light was wired to an electronic contact operate (ECO) unit on the computer so that the on-off status of this light could be programmed. A 20 volt 1 ampere capacity power supply unit was fabricated to provide current for the button lights.

The four coding buttons were tied into the first four bits of a digital input group on the computer. The fifth button was connected to an interrupt on the computer which when activated caused a program to read the coding on the other four buttons as well as close the circuit ECO which illuminated the light in the back of this button. When the program which corresponded to the button coding had finished its execution, the ECO was opened and the interrupt button light would go off. The computer pin labels and location are provided in Figure 2.4.

The output signal of the thermal conductivity cell in the gas chromatograph was wired to a 0-20 millivolt analogue input channel on the 1800. Accordingly, the attenuators on the process gas chromatograph were adjusted to prevent overdriving the maximum range of the channel.

For computer monitoring of a gas chromatograph, it was essential that the act of sample injection be tied into the monitor software on a real time basis that was reasonably repeatable. This was necessary because the user had to "a priori" specify to the monitor routine the absolute retention time of the reference peak and the time bands between which the peaks would come off. The real time linkage was achieved by making use of an ECO on the computer to close and open the circuit which initiated the motor drive on the gas chromatograph cam system programmer. An electrical diagram for this interface is shown in Figure 2.5. One of the cams on the programmer (timer control) closes another microswitch which sustains provision of power to the cam system motor drive after the ECO cuts out. At the end of the programmer cycle this microswitch opens and the cam system comes to rest at the same place from which the cycle was initiated. Only when the computer closes the ECO again will the cycle restart, and the time at which this occurs is known to the computer. Since sample injection is controlled at a specific point in the programmer cycle by a cam, the real time linkage was possible.

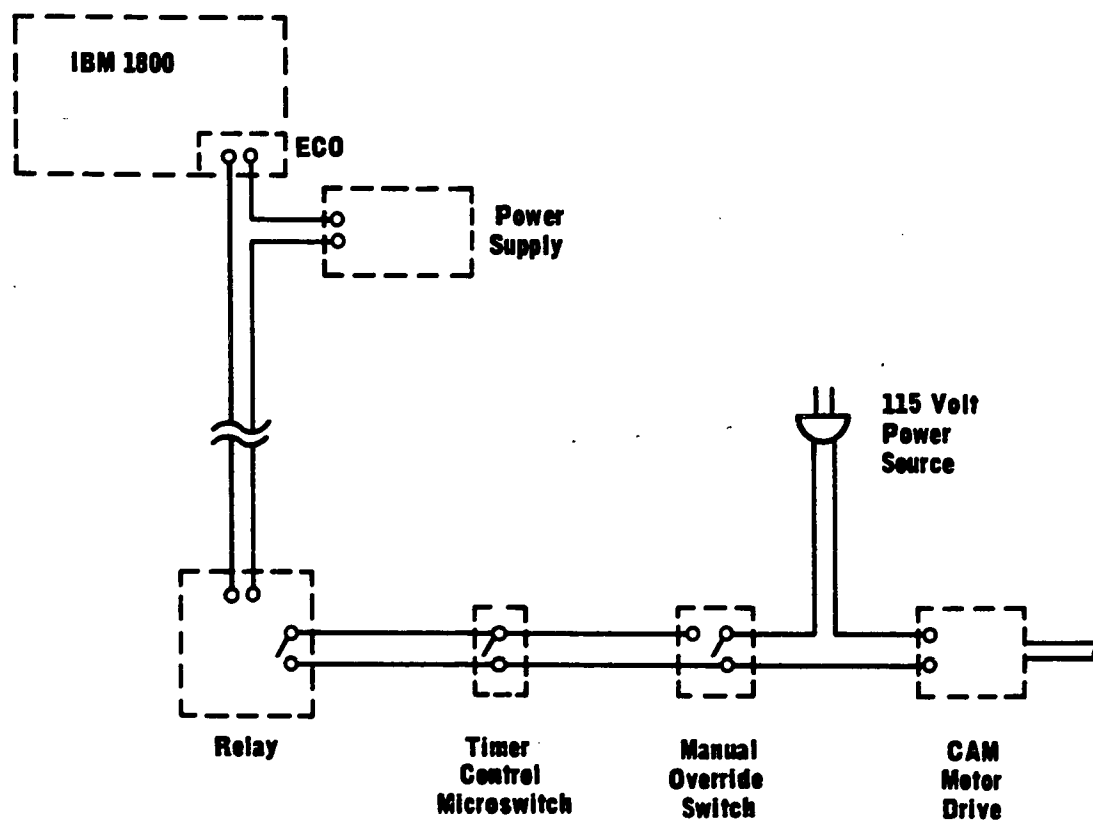


FIGURE 2.5: ELECTRICAL DIAGRAM OF COMPUTER-GC PROGRAMMER INTERFACE

2.3 Software Schemes

2.3.1 Software Implementation of Data Acquisition

Process measurements such as temperatures, absolute pressures, and orifice differential pressures were monitored every sixty-four seconds throughout the course of a run and a maximum of thirty data points per run could be stored. Only a small amount of user computer programming was required to institute data acquisition which was done through the use of loop records.

2.3.1.1 Loop Records

A loop record is the standard means by which the user can provide the computer with the specifications to be imposed on a control loop in a process or on computer monitoring of a process measurement. In the case of data acquisition, two loops can be used for each process variable to be measured. The first is a data acquisition loop which obtains the measurement and the second is a data accumulation loop in which a number of these measurements may be stored. A list of the information which the user supplies to the computer to "build a data acquisition loop" is given in Table 2.2. The coding which was used for this project is also included as well as the information specified by the coding. A computer listing of the eight data acquisition loops which were built is given in Table 2.3. Finally, the same approach is used to describe the data accumulation loops in Tables 2.4 and 2.5. Note that the example given for the data accumulation loop is the one which stores the measurements collected by the example used for a

data acquisition loop.

A documentation of the reactor/computer interface wiring is provided in Table 2.1 and Table 2.6 lists the loop record numbers and computer pin addresses which were applied to the process measurements taken from the recycle reactor. The scanning frequency of all process measurements was 64 seconds except for the thermal conductivity cell signal which was scanned every second.

2.3.2 Supervisory Software

Computer listings of all the software which was necessary are given in Appendix A. Two disk resident Fortran programs called DM001 and DM002 were developed to perform the tasks necessary to achieve online data acquisition and reduction capabilities in the user application sense. Both programs relied heavily on other system software which will not be dealt with extensively herein.

Three Assembler programs were written by the DACS centre staff to interface the laboratory coding buttons with DM001 and DM002. A skeleton subroutine called PNT05 responds to the laboratory interrupt button and queues PIC05. PIC05 reads the specified digital input group (i.e. the coding on the four coding buttons) and queues DM001 or DM002 dependent upon the value of the high order bit (i.e. the status of one of the coding buttons; on or off). The value of the remaining bits is saved for interrogation by BTNSW, which is the third program developed by the DACS center. BTNSW is queued by either DM001 or DM002 depending on which was queued by PIC05 and the value of the remaining bits (i.e. the

Table 2.2
Data Acquisition Loop Records - Description

<u>Word Number</u>	<u>Record Builder Form Name</u>	<u>Information Contained Therein</u>	<u>Coding Used</u>	<u>Information Specified by Coding</u>
00	ID	Name of loop record	0101	Record's name is 101
01	LPOUT ADCBT FLTYP ALGOP RECSZ	Loop status; operable or not Reading type Filter type Control algorithm type Number of words in the record	C00F	Loop operable ADC reading required No filter required No control algorithm Number of words is 15
02	POLLT FAZE INSUB INFRQ INDIT INHAL INHPR	Scan time = 2 POLLT seconds Phase time in seconds Calculation subroutine Time to execute subroutine Engineering units or percent Inhibit alarm; yes or no Inhibit printing, yes or no	600F	Scan time = 64 seconds Phase time = 0 seconds No subroutine used At poll time Engineering units Yes Yes
03	INMAD	Input multiplexer address	00067	Address is 67
04	CHECK FILCT	Filter status Filter constant	0000	No filter Filter constant = 0
05	EDTCH PUNIT INSW SAUD LPALM ALMOR LPMWT	Edit character position Input units Limit check or not Siren sounded or not Loop is or is not in alarm Alarm message originate Alarm message designation	9100	xx.xx Percent No limit check No siren sounded Disregard Disregard Disregard

Table 2.2 (continued)

Word Number	Record Builder Form Name	Information Contained Therein	Coding Used	Information Specified by Coding
06	CONA	Two times span in eng. units	+20000	Span is 100
07	CONB	B in $Y = \text{CONA} * X + B$ The equation is used for changing input-related values from machine to eng. units	0000	B = 0
08	MEAS	The most current input value	0000	Current input value = 0
09	SETPT	The setpoint of the loop	0000	Loop setpoint = 0
10	SPCHI SPCLO	Value of high setpoint Change limit and the low one	7FFF	No limits
11	ERRHI ERRLO	Value of high and low error limits	7FFF	No limits
12	FRAST ERADB ERAHI ERALO INBAD	Error alarm status Error deadband Hi error action instruction Lo error action instruction Bad input counter	3000	No alarm Error deadband = 10 No action for high error No action for low error No bad input
13	INHIL	Value of high input limit	7FFF	No limit
14	INLOL	Value of low input limit	0000	No limit
15	INAST INADB INAHIL INALO INCNT	Input alarm status Input deadband High input action instruction Low input action instruction Input out of limit counter	0000	No alarm Input deadband = 0.1 No action No action No out of limit input

Table 2.3

Data Acquisition Loop Records - Listing

010101	C00F	600F+00067	0000	9100+20000	0000	0000	0000	7FFF
010102	7FFF	3000 7FFF	0000	0000				
010201	C00F	600F+00069	0000	9100+20000	0000	0000	0000	7FFF
010202	7FFF	3000 7FFF	0000	0000				
010301	C00F	600F+00074	0000	9100+20000	0000	0000	0000	7FFF
010302	7FFF	3000 7FFF	0000	0000				
010401	C00F	600F+00060	0000	9100+20000	0000	0000	0000	7FFF
010402	7FFF	3000 7FFF	0000	0000				
010501	C00F	600F+00061	0000	9100+20000	0000	0000	0000	7FFF
010502	7FFF	3000 7FFF	0000	0000				
010601	C00F	600F+00036	0000	9100+20000	0000	0000	0000	7FFF
010602	7FFF	3000 7FFF	0000	0000				
010701	C00F	600F+00037	0000	9100+20000	0000	0000	0000	7FFF
010702	7FFF	3000 7FFF	0000	0000				
010801	C00F	600F+00034	0000	9100+20000	0000	0000	0000	7FFF
010802	7FFF	3000 7FFF	0000	0000				

Table 2.4

<u>Data Accumulation Loop Records - Description</u>			
<u>Word Number</u>	<u>Record Builder Form Name</u>	<u>Information Contained Therein</u>	<u>Coding Used</u> <u>Information Specified by Coding</u>
00	ID	Name of loop record	0111 Record's name is 111
01	LPOUT ADCBT ALGOP RECSZ	Loop status; operable or not Reading type Control algorithm type Number of words in the record	0625 Loop not operable No ADC reading required Data acquisition Number of words is 37
02	POLLT FAZE INSUB INFRQ VCODE	Scan time = 2 POLLT seconds Phase time in seconds Calculation subroutine Time to execute subroutine Source of reading	6008 Scan time = 64 seconds Phase time = 0 seconds No subroutine Calculate at poll time Measurement from loop INMAD
03	INMAD	Name of donor loop	0101 Donor loop is 101
04	These three words contain information such as the relative location of the last value stored in the loop, the time it was stored there and other specifications concerning buffering to disk. The coding for each word is 0000.		
05			
06			

Table 2.5
Data Accumulation Loop Records - Listing

011101	0625	6008	0101	0000	0000	0000
011201	0625	6008	0102	0000	0000	0000
011301	0625	6008	0103	0000	0000	0000
011401	0625	6000	0104	0000	0000	0000
011501	0625	6008	0105	0000	0000	0000
011601	0625	6008	0106	0000	0000	0000
011701	0625	6008	0107	0000	0000	0000
011801	0625	6008	0108	0000	0000	0000

Table 2.6

Loop Record Names and Purposes

<u>Loop Record Number</u>	<u>Computer Pin Address</u>	<u>Purpose of the Loop Record</u>
0101	67	Acquire reactor bed temperature
0102	69	Acquire reactor wall temperature
0103	74	Acquire fluidized bath temperature
0104	60	Acquire G.C. temperature
0105	61	Acquire feed temperature
0106	36	Acquire feed absolute pressure
0107	37	Acquire reactor absolute pressure
0108	34	Acquire feed d/p cell reading
0109		Acquire thermoconductivity cell signal
0111		Accumulate data from loop 0101
0112		Accumulate data from loop 0102
.		
.		
.		
0118		Accumulate data from loop 0108
0119		Accumulate data from loop 0109 and buffer to disk

coding on the buttons) is used to direct command to a particular part of the queued coreload for execution.

The tasks to which DM001 has access include supervision of loop records, disk files and reduction of process measurements and kinetic data. Dependent upon the laboratory button coding, the following commands are executed by DM001:

- (i) Turn loop records on
- (ii) Turn loop records off
- (iii) Extract data from accumulation records and files, reduce it, and store it on files
- (iv) Zero accumulation records
- (v) Execute data file house keeping procedures .

Turning a loop record on or off and zeroing an accumulation record are relatively simple to program by using system subroutines, OPER, NONOP and RSLP, respectively. The programming technique is available in the listing of DM001. Extraction of data from accumulation records involves the use FNDLP and LPAD system subroutines and an understanding of loop record configuration which must be learned from system documentation. Similarly, recovery of data from disk files and disk file housekeeping work can be programmed in Fortran by the user and the techniques are shown in the program listing.

The reduction of data which is performed by DM001 is calculated in virtually the same fashion as in the offline mode which has been described in Part I of this thesis. In fact, 90% of the offline

data reduction program has been incorporated into DM001 for this purpose. Calibration coefficients had to be altered for the online program and these were shown in Appendix A of Part I. The necessary GC data for data reduction were recovered from disk files and the way in which these data were determined is dealt with later.

The three disk files which were used will now be described. FILE 80 provided storage space for reduced analog measurement data which is recovered for run documentation when output is desired. FILE 81 was a temporary storage file for chromatogram area measurements. DM001 called on this file when in the process of data reduction. FILE 82 was a storage file for reduced kinetic data. DM006, which was another disk resident Fortran program, could be queued upon demand while in the computer room. This program would read the data files and print the run documentation on the line printer and punch the results on cards for future machine reproduction.

DM002 carried out the following operations, again depending on the button coding in the laboratory:

- (i) Initiate CG monitoring and control
- (ii) Terminate GC monitoring
- (iii) Label chromatogram results on disk files (i.e. feed or product)
- (iv) Indicate the attenuation level of the H_2S peak (N_2 and SO_2 attenuations were constant).

GC monitoring software was devised such that after it had been initiated,

the appropriate coreload would requeue itself every seven minutes which became the cycle time of the process GC. Termination of GC monitoring prevented this cycle from continuing. This software is dealt with later. After a GC run was completed, it was necessary to tell the computer which of the feed or product streams had been analyzed. This was done by entering the appropriate coding at the end of each GC run. Similarly the H₂S attenuation level was required for proper GC data analysis and this also was entered through the coding buttons.

Both DM001 and DM002 were programmed to type on the 1053 typewriter which was located in the laboratory. This was very useful for confirming that the operation which was requested by the coding buttons had actually been performed by the computer. Also, DACS centre personnel had a system program which would relay warnings to the laboratory typewriter if the computer was having stability problems which could jeopardize the success of online data acquisition and reduction of an experiment.

2.3.3 Gas Chromatograph Monitoring Program

As was stated in the Abstract, a reliable gas chromatograph monitoring package of programs was not available for this project. Mr. P. Coxhead, in his M.Sc. thesis (2), modified a generalized set of "IBM" written programs so that it would simultaneously monitor four gas chromatographs on the University of Alberta IBM 1800 computer. Pursuant to Mr. Coxhead's efforts, this author, with considerable assistance from University of Alberta DACS Centre personnel and an IBM systems

engineer, spent four months attempting to utilize the revised software. The effort was unsuccessful and IBM made the decision to commit themselves to reorganizing and condensing their GC software package which consisted of no fewer than 108 separate coreloads.

Independent of the IBM GC system, Mr. M.W. Berry (1) developed a GC monitoring scheme which was adequate for a particular distillation column control application, but was intolerably inaccurate for use in this author's kinetic study. The problem was that the highest attainable scanning frequency of the thermal conductivity cell signal was one point per second. A ten points per second scanning rate was necessary to achieve accurate integration of the N_2 and H_2S peaks, which were much sharper than those in Mr. Berry's application. However, his program was modified and adapted for demonstration purposes to the software scheme used in this study. The modified version was called DMGC.

Fundamental to integrating chromatogram peak areas while online is the necessity to provide the computer with the capability of recognizing the start and end of a chromatogram peak. This has been achieved by examining the derivatives of the thermal conductivity cell signal with respect to time. The relationships between a chromatogram peak and its derivatives are shown in Figure 2.6 and are self-explanatory. The behaviour of the derivatives are used to detect the beginning and end of a peak as shown in Table 2.7.

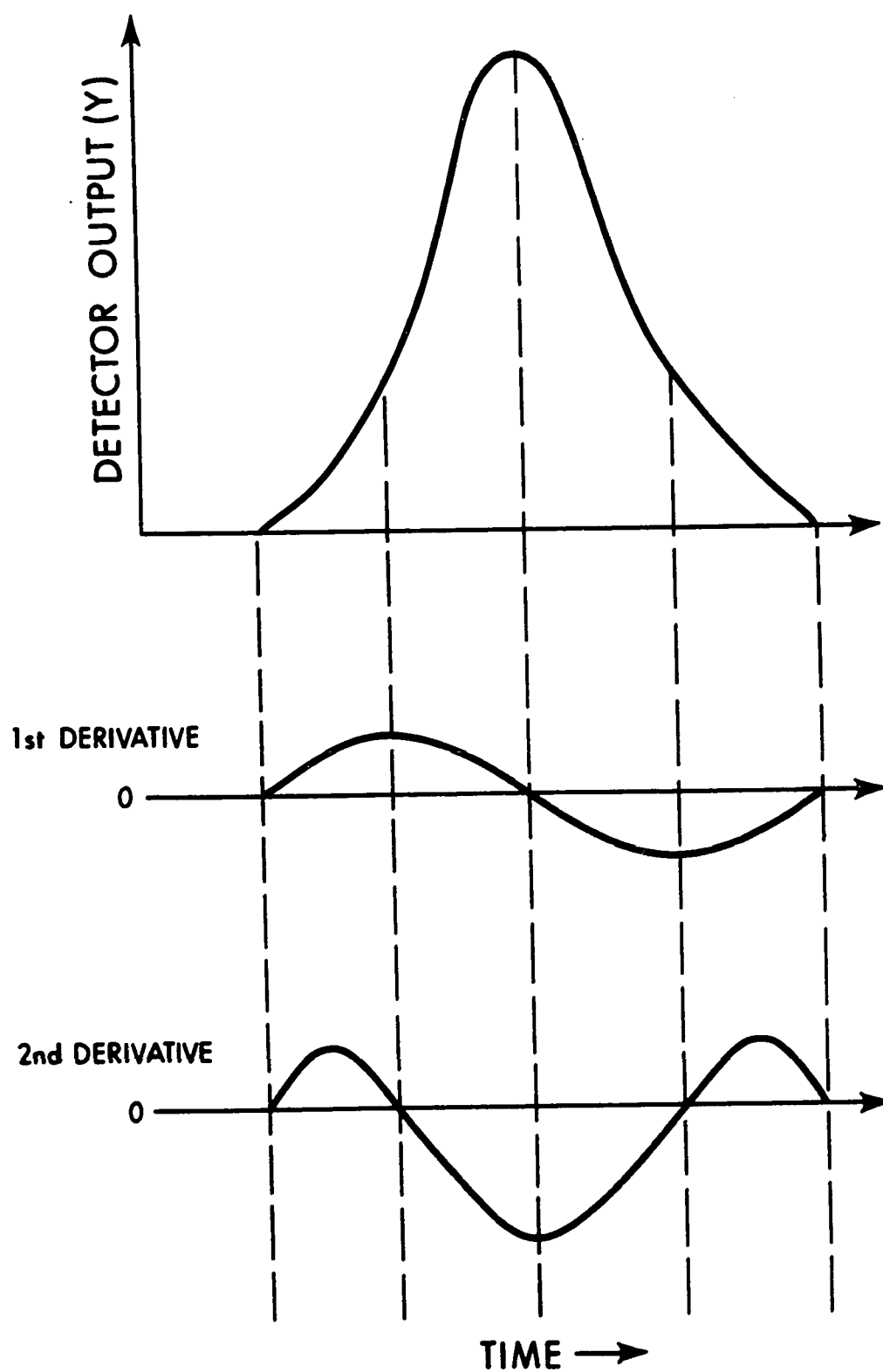


FIGURE 2.6: RELATIONSHIP BETWEEN CHROMATOGRAPH PEAK AND THE CURVE DERIVATIVES

Table 2.7
Signal Derivative Behaviour with

Event	<u>GC Peak Events</u>	
	<u>First Derivative Behaviour</u>	<u>Second Derivative Behaviour</u>
Peak Start	0 → + ve	0 → + ve
Peak Maximum	+ ve → - ve	minimum
Peak Finish	- ve → 0	+ ve → 0

Peak areas were integrated numerically using Simpson's Rule. To improve the accuracy of the integration at the apex of the sharp N_2 and H_2S peaks, a short subroutine called APEX was added to Mr. Berry's program. APEX curve fitted the last three points before a peak maximum to a line in order to obtain the slope and similarly the first three points after a peak maximum. From the slopes of these lines, the apex area which lay between the last point before a peak maximum and the first point after the maximum could be determined. This procedure was essential even for demonstration purposes. Area correction to compensate for baseline drift of the GC was also provided in the original program. Since this program is documented in Mr. Berry's M.Sc. thesis (1), the reader is directed to this reference for a more detailed explanation of the operation of the program.

The thermal conductivity cell signal was monitored at one point per second and temporarily stored in a data accumulation record which

periodically buffered its contents to disk. The monitoring started when the appropriate section of DM002 was executed. This part of DM002 was also responsible for closing the ECO on the computer which started the process GC programmer operating. Also, by using system subroutines DEFER and QUEUE, DM002 at this point was arranging for DMGC to be queued at the end of the programmer cycle seven minutes later. When DMGC was executed at the end of the cycle, it recovered the numerical version of the thermal conductivity cell signal from disk buffer files using system subroutine NIGBD and disk FILES 83 and 84. DMGC with its subroutines reduced the data to peak area measurements and transferred these results to FILE 81 for later use by the data reduction section of DM001.

CHAPTER III

OPERATION OF THE RECYCLE REACTOR ONLINE

The procedure for operating the recycle reactor online was the same as that described in Part I. After the equipment was operating at steady state with the desired set of process variables, the buttons in the laboratory were given the appropriate codes and the computer would execute the operating commands upon demand from the interrupt button. A typical run required the following instructions to be entered by the coding buttons and the computer would send the corresponding message of confirmation (between asterisks) back to the laboratory via the 1053 typewriter:

- (i) Turn loop records off
LOOP RECORDS ARE OFF
- (ii) Zero loop records
LOOP RECORDS ARE ZEROED
- (iii) Initialize GC area file
GC FILE INITIALIZED
- (iv) Initialize analog data file
ANALOG MSMT. DATA FILE CLEARED
- (v) Initialize kinetic data storage file
KINETIC DATA STORAGE FILE CLEARED
- (vi) Turn loop records on
LOOP RECORDS ARE ON

(vii) Initiate GC monitoring

GC NOW BEING SCANNED

At this stage the computer would start the process GC programmer which controlled sample injection, output signal attenuation changes, and back flushing. At the end of the chromatogram, DMGC would analyze and reduce the data to area measurements, send the results to FILE 81 and restart the programmer. Again, another ***GC NOW BEING SCANNED*** message would be sent to the laboratory typewriter. Enough space was provided in FILE 81 for eight sets of GC results, however a typical run would only require two sets of results; two feed analyses and two product analyses. Following these four analyses, the commands which remained were:

(viii) Turn loop records off

LOOP RECORDS ARE OFF

(ix) Enter H₂S attenuator reading

H₂S ATTENUATION = 9.4

(x) Label chromatograms (feed = 1, product = 2)

CHROMATOGRAM LABELLED 1

CHROMATOGRAM LABELLED 1

CHROMATOGRAM LABELLED 2

CHROMATOGRAM LABELLED 2

(xi) Reduce the measurements to kinetic data

DATA REDUCTION COMMENCING

NO. ANALOG DATA SAMPLES IS 22

NO. RUNS STORES IS 1

DATA REDUCTION COMPLETED

GC AREA STORAGE FILE CLEARED

After such an online run was completed, subsequent experi-

ments required only the following commands:

- (i) Zero loop records
- (ii) Turn loop records on
- (iii) Initiate GC monitoring
Run the experiment to completion
- (iv) Turn loop records off
- (v) Enter H₂S attenuator reading
- (vi) Label chromatograms
- (vii) Reduce the data

Sufficient storage space was available to allow the kineticist to carry out eight experiments without having to leave the laboratory.

The stored kinetic data were recovered in the computer room where DM006 could be executed by queuing it from one of the 1816 typewriters. DM006 would read the files, print the results on the line printer and also punch the numerical data on computer cards for future machine reproduction.

CHAPTER IV

PRESENTATION AND DISCUSSION OF RESULTS

On the first three pages of Appendix II-A, the results of the only online run which was successfully completed are given. They are self explanatory and so, a description will not be dealt with here.

A much more comprehensive statistical analysis could have been given to the analog measurement data such as the confidence limits on each process variable. Data such as these could ultimately be used for establishing the reliability of correlation parameter estimates.

The repeatability of the SO_2 peak area measurement (the broadest peak) was reasonable however, it was poor for both the nitrogen and H_2S peaks which accounts for the poor material balance results on the third page of output. The latter two peaks were very sharp and, as was previously explained, their areas could not be accurately measured with a scanning frequency of only one point per second. It is worth mentioning that at a scanning frequency of 10 points per second on the original IBM GC pack, the repeatability of nitrogen peak integration was one part in 10,000 for the runs which were attempted. In this run it was 4 in 60 and the chromatograms on both feed and product indicated much better repeatability than this on the chart recorder and disk integrator.

Although the coding buttons provided sufficient flexibility for sending instructions to the computer, a keyboard typewriter which could afford conversational communication with the 1800 could obviate the need for the 1053 and the coding buttons and provide a much more

versatile interface between the kineticist and the computer. Such an arrangement would be a necessity if computer control of the experiment were to be implemented.

The programming could have been arranged to reduce the number of operating commands which were necessary during an online run. Nonetheless, to enter a command required less than 5 seconds so that no more than a minute was spent pushing coding buttons during an experiment. The online user software was developed in stages and as the need for a new instruction was recognized, it was developed and assigned a new code. Over the long term, all the programs should be improved in organization.

Operating the equipment online provided the following advantages:

- (i) Unbiased data measurement free from human error (conditional that programs and hardware are error free);
- (ii) Capability of multiple data samples for statistical analysis with no human effort;
- (iii) Hardcore documentation of experimental results and, of course, machine calculation of these results.

Ultimately, computer control of the experimental apparatus would provide the following additional benefits.

- (i) Potentially around the clock operation of the apparatus rather than just while the operator is present.
- (ii) Online design of experiments based on stored results, data trends, and requirements for more accurate correlation parameter estimates.

CHAPTER V

CONCLUSIONS AND RECOMMENDATIONS

The operation of a kinetic research reactor with data acquisition capabilities has been successfully demonstrated. Although this author did not have the satisfaction of a complete online kinetic program, the online approach is recommended based on the previously discussed benefits which were experienced for the one demonstration run.

The need for a user-oriented, trouble-free and reliable gas chromatograph monitoring package of programs is a prerequisite to this type of research. Existing software at the University of Alberta was not satisfactory and it is recommended that a concerted effort be applied to this need immediately and before future online kinetic research endeavours commence. Examination of other proven software schemes such as those of Varian or Digital Equipment Corporation may prove expeditious. It is stressed that a proven system should be operational before future kinetic research programs be attempted online. This may require the equivalent of another M.Sc. endeavour.

BIBLIOGRAPHY

1. Berry, M.W., M.Sc. Thesis, University of Alberta, 1971.
2. Coxhead, P.J., M.Sc. Thesis, University of Alberta, 1968.
3. Fehr, M., M.Sc. Thesis, University of Alberta, 1969.
4. Orr, C.H. and Norris, J.A. Editors, "Computers in Analytical Chemistry", Vol. 4, Progress in Analytical Chemistry, 1970, Plenum Press.

PART I
APPENDICES

APPENDIX A
CALIBRATION OF EXPERIMENTAL EQUIPMENT

A.1 Introduction to Equipment Calibration

This appendix is concerned with describing calibration procedures, documenting the calibration data, and fitting experimental and calculated results to power series using linear least squares. A power series polynomial is of the following form:

$$y = a_0 + a_1x + a_2x^2 + \dots \quad (A.1)$$

Calibration in the form of curves, in most cases, has been preempted by fitting the data using least squares and indicating the standard deviation and variance of the fit. This is reasonable, since graphical plots of calibration data were not used for reducing measurements to meaningful kinetic data, only the polynomials generated by the curve-fitting process. In calibrating the gas chromatograph, the data were necessarily plotted to demonstrate that the analyses were being carried out in the linear range. Table A.1 summarizes the values of the correlation parameters which were employed in the data reduction programs for calculating the kinetic data. Independent variables in this table which are indicated as percent have been read from a recorder with a scale of 0-100. For the IBM 1800 computer, the percent means 100 times the digital reading of the analog input channel divided by 32767.

Tables of data in this appendix which display the results of the least squares fitting process in most cases provide more significant figures in the numbers than is justified. This is because the computer

TABLE A.1 SUMMARY OF CORRELATION COEFFICIENTS FOR INSTRUMENT CALIBRATION

DEPENDENT VARIABLE.....UNITS	INDEPENDENT VARIABLE AND MEASUREMENT DEVICE	CORRELATION PARAMETERS		
		A0	A1	A2
REACTOR BED TEMP.....DEG C	VOLTAGE...L&N RECORDER	5.3155	18.0706	-----
REACTOR WALL TEMP.....DEG C	VOLTAGE...L&N RECORDER	6.6860	17.9544	-----
FLUIDIZED BATH TEMP.....DEG C	VOLTAGE...L&N RECORDER	6.3627	17.9853	-----
FEED ABSOLUTE PRESS.....PSIA	PERCENT...FOXBORO RECORDER	15.000	0.2500	-----
	PERCENT...IBM 1800 COMPUTER	8.7012	0.3159	-----
REACTOR ABSOLUTE PRESS...MM HG	PERCENT...FOXBORO RECORDER	-534.851	24.806	-----
	PERCENT...IBM 1800 COMPUTER	-1123.63	30.850	-----
FEED FLOW RATE.....SCFH	PERCENT...FOXBORO RECORDER	1.2265	1.5367	0.0381
(22.5 PSIA)	PERCENT...FOXBORO RECORDER	0.8985	1.6844	0.0212
(25 PSIA)	PERCENT...FOXBORO RECORDER	0.7409	1.9429	0.0178
(30 PSIA)	PERCENT...FOXBORO RECORDER	0.7955	2.0629	0.0246
(35 PSIA)				
FEED FLOW RATE.....SCFH	PERCENT...IBM 1800 COMPUTER	-13.1032	4.1620	-0.0822
(22.5 PSIA)	PERCENT...IBM 1800 COMPUTER	-13.7117	4.3797	-0.1022
(25 PSIA)	PERCENT...IBM 1800 COMPUTER	-15.8658	5.0301	-0.1249
(30 PSIA)	PERCENT...IBM 1800 COMPUTER	-16.9059	5.3198	-0.1239
(35 PSIA)				
100X H2S/N2 MOLAR RATIO	100X H2S/N2 AREA RATIO	0.0418	0.5888	-----
(H2S ATTEN.-9.8)	...SARGENT RECORDER WITH	0.1129	0.6921	-----
(H2S ATTEN.-9.6)	DISK INTEGRATOR	0.0547	0.7756	-----
(H2S ATTEN.-9.4)				
100X SO2/N2 MOLAR RATIO	100X SO2/N2 AREA RATIO	0.0044	0.4950	-----
(SO2 ATTEN.-9.8)	...SARGENT RECORDER WITH			
	DISK INTEGRATOR			

correlation program was written with F-type output formats which could be useful over a wide range of number magnitudes and yet remain more readable than E-type formats.

Throughout this appendix, reference is made to calibration coefficients for variables whose values were measured by an IBM 1800 computer. These parameters were used for the online procurement of kinetic data which is discussed in Part II of this thesis. The information is included here since the equipment calibration for both off-line and online modes of operation was performed simultaneously.

A.2 Calibration of Thermocouples

Ten thermocouples were tested before they were installed in the equipment. The test procedure involved immersing each thermocouple and a mercury thermometer in a stirred, temperature-controlled oil bath and noting the electrical signal produced by the thermocouple and simultaneously the temperature registered on the mercury thermometer. The reading of a second mercury thermometer, placed at the midpoint of the exposed length of the first thermometer's mercury thread, was also taken for purposes of stem correction calculations. Figure A.1 shows the physical arrangement which was used for obtaining the calibration data.

Voltages were measured by a Leeds and Northrup model number 8686 millivolt potentiometer which had a marked resolution of 0.005 millivolts. The mercury thermometers which were used were manufactured by Dr. Siebert and Kühn Company, Oberkaufungen, West Germany. The North American distributor, Fisher Scientific, indicated that these thermo-

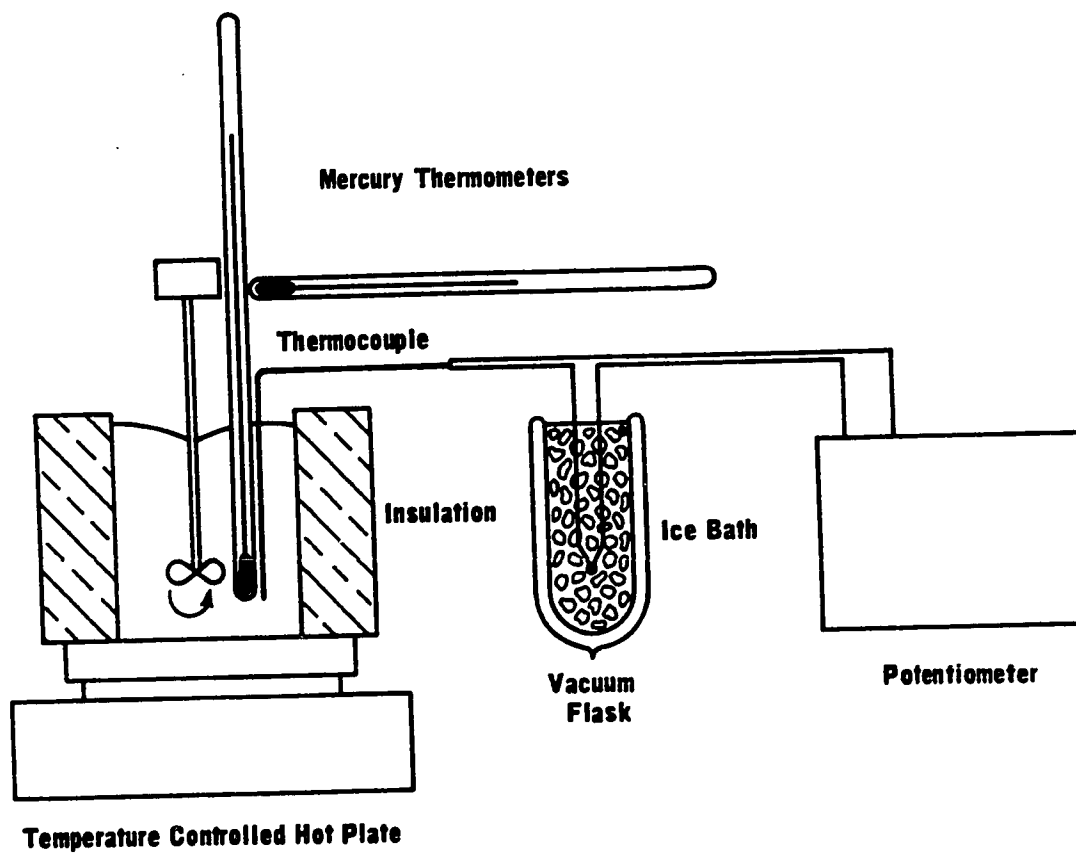


FIGURE A.1: CALIBRATION OF THERMOCOUPLES

imeters were manufactured according to the specifications and accuracy set forth by the National Bureau of Standards which require the accuracy to be within $\pm 1/2$ of the resolution (i.e. the finest marked gradation). The following table gives the range and resolution of these thermometers.

TABLE A.2 RANGE AND RESOLUTION OF CALIBRATION
THERMOMETERS FOR THERMOCOUPLES

<u>Temperature Range (°C)</u>	<u>Resolution(°C)</u>
0 - 60	0.1
50 - 100	0.1
100 - 150	0.1
150 - 200	0.1
200 - 350	0.2

The uncorrected calibration data are recorded in Table A.3. Since the thermometers were of the immersion type, the readings had to be stem-corrected. The stem-corrected temperature is given by equation A.2⁽¹⁾.

$$t_c = 0.000156L(t_o - t_e) + t_o \quad (A.2)$$

where, t_c = corrected temperature

(1) Shoemaker, D.P. and Garland, C.W., "Experiments in Physical Chemistry" p. 379, McGraw-Hill Book Publishing Company, Inc., New York, 1962.

TABLE A.3 THERMOCOUPLE CALIBRATION DATA

Thermocouple Description	Temperature (°C)					
	Millivolts					
Feed	0.00	54.60	98.50			
Temperature	0.015	2.816	5.16			
Gas I	0.00	54.55	98.10			
Chromatograph	0.013	2.831	5.191			
Gas II	0.00	54.55	97.95			
Chromatograph	0.013	2.831	5.183			
Sulphur I	0.00	54.65	98.00	194.7	194.6	
Condenser	-0.018	2.865	5.242	10.641	10.615	
Sulphur II	0.00	54.55	98.10	199.2	199.9	
Condenser	-0.004	2.841	5.199	10.785	10.826	
Catalyst	0.00		98.60	195.4	249.0	307.6
Bed	-0.015		5.220	10.622	13.537	16.902
Reactor	0.00		98.60	193.50	248.3	308.6
Wall	-0.021		5.229	10.501	13.510	16.977
Preheater			97.10	193.00		
			5.094	10.404		
Fluidized	0.00	54.75	98.20	196.20	246.6	309.2
Bed	+0.015	2.840	5.181	10.641	13.409	17.000
Recycle	0.00		97.45	191.9	249.2	
Valve	+0.015		5.073	10.361	13.512	

Note: The above data do not have stem corrections applied to the thermometers.

TABLE A.4 STEM CORRECTED THERMOCOUPLE CALIBRATION DATA

Thermocouple Description	Temperature (°C) Millivolts					
Feed	0.00	54.60	98.90			
Temperature	0.015	2.816	5.16			
Gas I	0.00	54.55	98.50			
Chromatograph	0.013	2.831	5.191			
Gas II	0.00	54.55	98.35			
Chromatograph	0.013	2.831	5.183			
Sulphur I	0.00	54.65	98.40	195.5		
Condenser	-0.018	2.865	5.242	10.64		
Sulphur II	0.00	54.55	98.50	200.0		
Condenser	-0.018	2.841	5.199	10.785		
Catalyst	0.00		99.0	196.2	249.9	310.5
Bed	-0.015		5.22	10.622	13.537	16.902
Reactor	0.00		99.0	194.3	249.2	311.5
Wall	-0.021		5.23	10.501	13.510	16.977
Preheater			97.50	193.8		
			5.094	10.404		
Fluidized	0.00	54.75	98.60	197.0	247.5	312.1
Bed	+0.015	2.84	5.181	10.641	13.409	17.000
Recycle	0.00		97.85	192.7	250.1	
Valve	+0.015		5.073	10.361	13.512	

TABLE A.5

LEAST SQUARES FIT OF STD. IRON CONSTANTAN THERMOCOUPLE DATA

X MEASURED = VOLTAGE (MILLIVOLTS)

Y OBSERVED = TEMPERATURE (DEGREES CENTIGRADE)

THE COEFFICIENTS OF THE POLYNOMIAL ARE

A0 = 5.41754

A1 = 18.04088

REGENERATED DATA

X MEASURED	Y OBSERVED	Y CALCULATED	PCT ERROR
10.780	200.000	199.898	0.050
11.890	220.000	219.923	0.034
13.010	240.000	240.129	0.053
14.120	260.000	260.154	0.059
15.220	280.000	279.999	0.000
16.330	300.000	300.025	0.008
17.430	320.000	319.870	0.040

VARIANCE = 0.012399

STANDARD DEVIATION = 0.111354

MAXIMUM PCT ERROR = 0.059509...

L = length of emergent stem measured in scale degrees

t_o = observed temperature

t_e = average temperature of emergent mercury column.

The stem-corrected calibration data are given in Table A.4.

The three most important temperature readings are taken at the reactor bed, the reactor wall and in the fluidized bath. To compare their calibration results with standard iron-constantan thermal electric data, the standard data were fitted using linear least squares between 200 and 320 degrees Centigrade. The results of this fit are given in Table A.5 and it is noted that the standard deviation is close to 0.1 degree Centigrade. Using the coefficients generated by the straight-line fitting process, the electrical data obtained in the calibration were inserted into the straight line equation and the calculated temperature was compared to that observed. This comparison is given in Table A.6.

TABLE A.6 COMPARISON OF THERMOCOUPLE CALIBRATION
DATA WITH STANDARD DATA

Thermocouple Description	Measured Voltage (mv)	Measured Temperature (°C)	Calculated Temperature (°C)	Error (°C)
Reactor Bed	13.537	249.9	249.6	0.3
Reactor Bed	16.902	310.5	310.3	0.2
Reactor Wall	13.510	249.2	249.1	0.1
Reactor Wall	16.977	311.5	311.7	-0.2
Fluidized Bath	13.409	247.5	247.3	0.2
Fluidized Bath	17.000	312.1	312.1	0.0

Considering the errors which were observed between the standard data⁽²⁾ and the calibration data, the coefficients for the straight-line fit of each thermocouple were adjusted so that no error would exist between measured and observed temperatures. These coefficients are given in Table A.7.

TABLE A.7 CALIBRATION COEFFICIENTS FOR THERMOCOUPLES
STRAIGHT LINE COEFFICIENTS

Thermocouple Description	Straight Line Coefficients	
	a_0	a_1
Standard Data	5.4175	18.0409
Reactor Bed	5.3155	18.0706
Reactor Wall	6.6860	17.9544
Fluidized Bath	6.3627	17.9853

A.3 Calibration of Feed Pressure Transducer

The Foxboro 611 AH absolute pressure transmitter was calibrated by using a five foot mercury manometer which had a resolution of 1 millimeter. A nitrogen cylinder was fitted with a Moore nullmatic pressure regulator (model number 41-50) and connected to the transmitter and manometer. The Foxboro 6430 HF electronic control recorder was operational during the calibration and readings were taken at five psia intervals between 15 psia and 40 psia. Also, the voltage signal obtained by

(2) Weast, R.C., editor, "Handbook of Chemistry and Physics", 49th edition, E-107, The Chemical Rubber Co., Cleveland, Ohio, (1968).

dropping the 10-50 milliamperes signal from the transducer across a 100 ohm resistor, was measured by the IBM 1800 computer. The points obtained are given in Table A.8.

These data were fitted to a straight line using linear least squares and the results of the fit are given in Tables A.9 and A.9A.

TABLE A.8 FEED PRESSURE TRANSMITTER CALIBRATION DATA

Barometric pressure = 70.06 cm.Hg.

<u>Manometer Reading (cm Hg)</u>	<u>Absolute Pressure (psia)</u>	<u>Recorder Chart Reading (%)</u>	<u>Computer Reading (%)</u>
7.56	15.0	0.0	19.94
33.43	20.0	20.0	35.77
59.31	25.0	40.0	51.59
85.18	30.0	60.0	67.42
111.06	35.0	80.0	83.25
136.93	40.0	100.0	99.08

A.4 Calibration of Reactor Pressure Transducer

The Statham PA732TC-50-350 absolute pressure transducer was calibrated with the same technique used with the feed pressure transmitter except that the reactor pressure transducer was calibrated at 245°C, the anticipated reactor temperature. This pressure transducer is temperature-compensated and tests carried out at 200 and 260°C showed that the drift in the instrument's output at constant pressure over this

TABLE A.9

LEAST SQUARES FIT OF FEED ABSOLUTE PRESSURE TRANSDUCER DATA

X MEASURED = FOXBORO RECORDER CHART READING (PERCENT)

Y OBSERVED = ABSOLUTE PRESSURE (PSIA)

THE COEFFICIENTS OF THE POLYNOMIAL ARE

A0 = 15.00000

A1 = 0.25000

REGENERATED DATA

X MEASURED	Y OBSERVED	Y CALCULATED	PCT ERROR
0.000	15.000	15.000	0.000
20.000	20.000	20.000	0.000
40.000	25.000	25.000	0.000
60.000	30.000	30.000	0.000
80.000	35.000	35.000	0.000
100.000	40.000	40.000	0.000

VARIANCE = 0.000000

STANDARD DEVIATION = 0.000000

MAXIMUM PCT ERROR = 0.000000

TABLE A.9A

LEAST SQUARES FIT OF FEED ABSOLUTE PRESSURE TRANSDUCER DATA

X MEASURED = IBM 1800 COMPUTER READING (PERCENT)

Y OBSERVED = ABSOLUTE PRESSURE (PSIA)

THE COEFFICIENTS OF THE POLYNOMIAL ARE

A0 = 8.70123

A1 = 0.31590

REGENERATED DATA

X MEASURED	Y OBSERVED	Y CALCULATED	PCT ERROR
19.940	15.000	15.000	0.002
35.770	20.000	20.001	0.005
51.590	25.000	24.998	0.005
67.420	30.000	29.999	0.002
83.250	35.000	35.000	0.000
99.080	40.000	40.000	0.001

VARIANCE = 0.000000

STANDARD DEVIATION = 0.000913

MAXIMUM PCT ERROR = 0.005645

temperature range was negligible. However, when the temperature was lowered to 20°C, the drift in output was perceptible.

The results of the calibration procedure are given in Table A.10 and the least squares fit of this data is given in Tables A.11 and A.11A.

TABLE A.10 REACTOR PRESSURE TRANSMITTER
CALIBRATION DATA

Barometric Pressure = 704.4 mm.Hg.

Fluidized Bath Temperature = 244°C

Manometer Reading (mm Hg)	Absolute Pressure (mm Hg)	Recorder Chart Reading (%)	Computer Reading (%)
0.0	704.4	49.90	59.25
42.5	746.9	51.75	60.66
70.5	774.9	52.80	61.52
120.0	824.4	54.80	63.14
183.0	887.4	57.30	65.19
234.0	938.4	59.40	66.84

A.5 Calibration of Feed Differential Pressure Cell

The D/P cell for the reactor feed line was calibrated by passing a constant flow of nitrogen through it and measuring the nitrogen flow-rate with a dry test meter and stopwatch. Before the calibration

TABLE A.11

LEAST SQUARES FIT OF REACTOR ABSOLUTE PRESSURE TRANSDUCER

X MEASURED = IBM 1800 COMPUTER READING (PERCENT)

Y OBSERVED = ABSOLUTE PRESSURE (MM HG)

THE COEFFICIENTS OF THE POLYNOMIAL ARE

A0 = -1123.63061

A1 = 30.85020

REGENERATED DATA

X MEASURED	Y OBSERVED	Y CALCULATED	PCT ERROR
59.250	704.400	704.244	0.022
60.650	746.900	747.742	0.112
61.520	774.900	774.274	0.080
63.140	824.400	824.251	0.018
65.190	887.400	887.494	0.010
66.840	938.400	938.397	0.000

VARIANCE = 0.231465

STANDARD DEVIATION = 0.481108

MAXIMUM PCT ERROR = 0.112852

TABLE A.11A

LEAST SQUARES FIT OF REACTOR ABSOLUTE PRESSURE TRANSDUCER

X MEASURED = FOXBORO RECORDER CHART READING (PERCENT)

Y OBSERVED = ABSOLUTE PRESSURE (MM HG)

THE COEFFICIENTS OF THE POLYNOMIAL ARE

$$A_0 = -534.85083$$

$$A_1 = 24.80598$$

REGENERATED DATA

X MEASURED	Y OBSERVED	Y CALCULATED	PCT ERROR
49.900	704.400	702.967	0.203
51.750	746.900	748.858	0.262
52.800	774.900	774.904	0.000
54.800	824.400	824.516	0.014
57.300	887.400	886.531	0.097
59.400	938.400	938.624	0.023

$$\text{VARIANCE} = 1.341284$$

$$\text{STANDARD DEVIATION} = 1.158138$$

$$\text{MAXIMUM PCT ERROR} = 0.262233$$

was carried out, the accuracy of the dry test meter (American Meter Company, Model Number 5M210, Serial Number 7838179) was checked against a gasometer.

Nitrogen was passed through the dry test meter and into the five cubic foot gasometer. The gasometer had previously been calibrated by filling the bell shaped top with water and noting the net weight change with change in height of water. Three runs were carried out at three different volumetric flow-rates in order to obtain the calibration factor for the meter and to see if this factor varied with different flow-rates passing through the meter. The average results of runs taken at the three flow-rates are given in Table A.12 and the calibration factor is plotted in Figure A.2.

At four different levels of absolute pressure (22.5, 25, 30 and 35 psia), as indicated by the feed absolute pressure transducer, the D/P cell was calibrated using the calibration factor established in the gasometer test to correct the apparent nitrogen flow-rate. A short computer program called FDCAL was written to document the measurements which were taken and the calculated results are given in Tables A.13 and A.14. FDCAL was also used to translate the calculated results onto punched cards to provide input for a least squares fitting program. The results of the least squares fit of the calculated results are presented in Tables A.15A to A.15H. Here the flow-rate in standard cubic feet per hour (60°F, 1 atm pressure) is correlated by a second degree polynomial to the square root of the percent reading taken by the recorder or computer, as the case may be.

TABLE A.12 CALIBRATION DATA FOR DRY TEST METER

Run Number	Apparent Volume (Dry Test Meter) (cu ft)	Actual Volume (gasometer) (cu ft)	Apparent Flow Rate (cuft/min)	Calibration Factor
1	1.890	1.870	0.151	0.990
2	1.852	1.870	0.362	1.010
3	1.804	1.870	0.584	1.037

Note: Actual Volume = (Dry Test Meter Reading)(Calibration Factor)

Barometric Pressure = 694.4 mm Hg

Room Temperature = 72°F

When flow data are obtained at pressures between 22.5 and 35 psia, the flow-rate is calculated according to the curve fitted data at 22.5, 25, 30 and 35 psia by using the square root of the D/P cell reading, and the flow at the intermediate pressure is obtained by a Newton interpolation polynomial routine. This is described in Appendix C, Reduction of Data.

The purpose of FDCAL and description of the input data is given at the start of the Fortran listing of the program. The only calculations performed by the program are the calculation of the square root of the D/P cell reading taken by the Foxboro recorder and the IBM 1800 computer and the calculation of the flow rate in scfh using the following equation

$$Q = \left(\frac{P}{760.}\right)\left(\frac{520}{460.+T}\right)\left(\frac{60.}{t}\right)(C.F.) \quad (A.3)$$

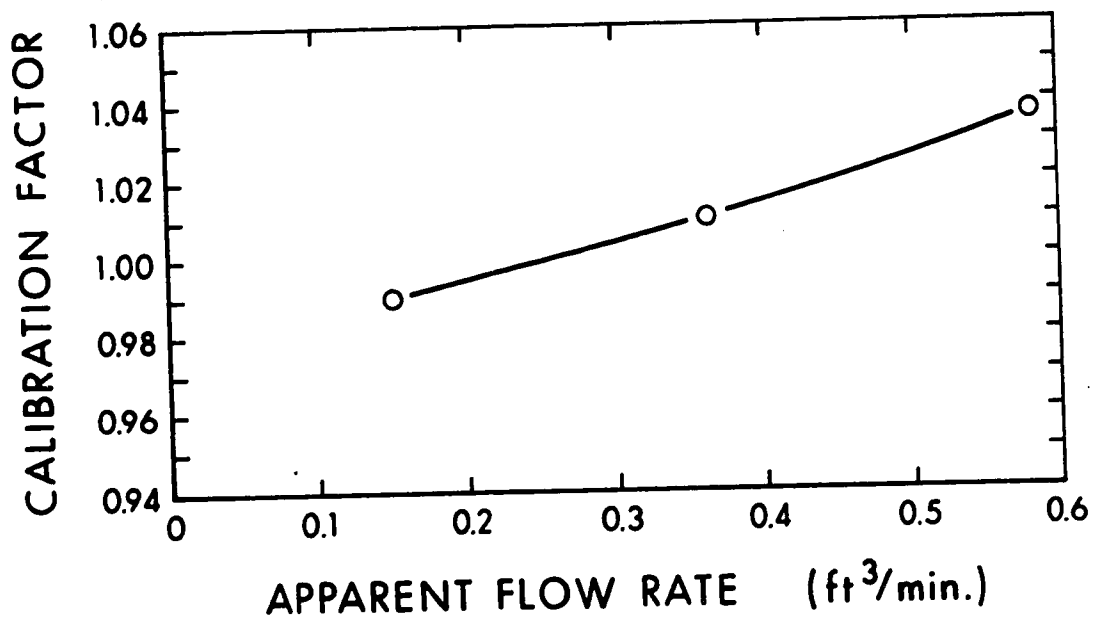


FIGURE A.2: DRY TEST METER CALIBRATION FACTOR VARIATION WITH APPARENT FLOW RATE.

TABLE A.13

EXPERIMENTAL RESULTS FOR D/P CELL CALIBRATION

TIME FOR 1 CUBIC FOOT OF GAS FLOW (MINUTES)	ATMOSPHERIC PRESS (MM HG)	TEMP (DEG F)	FOXBORO RECORDER D/P CELL (PCT)	IBM 1800 ABS PRESS (PCT)	COMPUTER (PCT)
3.000	704.8	68.0	90.00	39.80	90.72
3.267	704.8	68.0	75.10	40.10	78.98
4.030	704.8	68.0	49.80	40.10	59.04
5.167	704.8	68.0	30.25	40.10	43.63
6.207	704.8	68.0	20.20	40.00	35.71
8.676	709.5	64.0	10.00	39.90	27.67
2.533	709.5	64.0	90.50	80.60	91.11
2.796	709.6	64.0	74.80	80.00	78.74
3.425	709.7	64.0	49.70	80.20	58.96
4.363	709.0	66.3	30.10	79.40	43.51
5.357	709.0	66.3	20.00	80.00	35.55
7.301	705.0	64.0	10.10	80.20	27.75
7.820	704.8	67.0	10.00	60.00	27.67
5.658	704.8	67.0	20.00	60.00	35.55
4.697	704.8	67.0	30.00	60.20	43.44
3.640	704.8	67.0	50.00	60.00	59.20
3.000	706.9	64.0	75.20	59.90	79.06
2.747	706.9	64.0	90.00	60.00	90.72
8.590	707.2	66.0	10.00	30.00	27.67
6.281	707.2	66.0	20.00	30.00	35.55
4.815	707.2	66.0	35.00	30.00	47.30
4.000	706.9	67.0	50.00	30.00	59.20
3.500	706.9	66.0	65.00	30.00	71.12
3.141	706.5	65.0	80.00	30.00	82.85

TABLE A.14

CALCULATED RESULTS FOR D/P CELL CALIBRATION

RUN NO.	FEED FLOW METERING SYSTEM			FLOW RATE (SCFH)
	ABS PRESS (PSIA)	D/P CELL SQRT(PCT)	COMPUTER SQRT(PCT)	
1	24.95	9.48	9.52	18.01
2	25.02	8.66	8.88	18.01
3	25.02	7.05	7.68	18.01
4	25.02	5.49	6.60	18.01
5	25.00	4.49	5.97	18.01
6	24.97	3.16	5.26	18.01
7	35.15	9.51	9.54	18.01
8	35.00	8.64	8.87	18.01
9	35.05	7.04	7.67	18.01
10	34.85	5.48	6.59	18.01
11	35.00	4.47	5.96	18.01
12	35.05	3.17	5.26	18.01
13	30.00	3.16	5.26	18.01
14	30.00	4.47	5.96	18.01
15	30.05	5.47	6.59	18.01
16	30.00	7.07	7.69	18.01
17	29.97	8.67	8.89	18.01
18	30.00	9.48	9.52	18.01
19	22.50	3.16	5.26	18.01
20	22.50	4.47	5.96	18.01
21	22.50	5.91	6.87	18.01
22	22.50	7.07	7.69	18.01
23	22.50	8.06	8.43	18.01
24	22.50	8.94	9.10	18.01

TABLE A.15

LEAST SQUARES FIT OF FEED D/P CELL AT 22.5 PSIA

X MEASURED = FOXBORO RECORDER CHART READING (SQRT(PCT))

Y OBSERVED = FLOW RATE (SCFH)

THE COEFFICIENTS OF THE POLYNOMIAL ARE

A0 = -0.62199

A1 = 0.61645

A2 = -0.00476

REGENERATED DATA

X MEASURED	Y OBSERVED	Y CALCULATED	PCT ERROR
6.460	3.160	3.161	0.049
8.870	4.470	4.471	0.028
11.620	5.910	5.898	0.200
14.010	7.070	7.079	0.137
16.090	8.060	8.063	0.046
18.010	8.940	8.935	0.049

VARIANCE = 0.000054

STANDARD DEVIATION = 0.007393

MAXIMUM PCT ERROR = 0.200529

TABLE A.15A

LEAST SQUARES FIT OF FEED D/P CELL AT 22.5 PSIA

X MEASURED = IBM 1800 COMPUTER READING (SQRT(PCT))

Y OBSERVED = FLOW RATE (SCFH)

THE COEFFICIENTS OF THE POLYNOMIAL ARE

A0 = 3.44361

A1 = 0.25890

A2 = 0.00310

REGENERATED DATA

X MEASURED	Y OBSERVED	Y CALCULATED	PCT ERROR
6.460	5.260	5.245	0.270
8.870	5.960	5.984	0.410
11.620	6.870	6.871	0.022
14.010	7.690	7.680	0.122
16.090	8.430	8.413	0.194
18.010	9.100	9.114	0.154

VARIANCE = 0.000272

STANDARD DEVIATION = 0.016496

MAXIMUM PCT ERROR = 0.410928

TABLE A.15B

LEAST SQUARES FIT OF FEED D/P CELL AT 25 PSIA

X MEASURED = FOXBORO RECORDER CHART READING (SQRT(PCT))

Y OBSERVED = FLOW RATE (SCFH)

THE COEFFICIENTS OF THE POLYNOMIAL ARE

A0 = 0.89847

A1 = 1.68443

A2 = 0.02117

REGENERATED DATA

X MEASURED	Y OBSERVED	Y CALCULATED	PCT ERROR
9.486	18.729	18.783	0.291
8.666	17.164	17.085	0.457
7.056	13.845	13.839	0.041
5.499	10.744	10.803	0.545
4.494	8.917	8.896	0.231
3.162	6.445	6.436	0.128

VARIANCE = 0.002624

STANDARD DEVIATION = 0.051226

MAXIMUM PCT ERROR = 0.545683

TABLE A.15C

LEAST SQUARES FIT OF FEED D/P CELL AT 25 PSIA

X MEASURED = IBM 1800 COMPUTER READING (SQRT(PCT))

Y OBSERVED = FLOW RATE (SCFH)

THE COEFFICIENTS OF THE POLYNOMIAL ARE

$$A_0 = -13.71168$$

$$A_1 = 4.37971$$

$$A_2 = -0.10222$$

REGENERATED DATA

X MEASURED	Y OBSERVED	Y CALCULATED	PCT ERROR
9.524	18.729	18.730	0.006
8.887	17.164	17.137	0.155
7.684	13.845	13.906	0.439
6.605	10.744	10.759	0.135
5.976	8.917	8.811	1.182
5.261	6.445	6.500	0.862

$$\text{VARIANCE} = 0.003769$$

$$\text{STANDARD DEVIATION} = 0.061397$$

$$\text{MAXIMUM PCT ERROR} = 1.182604$$

TABLE A.15D

LEAST SQUARES FIT OF FEED D/P CELL AT 30 PSIA

X MEASURED = FOXBORO RECORDER CHART READING (SQRT(PCT))

Y OBSERVED = FLOW RATE (SCFH)

THE COEFFICIENTS OF THE POLYNOMIAL ARE

A0 = 0.74086

A1 = 1.94287

A2 = 0.01777

REGENERATED DATA

X MEASURED	Y OBSERVED	Y CALCULATED	PCT ERROR
3.162	7.062	7.062	0.004
4.472	9.811	9.785	0.263
5.477	11.866	11.915	0.418
7.071	15.388	15.367	0.134
8.671	18.947	18.926	0.112
9.485	20.754	20.772	0.089

VARIANCE = 0.000873

STANDARD DEVIATION = 0.029553

MAXIMUM PCT ERROR = 0.418678

TABLE A.15E

LEAST SQUARES FIT OF FEED D/P CELL AT 30 PSIA

X MEASURED = IBM 1800 COMPUTER READING (SQRT(PCT))

Y OBSERVED = FLOW RATE (SCFH)

THE COEFFICIENTS OF THE POLYNOMIAL ARE

$$A_0 = -15.86578$$

$$A_1 = 5.03013$$

$$A_2 = -0.12491$$

REGENERATED DATA

X MEASURED	Y OBSERVED	Y CALCULATED	PCT ERROR
5.261	7.062	7.140	1.100
5.963	9.811	9.687	1.255
6.590	11.866	11.861	0.041
7.694	15.388	15.442	0.349
8.891	18.947	18.984	0.196
9.524	20.754	20.713	0.195

$$\text{VARIANCE} = 0.005432$$

$$\text{STANDARD DEVIATION} = 0.073707$$

$$\text{MAXIMUM PCT ERROR} = 1.255190$$

TABLE A.15F

LEAST SQUARES FIT OF FEED D/P CELL AT 35 PSIA

X MEASURED = FOXBORO RECORDER CHART READING (SQRT(PCT))

Y OBSERVED = FLOW RATE (SCFH)

THE COEFFICIENTS OF THE POLYNOMIAL ARE

A0 = 0.79547

A1 = 2.06285

A2 = 0.02462

REGENERATED DATA

X MEASURED	Y OBSERVED	Y CALCULATED	PCT ERROR
9.513	22.657	22.648	0.040
8.648	20.447	20.478	0.148
7.049	16.595	16.562	0.203
5.486	12.880	12.854	0.205
4.472	10.448	10.513	0.620
3.178	7.625	7.600	0.338

VARIANCE = 0.001541

STANDARD DEVIATION = 0.039262

MAXIMUM PCT ERROR = 0.620169

TABLE A.15G

LEAST SQUARES FIT OF FEED D/P CELL AT 35 PSIA

X MEASURED = IBM 1800 COMPUTER READING (SQRT(PCT))

Y OBSERVED = FLOW RATE (SCFH)

THE COEFFICIENTS OF THE POLYNOMIAL ARE

A0 = -16.90591

A1 = 5.31977

A2 = -0.12390

REGENERATED DATA

X MEASURED	Y OBSERVED	Y CALCULATED	PCT ERROR
9.545	22.657	22.584	0.320
8.873	20.447	20.544	0.471
7.678	16.595	16.638	0.254
6.596	12.880	12.795	0.657
5.963	10.448	10.410	0.360
5.268	7.625	7.682	0.740

VARIANCE = 0.005624

STANDARD DEVIATION = 0.074994

MAXIMUM PCT ERROR = 0.740012

```

DIMENSION A(25,10),NR(25)
READ(5,9) N,NPAGE,NCOPY
9 FORMAT(3I5)
DO 2 I=1,N
2 READ(5,1) NR(I),(A(I,J),J=1,7)
1 FORMAT(I5,5X,7F10.5)
DO 5 NC=1,NCOPY
WRITE(6,3) NPAGE
3 FORMAT('1', ///56X,'A-',I2,//////
1 35X,'TABLE A.13'/// ,18X
5,'EXPERIMENTAL RESULT
15 FOR D/P CELL CALIBRATION' / )
WRITE(6,4)
4 FORMAT( 10X,'TIME FOR 1 ATMOSPHERIC FOXBORO
5 RECORDER IB
2X 1800' / 10X,'CUBIC FOOT PRESS TEMP D/P CELL
5 ABS PRESS CO
3MPUTER' / 10X,'OF GAS FLOW (MM HG) (DEG F) (PCT)
5 (PCT)
4 (PCT)' / 11X,'(MINUTES)' / )
DO 5 I=1,N
5 WRITE(6,6) (A(I,J),J=1,6)
6 FORMAT(13X,F5.3,5X,F5.1,5X,F4.1,4X,F5.2,6X,F5.2,5X
5,F5.2)
NPAGE=NPAGE+1
DO 17 I=1,N
TPCOR=A(I,2)/760.*530./(A(I,3)+460.)

```


MAINLINE FDCAL ... (CONT'D)

```

FLO=TPCOR*1./A(I,1)*60.*A(I,7)
A(I,4)=A(I,4)**0.5
A(I,6)=A(I,6)**0.5
A(I,5)=A(I,5)*0.25+15.
17 CONTINUE
DO 7 NC=1,NCOPY
WRITE(6,20)NPAGE
20 FORMAT('1', ///,66X,'A-',I2,///)
WRITE(6,10)
10 FORMAT( ///,32X,'TABLE A.14'// 15X,'CALCULATED RESULTS
$ FOR D/P CEL
1L CALIBRATION'//)
WRITE(6,11)
11 FORMAT(16X,'RUN        FEED FLOW METERING SYSTEM    FLOW'
$/ 16X,'NO.
1ABS PRESS   D/P CELL    COMPUTER   RATE'/ 22X,'(PSIA)
$ SQRT(PCT) SQ
2RT(PCT) (SCFH)'//)
DO 7 I=1,N
WRITE(6,8) NR(I),A(I,5),A(I,4),A(I,6),FLO
7 CONTINUE
8 FORMAT(14X,I5,3X,F5.2,1X,3(5X,F5.2))
CALL EXIT
END

```

where, Q = flow rate (scfh)
 P = barometric pressure (mm Hg)
 T = room temperature ($^{\circ}\text{F}$)
 t = time required for one apparent cubic foot of gas
 flow (min)

A.6 Correction Applied to Differential Pressure Cell

The d/p cell was calibrated at 22°C with pure nitrogen. Since the orifice meter was used for measuring the flow-rate of a mixture of N_2 , H_2S and SO_2 , this flow rate was corrected to allow for the difference in density between the mixture and the pure nitrogen.

In orifice meters, the pressure loss from form friction is considerable and, in fact, the orifice plate is a meter which maximizes form drag. Thus the general meter equation may be written in the following form:

$$\bar{v}_1 = C_0 \sqrt{\frac{2g_c(-\frac{\Delta P}{\rho})}{\frac{S_1^2}{S_0^2} - 1}} \quad (\text{A.4})$$

where: C_0 = orifice coefficient
 g_c = dimensional constant
 ΔP = pressure drop across orifice
 ρ = gas density
 S_1 = cross sectional area of pipe

S_0 = cross sectional area of orifice hole

\bar{v}_1 = average gas velocity through pipe

The variation of discharge coefficient with Reynolds number for sharp edged orifices, as presented by Brown and Associates⁽³⁾, indicated that no correction of the orifice coefficient was necessary for the mixed gas stream. From Tables A.16 and A.17 it is apparent that the change in C_0 is less than 0.5 percent between pure nitrogen and a gas mixture of 90% N_2 , 5% H_2S and 5% SO_2 . Hence no correction was applied to account for variation of discharge coefficient.

Physical property data shown in Table A.16 were taken from Perry⁽⁴⁾ and the following equations were used for calculating the density⁽⁵⁾ and viscosity⁽⁶⁾ of the gas stream mixtures:

$$\rho_{Mix} = \sum_{i=1}^3 x_i \rho_i \quad (A.5)$$

where, ρ_{Mix} = density of gas mixture (1atm, 60°F)

x_i = mole fraction of component i

ρ_i = density of component i (1atm, 60°F)

(3) Brown G.G. and Associates, "Unit Operations", John Wiley and Sons, Inc., New York, p. 158 (1950).

(4) Perry, J.H., (ed.), "Perry's Chemical Engineers' Handbook", 4th ed., p.3-71 and 3-197, McGraw Hill Book Company, Inc., New York, 1963.

(5) Smith, J.M. and Van Ness, H.C., "Introduction to Chemical Engineering Thermodynamics", pp 103-107, McGraw Hill Book Company, Inc., New York, 1959.

(6) Bird, R.B., Stewart, W.E., and Lightfoot, E.N., "Transport Phenomena", p. 24, John Wiley and Sons, Inc., New York, 1960.

TABLE A.16 PHYSICAL PROPERTIES OF PURE NITROGEN
AND REACTOR FEED MIXTURE (1 atm, 60°F)

	<u>Nitrogen</u>	<u>Feed Mixture</u>
Density (lb/cuft)	0.074	0.084
Viscosity (c p)	0.0171	0.0164
N_{Re} (6.0 scfh)	8200	9700
N_{Re} (16.0 scfh)	21,900	25,900

Note: Feed mixture is 95% N_2 , 5% H_2S , 5% SO_2 (molar basis)

Reynolds number is based on orifice diameter of
0.020 in.

TABLE A.17 VARIATION OF ORIFICE
COEFFICIENT WITH N_{Re}

N_{Re}	Orifice Coefficient ($D_o/D_p = 0.20$)
8,000	0.617
10,000	0.616
20,000	0.613
30,000	0.610

$$\mu_{Mix} = \frac{\sum_{i=1}^3 x_i \mu_i}{\sum_{j=1}^3 x_j \phi_{ij}} \quad (A.6)$$

where, μ_{Mix} = viscosity of gas mixture

$$\phi_{ij} = \frac{1}{\sqrt{8}} \left(1 + \frac{M_i}{M_j}\right)^{-\frac{1}{2}} \left[1 + \left(\frac{\mu_i}{\mu_j}\right)^{-\frac{1}{2}} \left(\frac{M_j}{M_i}\right)^{\frac{1}{4}}\right]^2$$

μ_i = viscosity of component i

M_i = molecular weight of component i

It is apparent from Table A.16 that there is a considerable difference between the density of pure nitrogen and the gas mixture, thus the necessity for the flow correction.

Since the orifice geometry and C_0 remained constant for both pure nitrogen and the gas mixture, equation A.2 can be rewritten to give:

$$Q = k \left(\frac{\Delta P}{\rho}\right)^{\frac{1}{2}} \quad (A.7)$$

where: Q = volumetric flow rate

$$k = k' C_0 \left(\frac{2g_c}{S_1^2 - S_0^2}\right)^{1/2}$$

k' = constant to convert from average velocity to volumetric flow rate.

For pure nitrogen:

$$Q_{N_2} = k \left(\frac{\Delta p}{\rho_{N_2}} \right)^{\frac{1}{2}} \quad (A.8)$$

For a gas mixture:

$$Q_{Mix} = k \left(\frac{\Delta p}{\rho_{Mix}} \right)^{\frac{1}{2}} \quad (A.9)$$

Dividing equation A.8 by A.9 gives:

$$\frac{Q_{N_2}}{Q_{Mix}} = \left(\frac{\rho_{Mix}}{\rho_{N_2}} \right)^{\frac{1}{2}} \quad (A.10)$$

Therefore, the corrected volumetric flow rate for the gas mixture is

$$Q_{Mix} = Q_{N_2} \left(\frac{\rho_{N_2}}{\rho_{Mix}} \right)^{\frac{1}{2}} \quad (A.11)$$

This correction is applied in the data reduction program.

A.7 Calibration of Gas Chromatograph

It was necessary in this investigation to design an apparatus which could be used for making mixtures of nitrogen and hydrogen sulfide or of nitrogen and sulfur dioxide of accurately known composition within a reasonably short time period. A description of this apparatus and the procedure followed for making up a known calibration mixture is given first, followed by the documentation and discussion of the experimental and calculated results.

A five litre capacity lucite cylinder equipped with a circulation fan and moveable lucite piston was used for preparing calibration mixtures of known composition. Lucite, stainless steel 316 and teflon all exhibited inertness toward nitrogen diluted H_2S and SO_2 in this equipment. The fan was driven by a magnetic-coupled motor. The magnet on the process side of the cylinder was coated with a spray-on form of teflon.

To make accurate samples of calibration gases, it was necessary to determine the volume of the calibration equipment accurately. The estimation of this volume included taking into account the irregularities which are found at each end of the cylinder. The mixing fan volume was determined by water displacement and along with the volume of the "hex" nut and piston rod protrusion, this combined volume is subtracted from the total volume. The residual volume from these calculations measured 11. cu cm. The cross-sectional area of the cylinder was 151.192 sq cm (diameter = 13.876 cm) and so, the volume of the cylinder was given by

$$V_c = 11. + (151.192)(L) \quad (A.12)$$

where, L = distance in cm between piston and end of cylinder

V_c = volume in cu cm

TABLE A.18 VOLUME OF GEOMETRIC IRREGULARITIES
IN GAS CHROMATOGRAPH CALIBRATION EQUIPMENT

<u>Description</u>	<u>Volume</u>
Magnet housing, valves	+ 66 cu cm
Hex nut, washer, piston rod	- 15 cu cm
Impeller, magnet, bracket	- 40 cu cm
Residual Volume	11 cu cm

Referring to Figure A.3, the procedure for making up calibration mixtures is now described step-by-step:

1. Note the barometric pressure, room temperature and the temperature of the water bath.
2. Fill the gas burette with mercury up to the top valve as shown in Figure A.3.
3. With the mixing fan on, flush the cylinder with pure nitrogen for three up-and-down cycles of the piston to remove previous gas contents.
4. Flush line B with pure nitrogen to eliminate any H_2S or SO_2 gas which may be present.
5. Fill the cylinder with pure nitrogen to the desired volume (i.e. piston position) through line A and then close the valve on this line at the cylinder.

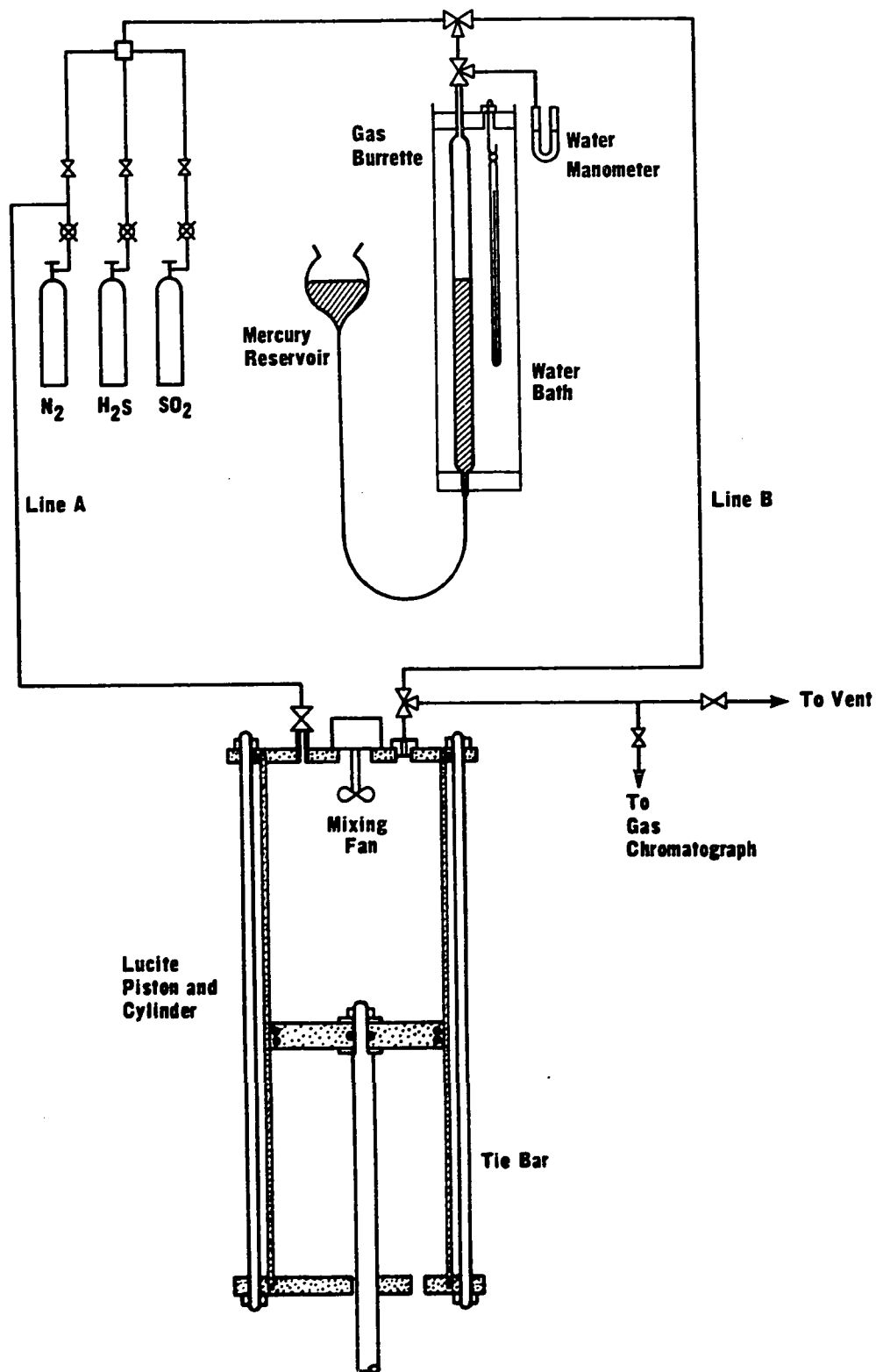


FIGURE A.3: PREPARATION OF GAS MIXTURE FOR CALIBRATION OF GAS CHROMATOGRAPH

6. Open the cylinder to vent for 60 seconds to enable the nitrogen in the cylinder time to equilibrate with atmospheric pressure, and then close the three-way valve at the cylinder.
7. Purge line B with the desired calibration gas, e.g., H_2S , for 60 seconds at least, to fill it with pure H_2S . Note that the flow goes from the H_2S bottle through to vent.
8. Fill the gas burette to the desired volume of H_2S with the H_2S flow still in the purge mode. Remaining in the purge mode is a safety precaution taken to prevent blowing out the gas burette with H_2S .
9. Isolate the gas burette from the H_2S flow using the top valve.
10. Turn off the H_2S flow, but leave line B open to vent to give it a chance to reach atmospheric pressure.
11. Measure the exact volumetric reading at atmospheric pressure by manipulation of the mercury reservoir and using the water manometer as the reference pressure.
12. Isolate the burette from the water manometer, isolate line B from vent, lift the mercury reservoir, and then open the burette to line B. Keeping at least a 5 cm head of pressure in line B, open the cylinder and force the H_2S into it. Close the valve on the cylinder, bring line B back to atmospheric pressure by adjusting the mercury level in the burette

and checking with the reference water manometer, and again note the reading of the burette.

13. Allow the fan to mix the cylinder contents for at least ten minutes.

During the calibration process, a large amount of experimental data was recorded for each run. To organize this data, document it and calculate meaningful results, a computer program, GCCAL, was written. A computer listing of GCCAL is given on the following pages, and the data are documented on the next 21 pages. A summary of the calculated results is presented in Table A.19 for the peak areas obtained by the disk integrator on the recorder.

The internal standard calibration method was employed. While several methods for obtaining quantitative gas chromatographic data are available, the internal standard technique was selected because the form of data correlation lends itself easily to curve fitting. For unknown mixtures, the repeatability of sample size within limits is not necessary and it is also applicable to the relatively low concentration levels which were used in this investigation. This method is fully described in a report published by Hewlett Packard⁽⁷⁾.

Following the selection of an internal standard (in this case, nitrogen), the response characteristics of standard mixtures (prepared with the previously described equipment and procedures) must be deter-

mined.

Each standard mixture was analyzed under the same conditions (described in Chapter 3). The areas of the peaks were determined simultaneously by the disk integrator on the recorder and the IBM 1800 computer GC-pack (described in Part II) two times, and the area response ratios were determined (e.g. $100 \times \text{H}_2\text{S}$ peak area/nitrogen peak area) and plotted as abscissas. The corresponding molar ratios were plotted as ordinates to obtain the straight lines shown in Figures A.4 and A.5. A summary of this data for the disk integrator appears in Table A.19 and the least squares coefficients for straight line fitting of the data is given in Tables A.20 to A.20.C.

Since nitrogen was used for diluting the reactor feed constituents, the internal standard is present in all gas stream analyses. From the area response ratios ($100 \times \text{H}_2\text{S}$ area and $100 \times \text{SO}_2$ area/ N_2 area), the molar ratios (Y_1 and Y_2) can be determined from the previously fitted data and from this the sample composition calculated by solving the following equations.

$$Y_{\text{N}_2} + Y_{\text{H}_2\text{S}} + Y_{\text{SO}_2} = 1 \quad (\text{A.13})$$

$$Y_{\text{H}_2\text{S}}/Y_{\text{N}_2} = Y_1 \quad (\text{A.14})$$

$$Y_{\text{SO}_2} / Y_{\text{N}_2} = Y_2 \quad (\text{A.15})$$

TABLE A.19 GAS CHROMATOGRAPH CALIBRATION RESULTS

<u>Run Number</u>	<u>Component Calibrated</u>	<u>Component Attenuation</u>	<u>Component/Nitrogen Ratios</u>	
			<u>100x Molar Ratio</u>	<u>100x Area Ratio</u>
1	H ₂ S	9.8	1.05	1.70
2	H ₂ S	9.8	2.12	3.52
3	H ₂ S	9.8	3.48	5.83
4	H ₂ S	9.8	4.40	7.51
5	H ₂ S	9.8	5.48	9.16
6	H ₂ S	9.6	2.12	2.91
7	H ₂ S	9.6	3.48	4.83
8	H ₂ S	9.6	4.40	6.24
9	H ₂ S	9.6	5.48	7.73
10	H ₂ S	9.6	7.91	11.27
11	H ₂ S	9.4	3.48	4.42
12	H ₂ S	9.4	4.40	5.61
13	H ₂ S	9.4	5.48	6.98
14	H ₂ S	9.4	7.91	10.13
15	H ₂ S	9.4	10.12	12.98
16	SO ₂	9.8	2.26	4.52
17	SO ₂	9.8	4.64	9.37
18	SO ₂	9.8	6.23	12.69
19	SO ₂	9.8	6.60	13.29
20	SO ₂	9.8	8.63	17.39
21	SO ₂	9.8	11.27	22.75

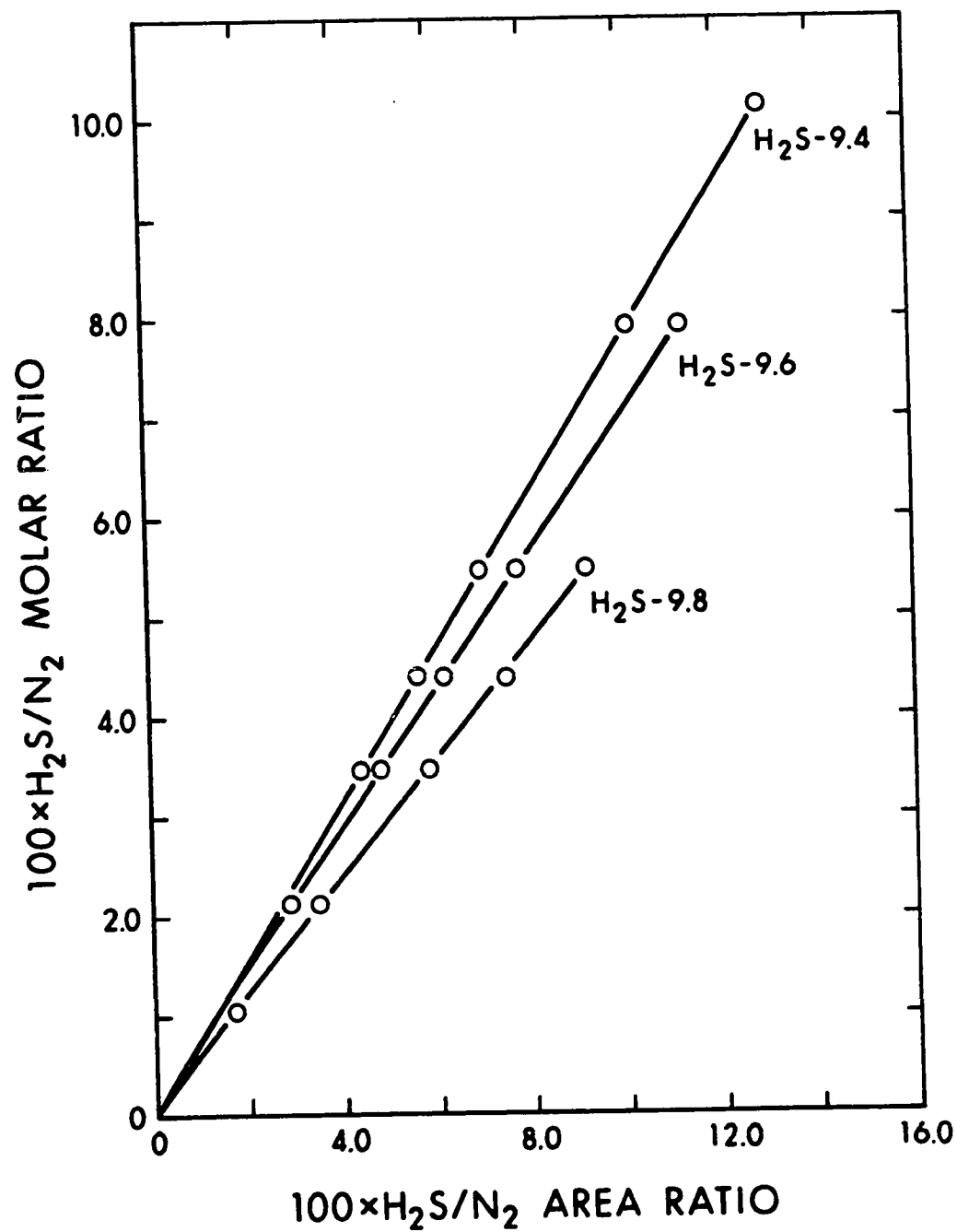


FIGURE A.4: GAS CHROMATOGRAPH CALIBRATION OF H_2S

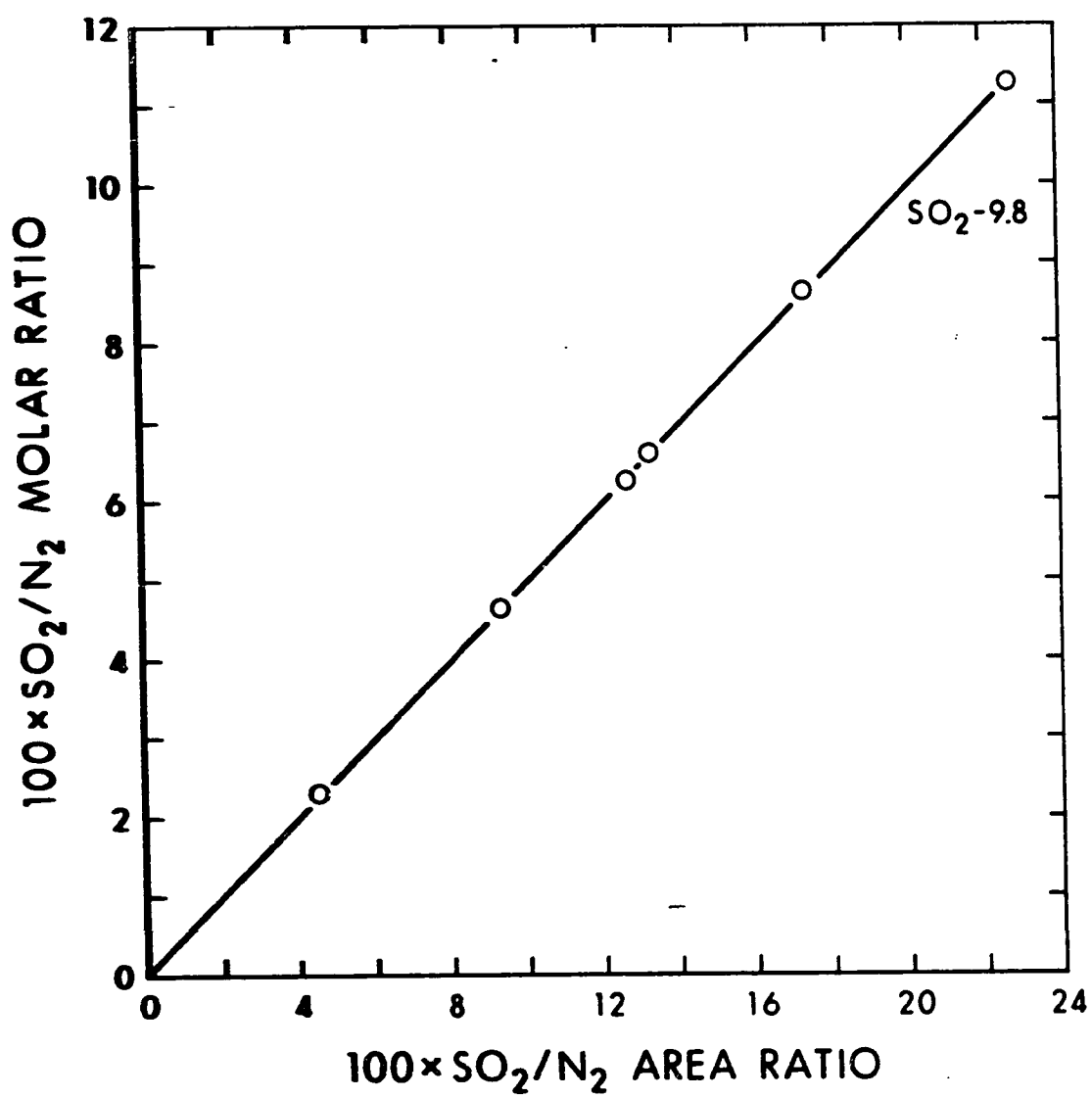


FIGURE A.5: GAS CHROMATOGRAPH CALIBRATION FOR SO_2 .

TABLE A.20

LEAST SQUARES FIT OF GAS CHROMATOGRAPH DATA

X MEASURED = 100X H₂S/N₂ AREA RATIO

Y OBSERVED = 100X H₂S/N₂ MOLAR RATIO

NOTE - H₂S ATTENUATOR=9.8

- AREAS MEASURED BY DISK INTEGRATOR

THE COEFFICIENTS OF THE POLYNOMIAL ARE

A₀ = 0.04182

A₁ = 0.58877

REGENERATED DATA

X MEASURED	Y OBSERVED	Y CALCULATED	PCT ERROR
1.700	1.050	1.042	0.690
3.520	2.120	2.114	0.268
5.830	3.480	3.474	0.161
7.510	4.400	4.463	1.443
9.160	5.480	5.435	0.820

VARIANCE = 0.001544

STANDARD DEVIATION = 0.039295

MAXIMUM PCT ERROR = 1.443906

TABLE A.20A

LEAST SQUARES FIT OF GAS CHROMATOGRAPH DATA

X MEASURED = 100X H₂S/N₂ AREA RATIO

Y OBSERVED = 100X H₂S/N₂ MOLAR RATIO

NOTE - H₂S ATTENUATOR=9.6

- AREAS MEASURED BY DISK INTEGRATOR

THE COEFFICIENTS OF THE POLYNOMIAL ARE

A₀ = 0.11291

A₁ = 0.69209

REGENERATED DATA

X MEASURED	Y OBSERVED	Y CALCULATED	PCT ERROR
2.910	2.120	2.126	0.326
4.830	3.480	3.455	0.696
6.240	4.400	4.431	0.718
7.730	5.480	5.462	0.313
11.270	7.910	7.912	0.036

VARIANCE = 0.000484

STANDARD DEVIATION = 0.022010

MAXIMUM PCT ERROR = 0.718485

TABLE A.20B

LEAST SQUARES FIT OF GAS CHROMATOGRAPH DATA

X MEASURED = 100X H₂S/N₂ AREA RATIOY OBSERVED = 100X H₂S/N₂ MOLAR RATIONOTE - H₂S ATTENUATOR=9.4

- AREAS MEASURED BY DISK INTEGRATOR

THE COEFFICIENTS OF THE POLYNOMIAL ARE

A₀ = 0.05473A₁ = 0.77558

REGENERATED DATA

X MEASURED	Y OBSERVED	Y CALCULATED	PCT ERROR
4.420	3.480	3.482	0.080
5.610	4.400	4.405	0.130
6.980	5.480	5.468	0.213
10.130	7.910	7.911	0.017
12.980	10.120	10.121	0.017

VARIANCE = 0.000045

STANDARD DEVIATION = 0.006763

MAXIMUM PCT ERROR = 0.213619

TABLE A.20C
LEAST SQUARES FIT OF GAS CHROMATOGRAPH DATA

X MEASURED = 100X SO₂/N₂ AREA RATIO

Y OBSERVED = 100X SO₂/N₂ MOLAR RATIO

NOTE - SO₂ ATTENUATOR=9.8

- AREAS MEASURED BY DISK INTEGRATOR

THE COEFFICIENTS OF THE POLYNOMIAL ARE

A₀ = 0.00437

A₁ = 0.49498

REGENERATED DATA

X MEASURED	Y OBSERVED	Y CALCULATED	PCT ERROR
4.520	2.260	2.241	0.809
9.370	4.640	4.642	0.051
12.690	6.230	6.285	0.894
13.290	6.600	6.582	0.261
17.390	8.630	8.612	0.206
22.750	11.270	11.265	0.041

VARIANCE = 0.000817

STANDARD DEVIATION = 0.028584

MAXIMUM PCT ERROR = 0.894632

A.8 Gas Chromatograph Data Reduction Program

A computer program, GCCAL, was written in Fortran to document the calibration data for the gas chromatograph. The required input data is indicated in the program heading and the input data formats can be found in the program listing which follows.

The calculations performed by GCCAL are listed below.

1. Calculate the number of moles of nitrogen in the cylinder using

$$NN_2 = (11. + (151.192)(L))\left(\frac{273.}{RT}\right)\left(\frac{BP}{760.}\right)\left(\frac{1.}{MVN_2}\right) \quad (A.16)$$

where, NN_2 = number of moles of nitrogen

L = distance between piston and end of cylinder
(cm)

RT = room temperature ($^{\circ}K$)

BP = barometric pressure (mm Hg)

MVN_2 = molecular volume of nitrogen (cu cm at $0^{\circ}C$)

2. Calculate the number of moles of calibration gas (either H_2S or SO_2) using

$$NCG = (VCG)\left(\frac{273.}{BT}\right)\left(\frac{BP}{760.}\right)\left(\frac{1.}{MVCG}\right) \quad (A.17)$$

where, NCG = number of moles of calibration gm of gas

VCG = volume of calibration gas admitted to
cylinder (cu cm)

BT = water bath temperature (°F)

MVCG = molecular volume of calibration gas (cu cm
at 0°C)

3. Calculate molar ratio and sample composition

$$MR_{100} = (100.)(NCG)/(NN_2) \quad (A.18)$$

where, MR_{100} = 100 times the molar ratio of the calibration
gas to the nitrogen

$$y_i = \frac{n_i}{n_1 + n_2} \quad (A.19)$$

where, y_i = mole fraction of component i

n_i = number of moles of component i

4. Calculate the corrected areas and obtain the area ratios
times 100.

$$CA_i = (MA_i)(21. - (2.)(ATTEN_i)) \quad (A.20)$$

where, CA_i = corrected area of component i peak

MA_i = measured area of component i peak

$ATTEN_i$ = attenuation used for component i.

Where applicable, averages are taken for measurements. The
results of the chromatograph calibration are given on the

pages following the program listing.

The molecular volumes which were used for the three gases are:⁽⁸⁾

N_2 - 22403.60 cu cm

H_2S - 22144.24 cu cm

SO_2 - 21889.30 cu cm

⁽⁸⁾The Matheson Company, Inc., "Matheson Gas Data Book" 4th ed., p. 287, 371 and 447, Herst Litho Inc., New York, N.Y., 1966.

```

C *****
C *
C *          MAINLINE GCCAL
C *
C * THIS PROGRAM WAS WRITTEN TO DOCUMENT THE DATA
C * TAKEN FOR THE CALIBRATION OF THE PROCESS GAS
C * CHROMATOGRAPH AND REDUCE THIS DATA TO CALCULATED
C * RESULTS USEFUL FOR THE INTERNAL STANDARD PROCEDURE
C * FOR THE CALIBRATION OF GAS CHROMATOGRAPHS.
C * INPUT DATA
C *   NSET - NUMBER OF SETS OF DATA
C *   NCOPY - NUMBER OF COPIES OF OUTPUT DESIRED
C *   NPAGE - PAGE NUMBER OF FIRST PAGE OF OUTPUT
C *   NRUN - CALIBRATION RUN NUMBER
C *   NCROM - NUMBER OF CHROMATOGRAMS TAKEN
C *   IPEAK - PEAK NUMBER CALIBRATED
C *           ...2 - H2S
C *           ...3 - SO2
C *   ICOMP - AREA FLAG
C *           ...1 - COMPUTER AREAS INCLUDED
C *           ...0 - NO COMPUTER AREAS
C *   RTEM - ROOM TEMPERATURE (DEG F)
C *   APRES - ATMOSPHERIC PRESSURE (MM HG)
C *   BTEM - WATER BATH TEMPERATURE (DEG F)
C *   V(1) - DISTANCE BETWEEN PISTON AND END OF
C *           CYLINDER (CM)
C *   V(2) - VOLUME OF CALIBRATION GAS (CU CM)
C *   RDG(1)- AREA OF NITROGEN PEAK
C *   RDG(2)- AREA OF CALIBRATION GAS
C *   RDG(3)- ATTENUATION FOR NITROGEN
C *   RDG(4)- ATTENUATION FOR CALIBRATION GAS
C *
C *****

```

```

      DIMENSION SNAM(4,2),SMV(3),V(2),RDG(7),AVG(7),STORE(20
      S,7)

```

```

      DATA SMV/22403.60,22144.24,21689.30/
      DATA SNAM/'HYDR','OGEN','SUL','FIDE','SULF','UR D'
      S,'IOXI','DE ' /

```

```

      READ(5,1) NSET,NCOPY,NPAGE
      DO 2 ISET=1,NSET
      READ(5,1) NRUN,NCROM,IPEAK,ICOMP
      READ(5,3) RTEM,BTEM,APRES,V(1),V(2)
      STEMP=273.
      SPRES=760.
      RTEX=(RTEM+460.)/1.8
      BTEM=(BTEM+460.)/1.8

```

```

C
C CALCULATION OF SAMPLE COMPOSITION

```

```

      XN2=(11.+151.192*V(1))*STEMP/RTEM*APRES/SPRES/SMV(1)

```

MAINLINE GCCAL ... (CONT'D)

```

V(1)=(11.+151.192*V(1))
XMCAL=V(2)*STEMP/BTEM*APRES/SPRES/SMV(IPEAK)
TOTM=XMN2+XMCAL
XMN2=XMN2/TOTM*100.
XMCAL=XMCAL/TOTM*100.
RMOL=XMCAL/XMN2*100.
KPEAK=IPEAK-1

```

C READ AND PROCESS PEAK AREA DATA
C

```

NCAT=0
14 DO 4 I=1,7
  4 AVG(I)=0.0
    DO 5 ICROM=1,NCROM
      NCAT=NCAT+1
      READ(5,3) RDG
      RDG(5)=RDG(2)*(21.-2.*RDG(4))
      RDG(4)=RDG(2)
      RDG(2)=RDG(1)*(21.-2.*RDG(3))
      TOTA=RDG(2)+RDG(5)
      RDG(3)=RDG(2)/TOTA*100.
      RDG(6)=RDG(5)/TOTA*100.
      RDG(7)=RDG(5)/RDG(2)*100.
    DO 6 I=1,7
      6 AVG(I)=RDG(I)+AVG(I)
      DO 20 J=1,7
        20 STORE(NCAT,J)=RDG(J)
      5 CONTINUE
      DO 7 I=1,7
        7 AVG(I)=AVG(I)/NCROM
        NCAT=NCAT+1
        DO 21 J=1,7
          21 STORE(NCAT,J)=AVG(J)
          IF(ICOMP) 9,9,8
        8 ICOMP=0
        GO TO 14
      9 CONTINUE
      NN=NCROM+1
      N1=NN+1
      N2=2*NN
      DO 23 IC=1,NCOPY
        WRITE(6,17) NPAGE
        WRITE(6,10) NRUN,RTEN,BTEM,APRES,V(1),(SNAM(J,KPEAK)
        S,J=1,4),V(2)
        WRITE(6,11) XMN2,(SNAM(J,KPEAK),J=1,4),XMCAL,RMOL
        WRITE(6,12)
        WRITE(6,13) (SNAM(J,KPEAK),J=1,4)
        WRITE(6,15) ((STORE(I,J),J=1,7),I=1,NN)
        IF(ICOMP-1)23,24,24

```


MAINLINE GCCAL ... (CONT'D)

```

24 CONTINUE
  WRITE(6,16)
  WRITE(6,15) ((STORE(I,J),J=1,7),I=N1,N2)
23 CONTINUE
  NPAGE=NPAGE+1
  2 CONTINUE
  1 FORMAT(5I5)
  3 FORMAT(7F10.5)
10 FORMAT(      15X,'CALIBRATION SAMPLE NUMBER',I3,///10X
  S,'SAMPLE PREP
  LARATION CONDITIONS'//12X,'ROOM TEMPERATURE.....'
  S,F7.1,' DEG K
  2',//12X,'BATH TEMPERATURE.....',F7.1,' DEG K',/
  S/12X,'ATMOSPHE
  RIC PRESSURE.....',F7.1,' MM HG',//12X,'VOLUME OF
  S NITROGEN.....
  4.',F7.1,' CC',//12X,'VOLUME OF ',4A4,F7.1,' CC')
11 FORMAT( //,10X,'SAMPLE COMPOSITION (MOLE PERCENT)'/
  S/12X,'NITROGEN.
  1.....',F6.2,//12X,4A4,'... ',F6.2,//12X,'100X
  S MOLAR RATIO... ',
  2F6.2)
12 FORMAT( //,10X,'DISK INTEGRATOR AREA RESULTS (THE LAST
  S SET IS THE
  1AVERAGE)'/)
13 FORMAT(      19X,'NITROGEN',13X,4A4,9X,'100X',//11X
  S,'INPUT',3X,'CORR'
  2,4X,'PCT OF',5X,'INPUT',3X,'CORR',4X,'PCT OF',5X
  S,'AREA' /11X,'AREA
  3',4X,'AREA',4X,'TOTAL',6X,'AREA',4X,'AREA',4X,'TOTAL'
  S,6X,'RATIO'/)
15 FORMAT(9X,F6.1,2X,F7.1,2X,F6.2,5X,F6.1,2X,F6.1,2X,F6.2
  S,5X,F6.2/)
16 FORMAT( //,10X,'COMPUTER AREA RESULTS (THE LAST SET IS
  S THE AVERAGE
  1)'/)
17 FORMAT('1',///66X,'A-',I2,/)
  CALL EXIT
  END

```

CALIBRATION SAMPLE NUMBER 1

SAMPLE PREPARATION CONDITIONS

ROOM TEMPERATURE..... 293.3 DEG K
 BATH TEMPERATURE..... 293.3 DEG K
 ATMOSPHERIC PRESSURE..... 706.1 MM HG
 VOLUME OF NITROGEN..... 3851.2 CC
 VOLUME OF HYDROGEN SULFIDE 40.0 CC

SAMPLE COMPOSITION (MOLE PERCENT)

NITROGEN..... 98.96
 HYDROGEN SULFIDE... 1.03
 100X MOLAR RATIO... 1.05

DISK INTEGRATOR AREA RESULTS (THE LAST SET IS THE AVERAGE)

NITROGEN			HYDROGEN SULFIDE			100X
INPUT AREA	CORR AREA	PCT OF TOTAL	INPUT AREA	CORR AREA	PCT OF TOTAL	AREA RATIO
103.0	5047.0	98.31	61.8	86.5	1.68	1.71
101.0	4949.0	98.33	60.0	84.0	1.66	1.69
102.0	4998.0	98.32	60.9	85.2	1.67	1.70

CALIBRATION SAMPLE NUMBER 2

SAMPLE PREPARATION CONDITIONS

ROOM TEMPERATURE..... 293.8 DEG K
 BATH TEMPERATURE..... 293.3 DEG K
 ATMOSPHERIC PRESSURE..... 706.1 MM HG
 VOLUME OF NITROGEN..... 3851.2 CC
 VOLUME OF HYDROGEN SULFIDE 80.8 CC

SAMPLE COMPOSITION (MOLE PERCENT)

NITROGEN..... 97.91
 HYDROGEN SULFIDE... 2.08
 100X MOLAR RATIO... 2.12

DISK INTEGRATOR AREA RESULTS (THE LAST SET IS THE AVERAGE)

NITROGEN			HYDROGEN SULFIDE			100X
INPUT AREA	CORR AREA	PCT OF TOTAL	INPUT AREA	CORR AREA	PCT OF TOTAL	AREA RATIO
94.0	4606.0	96.59	116.0	162.4	3.40	3.52
94.8	4645.2	96.59	117.0	163.8	3.40	3.52
94.4	4625.6	96.59	116.5	163.1	3.40	3.52

CALIBRATION SAMPLE NUMBER 3

SAMPLE PREPARATION CONDITIONS

ROOM TEMPERATURE..... 293.6 DEG K
BATH TEMPERATURE..... 293.8 DEG K
ATMOSPHERIC PRESSURE..... 703.7 MM HG
VOLUME OF NITROGEN..... 3851.2 CC
VOLUME OF HYDROGEN SULFIDE 132.7 CC

SAMPLE COMPOSITION (MOLE PERCENT)

NITROGEN..... 96.63
HYDROGEN SULFIDE... 3.36
100X MOLAR RATIO... 3.48

DISK INTEGRATOR AREA RESULTS (THE LAST SET IS THE AVERAGE)

NITROGEN			HYDROGEN SULFIDE			100X
INPUT AREA	CORR AREA	PCT OF TOTAL	INPUT AREA	CORR AREA	PCT OF TOTAL	AREA RATIO
95.6	4684.4	94.46	196.0	274.4	5.53	5.85
97.0	4753.0	94.51	197.0	275.8	5.48	5.80
96.3	4718.7	94.49	196.5	275.1	5.50	5.83

CALIBRATION SAMPLE NUMBER 4

SAMPLE PREPARATION CONDITIONS

ROOM TEMPERATURE..... 294.1 DEG K
BATH TEMPERATURE..... 294.1 DEG K
ATMOSPHERIC PRESSURE..... 696.5 MM HG
VOLUME OF NITROGEN..... 3851.2 CC
VOLUME OF HYDROGEN SULFIDE 167.6 CC

SAMPLE COMPOSITION (MOLE PERCENT)

NITROGEN..... 95.78
HYDROGEN SULFIDE... 4.21
100X MOLAR RATIO... 4.40

DISK INTEGRATOR AREA RESULTS (THE LAST SET IS THE AVERAGE)

NITROGEN			HYDROGEN SULFIDE			100X
INPUT AREA	CORR AREA	PCT OF TOTAL	INPUT AREA	CORR AREA	PCT OF TOTAL	AREA RATIO
90.0	4410.0	93.00	236.8	331.5	6.99	7.51
89.8	4400.2	93.00	236.3	330.8	6.99	7.51
89.9	4405.1	93.00	236.5	331.1	6.99	7.51

CALIBRATION SAMPLE NUMBER 5

SAMPLE PREPARATION CONDITIONS

ROOM TEMPERATURE..... 293.0 DEG K
 BATH TEMPERATURE..... 293.0 DEG K
 ATMOSPHERIC PRESSURE..... 701.7 MM HG
 VOLUME OF NITROGEN..... 3851.2 CC
 VOLUME OF HYDROGEN SULFIDE 208.6 CC

SAMPLE COMPOSITION (MOLE PERCENT)

NITROGEN..... 94.80
 HYDROGEN SULFIDE... 5.19
 100X MOLAR RATIO... 5.48

DISK INTEGRATOR AREA RESULTS (THE LAST SET IS THE AVERAGE)

NITROGEN			HYDROGEN SULFIDE			100X
INPUT AREA	CORR AREA	PCT OF TOTAL	INPUT AREA	CORR AREA	PCT OF TOTAL	AREA RATIO
90.8	4449.2	91.59	291.5	408.1	8.40	9.17
91.5	4483.5	91.61	293.0	410.2	8.38	9.14
91.1	4466.3	91.60	292.2	409.1	8.39	9.16

CALIBRATION SAMPLE NUMBER 6

SAMPLE PREPARATION CONDITIONS

ROOM TEMPERATURE..... 293.8 DEG K
 BATH TEMPERATURE..... 293.3 DEG K
 ATMOSPHERIC PRESSURE..... 706.1 MM HG
 VOLUME OF NITROGEN..... 3851.2 CC
 VOLUME OF HYDROGEN SULFIDE 80.8 CC

SAMPLE COMPOSITION (MOLE PERCENT)

NITROGEN..... 97.91
 HYDROGEN SULFIDE... 2.08
 100X MOLAR RATIO... 2.12

DISK INTEGRATOR AREA RESULTS (THE LAST SET IS THE AVERAGE)

NITROGEN			HYDROGEN SULFIDE			100X
INPUT AREA	CORR AREA	PCT OF TOTAL	INPUT AREA	CORR AREA	PCT OF TOTAL	AREA RATIO
94.0	4606.0	97.17	74.5	134.1	2.82	2.91
94.0	4606.0	97.17	74.5	134.1	2.82	2.91
94.0	4606.0	97.17	74.5	134.1	2.82	2.91

CALIBRATION SAMPLE NUMBER 7

SAMPLE PREPARATION CONDITIONS

ROOM TEMPERATURE..... 293.6 DEG K
 BATH TEMPERATURE..... 293.8 DEG K
 ATMOSPHERIC PRESSURE..... 703.7 MM HG
 VOLUME OF NITROGEN..... 3851.2 CC
 VOLUME OF HYDROGEN SULFIDE 132.7 CC

SAMPLE COMPOSITION (MOLE PERCENT)

NITROGEN..... 96.63
 HYDROGEN SULFIDE... 3.36
 100X MOLAR RATIO... 3.48

DISK INTEGRATOR AREA RESULTS (THE LAST SET IS THE AVERAGE)

NITROGEN			HYDROGEN SULFIDE			100X
INPUT AREA	CORR AREA	PCT OF TOTAL	INPUT AREA	CORR AREA	PCT OF TOTAL	AREA RATIO
97.0	4753.0	95.39	127.5	229.5	4.60	4.82
97.0	4753.0	95.37	128.0	230.4	4.62	4.84
97.0	4753.0	95.38	127.7	229.9	4.61	4.83

CALIBRATION SAMPLE NUMBER 8

SAMPLE PREPARATION CONDITIONS

ROOM TEMPERATURE..... 294.1 DEG K
 BATH TEMPERATURE..... 294.1 DEG K
 ATMOSPHERIC PRESSURE..... 696.5 MM HG
 VOLUME OF NITROGEN..... 3851.2 CC
 VOLUME OF HYDROGEN SULFIDE 167.6 CC

SAMPLE COMPOSITION (MOLE PERCENT)

NITROGEN..... 95.78
 HYDROGEN SULFIDE... 4.21
 100X MOLAR RATIO... 4.40

DISK INTEGRATOR AREA RESULTS (THE LAST SET IS THE AVERAGE)

NITROGEN			HYDROGEN SULFIDE			100X
INPUT AREA	CORR AREA	PCT OF TOTAL	INPUT AREA	CORR AREA	PCT OF TOTAL	AREA RATIO
90.6	4439.4	94.15	153.0	275.4	5.84	6.20
91.7	4493.3	94.08	157.0	282.6	5.91	6.28
91.1	4466.3	94.12	155.0	279.0	5.87	6.24

CALIBRATION SAMPLE NUMBER 9

SAMPLE PREPARATION CONDITIONS

ROOM TEMPERATURE..... 293.0 DEG K
 BATH TEMPERATURE..... 293.0 DEG K
 ATMOSPHERIC PRESSURE..... 701.7 MM HG
 VOLUME OF NITROGEN..... 3851.2 CC
 VOLUME OF HYDROGEN SULFIDE 208.6 CC

SAMPLE COMPOSITION (MOLE PERCENT)

NITROGEN..... 94.80
 HYDROGEN SULFIDE... 5.19
 100X MOLAR RATIO... 5.48

DISK INTEGRATOR AREA RESULTS (THE LAST SET IS THE AVERAGE)

NITROGEN			HYDROGEN SULFIDE			100X
INPUT AREA	CORR AREA	PCT OF TOTAL	INPUT AREA	CORR AREA	PCT OF TOTAL	AREA RATIO
94.6	4635.4	92.82	199.0	353.2	7.17	7.72
95.0	4655.0	92.82	200.0	360.0	7.17	7.73
94.8	4645.2	92.82	199.5	359.1	7.17	7.73

CALIBRATION SAMPLE NUMBER 10

SAMPLE PREPARATION CONDITIONS

ROOM TEMPERATURE..... 293.8 DEG K
 BATH TEMPERATURE..... 293.8 DEG K
 ATMOSPHERIC PRESSURE..... 702.8 MM HG
 VOLUME OF NITROGEN..... 3851.2 CC
 VOLUME OF HYDROGEN SULFIDE 301.4 CC

SAMPLE COMPOSITION (MOLE PERCENT)

NITROGEN..... 92.66
 HYDROGEN SULFIDE... 7.33
 100X MOLAR RATIO... 7.91

DISK INTEGRATOR AREA RESULTS (THE LAST SET IS THE AVERAGE)

NITROGEN			HYDROGEN SULFIDE			100X
INPUT AREA	CORR AREA	PCT OF TOTAL	INPUT AREA	CORR AREA	PCT OF TOTAL	AREA RATIO
93.1	4561.9	89.85	286.0	514.8	10.14	11.28
89.0	4361.0	89.83	272.7	490.8	10.11	11.25
91.0	4461.4	89.87	279.3	502.8	10.12	11.27

CALIBRATION SAMPLE NUMBER 11

SAMPLE PREPARATION CONDITIONS

ROOM TEMPERATURE..... 293.6 DEG K
 BATH TEMPERATURE..... 293.8 DEG K
 ATMOSPHERIC PRESSURE..... 703.7 MM HG
 VOLUME OF NITROGEN..... 3851.2 CC
 VOLUME OF HYDROGEN SULFIDE 132.7 CC

SAMPLE COMPOSITION (MOLE PERCENT)

NITROGEN..... 96.63
 HYDROGEN SULFIDE... 3.36
 100X MOLAR RATIO... 3.48

DISK INTEGRATOR AREA RESULTS (THE LAST SET IS THE AVERAGE)

NITROGEN			HYDROGEN SULFIDE			100X
INPUT AREA	CORR AREA	PCT OF TOTAL	INPUT AREA	CORR AREA	PCT OF TOTAL	AREA RATIO
91.0	4459.0	95.75	89.8	197.5	4.24	4.43
97.0	4753.0	95.76	95.5	210.1	4.23	4.42
94.0	4606.0	95.76	92.6	203.8	4.23	4.42

CALIBRATION SAMPLE NUMBER 12

SAMPLE PREPARATION CONDITIONS

ROOM TEMPERATURE..... 294.1 DEG K
 BATH TEMPERATURE..... 294.1 DEG K
 ATMOSPHERIC PRESSURE..... 696.5 MM HG
 VOLUME OF NITROGEN..... 3851.2 CC
 VOLUME OF HYDROGEN SULFIDE 167.6 CC

SAMPLE COMPOSITION (MOLE PERCENT)

NITROGEN..... 95.78
 HYDROGEN SULFIDE... 4.21
 100X MOLAR RATIO... 4.40

DISK INTEGRATOR AREA RESULTS (THE LAST SET IS THE AVERAGE)

NITROGEN			HYDROGEN SULFIDE			100X
INPUT AREA	CORR AREA	PCT OF TOTAL	INPUT AREA	CORR AREA	PCT OF TOTAL	AREA RATIO
94.6	4635.4	94.67	118.5	260.7	5.32	5.62
92.0	4508.0	94.68	115.0	253.0	5.31	5.61
93.3	4571.7	94.68	116.7	256.8	5.31	5.61

CALIBRATION SAMPLE NUMBER 13

SAMPLE PREPARATION CONDITIONS

ROOM TEMPERATURE..... 293.0 DEG K
 BATH TEMPERATURE..... 293.0 DEG K
 ATMOSPHERIC PRESSURE..... 701.7 MM HG
 VOLUME OF NITROGEN..... 3851.2 CC
 VOLUME OF HYDROGEN SULFIDE 208.6 CC

SAMPLE COMPOSITION (MOLE PERCENT)

NITROGEN..... 94.80
 HYDROGEN SULFIDE... 5.19
 100X MOLAR RATIO... 5.48

DISK INTEGRATOR AREA RESULTS (THE LAST SET IS THE AVERAGE)

NITROGEN			HYDROGEN SULFIDE			100X
INPUT AREA	CORR AREA	PCT OF TOTAL	INPUT AREA	CORR AREA	PCT OF TOTAL	AREA RATIO
94.0	4606.0	93.46	146.5	322.3	6.53	6.99
98.6	4831.4	93.47	153.2	337.0	6.52	6.97
96.3	4718.7	93.46	149.8	329.6	6.53	6.98

CALIBRATION SAMPLE NUMBER 14

SAMPLE PREPARATION CONDITIONS

ROOM TEMPERATURE..... 293.8 DEG K
 BATH TEMPERATURE..... 293.8 DEG K
 ATMOSPHERIC PRESSURE..... 702.8 MM HG
 VOLUME OF NITROGEN..... 3851.2 CC
 VOLUME OF HYDROGEN SULFIDE 301.4 CC

SAMPLE COMPOSITION (MOLE PERCENT)

NITROGEN..... 92.66
 HYDROGEN SULFIDE... 7.33
 100X MOLAR RATIO... 7.91

DISK INTEGRATOR AREA RESULTS (THE LAST SET IS THE AVERAGE)

NITROGEN			HYDROGEN SULFIDE			100X
INPUT AREA	CORR AREA	PCT OF TOTAL	INPUT AREA	CORR AREA	PCT OF TOTAL	AREA RATIO
92.5	4532.5	90.82	208.0	457.6	9.17	10.09
91.4	4478.6	90.77	207.0	455.4	9.22	10.16
91.9	4505.5	90.80	207.5	456.5	9.20	10.13

CALIBRATION SAMPLE NUMBER 15

SAMPLE PREPARATION CONDITIONS

ROOM TEMPERATURE..... 294.4 DEG K
 BATH TEMPERATURE..... 294.7 DEG K
 ATMOSPHERIC PRESSURE..... 702.3 MM HG
 VOLUME OF NITROGEN..... 3851.2 CC
 VOLUME OF HYDROGEN SULFIDE 385.9 CC

SAMPLE COMPOSITION (MOLE PERCENT)

NITROGEN..... 90.80
 HYDROGEN SULFIDE... 9.19
 100X MOLAR RATIO... 10.12

DISK INTEGRATOR AREA RESULTS (THE LAST SET IS THE AVERAGE)

NITROGEN			HYDROGEN SULFIDE			100X
INPUT AREA	CCRR AREA	PCT OF TOTAL	INPUT AREA	CORR AREA	PCT OF TOTAL	AREA RATIO
93.5	4581.5	88.52	270.0	594.0	11.47	12.96
93.5	4581.5	88.48	271.0	596.2	11.51	13.01
93.5	4581.5	88.50	270.5	595.1	11.49	12.98

CALIBRATION SAMPLE NUMBER 16

SAMPLE PREPARATION CONDITIONS

ROOM TEMPERATURE..... 295.5 DEG K
 BATH TEMPERATURE..... 295.5 DEG K
 ATMOSPHERIC PRESSURE..... 703.6 MM HG
 VOLUME OF NITROGEN..... 3851.2 CC
 VOLUME OF SULFUR DIOXIDE 85.2 CC

SAMPLE COMPOSITION (MOLE PERCENT)

NITROGEN..... 97.78
 SULFUR DIOXIDE ... 2.21
 100X MOLAR RATIO... 2.26

DISK INTEGRATOR AREA RESULTS (THE LAST SET IS THE AVERAGE)

NITROGEN			SULFUR DIOXIDE			100X
INPUT AREA	CORR AREA	PCT OF TOTAL	INPUT AREA	CORR AREA	PCT OF TOTAL	AREA RATIO
92.8	4547.2	95.65	147.4	206.3	4.34	4.53
97.6	4782.4	95.68	154.0	215.6	4.31	4.50
95.2	4664.7	95.67	150.7	210.9	4.32	4.52

CALIBRATION SAMPLE NUMBER 17

SAMPLE PREPARATION CONDITIONS

ROOM TEMPERATURE..... 296.1 DEG K
 BATH TEMPERATURE..... 296.6 DEG K
 ATMOSPHERIC PRESSURE..... 697.4 MM HG
 VOLUME OF NITROGEN..... 3851.2 CC
 VOLUME OF SULFUR DIOXIDE 175.3 CC

SAMPLE COMPOSITION (MOLE PERCENT)

NITROGEN..... 95.55
 SULFUR DIOXIDE ... 4.44
 100X MOLAR RATIO... 4.64

DISK INTEGRATOR AREA RESULTS (THE LAST SET IS THE AVERAGE)

NITROGEN			SULFUR DIOXIDE			100X
INPUT AREA	CORR AREA	PCT OF TOTAL	INPUT AREA	CORR AREA	PCT OF TOTAL	AREA RATIO
92.5	4522.5	91.41	304.0	425.6	8.58	9.38
91.8	4498.2	91.43	301.0	421.4	8.56	9.36
92.1	4515.3	91.42	302.5	423.5	8.57	9.37

CALIBRATION SAMPLE NUMBER 18

SAMPLE PREPARATION CONDITIONS

ROOM TEMPERATURE..... 296.6 DEG K
 BATH TEMPERATURE..... 296.6 DEG K
 ATMOSPHERIC PRESSURE..... 696.6 MM HG
 VOLUME OF NITROGEN..... 3851.2 CC
 VOLUME OF SULFUR DIOXIDE 234.6 CC

SAMPLE COMPOSITION (MOLE PERCENT)

NITROGEN..... 94.13
 SULFUR DIOXIDE ... 5.86
 100X MOLAR RATIO... 6.23

DISK INTEGRATOR AREA RESULTS (THE LAST SET IS THE AVERAGE)

NITROGEN			SULFUR DIOXIDE			100X
INPUT AREA	CORR AREA	PCT OF TOTAL	INPUT AREA	CORR AREA	PCT OF TOTAL	AREA RATIO
92.5	4232.5	88.66	414.0	579.6	11.33	12.78
92.8	4347.2	88.81	409.0	572.6	11.18	12.59
92.6	4339.8	88.73	411.5	576.1	11.26	12.69

CALIBRATION SAMPLE NUMBER 19

SAMPLE PREPARATION CONDITIONS

ROOM TEMPERATURE..... 296.6 DEG K
 BATH TEMPERATURE..... 296.6 DEG K
 ATMOSPHERIC PRESSURE..... 696.1 MM HG
 VOLUME OF NITROGEN..... 3851.2 CC
 VOLUME OF SULFUR DIOXIDE 248.3 CC

SAMPLE COMPOSITION (MOLE PERCENT)

NITROGEN..... 93.80
 SULFUR DIOXIDE ... 6.19
 100X MOLAR RATIO... 6.60

DISK INTEGRATOR AREA RESULTS (THE LAST SET IS THE AVERAGE)

NITROGEN			SULFUR DIOXIDE			100X
INPUT AREA	CORR AREA	PCT OF TOTAL	INPUT AREA	CORR AREA	PCT OF TOTAL	AREA RATIO
91.3	4473.7	88.25	425.2	595.2	11.74	13.30
93.2	4566.8	88.28	433.0	606.2	11.71	13.27
92.2	4520.2	88.26	429.1	600.7	11.73	13.29

CALIBRATION SAMPLE NUMBER 20

SAMPLE PREPARATION CONDITIONS

ROOM TEMPERATURE..... 296.6 DEG K
 BATH TEMPERATURE..... 296.9 DEG K
 ATMOSPHERIC PRESSURE..... 694.8 MM HG
 VOLUME OF NITROGEN..... 3851.2 CC
 VOLUME OF SULFUR DIOXIDE 325.3 CC

SAMPLE COMPOSITION (MOLE PERCENT)

NITROGEN..... 92.04
 SULFUR DIOXIDE ... 7.95
 100X MOLAR RATIO... 8.63

DISK INTEGRATOR AREA RESULTS (THE LAST SET IS THE AVERAGE)

NITROGEN			SULFUR DIOXIDE			100X
INPUT AREA	CORR AREA	PCT OF TOTAL	INPUT AREA	CORR AREA	PCT OF TOTAL	AREA RATIO
89.4	4380.6	85.25	541.2	757.6	14.74	17.29
88.6	4341.4	85.11	542.4	759.3	14.88	17.49
89.0	4360.9	85.18	541.8	758.5	14.81	17.39

CALIBRATION SAMPLE NUMBER 21

SAMPLE PREPARATION CONDITIONS

ROOM TEMPERATURE..... 295.8 DEG K
 BATH TEMPERATURE..... 295.8 DEG K
 ATMOSPHERIC PRESSURE..... 697.0 MM HG
 VOLUME OF NITROGEN..... 3851.2 CC
 VOLUME OF SULFUR DIOXIDE 424.2 CC

SAMPLE COMPOSITION (MOLE PERCENT)

NITROGEN..... 89.86
 SULFUR DIOXIDE ... 10.13
 100X MOLAR RATIO... 11.27

DISK INTEGRATOR AREA RESULTS (THE LAST SET IS THE AVERAGE)

NITROGEN			SULFUR DIOXIDE			100X
INPUT AREA	CORR AREA	PCT OF TOTAL	INPUT AREA	CORR AREA	PCT OF TOTAL	AREA RATIO
85.4	4124.6	81.51	678.0	949.2	18.48	22.68
85.1	4169.9	81.41	679.8	951.7	18.58	22.82
85.2	4177.2	81.46	678.9	950.4	18.53	22.75

A.9 Least Squares Data Correlation Program

A computer program was written in Fortran IV basic to estimate the parameters of power series polynomials which were fitted to the calibration data. The program is divided into a mainline and three sub-routines and comment cards at the start of each routine describe its purpose. The form of the polynomial is

$$y = a_0 + a_1x + a_2x^2 + \dots \quad (\text{A.1})$$

and it is suggested that Fröberg⁽⁹⁾ be consulted for the mathematical details of the curve-fitting process.

(9) Fröberg, C.E., "Introduction to Numerical Analysis", p. 278, Addison-Wesley Publishing Company, Reading, Mass., 1965.

```

C *****
C *
C *
C *          MAINLINE LEAST
C *
C * THIS PROGRAM WAS WRITTEN FOR FITTING A MAXIMUM OF
C * 50 DATA POINTS TO POWER SERIES TYPE POLYNOMIALS OF
C * ANY ORDER UP TO A MAXIMUM OF FOURTH DEGREE.
C *
C *   INPUT DATA
C *
C *   NCASE  - NUMBER OF SETS OF DATA
C *   NCOPY  - NUMBER OF COPIES OF OUTPUT DESIRED
C *   N      - NUMBER OF DATA POINTS
C *   M      - DEGREE OF POLYNOMIAL
C *   NTL    - NUMBER OF CARDS FOR TITLE
C *   NPAGE  - PAGE NUMBER OF OUTPUT
C *   NPLT   - DATA REGENERATION FLAG
C *             ...0-REGENERATE GIVEN DATA ONLY
C *             ...1-REGENERATE GIVEN DATA PLUS 20
C *             INTERMEDIATE POINTS
C *   DES(K) - ALPHANUMERIC DESCRIPTION OF THE TITLE
C *   Y(I)   - DEPENDENT VARIABLE
C *   X(I)   - INDEPENDENT VARIABLE
C *
C *****

```

```

      DIMENSION X(50),Y(50),A(50,5),P(20,20),V(20),Z(20)
      S,DES(10,15),SNAM
      1(5)
      DATA SNAM/'A0 = ','A1 = ','A2 = ','A3 = ','A4 = '/
      READ(5,1) NCASE,NCOPY
      DO 9 NC=1,NCASE
      READ(5,1) N,M,NTL,NPAGE,NPLT
      1 FORMAT(5I5)
      DO 11 NT=1,NTL
      11 READ(5,12) (DES(NT,K),K=1,15)
      12 FORMAT(15A4)
      13 FORMAT(10X,15A4/)
      MM=M+1
      DO 2 I=1,N
      2 READ(5,3) X(I),Y(I)
      3 FORMAT(2F10.5)
      DO 4 I=1,N
      DO 4 J=1,MM
      4 A(I,J)=X(I)**(J-1)
      DO 5 I=1,MM
      DO 5 J=1,MM
      P(I,J)=0.
      DO 5 K=1,N
      5 P(I,J)=P(I,J)+A(K,I)*A(K,J)
      DO 6 I=1,MM
      V(I)=0.
      DO 6 J=1,N
      6 V(I)=V(I)+Y(J)*A(J,I)

```


MAINLINE LEAST ... (CONT'D)

```
CALL GAUSS(P,V,MM,Z)
DO 16 ICOP=1,NCOPY
WRITE(6,10) NPAGE
10 FORMAT('1',///,66X,'A-',I2,/)
DO 17 I=1,NTL
17 WRITE(6,13)(DES(I,K),K=1,15)
WRITE(6,8)
8 FORMAT(   ///,10X,'THE COEFFICIENTS OF THE POLYNOMIAL
$ ARE '/')
DO 15 I=1,MM
15 WRITE(6,7) SNAM(I),Z(I)
7 FORMAT(15X,A4,F11.5/)
16 CALL REGEN(X,Y,Z,MM,N)
IF(NPLT) 9,9,14
14 CALL POLYN (X,Z,N,MM)
9 CONTINUE
CALL EXIT
END
```

```

C *****
C *
C *          SUBROUTINE POLYN
C *
C * POLYN SUPPLIES REGENERATED DATA AT POINTS INTER-
C * MEDIATE TO THE GIVEN DATA.
C *
C *****

```

```

SUBROUTINE POLYN(X,Z,N,MM)
  DIMENSION X(50),Z(20)
  WRITE(6,1)
1  FORMAT(///,32X,'PLOT TEST DATA'//25X'X CALCULATED',4X
  5,'Y CALCULATE
  1D'//)
  XMAX=0.
  XMIN=99999.
  DO 2 I=1,N
    IF(XMAX-X(I)) 3,3,4
3  XMAX=X(I)
4  IF(X(I)-XMIN) 5,5,2
5  XMIN=X(I)
2  CONTINUE
  DELX=(XMAX-XMIN)/20.
  XY=XMIN
  DO 6 I=1,20
    CAL=0.
    DO15 J=1,MM
15  CAL=CAL+Z(J)*XY**(J-1)
    WRITE(6,7) XY,CAL
7  FORMAT(24X,2(F10.3,5X))
6  XY=XY+DELX
  RETURN
  END

```

```

C *****
C *
C *          SUBROUTINE REGEN
C *
C * THIS SUBROUTINE REGENERATES THE GIVEN DATA AND
C * CALCULATES THE VARIANCE AND STANDARD DEVIATION OF
C * THE FIT.
C *
C *****

SUBROUTINE REGEN(X,Y,Z,MM,N)
  DIMENSION X(50),Y(50),Z(20)
  WRITE(6,1)
1  FORMAT(///,29X,'REGENERATED DATA'//10X,'X MEASURED',5X
  $,'Y OBSERVED
  1',5X,'Y CALCULATED',3X,'PCT ERROR',/)
  VAR=0.
  HI=0.
  DO 2 I=1,N
    CAL=0.
    DO 3 J=1,MM
3  CAL=CAL+Z(J)*X(I)**(J-1)
    CAT=ABS(Y(I)-CAL)
    PCE=CAT/Y(I)*100.
    VAR=VAR+CAT**2
    IF(HI-PCE)4,4,2
4  HI=PCE
2  WRITE(6,5) X(I),Y(I),CAL,PCE
5  FORMAT( 9X,4(F10.3,5X)/)
  VAR=VAR/(N-1)
  DEV=VAR**0.5
  WRITE(6,6) VAR,DEV,HI
6  FORMAT(//,10X'VARIANCE          =',F10.6//10X
  $,'STANDARD DEVIATION
  1 =',F10.6//10X,'MAXIMUM PCT ERROR  =',F10.6)
  RETURN
  END

```

```

C *****
C *
C *          SUBROUTINE GAUSS          *
C *
C * THE FUNCTION OF THIS SUBROUTINE IS TO SOLVE THE *
C * SET OF EQUATIONS A*X=B USING GAUSSIAN ELIMINATION *
C * AND BACK SUBSTITUTION ROTATING ABOUT THE ELEMENT *
C * OF MAXIMUM MODULUS. *
C *
C *****

```

```

SUBROUTINE GAUSS (A,R,N,X)
DIMENSION A(20,20),R(20),X(20)
M=N-1
DO 11 J=1,M
  S=0.
  DO 12 I=J,N
    U= ABS(A(I,J))
    IF(U-S) 12,12,112
112 S=U
    L=I
  12 CONTINUE
  IF(L=J) 119,19,119
119 DO 14 I=J,N
    S=A(L,I)
    A(L,I)=A(J,I)
  14 A(J,I)=S
    S=R(L)
    R(L)=R(J)
    R(J)=S
  19 IF( ABS(A(J,J))-1.E-30) 115,115,15
115 WRITE(6,3)
  GO TO 500
  15 MM=J+1
  DO 11 I=MM,N
    IF( ABS(A(I,J))-1.E-30) 11,111,111
111 S=A(J,J)/A(I,J)
    A(I,J)=0.0
    DO 16 K=MM,N
      16 A(I,K)=A(J,K)-S*A(I,K)
      R(I)=R(J)-S*R(I)
  11 CONTINUE
  DO 17 K=1,N
    I=N+1-K
    S=0.0
    IF(I=N) 117,17,117
117 MM=I+1
    DO 18 J=MM,N
      18 S=S+A(I,J)*X(J)
  17 X(I)=(R(I)-S)/A(I,I)
500 RETURN
  3 FORMAT (1H , 'MATRIX SINGULAR')

```

A-83

SUBROUTINE GAUSS ... (CONT'D)

END

APPENDIX B
DOCUMENTATION OF THE FREE ENERGY MINIMIZATION METHOD

The free energy minimization procedure was programmed in Fortran IV basic to solve the problem of finding the composition of a given mixture of gases when it reaches thermodynamic equilibrium at a given temperature and pressure.

The Fortran program, listed on the following pages, is broken up into a mainline and five subroutines. The purpose of each subroutine is stated in the comment cards at its beginning. Comment cards in the mainline program define each variable that is read in as data, and the format for the data is easily found by noting the appropriate READ and FORMAT statements in the program listing.

Output from the program includes one copy of the data, entitled Data Echo Check, and the specified number of copies of the tabulated equilibrium data. Following the program listing is an example of the data input (as used for Example 1), its data echo check and the eleven examples which were solved using the free energy minimization program, FREM.

It is pointed out that the expression for F/RT which is used in this program is taken from McBride and associates⁽¹⁾ where the coefficients for many compounds are available.

$$\frac{F}{RT} = a_1(1.-\ln T) - a_2 \frac{T}{2} - a_3 \frac{T^2}{6} - a_4 \frac{T^3}{16} - a_5 \frac{T^4}{20} + \frac{a_6}{T} - a_7 \quad .(B.1)$$

Two ways are provided which may be used for calculation of percent conversion of a particular starting component. For NCON = 1

(1) McBride, B.J., Helmel, S., Ehlers, J.G., and Gordon, S., "Thermodynamic Properties to 6000°K for 210 substances involving the first 18 Elements", NASA, 1963.

(refer to program listing), the percent conversion of the first component for which mass balance data was read in is calculated using the following equation.

$$\text{Pct. Conv.} = (X(1)_0 - X(1)_E) / X(1)_0 \quad (\text{B.2})$$

where $X(1)_0$ = number of moles of component number 1 initially
 $X(1)_E$ = number of moles of component number 1 at equilibrium.
 For NCON = 2, the conversion of H_2S to sulfur is calculated and the mass balance data for the first five compounds should be entered in the sequence indicated in the program listing.

$$\text{Pct. Conv.} = (8.X(1)_E + 6.X(2)_E + 2X(3)_E + X(4)_E) / X(5)_0 \quad (\text{B.3})$$

where $X(1)_E$ = number of S_8 moles at equilibrium
 $X(2)_E$ = number of S_6 moles at equilibrium
 $X(3)_E$ = number of S_2 moles at equilibrium
 $X(4)_E$ = number of S moles at equilibrium
 $X(5)_0$ = number of H_2S moles initially .

It is assumed in this second method of conversion calculation that there was no sulfur existent in the starting chemical mixture.

H*****ON*

C

```

*** READ IN DATA

READ (5,1) NCASE
DO 205 ICASE=1,NCASE
  READ(5,64) (DES(J),J=1,20)
64  FORMAT(20A4)
  READ(5,1) M,N,NCON,NCOPY
  1  FORMAT(5I5)
  N1=N+2
  READ(5,4) (ANAM(J),J=1,M)
  4  FORMAT(20A1)
  DO 2 I=1,N
    READ(5,3) SNAM(I),(A(I,J),J=1,M),X(I)

```

FREM ... (CONT'D)

```

3 FORMAT(A4,1X,10F5.0)
2 READ(5,5) (FRE(I,K),K=1,7)
5 FORMAT (5E15.7)

```

C *** ECHO CHECK DATA

```

DO 43 NCOP=1,NCOPY
WRITE(6,6) (ANAM(J),J=1,M),XNAM
6 FORMAT('1',////,39X,'DATA ECHO CHECK',//37X,'MASS
$ BALANCE MATRIX'/
1 /25X,'MOLECULAR',2X,10(2X,A1,2X))
WRITE(6,65)
65 FORMAT(25X,'SPECIE'//)
DO 66 I=1,N
66 WRITE(6,40) SNAM(I), (A(I,J),J=1,M),X(I)
WRITE(6,41)
40 FORMAT(27X,A4,5X,10(F4.2,1X)/)
41 FORMAT(/,36X,'FREE ENERGY DATA'//)
DO 43 I=1,N
43 WRITE(6,42) SNAM(I),(FRE(I,J),J=1,7)
42 FORMAT(10X,A4,4E15.7/14X,3E15.7/)
CALL DISTR(X,Y,B,N,M,A)
JBI=2
DO 208 ICAT=1,50
DO 10 NC=1,10
READ(5,11)PRESS,T
11 FORMAT(5F10.5)
IF(T-.01) 206,206,13
13 OTPT(1,NC)=T
OTPT(2,NC)=PRESS

```

C *** CALCULATE F/RT RATIOS

```

DO 12 I=1,N
NG1(I)=0
FRT=FRE(I,1)*(1.-ALOG(T))-FRE(I,2)*T/2.-FRE(I,3)*T**2
$/6
1.-FRE(I,4)*T**3/12.-FRE(I,5)*T**4/20.+FRE(I,6)/T-FRE(I
1,7)
12 C(I)=FRT+ALOG(PRESS)
DO 35 JB=1,JBI

```

C *** COMMENCE FREE ENERGY MINIMIZATION

```

DO 14 ITER=1,100
CALL FREN (Y,C,F,YBAR,N,NG1)
MG=M+1
CALL GSET (A,Y,GA,GB,B,F,M,MG,N)
CALL GAUSS(GA,GB,MG,GX)

```

FREM ... (CONT'D)

C *** CALCULATE THE CURRENT AMOUNT OF THE ITH SPECIE IN
C *** THE SYSTEM

```

DO 18 I=1,N
  IF(NG1(I)) 19,19,18
19 X(I)=-Y(I)*((C(I)+ALOG(Y(I)/YBAR))-GX(1))
  DO 21 J=1,M
    IG=J+1
21 X(I)=X(I)+GX(IG)*A(I,J)*Y(I)
18 CONTINUE
  CALL NEZE (X,Y,N,NG1)
  QUIT=1.

```

C *** TEST FOR CONVERGENCE

```

DO 22 I=1,N
  IF(NG1(I)) 23,23,22
23 TEST=(X(I)-Y(I))/X(I)
  IF(ABS(TEST)-0.1E-03) 22,22,24
24 QUIT=-1.
22 CONTINUE
  IF(QUIT) 25,25,26
25 DO 27 I=1,N
27 Y(I)=X(I)
14 CONTINUE
26 DO 32 I=1,N
  NG1(I)=0
  IF(X(I)) 33,33,34
34 Y(I)=X(I)
  GO TO 32
33 Y(I)=0.000001
32 CONTINUE
35 CONTINUE
  DEN=0.0
  DO 150 I=1,N
150 DEN=DEN+Y(I)
  DO 151 I=1,N
151 FRC(I)=Y(I)/DEN
  DO 36 I=3,N1
    II=I-2
36 OTPT(I,NC)=FRC(II)
  JBI=1
  IF(NCON)10,10,7
7 NCP=N+3
  OTPT(NCP,NC)=8.*FRC(1)+6.*FRC(2)+2.*FRC(3)+FRC(4)
  OTPT(NCP,NC)=OTPT(NCP,NC)*100./(OTPT(NCP,NC)+FRC(5)
  +FRC(6))
10 CONTINUE

```

C *** PUNCH OUT RESULTS

FREM ... (CONT'D)

```
206 NPT=NC-1
   IF(NPT-1)205,205,207
207 DO 208 NCOP=1,NCOPY
   WRITE(6,45) (DES(J),J=1,20),(OTPT(1,J),J=1,NPT)
45  FORMAT('1'////////20X,20A4///10X'TEMP (DEG K) ',10(F5.0
   $,2X))
   WRITE(6,300) (OTPT(2,J),J=1,NPT)
300 FORMAT(10X,'PRESS (ATM) ',10(F5.3,2X)/)
   WRITE(6,75)
75  FORMAT(10X,'MOLECULAR',23X,'EQUILIBRIUM MOLE
   $ FRACTIONS',/10X,'SPEC
   1IE'/)
   DO 47 I=3,N1
   II=I-2
47  WRITE(6,46) SNAM(II),(OTPT(I,J),J=1,NPT)
46  FORMAT(12X,A4,6X,10(F6.4,1X)/)
   IF(NCON)208,208,203
203 L=N1+1
   DO 2000 J=1,10
2000 OTPT(L,J)=99.99
   WRITE(6,204) (OTPT(L,J),J=1,NPT)
204 FORMAT(/,10X,'PCT CONV',5X,10(F5.2,2X))
208 CONTINUE
205 CONTINUE
   CALL EXIT
   END
```

```

C *****
C *
C *
C *
C *
C *
C *
C *****

```

GAUSS

THIS SUBROUTINE IS LISTED IN APPENDIX A

END

```

C *****
C *
C *
C *
C *
C *
C *
C *
C *
C *
C *
C *****

```

GSET

THIS SUBROUTINE SETS UP THE MATRIX EQUATION WHICH
 CORRESPONDS TO EQUATION (16) IN THE REVIEW OF THE
 METHOD. THIS MATRIX EQUATION IS SOLVED USING
 SUBROUTINE GAUSS.

```

      DIMENSION R(20,20),A(20,20),Y(20),GA(20,20),GB(20)
      S,B(20),F(20)
      DO 1 K=1,M
      DO 1 J=1,K
      R(J,K)=0.0
      DO 2 I=1,N
2  R(J,K)=R(J,K)+A(I,J)*A(I,K)*Y(I)
1  R(K,J)=R(J,K)
      DO 3 I=1,MG
      DO 3 J=1,MG
3  GA(I,J)=0.0
      DO 4 IG=1,M
      DO 5 I=1,N
5  GA(IG,1)=GA(IG,1)+A(I,IG)*Y(I)
      DO 9 J=1,M
      JG=J+1
9  GA(IG,JG)=R(IG,J)
      JG=IG+1
      IGG=M+1
4  GA(IGG,JG)=GA(IG,1)
      DO 10 J=1,M
      GB(J)=B(J)
      DO 10 I=1,N
10 GB(J)=GB(J)+A(I,J)*F(I)
      JGB=M+1
      GB(JGB)=0.0
      DO 11 I=1,N
11 GB(JGB)=GB(JGB)+F(I)
      RETURN
      END

```

```

*****
*
*
*           NEZE
*
* THIS SUBROUTINE TESTS FOR NEGATIVE OR ZERO AMOUNTS
* OF MOLECULAR SPECIES AND TAKES THE CORRECTIVE
* ACTION AS INDICATED IN THE METHOD REVIEW.
*
*****

```

```

DIMENSION X(20),Y(20),NG1(20)
TEST=1.0
DO 1 I=1,N
  IF(NG1(I)) 2,2,1
2  IF(X(I)) 3,3,1
3  SLAM=-0.99*Y(I)/(X(I)-Y(I))
  IF(SLAM-TEST)4,4,1
4  TEST=SLAM
1  CONTINUE
  DO 5 I=1,N
    IF(NG1(I))7,7,5
7  X(I)=Y(I)+TEST*(X(I)-Y(I))
    IF(X(I)-0.10E-10) 6,6,5
6  X(I)=0.0
    NG1(I)=1
5  CONTINUE
  RETURN
  END

```

```

C *****
C *
C *
C *
C *
C *
C *
C *
C *
C *
C *
C *****

```

DISTR

```

* THIS SUBROUTINE IS USED TO GENERATE A POSITIVE SET *
* OF MOLE NUMBERS FOR ALL SPECIES IN THE SYSTEM. *
*

```

```

DIMENSION X(20),Y(20),B(20),A(20,20)
DO 1 I=1,N
  IF(X(I)) 2,2,1
2 X(I)=0.0000001
1 Y(I)=X(I)
  DO 3 J=1,M
    B(J)=0.0
    DO 3 I=1,N
3 B(J)=B(J)+A(I,J)*Y(I)
  RETURN
END

```

```

C
C
C
C
C
C
C
C
C
*****
*
*                               FREN
*
* THIS SUBROUTINE CALCULATES THE FREE ENERGY
* CONTRIBUTION OF EACH SPECIE TO THE SYSTEM.
*
*****

SUBROUTINE FREN (Y,C,F,YBAR,N,NG1)
  DIMENSION Y(20),C(20),F(20),NG1(20)
  YBAR=0.0
  DO 1 I=1,N
1  YBAR=YBAR+Y(I)
  DO 2 I=1,N
    IF(NG1(I)) 3,3,4
3  F(I)=Y(I)*(C(I)+ALOG(Y(I)/YBAR))
    GO TO 2
4  F(I)=0.0
2  CONTINUE
  RETURN
  END

```


INPUT DATA FOR FREE ENERGY MINIMIZATION PROGRAM

11		TABLE B-1 EQUILIBRIUM DATA FOR THE CLAUS REACTION			
	4	10	2	13	
HNOS					
S8	0.	0.	0.	8.	0.
	+7.7838968E+00	+2.5099820E-02	-3.7148310E-05	+2.6157310E-08	-7.1209128E-12
	+1.0114584E+04	+4.7621792E+00			
S6	0.	0.	0.	6.	0.
	+6.0892429E+00	+1.8824865E-02	-2.7861233E-05	+1.9617983E-08	-5.3406846E-12
	+1.1264370E+04	+7.3202322E+00			
S2	0.	0.	0.	2.	0.
	+2.6999349E+00	+6.2749549E-03	-9.2870775E-06	+6.5393276E-09	-1.7802282E-12
	+1.4504935E+04	+1.0534222E+01			
S	0.	0.	0.	1.	0.
	+2.9137258E+00	+3.1294061E-04	-2.6092508E-06	+3.1382439E-09	-1.1708988E-12
	+3.2568272E+04	+3.5681154E+00			
H2S	2.	0.	0.	1.	2.
	+3.9163074E+00	-3.5138671E-04	+4.2191312E-06	-2.7453665E-09	+4.8584365E-13
	-3.6095585E+03	+2.3660042E+00			
O2	0.	0.	2.	0.	1.
	+3.7189946E+00	-2.5167288E-03	+8.5837353E-06	-8.2998716E-09	+2.7082180E-12
	-1.0576706E+03	+3.9080704E+00			
S02	0.	0.	2.	1.	0.
	+3.2257132E+00	+5.6551207E-03	-2.4970208E-07	-4.2206766E-09	+2.1392733E-12
	-3.6904476E+04	+9.8177036E+00			
N2	0.	2.	0.	0.	3.76
	+3.6916148E+00	-1.3332552E-03	+2.6503100E-06	-9.7688341E-10	-9.9772234E-14
	-1.0628336E+03	+2.2874980E+00			
H2O	2.	0.	1.	0.	0.
	+4.1565016E+00	-1.7244334E-03	+5.6982316E-06	-4.5930044E-09	+1.4233654E-12
	-3.0288770E+04	-6.8616246E-01			
H2	2.				
	+2.8460849E+00	+4.1932116E-03	-9.6119332E-06	+9.5122662E-09	-3.3093421E-12
	-9.6725372E+02	-1.4117850E+00			
	1.	400.			
	1.	450.			
	.	.			
	.	.			
	1.	1750.			
	0.	0.			

DATA ECHO CHECK

MASS BALANCE MATRIX

MOLECULAR SPECIE	H	N	O	S	X
S8	0.00	0.00	0.00	8.00	0.00
S6	0.00	0.00	0.00	6.00	0.00
S2	0.00	0.00	0.00	2.00	0.00
S	0.00	0.00	0.00	1.00	0.00
H2S	2.00	0.00	0.00	1.00	2.00
O2	0.00	0.00	2.00	0.00	1.00
SO2	0.00	0.00	2.00	1.00	0.00
N2	0.00	2.00	0.00	0.00	3.76
H2O	2.00	0.00	1.00	0.00	0.00
H2	2.00	0.00	0.00	0.00	0.00

FREE ENERGY DATA

S8	0.7783897E 01 -0.7120913E-11	0.2509982E-01 0.1011458E 05	-0.3714831E-04 0.4762179E 01	0.2615731E-07
S6	0.6089242E 01 -0.5340685E-11	0.1882486E-01 0.1126437E 05	-0.2786123E-04 0.7320232E 01	0.1961798E-07
S2	0.2699934E 01 -0.1780228E-11	0.6274955E-02 0.1450493E 05	-0.9287077E-05 0.1053422E 02	0.6539328E-08
S	0.2913725E 01 -0.1170898E-11	0.3129406E-03 0.3256827E 05	-0.2609251E-05 0.3568115E 01	0.3138244E-08
H2S	0.3916307E 01 0.4858436E-12	-0.3513867E-03 -0.3609558E 04	0.4219131E-05 0.2366004E 01	-0.2745366E-08
O2	0.3718994E 01 0.2708218E-11	-0.2516728E-02 -0.1057670E 04	0.8583736E-05 0.3908070E 01	-0.8299872E-08
SO2	0.3225713E 01 0.2139273E-11	0.5655121E-02 -0.3690447E 05	-0.2497021E-06 0.9817705E 01	-0.4220677E-08
N2	0.3691615E 01 -0.9977224E-13	-0.1333255E-02 -0.1062833E 04	0.2650310E-05 0.2287498E 01	-0.9768834E-09
H2O	0.4156501E 01 0.1423365E-11	-0.1724433E-02 -0.3028877E 05	0.5698231E-05 -0.6861624E 00	-0.4593005E-08
H2	0.2846085E 01 -0.3309342E-11	0.4193211E-02 -0.9672537E 03	-0.9611934E-05 -0.1411785E 01	0.9512266E-08

TABLE B-1 EQUILIBRIUM DATA FOR THE CLAUSS REACTION

TEMP (DEG K) PRESS (ATM)	EQUILIBRIUM MOLE FRACTIONS									
	400.	450.	500.	550.	600.	650.	700.	750.	800.	825.
	1.000	1.000	1.000	1.000	1.000	1.000	1.000	1.000	1.000	1.000
MOLECULAR SPECIE										
S8	0.0403	0.0381	0.0340	0.0281	0.0210	0.0141	0.0083	0.0039	0.0011	0.0004
S6	0.0013	0.0037	0.0079	0.0137	0.0198	0.0240	0.0247	0.0204	0.0112	0.0065
S2	0.0000	0.0000	0.0000	0.0000	0.0005	0.0024	0.0084	0.0230	0.0483	0.0617
S	0.0000	0.0000	0.0000	0.0000	0.0000	0.0000	0.0000	0.0000	0.0000	0.0000
H2S	0.0008	0.0028	0.0071	0.0148	0.0265	0.0421	0.0601	0.0779	0.0908	0.0937
O2	0.0000	0.0000	0.0000	0.0000	0.0000	0.0000	0.0000	0.0000	0.0000	0.0000
SO2	0.0004	0.0014	0.0035	0.0074	0.0132	0.0210	0.0300	0.0390	0.0455	0.0470
N2	0.6252	0.6244	0.6229	0.6205	0.6170	0.6124	0.6060	0.5963	0.5833	0.5772
H2O	0.3316	0.3293	0.3242	0.3152	0.3016	0.2836	0.2621	0.2391	0.2192	0.2130
H2	0.0000	0.0000	0.0000	0.0000	0.0000	0.0000	0.0000	0.0001	0.0002	0.0002
PCT CONV	99.73	99.13	97.81	95.39	91.55	86.17	79.41	71.98	65.67	63.95

TABLE B-1 EQUILIBRIUM DATA FOR THE CLAUSS REACTION

TEMP (DEG K)	850.	875.	900.	950.	1000.	1050.	1100.	1150.	1200.	1250.
PRESS (ATM)	1.000	1.000	1.000	1.000	1.000	1.000	1.000	1.000	1.000	1.000
MOLECULAR SPECIE	EQUILIBRIUM MOLE FRACTIONS									
S8	0.0001	0.0000	0.0000	0.0000	0.0000	0.0000	0.0000	0.0000	0.0000	0.0000
S6	0.0030	0.0012	0.0005	0.0000	0.0000	0.0000	0.0000	0.0000	0.0000	0.0000
S2	0.0720	0.0785	0.0826	0.0877	0.0916	0.0948	0.0976	0.1001	0.1023	0.1042
S	0.0000	0.0000	0.0000	0.0000	0.0000	0.0000	0.0000	0.0000	0.0000	0.0000
H2S	0.0938	0.0920	0.0893	0.0835	0.0781	0.0732	0.0687	0.0645	0.0606	0.0568
O2	0.0000	0.0000	0.0000	0.0000	0.0000	0.0000	0.0000	0.0000	0.0000	0.0000
SO2	0.0471	0.0462	0.0450	0.0423	0.0400	0.0380	0.0365	0.0353	0.0344	0.0339
N2	0.5728	0.5704	0.5691	0.5677	0.5668	0.5660	0.5651	0.5643	0.5634	0.5625
H2O	0.2105	0.2108	0.2126	0.2172	0.2214	0.2249	0.2276	0.2295	0.2307	0.2313
H2	0.0003	0.0005	0.0006	0.0011	0.0018	0.0028	0.0042	0.0060	0.0083	0.0110
PCT CONV	63.57	64.21	65.32	67.81	70.10	72.13	73.96	75.61	77.14	78.57

TABLE B-1 EQUILIBRIUM DATA FOR THE CLAUSS REACTION

TEMP (DEG K)	1300.	1350.	1400.	1450.	1500.	1550.	1600.	1650.	1700.	1750.
PRESS (ATM)	1.000	1.000	1.000	1.000	1.000	1.000	1.000	1.000	1.000	1.000
MOLECULAR SPECIE	EQUILIBRIUM MOLE FRACTIONS									
S8	0.0000	0.0000	0.0000	0.0000	0.0000	0.0000	0.0000	0.0000	0.0000	0.0000
S6	0.0000	0.0000	0.0000	0.0000	0.0000	0.0000	0.0000	0.0000	0.0000	0.0000
S2	0.1058	0.1073	0.1085	0.1095	0.1103	0.1109	0.1113	0.1116	0.1117	0.1117
S	0.0000	0.0000	0.0000	0.0000	0.0000	0.0000	0.0000	0.0000	0.0000	0.0001
H2S	0.0531	0.0496	0.0462	0.0429	0.0398	0.0369	0.0341	0.0316	0.0292	0.0271
O2	0.0000	0.0000	0.0000	0.0000	0.0000	0.0000	0.0000	0.0000	0.0000	0.0000
SO2	0.0337	0.0338	0.0342	0.0349	0.0358	0.0369	0.0382	0.0396	0.0412	0.0428
N2	0.5616	0.5605	0.5595	0.5584	0.5573	0.5561	0.5550	0.5539	0.5528	0.5517
H2O	0.2311	0.2304	0.2290	0.2271	0.2247	0.2219	0.2187	0.2152	0.2116	0.2078
H2	0.0143	0.0181	0.0223	0.0269	0.0318	0.0370	0.0423	0.0477	0.0531	0.0585
PCT CONV	79.92	81.21	82.43	83.60	84.70	85.73	86.70	87.60	88.42	89.18

TABLE B-3 EQUILIBRIUM DATA FOR THE COS/SO2 REACTION

TEMP (DEG K)	500.	600.	700.	800.	900.	1000.	1100.	1300.	1500.	2000.
PRESS (ATM)	1.000	1.000	1.000	1.000	1.000	1.000	1.000	1.000	1.000	1.000
MOLECULAR SPECIE	EQUILIBRIUM MOLE FRACTIONS									
COS	0.0000	0.0000	0.0004	0.0011	0.0014	0.0016	0.0017	0.0020	0.0022	0.0026
SO2	0.0000	0.0000	0.0002	0.0005	0.0007	0.0008	0.0008	0.0010	0.0011	0.0013
CO2	0.0610	0.0609	0.0602	0.0584	0.0576	0.0575	0.0573	0.0571	0.0569	0.0565
S8	0.0092	0.0057	0.0024	0.0002	0.0000	0.0000	0.0000	0.0000	0.0000	0.0000
S6	0.0029	0.0074	0.0097	0.0034	0.0000	0.0000	0.0000	0.0000	0.0000	0.0000
S2	0.0000	0.0003	0.0061	0.0325	0.0430	0.0431	0.0430	0.0428	0.0426	0.0420
S	0.0000	0.0000	0.0000	0.0000	0.0000	0.0000	0.0000	0.0000	0.0000	0.0006
N2	0.9266	0.9253	0.9207	0.9036	0.8970	0.8969	0.8969	0.8970	0.8970	0.8968
PCT CONV	97.77	94.23	88.88	78.22	75.27	75.46	75.69	76.08	76.41	77.12

TABLE B-4 EQUILIBRIUM DATA FOR THE CS₂/SO₂ REACTION

TEMP (DEG K)	500.	600.	700.	800.	900.	1000.	1100.	1300.	1500.	2000.
PRESS (ATM)	1.000	1.000	1.000	1.000	1.000	1.000	1.000	1.000	1.000	1.000
MOLECULAR SPECIE	EQUILIBRIUM MOLE FRACTIONS									
CS ₂	0.0001	0.0001	0.0001	0.0001	0.0001	0.0002	0.0002	0.0002	0.0002	0.0003
SO ₂	0.0000	0.0000	0.0000	0.0000	0.0000	0.0001	0.0001	0.0001	0.0001	0.0002
CO ₂	0.0515	0.0514	0.0510	0.0497	0.0487	0.0486	0.0486	0.0486	0.0485	0.0485
S ₂	0.0000	0.0004	0.0073	0.0446	0.0720	0.0729	0.0729	0.0729	0.0728	0.0727
S ₆	0.0045	0.0116	0.0165	0.0088	0.0003	0.0000	0.0000	0.0000	0.0000	0.0000
S ₈	0.0159	0.0104	0.0048	0.0008	0.0000	0.0000	0.0000	0.0000	0.0000	0.0000
N ₂	0.9278	0.9259	0.9199	0.8957	0.8786	0.8780	0.8780	0.8780	0.8780	0.8780
PCT CONV	83.55	82.50	83.74	93.74	99.80	99.99	99.99	99.99	99.99	99.99

99.99

99.99

99.80

93.74

83.74

82.50

83.55

PCT CONV

TABLE B-5 EQUILIBRIUM DATA FOR THE COS/H₂O REACTION

TEMP (DEG K)	500.	600.	700.	800.	900.	1000.	1100.	1300.	1500.	2000.
PRESS (ATM)	1.000	1.000	1.000	1.000	1.000	1.000	1.000	1.000	1.000	1.000
MOLECULAR SPECIE	EQUILIBRIUM MOLE FRACTIONS									
COS	0.0008	0.0016	0.0026	0.0038	0.0049	0.0061	0.0072	0.0092	0.0109	0.0139
H ₂ O	0.0008	0.0016	0.0026	0.0038	0.0049	0.0061	0.0072	0.0092	0.0109	0.0139
CO ₂	0.0491	0.0483	0.0473	0.0461	0.0450	0.0438	0.0427	0.0407	0.0390	0.0360
H ₂ S	0.0491	0.0483	0.0473	0.0461	0.0450	0.0438	0.0427	0.0407	0.0390	0.0360
N ₂	0.9000	0.9000	0.9000	0.9000	0.9000	0.9000	0.9000	0.9000	0.9000	0.9000
PCT CONV	15.01	15.73	16.61	17.57	18.54	19.47	20.34	21.87	23.11	25.24

TABLE B-6 EQUILIBRIUM DATA FOR THE CS₂/H₂O REACTION

MOLECULAR SPECIE	EQUILIBRIUM MOLE FRACTIONS											
	TEMP (DEG K) PRESS (ATM)	500. 1.000	600. 1.000	700. 1.000	800. 1.000	900. 1.000	1000. 1.000	1100. 1.000	1300. 1.000	1500. 1.000	2000. 1.000	
CS ₂		0.0000	0.0002	0.0004	0.0007	0.0010	0.0014	0.0017	0.0025	0.0032	0.0047	
H ₂ O		0.0001	0.0004	0.0008	0.0014	0.0020	0.0028	0.0035	0.0050	0.0064	0.0095	
CO ₂		0.0299	0.0297	0.0295	0.0292	0.0289	0.0285	0.0282	0.0274	0.0267	0.0252	
H ₂ S		0.0598	0.0595	0.0591	0.0585	0.0579	0.0571	0.0564	0.0549	0.0535	0.0504	
N ₂		0.9100	0.9100	0.9100	0.9100	0.9100	0.9100	0.9100	0.9100	0.9100	0.9100	
PCT CONV		11.77	11.96	12.25	12.63	13.06	13.53	14.01	14.96	15.84	17.75	

TABLE B-7 EQUILIBRIUM DATA FOR THE H₂S/CO₂ REACTION

TEMP (DEG K) PRESS (ATM)	500. 1.000	600. 1.000	700. 1.000	800. 1.000	900. 1.000	1000. 1.000	1100. 1.000	1300. 1.000	1500. 1.000	2000. 1.000
MOLECULAR SPECIE	EQUILIBRIUM MOLE FRACTIONS									
H ₂ S	0.0491	0.0483	0.0473	0.0461	0.0450	0.0438	0.0427	0.0407	0.0390	0.0360
CO ₂	0.0491	0.0483	0.0473	0.0461	0.0450	0.0438	0.0427	0.0407	0.0390	0.0360
COS	0.0008	0.0016	0.0026	0.0038	0.0049	0.0061	0.0072	0.0092	0.0109	0.0139
H ₂ O	0.0008	0.0016	0.0026	0.0038	0.0049	0.0061	0.0072	0.0092	0.0109	0.0139
N ₂	0.9000	0.9000	0.9000	0.9000	0.9000	0.9000	0.9000	0.9000	0.9000	0.9000
PCT CONV	43.42	43.10	42.69	42.23	41.75	41.26	40.79	39.91	39.16	37.76

TABLE B-8 EQUILIBRIUM DATA FOR THE CH₄/SX REACTION

TEMP (DEG K)	500.	600.	700.	800.	900.	1000.	1100.	1300.	1500.	2000.
PRESS (ATM)	1.000	1.000	1.000	1.000	1.000	1.000	1.000	1.000	1.000	1.000
EQUILIBRIUM MOLE FRACTIONS										
MOLECULAR SPECIE										
CH ₄	0.0001	0.0001	0.0001	0.0001	0.0001	0.0002	0.0003	0.0004	0.0007	0.0013
S ₂	0.0000	0.0000	0.0000	0.0000	0.0001	0.0002	0.0004	0.0007	0.0012	0.0025
S ₆	0.0000	0.0000	0.0000	0.0000	0.0000	0.0000	0.0000	0.0000	0.0000	0.0000
S ₈	0.0000	0.0000	0.0000	0.0000	0.0000	0.0000	0.0000	0.0000	0.0000	0.0000
CS ₂	0.0199	0.0199	0.0199	0.0199	0.0199	0.0198	0.0197	0.0196	0.0193	0.0187
H ₂ S	0.0399	0.0399	0.0399	0.0399	0.0398	0.0397	0.0395	0.0392	0.0387	0.0374
N ₂	0.9399	0.9399	0.9399	0.9399	0.9399	0.9399	0.9399	0.9399	0.9399	0.9399
PCT CONV	1.52	1.43	1.81	2.64	3.98	5.78	7.93	12.88	18.17	31.98

TABLE B-9 EQUILIBRIUM DATA FOR THE COS/H₂S REACTION

TEMP (DEG K)	500.	600.	700.	800.	900.	1000.	1100.	1300.	1500.	2000.
PRESS (ATM)	1.000	1.000	1.000	1.000	1.000	1.000	1.000	1.000	1.000	1.000
MOLECULAR SPECIE	EQUILIBRIUM MOLE FRACTIONS									
COS	0.0495	0.0490	0.0485	0.0478	0.0472	0.0465	0.0459	0.0448	0.0438	0.0416
H ₂ S	0.0494	0.0490	0.0484	0.0477	0.0471	0.0464	0.0458	0.0447	0.0437	0.0415
CS ₂	0.0005	0.0009	0.0015	0.0022	0.0028	0.0035	0.0041	0.0052	0.0062	0.0084
H ₂ O	0.0005	0.0009	0.0015	0.0022	0.0028	0.0035	0.0041	0.0052	0.0062	0.0084
N ₂	0.8999	0.8999	0.8999	0.8999	0.8999	0.8999	0.8999	0.8999	0.8999	0.8999
PCT CONV	43.54	43.35	43.12	42.87	42.61	42.35	42.09	41.63	41.22	40.27

TABLE B-11 EQUILIBRIUM DATA FOR THE CO/SX REACTION (B)

MOLECULAR SPECIE	EQUILIBRIUM MOLE FRACTIONS										
	TEMP (DEG K)	500.	600.	700.	800.	900.	1000.	1100.	1300.	1500.	2000.
PRESS (ATM)	1.000	1.000	1.000	1.000	1.000	1.000	1.000	1.000	1.000	1.000	1.000
CO		0.0010	0.0042	0.0130	0.0361	0.0846	0.1493	0.2076	0.2691	0.2878	0.2969
S2		0.0000	0.0001	0.0028	0.0163	0.0417	0.0743	0.1035	0.1342	0.1436	0.1481
S6		0.0000	0.0003	0.0009	0.0004	0.0000	0.0000	0.0000	0.0000	0.0000	0.0000
S8		0.0000	0.0001	0.0001	0.0000	0.0000	0.0000	0.0000	0.0000	0.0000	0.0000
CO2		0.1751	0.1734	0.1684	0.1546	0.1259	0.0879	0.0536	0.0175	0.0065	0.0011
CS2		0.1751	0.1734	0.1684	0.1546	0.1259	0.0879	0.0536	0.0175	0.0065	0.0011
N2		0.6486	0.6482	0.6461	0.6377	0.6215	0.6004	0.5815	0.5615	0.5555	0.5525
PCT CONV		2.33	9.34	26.90	55.63	78.65	90.32	95.50	98.82	99.59	99.92

(

APPENDIX C
REDUCTION OF DATA AND ERROR ANALYSIS

C.1 Mathematics of Data Reduction and Sample Calculation

A step by step procedure is outlined below which indicates how a set of experimental measurements is reduced to kinetic data using the data reduction program, NPRDP. The sample calculation is given for run number CB-1 for which the following measurements were taken:

Reactor Bed Temperature	13.11 (millivolts)
Reactor Wall Temperature	13.10 (millivolts)
Feed Pressure Transducer	38.70 (chart pct.)
Reactor Pressure Transducer	55.00 (chart pct.)
D/P Cell	12.30 (chart pct.)
Catalyst Weight	0.4955 (grams)

Chromatogram Results

	N ₂	Feed H ₂ S	SO ₂	N ₂	Product H ₂ S	SO ₂
Attenuation	-14.	9.8	9.8	-14.	9.8	9.8
Area	90.5	222.	258.5	90.0	179.5	234.
Area	90.5	221.	259.0	90.0	178.5	234.

The following equations, many of which were developed by instrument calibrations, are used in NPRDP and the sample calculation is given below.

$$\text{Component area} = (\text{Average meas'd. area})(21.-2. \times \text{Attenuation})$$

$$\text{H}_2\text{S}:\text{N}_2 \text{ molar ratio} = 0.0418/100. + 0.5888 \times (\text{H}_2\text{S Area}/\text{N}_2 \text{ Area})$$

$$\text{SO}_2:\text{N}_2 \text{ molar ratio} = 0.0044/100. + 0.4950 \times (\text{SO}_2 \text{ Area}/\text{N}_2 \text{ Area})$$

$$\text{Reactor bed temp.} = 5.3155 + 18.0706 \times (\text{Meas'd. millivolts})$$

$$\text{Reactor wall temp.} = 6.6860 + 17.9544 \times (\text{Meas'd. millivolts})$$

$$\text{Feed system pressure} = 15. + 0.25 (\text{Meas'd. Chart Pct.})$$

$$\text{Reactor pressure} = - 534.85 + 24.806 (\text{Meas'd Chart Pct.})$$

$$\text{Feed Flow (22.5 psia)} = 1.2265 + 1.5367 \sqrt{Y} + 0.0381 Y$$

$$\text{Feed Flow (25.0 psia)} = 0.8985 + 1.6844 \sqrt{Y} + 0.0212 Y$$

$$\text{Feed Flow (30.0 psia)} = 0.7409 + 1.9429 \sqrt{Y} + 0.0178 Y$$

$$\text{Feed Flow (35.0 psia)} = 0.7955 + 2.0629 \sqrt{Y} + 0.0246 Y$$

The results of using these equations are given below:

$$\text{N}_2 \text{ area, FD.} = 4434.5$$

$$\text{H}_2\text{S area, FD.} = 310.1$$

$$\text{SO}_2 \text{ area, FD.} = 362.25$$

$$\text{N}_2 \text{ area, PR.} = 4410.0$$

$$\text{H}_2\text{S area, PR.} = 250.6$$

$$\text{SO}_2 \text{ area, PR.} = 327.6$$

$$\text{H}_2\text{S}/\text{N}_2 \text{ molar ratio, FD.} = 0.0415$$

$$\text{SO}_2/\text{N}_2 \text{ molar ratio, FD.} = 0.0405$$

$$\text{H}_2\text{S}/\text{N}_2 \text{ molar ratio, PR.} = 0.0336$$

$$\text{SO}_2/\text{N}_2 \text{ molar ratio, PR.} = 0.0368$$

By solving the set of equations given below, the feed composition may be calculated.

$$Y_{N_2} + Y_{H_2S} + Y_{SO_2} = 1.0$$

$$Y_{H_2S}/Y_{N_2} = 0.0415$$

$$Y_{SO_2}/Y_{N_2} = 0.0405$$

where Y_i = mole fraction of component i. The solution to these equations yields the following feed composition (molar basis):

$$N_2 - 92.41\% *$$

$$H_2S - 3.84\% *$$

$$SO_2 - 3.74\% *$$

$$\text{Feed } H_2S/SO_2 \text{ ratio} - 1.027 *$$

$$\text{Reactor bed temp.} = 242.2^\circ\text{C}$$

$$= 515.2^\circ\text{K}$$

$$\text{Reactor wall temp.} = 241.9^\circ\text{C}$$

$$= 514.9^\circ\text{K}$$

$$\text{Reaction temp.} = (515.2 + 514.9)/2$$

$$= 515.04^\circ\text{K} *$$

$$\text{Feed system press.} = 24.67 \text{ psia}$$

$$\text{Reactor press.} = 829.4 \text{ mm Hg} *$$

Feed Flow (22.5 psia) = 7.085 SCFH

Feed Flow (25.0 psia) = 7.067 SCFH

Feed Flow (30.0 psia) = 7.774 SCFH

Feed Flow (35.0 psia) = 8.333 SCFH

Since the feed system pressure is given as 24.67 psia, it is likely that the Newton Interpolation polynomial routine would calculate a flow of magnitude very close to that found for 25.0 psia. So this flow is selected as the flow rate of nitrogen at 1.0 atmosphere and 60°F (SCFH) which would exist at the measured conditions. The basis for flow rate density correction is given in Appendix A, and the formula is:

$$FF_{\text{Mix}} = FF_{\text{N}_2} \left(\frac{\rho_{\text{N}_2}}{\rho_{\text{Mix}}} \right)^{1/2} \left(\frac{492.}{520.} \right)$$

where FF_{Mix} = flow rate of mixture at 0°C, 1 atm.

FF_{N_2} = flow rate of nitrogen at 60°F, 1 atm.

ρ_{N_2} = density of nitrogen at 0°C, 1 atm.

ρ_{Mix} = density of mixture at 0°C, 1 atm.

As indicated in Chapter V, Section 2, the ideal gas law was assumed to apply so it makes little difference whether densities are taken at 0°C or 60°F. The molecular volumes indicated in Table 5.3 were used for calculating densities.

$$\rho_{\text{N}_2} = 28./22.403 = 1.2498$$

$$\begin{aligned}
 \rho_{\text{Mix}} &= \frac{\sum_{i=1}^3 \text{MW}_i \times y_i}{\sum y_i v_i} \\
 &= 29.574/22.3725 \\
 &= 1.32189
 \end{aligned}$$

where MW_i = molecular weight of component i
 y_i = mole fraction of component i
 v_i = molar volume of component i (litre)

$$\begin{aligned}
 \text{FF}_{\text{Mix}} &= 7.067 \left(\frac{1.2498}{1.3219} \right)^{1/2} \left(\frac{492.}{520.} \right) \\
 &= 6.5015 = \text{FF}_0
 \end{aligned}$$

This answer is very close to the computer output for CBI which is 6.484, therefore, selecting the flow of 7.067 as calculated for 25.0 psia is reasonable.

The material balance calculations have been described in Chapter V. The molar feed rate of a component is taken as

$$\text{FF}_i = (\text{FF}_0)(y_i)/(\sum y_i v_i)$$

where FF_i = molar feed rate of component i
 FF_0 = volumetric mixture feed rate at 0°C and 1 atmosphere
 y_i = mole fraction of component i
 v_i = molecular volume of component i at 0°C, 1 atmosphere

Taking F_0 as 6.484, the following molar feed rates are calculated.

$$\sum Y_i V_i = 22.3725 \text{ litre}$$

$$\begin{aligned} FF_{N_2} &= 6.484 \times 28.317016 \times 0.09241 / 22.3725 \\ &= 7.583 \text{ gm moles/hr} \quad * \end{aligned}$$

$$FF_{H_2S} = 0.315 \text{ gm moles/hr} \quad *$$

$$FF_{SO_2} = 0.306 \text{ gm moles/hr} \quad *$$

It has been pointed out that nitrogen passes through the system unreacted, so

$$FP_{N_2} = FF_{N_2} = 7.583 \quad *$$

$$\begin{aligned} FP_{H_2S} &= FP_{N_2} \text{ (molar ratio of } H_2S/N_2) \\ &= 7.583 \times 0.0336 \\ &= 0.256 \quad * \end{aligned}$$

$$\begin{aligned} FP_{SO_2} &= 7.583 \times 0.0368 \\ &= 0.279 \quad * \end{aligned}$$

The product rate of sulfur is calculated on the basis that all of the reacted H_2S and SO_2 go to the formation of sulfur.

$$\begin{aligned} FP_{S_x} &= (FH_{2S} + F_{SO_2} - P_{H_2S} - P_{SO_2}) / X \\ &= (0.315 + 0.306 - 0.256 - 0.279) / 7.4 \\ &= 0.011 \quad * \end{aligned}$$

The method of arriving at $X = 7.4$ will be discussed later.

The product rate of water is calculated on the basis of the amount of H_2S and SO_2 reacted.

$$\begin{aligned} P_{H_2O} &= (2(F_{SO_2} - P_{SO_2}) + F_{H_2S} - P_{H_2S})/2. \\ &= (2(.306 - .279) + .315 - .256)/2 \\ &= 0.057 \quad * \end{aligned}$$

Now, there will be an error in the material balance due to inaccuracies in the chromatogram area measurements. This error is established by calculating the product rate of hydrogen.

$$\begin{aligned} P_{H_2} &= F_{H_2S} - P_{H_2S} - P_{H_2O} \\ &= 0.315 - 0.256 - 0.057 \\ &= 0.002 \quad * \end{aligned}$$

The average molecular weight of sulfur, X , is calculated using free energy minimization as described in Chapter III. The average molecular weight is a function of the temperature (reaction temperature) and the total pressure of the sulfur species. A value of X is guessed and using it, P_{S_x} is calculated using the product flow rates to determine its mole fraction and subsequently its partial pressure. The free energy minimization routine, given the sulfur partial pressure and temperature, will calculate the average molecular weight of sulfur based

on sulfur specie distribution (see Chapter III, Figure 3.2). The latest value is compared to the last calculated and if the error exceeds 0.5%, the latest value of the average sulfur gas molecular weight is used for the next guess. The cycle continues until the error criteria is satisfied. This approach assumes that sulfur vapor is at equilibrium and the basis for this assumption is discussed in Section 2.2.3 of the literature review.

The partial pressures of each of the species in the reactor are calculated on the basis of the product stream composition assuming that the ideal gas law applies.

$$p_i = (\text{reactor pressure}) \left(\frac{FP_i}{\sum FP_i} \right)$$

$$P_{N_2} = 829.4 \left(\frac{7.583}{8.187} \right) = 768.2 \quad *$$

$$P_{H_2S} = 26.0 \quad *$$

$$P_{SO_2} = 28.2 \quad *$$

$$P_{H_2O} = 5.7 \quad *$$

$$P_{S_x} = 1.1 \quad *$$

$$P_{H_2} = 0 \quad *$$

Other data which is calculated by NPRDP and is printed out includes:

$$\begin{aligned}\text{Weight of Catalyst}/(\text{feed rate of H}_2\text{S}) &= 0.4955/0.315 \\ &= 1.57 = \text{WFA} \quad *\end{aligned}$$

$$\begin{aligned}\text{Reaction rate of H}_2\text{S} &= (F_{\text{H}_2\text{S}} - P_{\text{H}_2\text{S}})/\text{WC} \\ &= (0.315 - 0.256)/0.4955 \\ &= 0.1180 \quad *\end{aligned}$$

$$\begin{aligned}\text{Reaction rate of SO}_2 &= (0.306 - 0.297)/0.4955 \\ &= 0.0560 \quad *\end{aligned}$$

$$\begin{aligned}\text{Product H}_2\text{S/SO}_2 \text{ ratio} &= P_{\text{H}_2\text{S}}/P_{\text{SO}_2} \\ &= 0.256/0.297 \\ &= 0.9201 \quad *\end{aligned}$$

$$\begin{aligned}\text{Conversion of H}_2\text{S(Pct.)} &= 100 \cdot (F_{\text{H}_2\text{S}} - P_{\text{H}_2\text{S}})/F_{\text{H}_2\text{S}} \\ &= 100 \cdot (0.315 - 0.256)/0.315 \\ &= 18.55 \quad *\end{aligned}$$

$$\begin{aligned}\text{Conversion of SO}_2 \text{(Pct.)} &= 100 \cdot (0.306 - 0.297)/0.306 \\ &= 9.05 \quad *\end{aligned}$$

All of the foregoing numbers which are marked by an asterisk are part of the print out of the computer program.

C.2 Error Analysis of Kinetic Data

The estimation of the reliability of the kinetic measurements may be performed by replicating an experimental run several times, calculating the mean value of reaction rate or percent conversion or whatever and then estimating the standard deviation of the errors. Caution should be exercised when using this approach, however, because it is possible that instrument calibrations would remain constant during

the replication process, but be subject to drift throughout the ensuing experimental program.

Rather than use this approach, the experience which has been obtained from the long term operation of the equipment is built into the error analysis. The following represents what is felt to be the combined error of instrument reading and reading of the instrument by the operator:

Foxboro chart readings $\pm 0.25\%$

Thermocouple millivolt readings ± 0.005 MV

N₂ area measurement $\pm 0.25\%$

H₂S area measurement $\pm 0.50\%$

SO₂ area measurement $\pm 0.75\%$

Using these error estimates, the measurement readings for curve CB were perturbed and the results tabulated below were calculated using the data reduction program. It was found that the H₂S area measurement was the most important from the stand point of error in the data. Therefore, this was the only measurement perturbed to obtain the table below. The high conversion was estimated by increasing the feed H₂S area by the possible error and decreasing the H₂S area in the product chromatogram by the possible error.

From this it is seen that in the more pessimistic sense, the error in conversion level is as high as 0.85% which leads to a rate measurement maximum error of 12% which applies to run CB4. For run CB1 the error would be 4.55%. It is felt that since product chromatograms

TABLE C.1 ERROR ANALYSIS OF H₂S CONVERSION

<u>Run Number</u>	<u>Percent Conversion</u>		
	<u>High</u>	<u>Measured</u>	<u>Low</u>
CB1	19.36	18.55	17.73
CB2	13.31	12.47	11.61
CB3	10.71	9.85	8.99
CB4	7.93	7.10	6.25

were replicated twice and feed chromatograms were taken around six times in a series, that the most pessimistic case as given does not exist and that the average rate measurement error is in the neighbourhood of 5%.

C.3 Data Reduction Program, Reduced Data and Data Summary Tables

The data reduction program, NPRDP, was written in Fortran IV basic. Data input symbols and formats may be obtained by consulting the Fortran listing on the following pages which also describes the calculation sequence and the intent of the various subroutines.

Preceding the program listing are Tables C.2, C.3 and C.4 which summarize experimental finite rate data, catalytic activity test data and experimental initial rate data. Immediately following the program listing is the data output from NPRDP for every experiment which was carried out.

TABLE C-2 EXPERIMENTAL FINITE RATE DATA

RUN NO.	REACTION TEMP	REACTION PRESS	W/FA	RXN. RATE	PCT CONVERSION		REACTOR PARTIAL PRESSURES				
					H2S	TOTAL	N2	H2S	SO2	H2O	SX
AA-1	558.6	829.4	0.79	0.3140	25.05	25.97	737.7	49.6	21.9	16.8	3.3
AA-2	558.8	829.4	0.51	0.3582	18.30	18.64	735.9	54.5	24.4	11.9	2.4
AA-3	558.6	829.4	0.38	0.3838	14.71	15.78	735.7	56.4	24.8	10.3	2.0
AA-4	558.6	829.4	0.29	0.3977	11.78	11.81	735.0	58.3	26.9	7.5	1.5
AB-1	559.2	829.4	1.50	0.1667	25.05	19.04	768.6	24.3	26.8	7.9	1.6
AB-2	559.6	829.4	1.01	0.1826	18.61	14.38	768.5	26.1	27.4	6.0	1.2
AC-1	559.0	829.4	3.41	0.0797	27.19	13.76	783.9	11.6	28.6	4.2	0.9
AC-2	559.3	829.4	2.03	0.0910	18.53	9.71	783.8	13.0	28.9	3.0	0.6
BA-1	540.2	826.9	0.86	0.2319	19.97	20.27	736.5	51.9	23.1	12.6	2.6
BA-2	540.4	826.9	0.58	0.2725	15.92	16.49	730.1	58.0	25.5	11.0	2.2
BA-3	540.4	831.9	0.36	0.3051	10.98	11.38	733.7	61.9	27.1	7.6	1.5
BA-4	539.7	831.9	0.26	0.3337	8.84	9.21	733.3	63.3	27.8	6.1	1.2

TABLE C-2 EXPERIMENTAL FINITE RATE DATA

RUN NO.	REACTION TEMP	W/FA	RXN. RATE	PCT CONVERSION		REACTOR PARTIAL PRESSURES				SX	
				H2S	TOTAL	N2	H2S	SO2	H2O		
BB-1	542.1	826.9	2.03	0.1247	25.40	19.03	768.3	22.8	26.6	7.7	1.4
BB-2	542.1	829.4	1.34	0.1338	17.94	13.42	770.3	24.8	27.6	5.4	1.1
BB-3	541.9	831.9	0.92	0.1401	12.91	9.52	771.7	26.8	28.7	3.8	0.8
BB-4	541.9	831.9	0.62	0.1465	9.13	6.82	771.0	28.1	29.3	2.8	0.5
BC-1	541.3	831.9	4.02	0.0720	28.98	14.51	786.6	11.3	28.5	4.4	0.8
BC-2	541.7	831.9	3.31	0.0772	25.61	12.97	786.4	11.8	28.7	4.0	0.8
BC-3	541.9	831.9	2.78	0.0735	20.51	10.49	785.9	12.7	29.3	3.2	0.6
BC-4	542.3	829.4	1.90	0.0750	14.28	7.44	783.2	13.7	29.6	2.3	0.4
CA-1	515.8	831.9	0.75	0.2008	15.24	15.67	737.8	56.2	25.7	10.1	1.9
CA-2	516.3	829.4	0.58	0.2197	12.93	13.54	734.6	57.7	26.4	8.9	1.7
CA-3	515.8	826.9	0.48	0.2239	10.94	10.79	731.7	58.9	28.0	6.9	1.4
CA-4	515.8	826.9	0.44	0.2187	9.64	10.12	732.1	59.5	27.4	6.6	1.3

TABLE C-2 EXPERIMENTAL FINITE RATE DATA

RUN NO.	REACTION		W/FA	RXN. RATE	PCT CONVERSION		REACTOR PARTIAL PRESSURES				S _X
	TEMP	PRESS			H ₂ S	TOTAL	N ₂	H ₂ S	SO ₂	H ₂ O	
CB-1	515.0	829.4	1.57	0.1180	18.55	13.86	768.2	26.0	28.2	5.7	1.1
CB-2	515.2	831.9	1.02	0.1221	12.47	9.15	770.3	27.7	29.2	3.7	0.7
CB-3	515.0	829.4	0.80	0.1224	9.85	7.40	767.7	28.5	29.4	3.0	0.6
CB-4	515.2	829.4	0.55	0.1274	7.10	5.33	767.2	29.5	29.9	2.2	0.4
CC-1	514.8	828.2	3.28	0.0591	19.41	10.00	782.2	12.9	29.1	3.1	0.6
CC-2	514.9	831.9	2.58	0.0652	16.84	8.62	785.5	13.5	29.5	2.6	0.5
CC-3	514.8	828.2	2.15	0.0651	14.05	7.29	782.0	13.8	29.5	2.2	0.4
CC-4	514.8	828.2	1.67	0.0618	10.34	5.24	781.8	14.4	29.9	1.6	0.3
CD-1	513.8	829.4	0.67	0.2900	19.55	16.92	725.7	50.3	38.9	12.0	2.4
CD-2	513.9	829.4	0.42	0.2900	12.25	10.67	724.3	54.9	41.0	7.6	1.5
CE-1	513.4	829.4	0.62	0.1794	11.27	13.70	754.6	56.1	10.2	6.9	1.4
CE-2	513.7	829.4	0.42	0.1708	7.21	9.17	753.4	59.0	11.2	4.8	0.9

TABLE C-2 EXPERIMENTAL FINITE RATE DATA

RUN NO.	REACTION TEMP	REACTION PRESS	W/FA	RXN. RATE	PCT CONVERSION		REACTOR PARTIAL PRESSURES				
					H2S	TOTAL	N2	H2S	SO2	H2O	SX
CF-1	514.3	829.4	2.40	0.0852	20.46	8.20	769.4	12.8	43.2	3.3	0.6
CF-2	514.3	829.4	1.35	0.0958	12.95	5.01	769.1	13.9	43.9	2.0	0.4
CG-1	514.0	829.4	2.59	0.0543	14.09	11.42	798.9	14.6	12.9	2.3	0.4
CG-2	514.2	829.4	1.82	0.0573	10.47	8.71	799.0	15.0	13.1	1.8	0.3
CH-1	513.2	829.4	1.29	0.1595	20.64	12.37	751.9	25.4	44.3	6.5	1.2
CH-2	513.5	829.4	0.77	0.1658	12.78	7.55	751.1	27.7	45.8	3.9	0.8
CK-1	513.6	829.4	1.25	0.0961	12.06	12.62	783.7	28.4	12.5	3.9	0.7
CK-2	513.6	829.4	0.85	0.0967	8.23	8.55	783.5	29.6	13.1	2.6	0.5
DA-1	480.7	829.4	0.78	0.1367	10.68	11.29	734.4	59.7	26.4	7.4	1.5
DA-2	481.6	829.4	0.63	0.1376	8.71	8.65	733.8	61.0	27.8	5.5	1.1
DA-3	480.7	829.4	0.46	0.1371	6.42	6.65	733.7	62.3	28.2	4.3	0.8
DA-4	481.2	831.9	0.33	0.1373	4.60	4.76	735.8	63.6	28.7	3.0	0.6

TABLE C-2 EXPERIMENTAL FINITE RATE DATA

RUN NO.	REACTION		W/FA	RXN. RATE	PCT CONVERSION		REACTOR PARTIAL PRESSURES				
	TEMP	PRESS			H2S	TOTAL	N2	H2S	SO2	H2O	SX
DB-1	481.1	829.4	1.80	0.0732	13.24	10.31	768.9	27.5	27.8	4.2	0.8
DB-2	485.6	829.4	0.97	0.0742	7.25	5.30	766.7	30.2	29.8	2.1	0.4
DC-1	481.6	829.4	2.38	0.0421	10.03	5.54	782.7	15.0	29.5	1.7	0.3
DC-2	481.6	829.4	1.63	0.0456	7.45	3.89	782.4	15.5	29.9	1.2	0.2
FMS1	513.7	851.8	1.99	0.2476	49.43	49.90	767.4	32.4	14.8	31.2	5.8
FMS2	515.8	849.3	1.16	0.3438	40.05	39.64	763.3	38.3	18.3	24.4	4.8
FMS3	514.9	851.8	0.68	0.4321	29.47	29.91	764.0	44.8	20.6	18.5	3.6
AX-1	557.4	829.4	4.02	0.1495	60.25	61.36	742.5	27.0	11.3	40.5	7.9
AX-2	557.7	829.4	5.42	0.1206	65.45	66.61	743.3	23.5	9.6	43.9	9.0
AX-3	558.6	829.4	3.22	0.1666	53.66	54.28	741.6	31.2	13.8	35.4	7.3
AX-4	558.6	829.4	2.46	0.1886	46.55	47.21	740.0	36.0	16.0	30.9	6.3
BX-1	542.8	841.8	5.79	0.1091	63.23	64.03	754.6	25.0	10.8	42.4	8.8

TABLE C-2 EXPERIMENTAL FINITE RATE DATA

RUN NO.	REACTION		W/FA	RXN. RATE	PCT CONVERSION H2S	TOTAL	REACTOR PARTIAL PRESSURES				
	TEVP	PRESS					N2	H2S	SO2	H2O	SX
BX-2	542.8	854.2	4.65	0.1156	53.83	54.82	764.1	31.8	13.8	36.9	7.5
BX-3	540.6	846.8	3.53	0.1369	48.40	49.24	756.2	35.3	15.6	32.9	6.6
BX-4	541.3	829.4	2.54	0.1630	41.46	42.14	739.5	39.1	17.6	27.5	5.5
CX-1	514.5	841.8	5.93	0.0858	50.92	52.23	752.8	33.4	14.2	34.7	6.5
CX-2	514.5	849.3	4.67	0.1127	52.76	53.54	759.5	32.4	14.3	35.7	7.1
CX-3	514.5	849.3	3.61	0.1160	41.96	42.57	757.4	39.5	18.1	28.4	5.6
CX-4	514.7	849.3	2.56	0.1336	34.33	34.45	756.1	44.7	20.9	22.8	4.5
DX-1	481.1	829.4	5.31	0.0760	40.43	41.77	739.6	39.7	17.2	27.4	5.4
DX-2	478.9	829.4	3.88	0.0878	34.14	34.95	738.4	43.9	19.7	22.8	4.4
DX-3	478.9	829.4	2.79	0.0886	24.80	25.40	736.8	49.9	22.8	16.5	3.2
DX-4	481.3	829.4	2.30	0.1057	24.35	24.87	736.5	50.3	23.2	16.2	3.1
HW-1	515.8	829.4	2.08	0.1184	24.74	24.74	700.7	44.1	21.2	60.7	2.6

TABLE C-2 EXPERIMENTAL FINITE RATE DATA

RUN NO.	REACTION TEMP	REACTION PRESS	W/FA	RXN. RATE	PCT CONVERSION		REACTOR PARTIAL PRESSURES			
					H ₂ S	TOTAL	N ₂	H ₂ S	SO ₂	H ₂ O SX
HW-2	514.9	829.4	1.01	0.1643	16.70	17.43	719.5	50.5	23.3	33.9 2.0
HW-3	514.7	829.4	4.10	0.0678	27.82	22.92	727.5	21.2	23.7	55.1 1.7
HW-4	514.9	829.4	2.04	0.0850	17.42	13.31	747.7	24.8	27.0	28.7 1.0
HW-5	515.6	829.4	2.05	0.0848	17.47	17.38	640.8	44.4	21.2	121.0 1.8
HW-6	516.0	829.4	1.02	0.1223	12.51	12.65	687.1	50.4	23.8	66.6 1.3
HW-7	515.5	829.4	4.13	0.0465	19.23	14.96	665.0	21.7	23.8	117.8 1.0
HW-8	515.6	829.4	2.01	0.0629	12.70	9.04	714.8	25.0	27.1	61.8 0.6

TABLE C-3 EXPERIMENTAL CATALYTIC ACTIVITY TESTS

RUN NO.	REACTION TEMP	W/FA PRESS	RXN. RATE	PCT CONVERSION H2S	TOTAL	REACTOR PARTIAL PRESSURES			SX		
						N2	H2S	SO2			
CAT1	515.8	829.4	1.03	0.1249	12.96	9.75	767.9	27.7	28.9	4.0	0.7
CAT1	515.8	829.4	1.09	0.1278	14.02	11.07	767.9	27.2	28.6	4.7	0.9
CAT1	515.0	829.4	0.73	0.1188	8.72	6.80	767.3	28.9	29.6	2.8	0.5
CAT1	515.0	829.4	0.80	0.1305	10.48	7.62	767.6	28.5	29.5	3.1	0.6
CAT1	515.1	834.4	1.12	0.1271	14.34	10.85	772.2	27.5	29.1	4.5	0.9
CAT1	516.2	829.4	1.01	0.1223	12.42	9.20	767.6	28.0	29.1	3.8	0.7
CAT1	514.2	829.4	0.62	0.1144	7.17	5.80	767.0	29.6	29.7	2.5	0.4
CAT2	515.8	829.4	1.78	0.1147	20.52	15.83	768.1	25.4	27.7	6.7	1.3
CAT2	515.4	829.4	2.45	0.1043	25.57	19.87	768.8	23.7	26.7	8.4	1.6
CAT3	514.0	829.4	1.39	0.1216	17.01	12.93	768.1	26.4	28.3	5.4	1.0
CAT3	514.0	831.9	1.91	0.1104	21.16	16.17	770.8	25.1	27.7	6.8	1.3
CB-1	515.0	829.4	1.57	0.1180	18.55	13.86	768.2	26.0	28.2	5.7	1.1

TABLE C-3 EXPERIMENTAL CATALYTIC ACTIVITY TESTS

RUN NO.	REACTION TEMP	W/FA	RXN. RATE	PCT CONVERSION H2S	TOTAL	REACTOR N2	H2S	SO2	H2O	SX
C8-2	515.2	831.9	1.02	0.1221	12.47	9.15	770.3	27.7	29.2	3.7 0.7
C8-3	515.0	829.4	0.80	0.1224	9.85	7.40	767.7	28.5	29.4	3.0 0.6
C8-4	515.2	829.4	0.55	0.1274	7.10	5.33	767.2	29.5	29.9	2.2 0.4

TABLE C-4 EXPERIMENTAL INITIAL RATE DATA

RUN NO.	REACTION TEMP	W/FA	RXN. RATE	PCT CONVERSION H ₂ S	TOTAL	REACTOR PARTIAL PRESSURES				SX
						N ₂	H ₂ S	SO ₂	H ₂ O	
AA	558.7	829.0	0.00	0.4149	0.00	736.8	61.8	30.2	0.0	0.0
AB	559.3	829.0	0.00	0.2023	0.00	766.2	32.2	30.5	0.0	0.0
AC	559.2	829.0	0.00	0.0995	0.00	782.4	15.9	30.5	0.0	0.0
9A	540.1	827.0	0.00	0.3390	0.00	727.7	68.6	30.5	0.0	0.0
8B	542.0	830.0	0.00	0.1453	0.00	768.9	30.5	30.4	0.0	0.0
BC	541.5	832.0	0.00	0.0775	0.00	785.3	15.9	30.7	0.0	0.0
CA	515.8	828.0	0.00	0.2417	0.00	731.2	65.8	30.8	0.0	0.0
CB	515.1	829.0	0.00	0.1267	0.00	766.3	31.7	30.9	0.0	0.0
CC	514.8	828.0	0.00	0.0680	0.00	781.2	16.1	30.6	0.0	0.0
CD	513.9	829.0	0.00	0.2925	0.00	722.1	62.2	44.6	0.0	0.0
CE	513.6	829.0	0.00	0.1789	0.00	752.1	63.2	13.5	0.0	0.0
CF	514.3	829.0	0.00	0.1020	0.00	768.1	16.0	44.7	0.0	0.0

TABLE C-4 EXPERIMENTAL INITIAL RATE DATA

RUN NO.	REACTION TEMP	W/FA	RXN. RATE	PCT CONVERSION H ₂ S	REACTOR N ₂	PARTIAL H ₂ S	PRESSURES SO ₂	H ₂ O	SX
CG	514.1	829.0	0.00	0.0610	0.00	797.9	16.9	14.0	0.0
CH	513.4	829.0	0.00	0.1695	0.00	749.6	31.8	47.5	0.0
CK	513.6	829.0	0.00	0.0966	0.00	782.2	32.2	14.5	0.0
DA	481.0	829.0	0.00	0.1405	0.00	732.1	66.5	30.2	0.0
DB	481.0	831.0	0.00	0.0752	0.00	768.4	32.1	0.4	0.0
DC	482.0	829.0	0.00	0.0495	0.00	781.9	16.6	30.4	0.0
FMS	514.5	850.9	0.00	0.4788	0.00	757.8	63.3	29.6	0.0

```

C *****
C *
C *                                     *
C *                                     *
C *                                     *
C * THE INTENT OF NPRDP IS TO REDUCE RAW PROCESS *
C * MEASUREMENTS, TAKEN FROM LABORATORY RECORDERS, TO *
C * USEABLE KINETIC DATA. *
C * INPUT DATA *
C *   NCASE - NUMBER OF SETS OF DATA *
C *   NRUN  - RUN NUMBER *
C *   NFDCR - NUMBER OF FEED CHROMATOGRAMS *
C *   NPRCR - NUMBER OF PRODUCT CHROMAGRAMS *
C *   INCOM - COMPUTER GC RESULTS FLAG *
C *           ...0-NO RESULTS INCLUDED *
C *           ...1-RESULTS INCLUDED ARE TO BE *
C *               AVERAGED WITH DISK INTEGRATOR *
C *               RESULTS *
C *           ...2-USE ONLY COMPUTER RESULTS FOR GC *
C *               ANALYSIS *
C *   NCOPY - NUMBER OF COPIES OF OUTPUT DESIRED *
C *   TEMP  - HONEYWELL MV RECORDER READINGS FOR *
C *           REACTOR BED, WALL AND FLUIDIZED BATH *
C *   PRESS - FOXBORO RECORDER READINGS FOR FEED ABS *
C *           PRESSURE, REACTOR ABS PRESSURE AND FEED *
C *           DIFFERENTIAL PRESSURE CELL *
C *   WC    - WEIGHT OF CATALYST *
C *   ATTEN - GC ATTENUATION LEVELS FOR N2, H2S AND *
C *           SO2 *
C *   CR    - CHROMATAGRAM AREA RESULTS FOR N2, H2S *
C *           AND SO2 MEASURED BY THE DISK INTEGRATOR *
C *           AND THE COMPUTER *
C *****

```

```

DIMENSION CR(6,6),TEMP(3),PRESS(3),ATTEN(6),FDCOM(7)
S,PRCOM(7),BAL(
12,7), V(3),T(2,3),P(2,2),DINT(3),DP(3,3),FDP(3)
DATA V/22403.60,22144.24,21889.30/
DATA T/5.3155,18.0706,6.6860,17.9544,6.3627,17.9853/
DATA P/15.80.25,-534.851,24.806/
DATA DP/0.8985,1.6844,0.0212,0.7409,1.9429,0.0178
S,0.7955,2.0629,0.
10246/
DATA DINT/25.,30.,35./

```

```

C *** READ IN DATA

```

```

READ(5,1) NCASE
1 FORMAT(5I5)
DO 100 IN=1,NCASE
READ(5,1) NRUN,NFDCR,NPRCR,INCOM,NCOPY
READ (5,5) (TEMP(J),J=1,3),(PRESS(J),J=1,3),WC

```


NPRDP

...(CONT'D)

```

5 FORMAT(7F10.5)
  READ(5,5) (ATTEN(J),J=1,3)
  DO 8 I=1,NFDCR
8  READ(5,5) (CR(I,J),J=1,6)
  CALL CHROM (FDCOM,CR,ATTEN,NFDCR,INCOM)
  DO 9 I=1,NPRCR
9  READ(5,5) (CR(I,J),J=1,6)
  CALL CHROM (PRCOM,CR,ATTEN,NPRCR,INCOM)
  DO 14 J=1,3

C  *** CALCULATE TEMPERATURES FROM CALIBRATION COEFFS.

    TMP=0.
    DO 15 I=1,2
15  TMP=TMP+T(I,J)*TEMP(J)**(I-1)
14  TEMP(J)=TMP

C  *** CALCULATE ABS PRESSURES FROM CALIBRATION COEFFS.

    DO 16 J=1,2
    PRS=0.
    DO 17 I=1,2
17  PRS=PRS+P(I,J)*PRESS(J)**(I-1)
16  PRESS(J)=PRS

C  *** CALCULATE FLOW RATE

    M=3
    PRESS(3)=PRESS(3)**0.5
    DO 19 J=1,3
    FDP(J)=0.
    DO 19 I=1,3
19  FDP(J)=FDP(J)+DP(I,J)*PRESS(3)**(I-1)
    CALL NIP (M,DINT,FDP,PRESS(1),PRESS(3))

C  *** FLOW RATE COMPOSITION CORRECTION

    ROMIX=(28.*FDCOM(1)+34.*FDCOM(2)+64.*FDCOM(3))
    S/(FDCOM(1)*V(1)+FDCO
    1M(2)*V(2)+FDCOM(3)*V(3))
    PRESS(3)=PRESS(3)*(28./V(1)/ROMIX)**0.5

C  *** CALCULATE MATERIAL BALANCE

    DO 10 J=1,3
10  BAL(1,J)=FDCOM(J)*PRESS(3)/V(J)*28317.016
    BAL(2,1)=BAL(1,1)
    BAL(2,2)=BAL(2,1)*(PRCOM(2)*V(1)/PRCOM(1)/V(2))
    BAL(2,3)=BAL(2,1)*(PRCOM(3)*V(1)/PRCOM(1)/V(3))
    BAL(2,4)=2.*(BAL(1,3)-BAL(2,3))

```

NPRDP ... (CONT'D)

BAL(2,5)=BAL(1,2)+BAL(1,3)-BAL(2,2)-BAL(2,3)

C *** CALCULATE AVERAGE MOLECULAR WEIGHT OF SULFUR

```

      PRS=PRESS(2)/760.*BAL(2,5)/8.
22  CALL FREM(PRS,RTEMP,XS)
      PRS1=PRESS(2)/760.*BAL(2,5)/XS
      IF (ABS((PRS-PRS1)/PRS1)-0.005) 20,20,21
21  PRS=PRS1
      GO TO 22
20  BAL(2,5)=BAL(2,5)/XS
      RTEMP=(TEMP(1)+TEMP(2))/2.+273.
      BAL(2,6)=BAL(1,2)-BAL(2,2)-BAL(2,4)

```

C *** CALCULATE REACTION RATES

```

      RXH2S=(BAL(1,2)-BAL(2,2))/WC
      RXSO2=(BAL(1,3)-BAL(2,3))/WC

```

C *** CALCULATE FEED AND PRODUCT H2S/SO2 RATIOS

```

      FDRAT=BAL(1,2)/BAL(1,3)
      PRRAT=BAL(2,2)/BAL(2,3)

```

C *** CALCULATE CONVERSION OF H2S AND SO2

```

      H2SCN=(BAL(1,2)-BAL(2,2))/BAL(1,2)*100.
      SO2CN=(BAL(1,3)-BAL(2,3))/BAL(1,3)*100.
      PRESS(3)=PRESS(3)*28317.016

```

C *** CALCULATE PARTIAL PRESSURES IN REACTOR

```

      TOT=0.
      DO 12 J=1,5
      FDCOM(J)=FDCOM(J)*100.
12  TOT=TOT+BAL(2,J)
      DO 13 J=1,5
13  PRCOM(J)=BAL(2,J)*PRESS(2)/TOT

```

C *** DATA OUTPUT

```

      DO 100 ICOP=1,NCOPY
      CALL OUTPT(NRUN,RXH2S,RXSO2,RTEMP,PRESS,PRCOM,FDCOM
        ,FDRAT,PRRAT,BA
        ,1L,H2SCN,SO2CN)
100  CONTINUE
      CALL EXIT
      END

```

C
C
C
C
C
C
C

```

*****
*
*                               OUTPT
*
* OUTPT HAS THE SOLE FUNCTION OF WRITING OUT THE
* CALCULATED RESULTS ON THE LINE PRINTER
*
*****

```

```

SUBROUTINE OUTPT (NRUN,RXH2S,RXSO2,RTEMP,PRESS,PRCOM
$,FDCOM,FDRAT,P
1RRAT,BAL,H2SCN,SO2CN)
DIMENSION PRESS(3),PRCOM(7),FDCOM(7),BAL(2,7)
WRITE(6,5)
5 FORMAT('1')
WRITE(6,1) NRUN
1 FORMAT(///10X,'RUN NUMBER',I3, /37X,'UNITS'//18X
$, 'MASS.....'
1..GRAM'//18X,'PRESSURE.....MILLIMETERS OF MERCURY' /
$/18X,'TEMPER
1ATURE.....DEGREES KELVIN'//18X,'TIME.....HOURL' /
$/18X,'COMPOS
1ITION.....MOLE PERCENT'//18X,'VOLUME.....STANDARD
$ CUBIC CENTI
1METER'//18X,'REACTION RATE...GM MOLES/(HR-GM OF
$ CATALYST)'//)
WRITE(6,3) PRESS(3)
3 FORMAT(10X,'VOLUMETRIC FEED RATE MEASURED BY D/P CELL'
$,11X,F9.1/)
WRITE(6,2) RXH2S,RXSO2,RTEMP,PRESS(2)
2 FORMAT(10X,'REACTION RATE OF H2S',F7.4,5X , 'REACTION
$ RATE OF SO2
1'F7.4//10X,'REACTION TEMPERATURE',F7.2,5X , 'REACTION
$ PRESSURE
1'F7.1/)
WRITE(6,6) FDRAT,PRRAT,H2SCN,SO2CN
6 FORMAT(10X,'FEED H2S/SO2 RATIO ' ,F7.4,5X , 'PRODUCT
$ H2S/SO2 RATIO
10',F7.4//10X,'CONVERSION OF H2S ' ,F7.2,5X
$, 'CONVERSION OF SO2
1 ' ,F7.2,///)
WRITE(6,4) (FDCOM(J),PRCOM(J),BAL(1,J),BAL(2,J) ,J=1
$,6)
4 FORMAT(10X,'MOLECULAR',5X,'FEED',6X,'PARTIAL PRESSURE'
$,4X,'MATERIAL
1L BALANCE'//11X,'SPECIE',4X'COMPOSITION',4X,'IN
$ REACTOR',8X,'FEED
1 PRODUCT'//13X,'N2 ' ,7X,F6.2,9X,F6.1,9X,F7.3,3X
$,F7.3//13X,'H2S'
1,7X,F6.2,9X,F6.1,9X,F7.3,3X,F7.3//13X,'SO2',7X,F6.2,9X
$,F6.1,9X,F7.
13,3X,F7.3//13X,'H2O',7X,F6.2,9X,F6.1,9X,F7.3,3X,F7.3/

```

OUTPT ... (CONT'D)

```
$/13X,'SX ',7X  
1,F6.2,9X,F6.1,9X,2(F7.3,3X)//13X'H2'8X,F6.2,9X,F6.1,9X  
$,2(F7.3,3X))  
  RETURN  
  END
```

```

C *****
C *
C *
C *
C *
C * CHROM CALCULATES STREAM COMPOSITIONS FROM THE
C * CHROMATOGRAPHIC AREA RESULTS USING THE CALIBRATION *
C * COEFFICIENTS DETERMINED USING THE INTERNAL STANDARD*
C * PROCEDURE
C *
C *****

SUBROUTINE CHROM(COMP,CR,ATTEN,N,INCOM)
  DIMENSION COMP(7),CR(6,6),ATTEN(6),HSN2(2,3),SON2(2)
  $,CHSN2(2,3),CS
  1ON2(2)
  DATA HSN2/0.0418,0.5888,0.1129,0.6921,0.0547,0.7756/
  DATA SON2/0.0044,0.4950/
  DATA CHSN2/0.0620,0.5824,0.0232,0.7115,0.0224,0.7901/
  DATA CSON2/-0.1157,0.5037/
  XN=N
  DO 2 J=1,3
2  ATTEN(J+3)=ATTEN(J)
  DO 1 J=1,6
  CR(6,J)=0.
  DO 1 I=1,N
1  CR(6,J)=CR(6,J)+CR(I,J)*(21.-2.*ATTEN(J))/XN
  IF(9.6-ATTEN(2)) 3,4,5
3  M1=1
  GO TO 6
4  M1=2
  GO TO 6
5  M1=3
6  HNRAI=HSN2(1,M1)/100.+HSN2(2,M1)*CR(6,2)/CR(6,1)
  SNRAI=SON2(1)/100.+SON2(2)*CR(6,3)/CR(6,1)
  INCOM=INCOM+1
  GO TO (15,11,11),INCOM
15 HNRAI=HNRAI
  SNRAI=SNRAI
  GO TO 14
11 HNRAC=CHSN2(1,M1)/100.+CHSN2(2,M1)*CR(6,5)/CR(6,4)
  SNRAC=CSON2(1)/100.+CSON2(2)*CR(6,6)/CR(6,4)
  IF(INCOM=3) 12,13,13
12 HNRAT=(HNRAC+HNRAI)/2.
  SNRAT=(SNRAC+SNRAI)/2.
  GO TO 14
13 HNRAT=HNRAC
  SNRAT=SNRAC
14 COMP(1)=1./(1.+HNRAT+SNRAT)
  COMP(2)=1.-COMP(1)-SNRAT*COMP(1)
  COMP(3)=1.-COMP(1)-HNRAT*COMP(1)
  INCOM=INCOM-1
  RETURN

```

C-20

CHROM

... (CONT'D)

END

```

C *****
C *
C *                               NIP
C *
C * NIP CARRIES OUT AN INTERPOLATION USING NEWTONS
C * INTERPOLATION POLYNOMIAL
C *
C *****

```

```

SUBROUTINE NIP(M,X,Y,BX,SX)
DIMENSION X(3),Y(3),YX(3),F(3)
DO 1 I=1,M
  F(I)=0.
  DO 1 J=1,I
    D=1.
    DO 2 K=1,I
      CD=X(J)-X(K)
      IF(CD) 2,3,2
3    CD=1.
2    D=D*CD
1    F(I)=F(I)+Y(J)/D
    YX(1)=F(1)
    DO 4 I=2,M
      II=I-1
      D=1.
      DO 5 J=1,II
        C=BX-X(J)
5      D=C*D
4      YX(I)=D*F(I)
      SX=0.
      DO 6 I=1,M
6      SX=SX+YX(I)
    RETURN
  END

```

```
C *****  
C *  
C *  
C * SUBROUTINE FREM *  
C *  
C * THIS SUBROUTINE AND ASSOCIATED SUBROUTINES GSET, *  
C * GAUSS AND NEZE ARE USED FOR DETERMINING THE AVERAGE *  
C * MOLECULAR WEIGHT OF SULFUR AT THE TEMPERATURE AND *  
C * PRESSURE OF THE EXPERIMENTAL RUN. THESE SUB- *  
C * ROUTINES WILL NOT BE LISTED HERE SINCE THEY ALREADY *  
C * APPEAR IN APPENDIX B. THE F/RT DATA FOR THE SULFUR *  
C * SPECIES IS EMBEDDED IN FREM AS A DATA STATEMENT. *  
C *  
C *****  
  
SUBROUTINE FREM(PRESS,T,XS)  
END
```


APPENDIX D
ESTIMATION OF FILM AND PORE DIFFUSION RATES

D.1 Physical Properties

The physical properties of N_2 , H_2S and SO_2 must be known before mass transfer rates can be estimated. Table D.1 lists the physical properties which were used in this Appendix.

TABLE D.1 PHYSICAL PROPERTIES OF N_2 ,
 H_2S AND SO_2 AT 500°F, 1 Atm.

Physical Property	Units	Molecular Species			Reference
		N_2	H_2S	SO_2	
Density	lb/cu.ft.	0.0400	0.0492	0.0936	(1)
	gm/litre	0.640	0.788	1.498	
Viscosity	C_p	0.0275	0.0230	0.0204	(2)
Critical Temperature	°K	125.9	373.4	430.2	(3)
Molar Volume at Normal Boiling Point	ml/gm mole	31.2	32.9	44.8	(4)
Diffusivity in Nitrogen	cm^2/sec		0.436	0.342	Estimated

- (1) Perry, J.H., "Chemical Engineers Handbook", 4th Ed., McGraw Hill, New York (19), p 3-71
- (2) Ibid, p 3-197
- (3) Ibid, p 3-100
- (4) Ibid, p 14-20

D.2 Calculation of Film Diffusion Coefficients

Data on mass transfer from fluid to solid in gas systems are commonly expressed in terms of a mass transfer coefficient, k_G , defined by,

$$N_i = k_G(p_i - p_i^s) \quad . \quad (2.35)$$

Chilton and Colburn⁽⁵⁾ suggested the following basis for correlating mass transfer data,

$$\frac{k_G P}{G_M} N_{Sc} = f(N_{Re}) \quad . \quad (2.36)$$

It is usual to plot jD versus N_{Re} , where

$$jD = \frac{k_G P}{G_M} N_{Sc}^{2/3} \quad .$$

Figure 2.1 in Satterfield⁽⁶⁾ gives the variation of jD with N_{Re} , and this information combined with the physical property data was used for estimating mass transfer coefficients in the $N_2 - H_2S - SO_2$ system.

Mass transfer coefficients have been calculated for two examples which both use a gas stream composition of 94% N_2 , 4% H_2S and 2% SO_2 (molar basis). Using the methods described in Appendix A, the density and viscosity of this fluid mixture were found to be:

(5) Chilton, T.H. and Colburn, A.P., Ind. Eng. Chem., 26, 1183 (1934).

(6) Satterfield, C.N. and Sherwood, T.K., "The Role of Diffusion in Catalysis", Addison-Wesley Publishing Company, Inc., Reading Massachusetts (1963), p 33.

$$\rho = 0.000628 \text{ gm/ml (500°F)}$$

$$0.0765 \text{ lb/cu.ft. (60°F)}$$

$$\mu = 0.0269 \text{ cp}$$

The first example applies to the recycle reactor where the flow rate is expected to be 3.0 scfm through a bed of 28/35 mesh catalyst pellets and the bed has a cross-sectional area of 0.963 cm^2 .

The second example is for a sulfur plant using commercial Porocel catalyst pellets, cylindrical in shape, with a length of 1.25 cm and diameter 0.80 cm. Modern Claus type sulfur plants are designed with converter space velocities in the range of 650 to 900 scfh of gas per cubic foot of catalyst bed volume⁽⁷⁾. On this basis a converter space velocity of 775 scfh gas per cubic foot of catalyst is selected for this example. The catalyst is contained in horizontal drums 60 ft. long and 13 ft. in diameter with flow downward through the bed which is packed to a depth of 3 to 4 ft⁽⁷⁾. These numbers were used for determining that the cross sectional area of bed perpendicular to the mean flow path is $0.286 \text{ ft}^2/\text{ft}^3$ assuming that the gas is evenly distributed and the bed depth is 3.5 ft.

The calculation results for estimating the mass transfer coefficients for both examples are presented in Table D.2. The values for jD were obtained from Figure 2-1, Satterfield and Sherwood⁽⁶⁾.

The experimental program proved that film diffusion is not a

(7) Cunliffe, R.S., "Optimizing Conversion of Hydrogen Sulfide to Sulfur", paper at the 19th Canadian Chemical Engineering Conference and Third Symposium on Catalysis, Edmonton, Alberta, October, 1969.

rate controlling phenomena for the Claus reaction in the recycle reactor and also that, for all intents and purposes, only the external surface of the catalyst is effective for catalyzing the reaction. The non-existence of film diffusion control in the recycle reactor will now be verified, and the sulfur plant data will be examined to see if bulk mass transfer is limiting in the selected situation.

For 28/35 mesh catalyst, the external surface area per gram is calculated from

$$A_E = \frac{S_p}{\rho_p V_p} . \quad (D.1)$$

For both spherical and cubical particle geometry, Equation D.1 reduces to

$$A_E = \frac{6}{d_p \rho_p} . \quad (D.2)$$

Examination of the crushed catalyst particles leads one to believe that they are more cubical than spherical in shape. Equation D.2 yields $A_E = 46.2 \text{ cm}^2/\text{gm}$ when the average cube side length is taken as 0.051 cm and the density of bauxite as 2.55 gm/ml⁽⁸⁾.

At the given pressure and gas stream composition, the partial pressures of H_2S and SO_2 are 30.4 and 15.2 mm Hg respectively. Substituting these values into the following rate expression which was cor-

(8) Opcit, Perry, J.H., p 3-89.

related to the kinetic data, a value of 0.12 gm mole $\text{H}_2\text{S}/(\text{hr})(\text{gm catalyst})$ was obtained for the reaction rate.

$$r = k_1 E_{\text{XPF1}} P_A^{m_A} P_B^{n_B} \quad (\text{D.3})$$

TABLE D.2 CALCULATION RESULTS FOR ESTIMATION OF MASS
TRANSFER COEFFICIENTS FOR H_2S AND SO_2

	<u>Recycle Reactor</u>	<u>Sulfur Plant</u>
$d_p(\text{cm})$	0.051	1.149
$P(\text{atm})$	1.0	1.0
$G(\text{gm}/\text{sec}.\text{cm}^2)$	1.803	0.02814
$G_M(\text{gm mole}/\text{sec}.\text{cm}^2)$	0.0622	0.00097
N_{Re}	341.63	120.20
$N_{\text{Sc}}(\text{H}_2\text{S})$	0.982	0.982
$N_{\text{Sc}}(\text{SO}_2)$	1.252	1.252
j_D	0.078	0.14
$k_G(\text{H}_2\text{S}) (\frac{\text{gm moles}}{\text{sec}.\text{cm}^2\text{atm}})$	0.00486	0.000135
$k_G(\text{SO}_2)$	0.00417	0.000116

The values of the parameters and their confidence limits are given in Table 6.6.

Since the area per gram of catalyst is known for the 28/35 mesh catalyst that was used in the kinetic study, the reaction rate will be expressed in terms of external surface area for comparison with the diffusion equation.

$$r_{AE} = \frac{r}{A_E} \quad (D.4)$$

From Equation D.4, $r_{ae} = 0.12/46.2 = 0.0026$ gm-moles/(hr)(cm² catalyst).

If film diffusion is rate controlling, it is reasonable to assume that the partial pressure of H₂S on the catalyst surface is zero in Equation 2.35. This being the case, the possible diffusion flux was calculated at 0.70 gm-moles/(cm²)(hr) which is more than 250 times as rapid as the flux required to sustain the surface reaction.

Similarly, the H₂S diffusion flux for the sulfur plant example calculates at 0.0195 gm-moles/(cm²)(hr). This is 7.5 times as rapid as the flux required to sustain the surface reaction. In this case, it is evident that, as the partial pressure of H₂S further decreases and the same ratio (2:1) of H₂S to SO₂ mole fractions is maintained, the ratio of mass transfer rate to chemical reaction rate increases.

In conclusion, theoretical calculations as well as experimental data indicate that film diffusion does not limit the Claus reaction in the experimental apparatus. It also appears that the same

holds true for full scale sulfur plants.

D.3 Interrogation of a Pore Diffusion Rate Control Criterion

Pore diffusion phenomena and underlying theory have been treated in Section 2.4.2 of the literature survey, so it will only be stated here that the criterion of Hudgins was the one selected for testing. It was selected because it is simple to apply, and it was considered to be conservative (perhaps even more so than necessary (9)). This criterion requires that

$$(\bar{r}) \left(\frac{1}{C_0} \right) \left(\frac{\rho_0^2}{D_{\text{eff}}} \right) < \left(\frac{1}{C_0} \right) \left(\frac{r(C_0)}{r'(C_0)} \right) . \quad (2.48)$$

The same conditions which were used for estimating film diffusion rates will also be applied here. Since there was no measurement of reaction rate at these conditions, it will be assumed that $\bar{r} = r(C_0)$ and that Equation (2.48) can be approximated by Equation D.5.

$$\frac{d_p^2}{D_{\text{eff}}} < \frac{1}{r'(C_0)} \quad (D.5)$$

The empirical expression for reaction rate described by Equation (6.12) will be used for estimating $r'(C_0)$.

A decision must be made on how to calculate D_{eff} . Is the pore diffusion ordinary or of the Knudsen type? Rather than belabour

(9) Peterson, E.E., Chem. Eng. Sci., 23, 94, (1968).

the point of which mechanism predominated, the theory of the transition region as given by Scott et al⁽¹⁰⁾ was considered. These authors suggest that if D_{12}/D_k is large, $D_{eff} = D_{k,eff}$ and, conversely in the other limit with $D_{12}/D_{k,small}$, D_{eff} becomes a function of D_{12} . Therefore $D_{12,eff}$ and $D_{k,eff}$ were both calculated using Equations (2.39) and (2.40) respectively. Surface area measurements obtained using the BET method gave a total surface area of $148 \text{ m}^2/\text{gm}$ ⁽¹¹⁾ for the bauxite catalyst used in this investigation. Values of θ and τ (catalyst void fraction and tortuosity) are not available for bauxite and values of 0.812 and 0.85 are used in these calculations. These values were determined by Henry et al⁽¹²⁾ for pure alumina catalyst pellets. The results which were obtained for ordinary and Knudsen effective diffusion coefficients using the above data and previously described experimental conditions were 0.417 and $0.0158 \text{ cm}^2/\text{sec}$ respectively. Since the ratio of the two diffusion coefficients (D_{12}/D_k) is greater than 25, it is assumed that Knudsen diffusion is the predominant diffusion mechanism and that $D_{eff} = 0.0158 \text{ cm}^2/\text{sec}$.

Equation (6.12) was revised so that P_B could be expressed in terms of P_A . Since H_2S and SO_2 were fed to the reactor in stoichiometric proportions in the selected experimental conditions, then

$$P_B = \left(\frac{1}{2}\right)(P_A) \quad (\text{D.6})$$

(10) Scott, D.S., and Dullien, F.A.L., A.I.Ch.E.J., 8, 113, (1962).

(11) DeGermany, M., University of Alberta, Edmonton, Alberta, unpublished work, 1970.

(12) Henry, J.P.B., Chennakesavan, B., and Smith, J.M., A.I.Ch.E.J., 7, 10, (1961).

and Equation (6.12) becomes

$$r = (k_1)(E_{\text{XPF1}})(P_A)^m(P_A/2)^n \quad (\text{D.7})$$

Equation (D.7) is next adjusted so that the units of r correspond to those required by Equation (2.48).

$$r = \frac{(\rho_p)(k_1)(E_{\text{XPF1}})(RT)^{m+n}(C_A)^{m+n}}{(3600.)(2)^n} \quad (\text{D.8})$$

From Equation (D.8),

$$\begin{aligned} r' = \frac{dr}{dC_A} &= \frac{(\rho_p)(k_1)(E_{\text{XPF1}})(RT)^{m+n}(C_A)^{m+n-1}}{(3600.)(2)^n} \\ &= \frac{(\rho_p)(k_1)(E_{\text{XPF1}})(RT)(P_A)^{m+n-1}}{(3600.)(2)^n} \\ &= 92. \text{ sec}^{-1} \end{aligned}$$

For this calculation, the following numbers were used:

$$\begin{aligned} \rho_p &= 2.55 \text{ gm catalyst/cm}^3 \\ k_1 &= 2.198 \frac{(\text{gm-moles H}_2\text{S})(\text{mm Hg})^{-m-n}}{(\text{hr})(\text{gm-catalyst})} \\ E_{\text{XPF1}} &= \exp(-7589/1.98/533) \\ R &= 82.057 \times 760. (\text{mm Hg})(\text{cm}^3)/(\text{gm-mole})/(^{\circ}\text{K}) \\ T &= 533^{\circ}\text{K} \end{aligned}$$

$$P'_A = 30.4 \text{ mm Hg}$$

$$m = 0.963$$

$$n = 0.359$$

This result yields a value of 0.011 for $1/r'$.

The value of ρ_0^2/D_{eff} , which should be less than 0.011 for the absence of pore diffusion control, calculates at 0.04 when 0.0255 cm and 0.0158 cm²/sec are used for ρ_0 and D_{eff} respectively. It therefore is concluded that the criterion of Hudgins for the absence of pore diffusion control has not been satisfied.

APPENDIX E
DATA CORRELATION AND PARAMETER CONFIDENCE LIMITS

E.1 Parameter Estimation Procedure

The problem of optimizing functions with nonlinear parameters has been approached in a variety of ways. Most techniques involve an iterative scheme which hopefully converges on the correct solution after having started from an initial guess of the parameter values. Nonlinear Least Squares⁽¹⁾ is such a technique, however it is very sensitive to the initial parameter estimates, and when "bad guesses" are made for them, the method often will not converge.

Similarly, Rosenbrock's Method of Rotating Coordinates^(2,3) requires an initial set of parameter estimates however, the procedure is designed to be insensitive to bad guesses. It optimizes the convergence path by combined rotation of the ridge tracking vector and adjustment of the stepsize.

To describe Rosenbrock's Method, the following nomenclature is used:

$X = (x_1, x_2, \dots, x_M)$; a set of M independent variables

Y ; a single dependent variable

$\Lambda = (\lambda_1, \lambda_2, \dots, \lambda_P)$; a set of P parameters

$Y = f(X, \Lambda)$; a functional relationship either to be fitted to data
or optimized

(1) Rubin, D.I., Chem. Eng. Prog. Symp. Series, 59, 42, (1963).

(2) Rosenbrock, H.H. and Storey, C., "Computational Techniques for Chemical Engineers", 64, Pergamon Press, Toronto, 1966.

(3) Wilde, D.J., "Optimum Seeking Methods", 151, Prentice Hall, Inc., Englewood Cliffs, N.J., 1964.

$v_1, v_2, v_3, \dots, v_p$; a set of P unit orthogonal vectors

e_1, e_2, \dots, e_p ; a set of P step lengths

$\delta(Y, f(X, \Lambda))$; the variance of the fit. Simply replace this with Y if one is trying to optimize the function $y = f(X, \Lambda)$.

The computational procedure follows the sequence now given:

I A set of P unit orthogonal vectors is generated

$$v_1 = (1 \ 0 \ 0 \ \dots \ 0)$$

$$v_2 = (0 \ 1 \ 0 \ \dots \ 0)$$

$$\vdots$$

$$v_p = (0 \ 0 \ 0 \ \dots \ 1)$$

A set of P parameter estimates is guessed.

$$\Lambda = (\lambda_1, \lambda_2, \dots, \lambda_p)$$

A set of P stepsizes are provided

$$(e_1, e_2, \dots, e_p)$$

II $\delta(y, f(X, \Lambda))$ is evaluated using the initial estimates.

III Λ is now modified by changing it to $\Lambda'(\Lambda + v_1 e_1)$ and then $\delta(y, f(X, \Lambda'))$ is evaluated. If this change was favourable

(i.e., $\delta(y, f(X, \Lambda')) < \delta(y, f(X, \Lambda))$), then Λ is replaced by Λ' and e_1 is multiplied by 3. Next $\Lambda'(\Lambda + v_2 e_2)$ is used for calculating $\delta(y, f(X, \Lambda'))$ and so on. If a change was unsuccessful (i.e., $\delta(y, f(X, \Lambda')) > \delta(y, f(X, \Lambda))$), the e_i is multiplied by - 0.5. The successive changes in Λ then are $e_1 v_1, e_2 v_2, \dots, e_p v_p, e_1 v_1 \dots$. This process is continued until oscillation occurs. That is, until for each parameter a successful step has been followed immediately by an unsuccessful step. This definition of oscillation should be strictly adhered to.

IV Next, the axes are rotated according to the following procedure.

$$\begin{aligned} \text{Let } A_1 &= (\Lambda_{i+1} - \Lambda_i) = (a_{11} \ a_{12} \ \dots \ a_{1p}) \\ A_2 &= (0 \ a_{12} \ \dots \ a_{1p}) \\ &\vdots \\ &\vdots \\ A_p &= (0 \ 0 \ \dots \ a_{1p}) \end{aligned}$$

Note that $\Lambda_{i+1} - \Lambda_i$ is the total change in the parameter values which took place in part III. That is, a_{11} is the sum of the successful steps taken for λ_1 .

$$\text{Now } v_1^{(2)} = \frac{A_1}{(\sum a_i^2)^{1/2}} = \frac{A_1}{||A_1||} = (v_{11} \ v_{12} \ \dots \ v_{1p})$$

Then one uses A_2 to construct a vector B_2 , normal to v_1 .

$$B_2 = A_2 - (A_2' v_1^{(2)}) v_1^{(2)}$$

$$v_2^{(2)} = \frac{B_2}{\|B_2\|}$$

.....

$$B_p = A_p - \sum_{i=1}^{p-1} (A_p' v_i^{(2)}) v_i^{(2)}$$

$$v_p^{(2)} = \frac{B_p}{\|B_p\|}$$

Note that $A_i' v_i = \sum_{j=1}^p a_{ij} v_{ij}$

In the above equations, A_1 is the vector representing the total progress made since the axes were last rotated and $v_1^{(2)}$ is a unit vector parallel to A_1 . This procedure, set forth by Rosenbrock in his article⁽⁴⁾, is called the Gram Schmidt orthogonalization process.

A description of input data symbols and their formats is provided in the heading of the Fortran listing of the program. The number of parameters and independent variables which the program can handle is

⁽⁴⁾ Rosenbrock, H.H., article in "A Survey of Modern Algebra", 192, ed. Birkoff, G., and MacLane, S., The Macmillan Company, New York, N.Y. 1953.

limited to 5 each due to the dimensioning of vectors and matrices. This number of course can be increased by modifying the dimension statements.

It should be noted that the names which are assigned to the parameters should be entered on the appropriate card in the same order as they are used in the equation for the function. For example, suppose one desired to correlate the following expression to data:

$$\text{Rate} = K_0 e^{(-Z/RT)} P_A^{K_1} P_B^{K_2}$$

Here the parameters are K_0 , Z , K_1 and K_2 and the independent variables are P_A , P_B and T . If the cards on which the names of the parameters and independent variables were punched up to be entered as

K_0	Z	K_1	K_2
P_A	P_B	T	

then the equation which should be entered in ROSE and VARIA is:

```
FUNC = PAR1(1)*EXP(-PAR1(2)/(1.98*X(J,3)))*X(J,2)**PAR1(3)
      ...*X(J,2)**PAR1(4)
```

An alternate approach to entering the function to be correlated would be as follows:

```

R = 1.98
K0 = PAR1(L)
Z = PAR1(2)
K1 = PAR1(3)
K2 = PAR1(4)
PA = X(J,1)
PB = X(J,2)
T = X(J,3)
RATE = K0*EXP(-z)/(R*T))*PA**K1*PB**K2
FUNC = RATE

```

In both cases, there is a need for avoiding undefined variables and maintaining consistency with the input data.

Following the listing of ROSE, the parameter estimates and regenerated data for Equation 6.10 are given. A different set of values for the parameters are found in the computer output than what is found in Table 6.6. The reason for this is that the program was run in single precision on an IBM 1800 for demonstration purposes only. For accurate parameter estimates, the program was executed on the IBM 360 in double precision and the results of such runs are given in Table 6.6.

E.2 Estimation of Parameter Interval

It was assumed that the error of the fit was normally distributed and with such a distribution, the likelihood function may be written as

$$L(\epsilon) = (2\pi\sigma^2)^{-\frac{n}{2}} \exp\left[-\frac{1}{2\sigma^2} \sum_{i=1}^n (y_i - f(x_i, B))^2\right]$$

where n = number of observations

x = state variables vector

B = parameter values

σ^2 = variance estimate

$$= \sum_{i=1}^n (y_i - f(x_i, B))^2 / (n-1)$$

The inverse of the posterior variance-covariance matrix may be written as

$$C^{-1} = \begin{array}{cccc} \frac{-\partial^2 \ln L(\epsilon)}{\partial B_1^2} & \frac{-\partial^2 \ln L(\epsilon)}{\partial B_1 \partial B_2} & \dots & \frac{-\partial^2 \ln L(\epsilon)}{\partial B_1 \partial B_p} \\ \frac{-\partial^2 \ln L(\epsilon)}{\partial B_1 \partial B_2} & \frac{-\partial^2 \ln L(\epsilon)}{\partial B_2^2} & \dots & \frac{-\partial^2 \ln L(\epsilon)}{\partial B_2 \partial B_p} \\ \frac{-\partial^2 \ln L(\epsilon)}{\partial B_1 \partial B_p} & \frac{-\partial^2 \ln L(\epsilon)}{\partial B_p \partial B_2} & \dots & \frac{-\partial^2 \ln L(\epsilon)}{\partial B_p^2} \end{array}$$

This is a positive, definite, symmetric matrix which may be inverted by

using Brown's method⁽⁵⁾ to give the variance-covariance matrix.

The natural logarithm of the above likelihood function is written as:

$$\ln L(\epsilon) = \frac{-n}{2} \ln(2\pi\sigma^2) - \frac{1}{2\sigma^2} \left[\sum_{i=1}^n y_i - f(x_i, B) \right]^2 .$$

The partial derivatives of the natural logarithm of the likelihood function with respect to the parameters may be written as:

$$\frac{\partial \ln L(\epsilon)}{\partial B_j} = - \frac{1}{2\sigma^2} \sum_{i=1}^n (-2) \frac{\partial f_i}{\partial B_j} (y_i - f_i)$$

$$= \frac{1}{\sigma^2} \sum_{i=1}^n (y_i - f_i) \frac{\partial f_i}{\partial B_j}$$

$$\frac{\partial^2 \ln L(\epsilon)}{\partial B_j^2} = \frac{1}{\sigma^2} \left[\sum_{i=1}^n \left\{ (y_i - f_i) \frac{\partial^2 f_i}{\partial B_j^2} - \left(\frac{\partial f_i}{\partial B_j} \right)^2 \right\} \right]$$

$$\frac{\partial^2 \ln L(\epsilon)}{\partial B_j \partial B_k} = \frac{1}{\sigma^2} \left[\sum_{i=1}^n \left\{ (y_i - f_i) \frac{\partial^2 f_i}{\partial B_j \partial B_k} - \frac{\partial f_i}{\partial B_j} \cdot \frac{\partial f_i}{\partial B_k} \right\} \right] .$$

The covariance matrix, C, is a measure of the reliability of the parameter estimates. This matrix expresses the manner in which variations in the observations would affect the parameter estimates. The diagonal elements of C are the variances and their square roots

⁽⁵⁾ Brown, R.G., "Smoothing Forecasting and Prediction", 353, Prentice-Hall, Englewood Cliffs, N.J., 1962.

are the standard deviations of the parameter estimates. Off-diagonal elements indicate the interdependence of the estimates of the various parameters.

Below is an example of the partial derivatives of a rate expression which were required for calculating the partial derivatives of the logarithm of the likelihood function. The likelihood logarithm derivatives are the elements found in the inverse of the variance-covariance matrix.

$$r = f = k_1 p_A^m p_B^n - k_{-1} p_C^p$$

$$\frac{\partial f}{\partial k_1} = p_A^m p_B^n$$

$$\frac{\partial f}{\partial m} = (k_1 p_A^m p_B^n) (\ln p_A)$$

$$\frac{\partial f}{\partial n} = (k_1 p_A^m p_B^n) (\ln p_B)$$

$$\frac{\partial f}{\partial k_{-1}} = - p_C^p$$

$$\frac{\partial f}{\partial p} = - (k_{-1} p_C^p) (\ln p_C)$$

$$\frac{\partial^2 f}{\partial k_1^2} = 0.0$$

$$\frac{\partial^2 f}{\partial m^2} = (k_1 P_A^m P_B^n) (\ln P_A)^2$$

$$\frac{\partial^2 f}{\partial n^2} = (k_1 P_A^m P_B^n) (\ln P_B)^2$$

$$\frac{\partial^2 f}{\partial k_{-1}^2} = 0.0$$

$$\frac{\partial^2 f}{\partial p^2} = - (k_{-1} P_C^P) (\ln P_C)^2$$

$$\frac{\partial^2 f}{\partial k_1 \partial m} = (P_A^m P_B^n) (\ln P_A)$$

$$\frac{\partial^2 f}{\partial k_1 \partial n} = (P_A^m P_B^n) (\ln P_B)$$

$$\frac{\partial^2 f}{\partial k_1 \partial k_{-1}} = 0.0$$

$$\frac{\partial^2 f}{\partial k_1 \partial p} = 0.0$$

$$\frac{\partial^2 f}{\partial m \partial n} = (k_1 P_A^m P_B^n) (\ln P_A) (\ln P_B)$$

$$\frac{\partial^2 f}{\partial m \partial k_{-1}} = 0.0$$

$$\frac{\partial^2 f}{\partial m \partial p} = 0.0$$

$$\frac{\partial^2 f}{\partial n \partial k_{-1}} = 0.0$$

$$\frac{\partial^2 f}{\partial n \partial p} = 0.0$$

$$\frac{\partial^2 f}{\partial k_{-1} \partial p} = -(P_C^P)(\ln P_C) \quad .$$

The computer program, CONLM, which estimated the confidence limits was written in Fortran IV basic and is listed on the following pages. Following the listing is the variance-covariance matrix for the above example.

```

C *****
C *
C *
C *
C *
C * THIS PROGRAM WAS WRITTEN TO OPTIMIZE FUNCTIONS
C * WITH A MAXIMUM OF 5 NONLINEAR PARAMETERS USING
C * ROSEN BROCK'S METHOD OF ROTATING COORDINATES. IT
C * MAY BE USED TO MAXIMIZE OR MINIMIZE AN
C * UNCONSTRAINED UNIMODAL FUNCTION, AND, IN THE CASE
C * OF DATA CORRELATION, IT WILL ESTIMATE PARAMETERS
C * IN ACCORDANCE WITH THE MINIMUM VARIANCE CRITERION.
C * TO DETERMINE IF A FUNCTION IS UNIMODAL IN THE
C * REGION OF INTEREST, A NUMBER OF DIFFERENT INITIAL
C * GUESSES FOR THE PARAMETERS SHOULD BE ATTEMPTED.
C *
C *
C * INPUT DATA
C * PLEASE NOTE THAT FOR CURVE FITTING, ALL OF THE
C * DATA BELOW MUST BE ENTERED, BUT FOR FUNCTION
C * OPTIMIZATION ONLY THE DATA MARKED WITH A * IS
C * ENTERED.
C *
C * JTYPE - PROGRAM CONTROL FLAG
C *
C *     ...1-MAXIMIZE A FUNCTION
C *     ...2-MINIMIZE A FUNCTION
C *     ...3-CORRELATE DATA TO A FUNCTION
C *
C * NFIT1 - NUMBER OF SETS OF DATA TO BE
C *         CORRELATED
C *
C * M      - NUMBER OF INDEPENDENT VARIABLES
C * N      - NUMBER OF DATA POINTS TO BE FITTED
C * XNAM   - NAMES OF THE INDEPENDENT VARIABLES
C * X      - VALUES OF INDEPENDENT VARIABLES
C * Y      - VALUE OF DEPENDENT VARIABLE
C *
C * NFITS  - NUMBER OF FUNCTIONS TO BE CORRELATED
C * * NFUNC - FUNCTION NUMBER TO BE CORRELATED
C *
C * P      - THE NUMBER OF PARAMETERS
C *
C * KPN    - NORMALIZATION FLAG
C *
C *     ...0-NORMALIZATION DESIRED
C *     ...1-NORMALIZATION NOT DESIRED
C *
C * * M1    - MAX. NO. OF STEPS BETWEEN ROTATIONS
C * * M2    - MAX. NO. OF ROTATIONS
C * * NTL   - NUMBER OF CARDS FOR PROBLEM TITLE
C * * DES   - ALPHANUMERIC DESCRIPTION OF TITLE
C * * PNAME - NAMES OF PARAMETERS
C *
C * * SS    - STEPSIZE
C *
C * * PAR1  - INITIAL GUESSES FOR PARAMETER VALUES
C *
C *****

```

```

INTEGER P
REAL*8 K0,K1,K2,K3,K4
DOUBLE PRECISION SS,VAR1,VAR2,VAR3,CT,R
S,T,PA,PB,PC,
1PD,DEV,FUNC,SMXMN

```


MAINLINE ROSE ... (CONT'D)

```

DOUBLE PRECISION ELAM(5),OV(5,5),PAR1(5),PAR3(5),X(50
$,5),Y(50),BK(
1150,6)
DIMENSION DES(20),PNAM(6),XNAM(7),XRUN(100),IBK(4,10)
$,KS(5),KSF(5)
1,KF(5),ARUN(100),VX(6)
DATA XNAM/'H2S','SO2','H2O','SX ',' ',' ',' '/
DATA M1,M2/100,50/
DATA IBK/1,24,0,0,25,33,0,0,1,33,0,0,34,73,0,0,74,85,0
$,0,34,85,0,0
1,13,24,28,85,28,33,74,85,13,24,34,73,86,101,0,0/
DATA PNAM/' KO ',' K1 ',' K2 ',' K3 ',' K4 ','VAR.'/
SMXMN=1.D+00

```

C *** READ IN DATA BANKS

```

DO 400 I=1,150
READ(5,401) ARUN(I),(VX(J),J=1,6)
DO 372 J=1,6
372 BK(I,J)=DBLE(VX(J))
IF(BK(I,1)-1.D+03)400,400,402
400 CONTINUE
401 FORMAT(2X,A4,F7.1,12X,F7.4,12X,4F7.1)

```

C *** READ IN CORRELATION DETAILS

```

402 DO 300 NFT=1,100
READ(5,1) P,KPN,NTL,NFUNC,NBANK
1 FORMAT(5I5)
IF(P-10) 23,23,301
23 WRITE(6,28)
28 FORMAT(1H1,///)
DO 24 I=1,NTL
READ(5,2) (DES(J),J=1,20)
2 FORMAT(20A4)
24 WRITE(6,27) (DES(J),J=1,20)
27 FORMAT(10X,20A4)
READ(5,12) SS,(PAR1(J),J=1,P)
12 FORMAT(8D10.3)
NN1=IBK(1,NBANK)
NN2=IBK(2,NBANK)
NN3=IBK(3,NBANK)
NN4=IBK(4,NBANK)
J=0
253 DO 250 I=NN1,NN2
J=J+1
XRUN(J)=ARUN(I)
Y(J)=BK(I,2)
X(J,1)=BK(I,1)
DO 250 K=2,5

```

MAINLINE ROSE ... (CONT'D)

```

      JJ=K+2
250  X(J,K)=BK(I,JJ)
      IF(NN3) 251,251,252
252  NN1=NN3
      NN2=NN4
      NN3=-1
      GO TO 253
251  N=J
      WRITE(6,29) (PNAM(J),J=1,P),PNAM(6)
29  FORMAT(/,10X,'ROTATION NO.',6(5X,A4,6X)/)

C    *** GENERATE INITIAL SET OF ORTHOGONAL VECTORS AND
C    *** NULL SCALING FACTORS

      DO 5 I=1,P
      KSF(I)=0
      5  PAR3(I)=PAR1(I)
14  DO 67 I=1,P
      DO 6 J=1,P
      6  OV(I,J)=0.0D+00
      67 OV(I,I)=1.0D+00

C    *** CALCULATION OF FUNCTION VALUE FOR INITIAL GUESSES

      CALL VARIA (PAR1,KSF,P,VAR2,N,NFT,X,Y,NFUNC)
      VAR2=VAR2*SMXMN
      VAR1=VAR2
      VAR3=VAR1
      COUNT=0.

C    *** COMMENCE ROSENBROCK ALGORITHM

      DO 7 KKK=1,M1

C    *** GENERATE INITIAL STEPSIZES AND SUCCESS/FAILURE
C    *** FLAGS

      DO 85 I=1,P
      ELAM(I)=SS*(10.0D+00)**KSF(I)
      KS(I)=0
      85  KF(I)=0

C    *** COMMENCE RIDGE TRACKING

      DO 80 KLP=1,M2
      DO 90 II=1,P

C    *** ADJUSTMENT OF PARAMETERS

      DO 9 I=1,P

```

MAINLINE ROSE ... (CONT'D)

```

9 PAR1(I)=PAR1(I)+OV(II,I)*ELAM(II)

C   *** CALCULATE NEW FUNCTION VALUE AND COMPARE TO OLD
C   *** ONE

      CALL VARIA (PAR1,KS,P,VAR2,N,NFT,X,Y,NFUNC)
      VAR2=VAR2*SMXMN
      COUNT=COUNT+1.
      IF(VAR1-VAR2) 10,101,101

C   *** SUCCESSFUL STEP, ADJUST STEPSIZE AND SET SUCCESS
C   *** FLAG

101 VAR1=VAR2
      KS(II)=1
      ELAM(II)=ELAM(II)*3.0D+00
      GO TO 81

C   *** UNSUCCESSFUL STEP, RETURN TO PREVIOUS PARAMETER
C   *** VALUES, ADJUST STEPSIZE AND DIRECTION AND SET
C   *** FAILURE FLAG

10 DO 13 I=1,P
      PAR1(I)=PAR1(I)-ELAM(II)*OV(II,I)
13 CONTINUE
      ELAM(II)=ELAM(II)/(-2.0D+00)
      KF(II)=KS(II)
      KS(II)=0

C   *** TEST FOR OSCILLATORY STEPPING STATUS AND MAGNITUDE
C   *** OF STEPSIZE

81 DO 82 I=1,P
      CT=ELAM(I)/PAR1(I)
      CTEST=DABS(CT)
      IF(CTEST-1.0D-08) 82,82,505
505 IF(KF(I)) 82,90,82
      82 CONTINUE
      GO TO 83
      90 CONTINUE
      80 CONTINUE
      83 CONTINUE

C   *** ROTATION OF AXES

      CALL ROTAT(P,PAR1,PAR3,OV)

C   *** DATA OUTPUT

      DO 40 I=1,P

```

MAINLINE ROSE ... (CONT'D)

```

    PAR1(I)=PAR1(I)/((10.D+00)**KSF(I))
40 CONTINUE
    WRITE(6,26)KKK,(PAR1(I),I=1,P),VAR1
26  FORMAT(10X,I5,7X,7D15.8)
    DO 17 I=1,P
        PAR1(I)=PAR1(I)*((10.D+00)**KSF(I))
17  PAR3(I)=PAR1(I)
    IF(DABS(VAR1-VAR3)-1.D-12) 30,30,310
310 VAR3=VAR1
    IF(KPN) 7,30,7
    7 CONTINUE
    30 IF(KPN=1) 102,100,102
102 KPN=1
    CALL TORM (P,PAR1,KSF)
    DO 11 I=1,P
11  PAR3(I)=PAR1(I)
    GO TO 14
100 DO 31 I=1,P
31  PAR1(I)=PAR1(I)/((10.D+00)**KSF(I))
    WRITE(6,18) (XNAM(J),J=1,3)
18  FORMAT(//,40X,'DATA REGENERATION'//10X,'RUN
    $ DEVIATION CALCULATED
    1 OBSERVED ',4X,'TEMP.',2X,3(5X,A3,3X)/10X,'NO.',12X
    $,'FUNC VALUE FU
    INC VALUE'/)
    DO 15 J=1,N
    FUNC=0.D+00

```

C *** FOR DATA CORRELATION, INSERT FUNCTION NEXT

```

    R=1.98D+00
    T=X(J,1)
    PA=X(J,2)
    PB=X(J,3)
    PC=X(J,4)
    PD=X(J,5)
    K0=PAR1(1)
    K1=PAR1(2)
    K2=PAR1(3)
    K3=PAR1(4)
    K4=PAR1(5)
    GO TO (200,201,202,203,204,205,206,207,208,209),NFUNC
200 FUNC=K0*PA**1.5*PB/(1.+K1*PA**0.5)
    GO TO 210
201 FUNC=K0*PA**1.5*PB/(1.+K1*PA**0.5+K2*PB)
    GO TO 210
202 FUNC=K0*DEXP(-K1/(R*T))*PA**0.8624*PB**0.3563
    GO TO 210
203 FUNC=K0*DEXP(-K1/(R*T))*PA**K2*PB**0.3563
    GO TO 210

```

MAINLINE ROSE ... (CONT'D)

```
204 FUNC=K0*DEXP(-K1/(R*T))*PA**K2*PB**K3
    GO TO 210
205 FUNC=K0*PA**2*PB/(1.D+00+K1*PA+K2*PB)**3
    GO TO 210
206 FUNC=K0*PA*PB/(1.D+00+K1*PA)
    GO TO 210
207 FUNC=K0*PA*PB/(1.D+00+K1*PB)
    GO TO 210
208 FUNC=K0*PA*PB/(1.D+00+K1*PA**0.5+K2*PB)**3
    GO TO 210
209 FUNC=K0*PA**0.5*PB/(1.D+00+K1*PA**0.5+K2*PC)**2
210 CONTINUE
    DEV=Y(J)-FUNC
    WRITE(6,16) XRUN(J),DEV,FUNC,Y(J),(X(J,I),I=1,4)
    16 FORMAT(10X,A4,D10.2,D10.3,2X,2D10.3,3D11.3)
    15 CONTINUE
300 CONTINUE
301 CONTINUE
    STOP
    END
```

```

C *****
C *
C *          VARIA
C *
C * THIS SUBROUTINE CALCULATES THE VALUE OF THE
C * FUNCTION TO BE OPTIMIZED, OR THE VARIANCE FOR
C * CURVE FITTING.
C *
C *****

```

```

SUBROUTINE VARIA (PAR1,KSF,P,VAR2,N,NFT,X,Y,NFUNC)
INTEGER P
REAL*8 K0,K1,K2,K3,K4
DOUBLE PRECISION          DEV2,T,R,PA,PB,PC,PD
S,FUNC,VAR2
DOUBLE PRECISION PAR1(5) ,X(50,5),Y(50)
DIMENSION KSF(5)
DO 5 I=1,P
5 PAR1(I)=PAR1(I)/((10.D+00)**KSF(I))
DEV2=0.0D+00
DO 2 J=1,N

```

```

C *** FOR DATA CORRELATION, INSERT FUNCTION NEXT

```

```

T=X(J,1)
R=1.98D+00
PA=X(J,2)
PB=X(J,3)
PC=X(J,4)
PD=X(J,5)
K0=PAR1(1)
K1=PAR1(2)
K2=PAR1(3)
K3=PAR1(4)
K4=PAR1(5)
GO TO (200,201,202,203,204,205,206,207,208,209),NFUNC
200 FUNC=K0*PA**1.5*PB/(1.+K1*PA**.5)
GO TO 210
201 FUNC=K0*PA**1.5*PB/(1.+K1*PA**.5+K2*PB)
GO TO 210
202 FUNC=K0*DEXP(-K1/(R*T))*PA**.8624*PB**.3563
GO TO 210
203 FUNC=K0*DEXP(-K1/(R*T))*PA**K2*PB**.3563
GO TO 210
204 FUNC=K0*DEXP(-K1/(R*T))*PA**K2*PB**K3
GO TO 210
205 FUNC=K0*PA**2*PB/(1.D+00+K1*PA+K2*PB)**3
GO TO 210
206 FUNC=K0*PA*PB/(1.D+00+K1*PA)
GO TO 210
207 FUNC=K0*PA*PB/(1.D+00+K1*PB)
GO TO 210

```

VARIA ... (CONT'D)

```
208 FUNC=K0*PA*PB/(1.D+00+K1*PA**0.5+K2*PB)**3
    GO TO 210
209 FUNC=K0*PA**0.5*PB/(1.D+00+K1*PA**0.5+K2*PC)**2
210 CONTINUE
    DEV2=(Y(J)-FUNC)**2+DEV2
    2 CONTINUE
    CFT=FLOAT(N-1)
    VAR2=DEV2/DBLE(CFT)
    DO 3 I=1,P
    3 PAR1(I)=PAR1(I)*((10.D+00)**KSF(I))
    RETURN
    END
```

```

SUBROUTINE ROTAT(P,PAR1,PAR3,OV)
INTEGER P
DOUBLE PRECISION S,SO,DOG
DOUBLE PRECISION A(5,5),B(5,5),PAR1(5),PAR3(5),OV(5,5)
DO 1 I=1,P
DO 1 J=1,P
A(I,J)=0.0D+00
1 B(I,J)=0.0D+00
DO 2 I=1,P
DO 2 J=I,P
A(I,J)=PAR1(J)-PAR3(J)
2 B(I,J)=A(I,J)
SO=0.0D+00
DO 3 J=1,P
3 SO=SO+A(1,J)**2
S=SO**0.5
DO 4 J=1,P
4 OV(1,J)=A(1,J)/S
DO 5 I=2,P
MI=I-1
DO 6 K=1,MI
DOG=0.0D+00
DO 7 J=1,P
7 DOG=DOG+OV(K,J)*A(K,J)
DO 8 J=1,P
8 B(I,J)=B(I,J)-DOG*OV(K,J)
6 CONTINUE
SO=0.0 D+00
DO 9 J=1,P
9 SO=SO+B(I,J)**2
S=SO**0.5
DO 10 J=1,P
10 OV(I,J)=B(I,J)/S
5 CONTINUE
RETURN
END
```



```

C *****
C *
C *
C *
C *
C *
C *
C *
C *****

```

```

SUBROUTINE TORM (P,PAR1,KSF)
  INTEGER P
  DOUBLE PRECISION PAR1(5),PP1
  DIMENSION KSF(5)
  DO 1 I=1,P
1 KSF(I)=0
  DO 2 I=1,P
    PP1=DLOG10(PAR1(I))
    IF(PP1) 3,4,4
3 KSF(I)=PP1-1
    GO TO 2
4 KSF(I)=PP1
2 CONTINUE
  RETURN
  END

```

RATE=KO*PA**K1*PB**K2

ROTATION NO.	KO	K1	K2	VAR.
1	0.10002496E	01-0.639999950E	00-0.639999950E	00 0.22627755E-01
2	0.10588438E	01-0.14746153E	00-0.51145160E	00 0.92951711E-02
3	0.94246232E	00-0.10861639E	00-0.50649535E	00 0.89070033E-02
4	0.54032993E	00 0.25688149E-01	0.49180281E	00 0.76500689E-02
5	0.45946413E	00 0.66054567E-01	0.48761183E	00 0.73423767E-02
6	0.17780563E	00 0.35946899E	00-0.47230195E	00 0.53058322E-02
7	0.14025220E	00 0.41427910E	00-0.46946382E	00 0.50815558E-02
8	0.85500866E-01	0.55158269E	00-0.46351754E	00 0.46328371E-02
9	0.68352609E-01	0.60884606E	00-0.46170556E	00 0.45256838E-02
10	0.44538646E-01	0.72324728E	00-0.45819520E	00 0.44002439E-02
11	0.42340643E-01	0.73590564E	00-0.45780456E	00 0.43948218E-02
12	0.39956741E-01	0.75215160E	00-0.45720392E	00 0.43876636E-02
13	0.39835214E-01	0.75212383E	00-0.45574134E	00 0.43741110E-02
14	0.28830084E-01	0.74972152E	00-0.33517795E	00 0.33217323E-02
15	0.17283212E-01	0.74637591E	00-0.15421468E	00 0.20163590E-02
16	0.12049380E-01	0.74413347E	00-0.33480465E-01	0.13498924E-02
17	0.92625338E-02	0.74283039E	00 0.41873224E-01	0.10253358E-02
18	0.80077927E-02	0.74177467E	00 0.10207280E	00 0.81564474E-03
19	0.52661430E-02	0.73957180E	00 0.22302755E	00 0.49836258E-03
20	0.39349142E-02	0.73800194E	00 0.31636977E	00 0.36125094E-03
21	0.29696673E-02	0.73665773E	00 0.40241575E	00 0.31180970E-03
22	0.27531734E-02	0.73631668E	00 0.42535364E	00 0.30956120E-03
23	0.27531394E-02	0.73631203E	00 0.42535114E	00 0.30956120E-03

DATA REGENERATION

RUN NO.	DEVIATION	CALCULATED FUNC VALUE	OBSERVED FUNC VALUE	TEMP.	H2S	SO2	H2O
CA-1	-0.01	0.212	0.200	515.800	56.200	25.700	10.100
CA-2	0.00	0.219	0.219	516.300	57.700	26.400	8.900
CA-3	-0.00	0.228	0.223	515.800	58.900	28.000	6.900
CA-4	-0.00	0.228	0.218	515.800	59.500	27.400	6.600
CB-1	-0.00	0.125	0.118	515.000	26.000	28.200	5.700
CB-2	-0.01	0.133	0.122	515.200	27.700	29.200	3.700
CB-3	-0.01	0.136	0.122	515.000	28.500	29.400	3.000
CB-4	-0.01	0.141	0.127	515.200	29.500	29.900	2.200
CC-1	-0.01	0.075	0.059	514.800	12.900	29.100	3.100
CC-2	-0.01	0.078	0.065	514.900	13.500	29.500	2.600
CC-3	-0.01	0.080	0.065	514.800	13.800	29.500	2.200
CC-4	-0.02	0.083	0.061	514.800	14.400	29.900	1.600
CD-1	0.05	0.233	0.290	513.800	50.300	38.900	12.000
CD-2	0.03	0.255	0.290	513.900	54.900	41.000	7.600
CE-1	0.03	0.143	0.179	513.400	56.100	10.200	6.900
CE-2	0.01	0.154	0.170	513.700	59.000	11.200	4.800
CF-1	-0.00	0.089	0.085	514.300	12.800	43.200	3.300
CF-2	0.00	0.095	0.095	514.300	13.900	43.900	2.000
CG-1	-0.00	0.058	0.054	514.000	14.600	12.900	2.300
CG-2	-0.00	0.060	0.057	514.200	15.000	13.100	1.800
CH-1	0.01	0.149	0.159	513.200	25.400	44.300	6.500
CH-2	0.00	0.161	0.165	513.500	27.700	45.800	3.900
CK-1	0.00	0.094	0.096	513.600	28.400	12.500	3.900
CK-2	-0.00	0.099	0.096	513.600	29.600	13.100	2.600
CA	-0.01	0.258	0.241	515.800	65.800	30.800	0.000
CB	-0.02	0.150	0.126	515.100	31.700	30.900	0.000
CC	-0.02	0.091	0.068	514.800	16.100	30.600	0.000
CD	0.00	0.289	0.292	513.900	62.200	44.600	0.000
CE	0.00	0.176	0.178	513.600	63.200	13.500	0.000
CF	-0.00	0.106	0.102	514.300	16.000	44.700	0.000
CG	-0.00	0.067	0.061	514.100	16.900	14.000	0.000
CH	-0.01	0.181	0.169	513.400	31.800	47.500	0.000
CK	-0.01	0.110	0.096	513.600	32.200	14.500	0.000

```

C *****
C *
C *          MAINLINE CONLM
C *
C * THE PURPOSE OF THIS PROGRAM IS TO CALCULATE THE
C * VALUE OF THE ELEMENTS OF THE VARIANCE-COVARIANCE
C * MATRIX WHICH CORRESPONDS TO A PARTICULAR RATE
C * EXPRESSION WHICH HAS BEEN CORRELATED TO DATA
C * RESULTING IN A NORMALLY DISTRIBUTED ERROR OF FIT
C * INPUT DATA
C *   VX      - VECTOR OF RAW DATA TO WHICH RATE
C *             EXPRESSION WAS CORRELATED.
C *   M        - NUMBER OF PARAMETERS IN RATE EXPR'N
C *   NBANK    - DATA BANK NO. TO WHICH RATE EXPR'N
C *             WAS CORRELATED
C *   DES     - ALPHAMERIC DESCRIPTION OF RATE EXPR'N
C *
C *****

```

```

      DIMENSION X(100,5),Y(100),BK(100,6),DES(20),IBK(4,11)
      S,VX(6),A(6,6)
      1,D(6,6)
      DATA IBK/1,24,0,0,25,33,0,0,1,33,0,0,34,73,0,0,74,85,0
      S,0,34,85,0,0
      1,13,24,28,85,28,33,74,85,13,24,34,73,1,24,86,93,13,24
      S,34,73/
      DO 400 I=1,150
      READ(5,401)          (VX(J),J=1,6)
      DO 372 J=1,6
372  BK(I,J)=VX(J)
      IF(BK(I,1)-1.E+03)400,400,402
400  CONTINUE
401  FORMAT(2X,4X,F7.1,12X,F7.4,12X,4F7.1)

```

```

C *** READ IN CORRELATION DETAILS

```

```

402  READ(5,1) M,NBANK,NPAGE,NCOPY
      1 FORMAT(5I5)
      READ(5,2) (DES(J),J=1,20)
      2 FORMAT(20A4)
      NN1=IBK(1,NBANK)
      NN2=IBK(2,NBANK)
      NN3=IBK(3,NBANK)
      NN4=IBK(4,NBANK)
      J=0
253  DO 250 I=NN1,NN2
      J=J+1
      Y(J)=BK(I,2)
      X(J,1)=BK(I,1)
      DO 250 K=2,5
      JJ=K+2
250  X(J,K)=BK(I,JJ)

```

MAINLINE CONLM ... (CONT'D)

```

      IF(NN3) 251,251,252
252 NN1=NN3
      NN2=NN4
      NN3=-1
      GO TO 253
251 IF(NBANK-10) 2000,2000,2001
2001 NBANK=0
      NN1=86
      NN2=93
      GO TO 253
2000 N=J
      CALL VCOVM(X,Y,A,D,M,N)
      DO 5 I=1,M
      DO 5 J=1,M
5 D(I,J)=D(I,J)/(A(I,I)**0.5*A(J,J)**0.5)
      CALL NVERT(D,M)
      DO 6 I=1,M
6 VX(I)=1./A(I,I)**0.5
      DO 7 I=1,M
      DO 7 J=1,M
7 A(I,J)=D(I,J)*VX(I)*VX(J)
      DO 30 ML=1,NCOPY
      WRITE(6,28)
28 FORMAT(1H1,/////)
      WRITE(6,27) (DES(J),J=1,20)
27 FORMAT(10X,20A4)
      WRITE(6,29)
29 FORMAT(/,25X,'VARIANCE-COVARIANCE MATRIX FOR
$ PARAMETER ESTIMATES'
1)
      DO 30 I=1,M
30 WRITE(6,20)(A(I,J),J=1,M)
20 FORMAT(/,10X,6E15.5)
      CALL EXIT
      END

```

```

SUBROUTINE VCOVM(X,Y,A,D,M,N)
REAL K0,K1,K2,K3,K4,K5
DIMENSION A(6,6),D(6,6),G(6,6),GG(6),X(100,5),Y(100)
DATA K0,K1,K2,K3,K4,K5/0.0018,0.828,0.467,0.00215
S,0.757,0.0/
VAR2=0.
R=1.98
DO 10 I=1,M
DO 10 J=1,M
10 D(I,J)=0.0
DO 1 L=1,N
T=X(L,1)
PA=X(L,2)
PB=X(L,3)
PC=X(L,4)
PD=X(L,5)

```

C ***INSERT FUNCTION AND NECESSARY DERIVATIVES NEXT

```

FUNC=K0*PA**K1*PB**K2-K3*PC**K4
FFFF=K0*PA**K1*PB**K2
GG(1)=PA**K1*PB**K2
GG(2)=GG(1)*K0*ALOG(PA)
GG(3)=GG(1)*K0*ALOG(PB)
GG(4)=-PC**K4
GG(5)=-K3*PC**K4*ALOG(PC)
G(1,1)=0.
G(2,2)=FFFF*ALOG(PA)**2
G(3,3)=FFFF*ALOG(PB)**2
G(4,4)=0.
G(5,5)=-K3*PC**K4*ALOG(PC)**2
G(1,2)=FFFF/K0*ALOG(PA)
G(1,3)=FFFF/K0*ALOG(PB)
G(1,4)=0.
G(1,5)=0.
G(2,3)=FFFF*ALOG(PA)*ALOG(PB)
G(2,4)=0.0
G(2,5)=0.0
G(3,4)=0.0

```

SUBROUTINE VCO...(CONT'D)

```

G(3,5)=0.0
G(4,5)=-PC**K4*ALOG(PC)
DF=Y(L)-FUNC
VAR2=VAR2+DF**2

```

C

***SET UP MATRIX

```

DO 1 I=1,M
DO 1 J=I,M
IF(I-J) 3,2,1
2 D(I,I)=D(I,I)+DF*G(I,I)-GG(I)**2
GO TO 1
3 D(I,J)=D(I,J)+DF*G(I,J)-GG(I)*GG(J)
D(J,I)=D(I,J)
1 CONTINUE
VAR2=VAR2/FLOAT(N-1)
DO 4 I=1,M
DO 4 J=1,M
A(I,J)=-D(I,J)/VAR2
4 D(I,J)=A(I,J)
RETURN
END

```

CCCCCCCC

RATE=K0*PA**K1*PB**K2-K3*PC**K4

VARIANCE-COVARIANCE MATRIX FOR PARAMETER ESTIMATES

0.29193E-06	-0.19506E-04	-0.22390E-04	0.91998E-06	-0.83633E-04
-0.19506E-04	0.22640E-02	0.41944E-03	-0.63663E-04	0.58631E-02
-0.22390E-04	0.41944E-03	0.30867E-02	-0.38413E-04	0.33184E-02
0.91998E-06	-0.63663E-04	-0.38413E-04	0.10115E-04	-0.96161E-03
-0.83633E-04	0.58631E-02	0.33184E-02	-0.96161E-03	0.92246E-01

APPENDIX F
DEVELOPMENT OF A RATE EQUATION WITH MUTUALLY
RATE-CONTROLLING CATALYTIC PROCESS STEPS

F.1

As was discussed in Section 6.8.3, a rate equation was developed which featured mutually rate-controlling catalytic process steps. The development of this rate equation is given below. To simplify matters, the reverse reaction was ignored in this instance. In the development which follows; $A \equiv H_2S$, $B \equiv SO_2$, $L \equiv$ concentration of all sites on the catalyst, $P_A \equiv$ partial pressure of H_2S and $C_A \equiv$ concentration of H_2S adsorbed on the catalyst surface.

Adsorption of A:

$$r = K_A' \left(P_A C_L - \frac{C_A}{K_A} \right) \quad (F.1)$$

Adsorption of B:

$$r = K_B' \left(P_B C_L - \frac{C_B}{K_B} \right) \quad (F.2)$$

Surface Reaction of ads. A and ads. B ignoring reverse kinetics:

$$r = K_R' \frac{S}{L} C_A C_B \quad (F.3)$$

Ignore desorption of products:

From site inventory,

$$L = C_L + C_A + C_B \quad (F.4)$$

From these four equations, C_A , C_B and C_ℓ must be eliminated.

From equations (1) and (2)

$$C_A = \left(-\frac{r}{K_A} + P_A C_\ell \right) K_A \quad (F.5)$$

$$C_B = \left(-\frac{r}{K_B} + P_B C_\ell \right) K_B \quad (F.6)$$

These expressions for C_A and C_B may be substituted into the rate expression to give:

$$r = K_R' \frac{S}{L} K_A K_B \left(-\frac{r}{K_A} + P_A C_\ell \right) \left(-\frac{r}{K_B} + P_B C_\ell \right) \quad (F.7)$$

The C_ℓ may be eliminated from (7) by solving for it in (4) after replacing C_A and C_B by their expressions in (5) and (6). L is considered constant.

$$L = C + \left(-\frac{r}{K_A} + P_A C \right) K_A + \left(-\frac{r}{K_B} + P_B C \right) K_B \quad (F.8)$$

$$L = C_\ell - \frac{K_A}{K_A} r + P_A K_A C_\ell - \frac{K_B}{K_B} r + P_B K_B C_\ell$$

$$C = \frac{\left(L + \frac{K_A}{K_A} r + \frac{K_B}{K_B} r \right)}{\left(1 + P_A K_A + P_B K_B \right)} \quad (F.9)$$

Replacing equation (9) for C_L into equation (7) for rate results in:

$$r = K_R' \frac{S}{L} K_A K_B \left(-\frac{r}{K_A} + P_A \left[\frac{L + \frac{K_A}{K_A} r + \frac{K_B}{K_B} r}{1 + P_A K_A + P_B K_B} \right] \right) + \left(-\frac{r}{K_B} + P_B \left[\frac{L + \frac{K_A}{K_A} r + \frac{K_B}{K_B} r}{1 + P_A K_A + P_B K_B} \right] \right) \quad (10)$$

Let

$$D = 1 + K_A P_A + K_B P_B$$

$$K_0 = K_R' \frac{S}{L} K_A K_B$$

$$r = K_0 \left(-\frac{r}{K_A} + \frac{P_A}{D} \left(L + \frac{K_A}{K_A} r + \frac{K_B}{K_B} r \right) \right) + \left(-\frac{r}{K_B} + \frac{P_B}{D} \left(L + \frac{K_A}{K_A} r + \frac{K_B}{K_B} r \right) \right)$$

Let

$$M = \frac{K_A}{K_A} + \frac{K_B}{K_B}$$

$$\therefore r = K_0 \left(-\frac{r}{K_A} + \frac{P_A L}{D} + \frac{P_A M r}{D} \right) + \left(-\frac{r}{K_B} + \frac{P_B L}{D} + \frac{P_B M r}{D} \right) \quad (11)$$

This equation is now expanded:

$$\begin{aligned} \frac{r}{K_0} = & \frac{r^2}{K_A K_B} - \frac{P_B L r}{K_A D} - \frac{P_B M r^2}{K_A D} - \frac{P_A L r}{K_B D} + \frac{P_A P_B L^2}{D^2} + \frac{P_A P_B M_L r}{D^2} \\ & - \frac{P_A M r^2}{K_B D} + \frac{P_A P_B M_L r}{D^2} + \frac{P_A P_B M^2 r^2}{D^2} \end{aligned}$$

$$\begin{aligned}
 & r^2 \left(\frac{1}{K_A' K_B'} - \frac{P_B^M}{K_A' D} - \frac{P_A^M}{K_B' D} + \frac{P_A P_B^M}{D^2} \right) \\
 & + r \left(-\frac{1}{K_0} - \frac{P_B^L}{K_A' D} - \frac{P_A^L}{K_B' D} + 2 \frac{P_A P_B^M}{D^2} \right) \\
 & + \left(\frac{P_A P_B^L}{D^2} \right) = 0
 \end{aligned} \tag{12}$$

Equation (12) is of the form

$$Ar^2 + Br + C = 0$$

where

$$r = \frac{-B \pm \sqrt{B^2 - 4AC}}{2A}$$

Examination of equation (12) leads to the conclusion that the following parameters must be determined:

K_A'

K_B'

K_A

K_B

K_0

L

$$A = \left(\frac{1}{K_A K_B} - \frac{P_B^M}{K_A D} - \frac{P_A^M}{K_B D} + \frac{P_A P_B M^2}{D^2} \right)$$

$$B = \left(-\frac{1}{K_0} - \frac{P_B^L}{K_A D} - \frac{P_A^L}{K_B D} + 2 \frac{P_A P_B M^L}{D^2} \right)$$

$$C = \frac{P_A P_B L^2}{D^2}$$

PART II
APPENDIX

APPENDIX II-A
ONLINE DATA ACQUISITION AND REDUCTION PROGRAMS

H2S/SO2 PROJECT-RUN NUMBER 1

REACTOR DATA		LOOP RECORD DATA EXPRESSED IN PERCENT				
TEMPERATURES (DEG C)		RECORD NUMBER	AVERAGE RDG	MAXIMUM RDG	MINIMUM RDG	STD DEV
REACTOR BED	250.6	101	27.19	27.44	22.99	0.91E-01
REACTOR WALL	238.7	102	25.86	26.06	23.12	0.67E-01
FLUIDIZED BED	218.3	103	58.93	59.34	53.76	0.10E 00
GAS CHROM.	98.6	104	25.81	26.16	20.64	0.94E-01
REACTOR FEED	23.8	105	5.05	5.07	5.02	0.10E 00
ABSOLUTE PRESSURE (MM HG)						
REACTOR FEED	1160.3	106	43.54	44.97	14.72	0.11E 00
CATALYST BED	859.2	107	63.30	63.56	63.00	0.13E 00
FD RATE (SCFH)	6.012	108	27.29	27.70	27.02	0.70E-01

NUMBER OF DATA SAMPLES TAKEN WAS 22.

H2S/SO2 PROJECT-RUN NUMBER 1

STREAM DESCRIPTION	COMPUTER INTEGRATED PEAK AREAS		
	N2	H2S	SO2
FEED	0.61627E 05	0.14183E 06	0.18836E 06
FEED	0.56018E 05	0.14472E 06	0.18991E 06
PRODUCT	0.58984E 05	0.75039E 05	0.10861E 06
PRODUCT	0.61921E 05	0.72252E 05	0.11062E 06

MOLECULAR	FEED MOLE	PRODUCT MOLE
SPECIE	FRACTION	FRACTION
N2	0.8993	0.9458
H2S	0.0779	0.0410
SO2	0.0227	0.0130

RUN NUMBER 1

UNITS

MASS.....GRAM

PRESSURE.....MILLIMETERS OF MERCURY

TEMPERATURE.....DEGREES KELVIN

TIME.....HOUR

COMPOSITION.....MOLE PERCENT

VOLUME.....STANDARD CUBIC CENTIMETER

REACTION RATE...GM MOLES/(HR-GM OF CATALYST)

VOLUMETRIC FEED RATE MEASURED BY D/P CELL 221564.2

REACTION RATE OF H2S 0.3885 REACTION RATE OF SO2 0.1048

REACTION TEMPERATURE 244.60 REACTION PRESSURE 589.2

FEED H2S/SO2 RATIO 3.3808 PRODUCT H2S/SO2 RATIO 3.1105

CONVERSION OF H2S 49.85 CONVERSION OF SO2 45.49

MOLECULAR	FEED	PARTIAL PRESSURE	MATERIAL BALANCE	
SPECIE	COMPOSITION	IN REACTOR	FEED	PRODUCT
N2	89.93	775.1	8.894	8.894
H2S	7.79	33.9	0.779	0.390
SO2	2.27	10.8	0.230	0.125
H2O	0.00	26.0	0.000	0.299
SX	0.00	5.3	0.000	0.061
H2	0.00	7.7	0.000	0.089

DM001 ... (CONT'D)

LUN=9

```
C   *** BTNSW IS A SUBROUTINE WHICH READS THE STATUS (ON
C   *** OR OFF) OF THE COMMUNICATION BUTTONS AT THE
C   *** RECYCLE REACTOR

      CALL BTNSW(0,N1)
      CALL BTNSW(1,N2)
      CALL BTNSW(2,N3)
      INIT=2
      N=4*(N1-1)+2*(N2-1)+N3
      GO TO (2,3,4,5,6,7,8,9),N

C   *** TURN LOOP RECORDS ON

      2 DO 10 I=1,16
      10 CALL OPER(LPID(I))
         WRITE(LUN,101)
      101 FORMAT(5X,'****LOOP RECORDS ARE ON****',/)
         GO TO 100

C   *** TURN LOOP RECORDS OFF

      3 DO 11 I=1,16
      11 CALL NONOP(LPID(I))
         WRITE(LUN,300)
      300 FORMAT(5X,'****LOOP RECORDS ARE OFF****',/)
         GO TO 100

C   *** EXTRACT DATA FROM ACCUMULATION RECORDS

      4 DO 12 I=1,8
         CALL FNDLP(LPHEX(I),LPAD(I))
         LPI=LPAD(I)+4
         NWORD=LD(LPI)-7
         DO 12 J=1,NWORD
            LPI=LPAD(I)+6+J
         12 IDATA(I,J)=LD(LPI)
            WRITE(LUN,301)
      301 FORMAT(5X,'****DATA REDUCTION COMMENCING****',/)

C   *** PROCESS THE DATA

      LPI=LPAD(1)+4
      NWORD=LD(LPI)-7

C   *** CALCULATE MAXIMUM, MINIMUM, AVERAGE AND STANDARD
C   *** DEVIATION OF LOOP RECORD READINGS

      DO 14 I=1,8
```

DM001 ... (CONT'D)

```

    IAVG=0
    IMAX=0
    IMIN=32767
    DO 15 J=1,NWORD
    IAVG=IAVG+IDATA(I,J)/NWORD
    IF(IMAX-IDATA(I,J)) 16,16,17
16  IMAX=IDATA(I,J)
17  IF(IDATA(I,J)-IMIN) 18,18,15
18  IMIN=IDATA(I,J)
15  CONTINUE
    IDEV=0
    DO 19 J=1,NWORD
19  IDEV=IDEV+IABS(IDATA(I,J)-IAVG)**2
    IDEV=(IDEV/(NWORD-1))**0.5
    FDATA(1,I)=IAVG/327.67
    FDATA(2,I)=IMAX/327.67
    FDATA(3,I)=IMIN/327.67
    FDATA(5,I)=IDEV/327.67
14  CONTINUE
    WRITE(LUN,102) NWORD
102 FORMAT(10X,'NO. OF ANALOG DATA SAMPLES IS',I3,/)

C    *** ASSIGN SPAN TO AVERAGE RECORD READING

    DO 29 J=1,8
29  FDATA(4,J)=FDATA(1,J)*RGE(J)

C    *** CALCULATE TEMPERATURES

    DO 30 J=1,5
    JJ=J+5
30  FDATA(4,J)=T(J)+T(JJ)*FDATA(4,J)/100.

C    *** CALCULATE ABSOLUTE PRESSURES

    DO 31 J=1,2
    JJ=J+5
31  FDATA(4,JJ)=PRESS(1,J)+PRESS(2,J)*FDATA(4,JJ)

C    *** CALCULATE FEED FLOW RATE UNCORRECTED

    FDATA(4,8)=FDATA(1,8)**0.5
    DO 32 J=1,3
    FLO(J)=0.
    DO 32 I=1,3
32  FLO(J)=FLO(J)+DP(I,J)*FDATA(4,8)**(I-1)
    FD1=FDATA(4,6)
    CALL NIP(FLO,FD1,FD2)
    FDATA(4,8)=FD2
    FDATA(4,6)=FDATA(4,6)*760./14.7

```

DM001 ... (CONT'D)

```

      READ (80'1) NEXT, NRNS
      IPLAC=NEXT
      WRITE(80'IPLAC) (FDATA(4,J), LPID(J), FDATA(1,J), FDATA(2
      $, J), FDATA(3,
      1J), FDATA(5,J), J=1,8), NWORD
      NRNS=NRNS+1
      WRITE(LUN,103) NRNS
103  FORMAT(10X, 'NO. RUNS STORED IS', I3,/)
      NEXT=IPLAC
      FIND(80'1)
      WRITE(80'1) NEXT, NRNS

```

C *** PROCESS GAS CHROMATOGRAPH DATA

```

      NFD=0
      NPR=0
      READ(81'1) ICOUN
      READ(82'1) ILN30
      WRITE(82'ILN30) ICOUN
      DO 200 ICHRO=2, ICOUN
      READ(81'ICHRO) IFLAG, (CR(J), J=1,3)
      ILN30=ILN30+1
      WRITE(82'ILN30) IFLAG, (CR(J), J=1,3)
      IF(IFLAG) 200,200,201
201  IF(IFLAG-2) 202,203,200
202  NFD=NFD+1
      DO 204 I=1,3
204  FDCR(NFD,I)=CR(I)
      GO TO 200
203  NPR=NPR+1
      DO 205 I=1,3
205  PRCR(NPR,I)=CR(I)
200  CONTINUE

```

C *** OBTAIN FEED AND PRODUCT COMPOSITION

```

      CALL CHROM(FDCR, FDCOM, NFD)
      CALL CHROM(PRCR, PRCOM, NPR)
      ILN30=ILN30+1
      WRITE(82'ILN30) (FDCOM(J), J=1,3), (PRCOM(J), J=1,3)
      ILN30=ILN30+1

```

C *** DENSITY CORRECTION IN FEED FLOW RATE

```

      RON2=28./V(1)
      ROMIX=28./V(1)*FDCOM(1)+34./V(2)*FDCOM(2)+64./V(3)
      $*FDCOM(3)
      FDATA(4,8)=FDATA(4,8)*(RON2/ROMIX)**0.5

```

C *** TEMPERATURE CORRECTION IN FEED FLOW RATE

DM001 ... (CONT'D)

```

FDATA(4,8)=FDATA(4,8)*((FDATA(4,5)+273.)/295.)**0.5
PREN(1)=FDATA(4,6)
PREN(2)=FDATA(4,7)
PREN(3)=FDATA(4,8)
RTEMP=(FDATA(4,3)+FDATA(4,2)+FDATA(4,1))/3.
CALL BALAN (PREN,FDCOM,PRCOM,RTEMP,ILN30)
ILN30=ILN30+1
WRITE(82'1) ILN30

```

```

WRITE(LUN,302)
302 FORMAT(5X,'****DATA REDUCTION COMPLETED****',/)

```

C *** ZERO GC AREA STORAGE FILE

```

DO 40 I=1,30
40 WRITE(81'I) (IDUM(J),J=1,7)
WRITE(81'1) INIT,INIT
WRITE(LUN,303)
303 FORMAT(5X,'****GC AREA STORAGE FILE CLEARED****',/)
GO TO 100

```

C *** ZERO THE LOOP RECORDS

```

5 DO 13 I=1,8
13 CALL RSLP(LPHEX(I),K)
WRITE(LUN,304)
304 FORMAT(5X,'****LOOP RECORDS ZEROED****',/)
GO TO 100

```

C *** ZERO STORAGE FILE ANALOG MSMT. DATA

```

6 DO 41 I=1,9
41 WRITE(80'I) (IDUM(J),J=1,100)
WRITE(80'1) INIT
WRITE(LUN,305)
305 FORMAT(5X,'****ANALOG MSMT. DATA FILE CLEARED****',/)
GO TO 100

```

C *** ZERO KINETIC DATA STORAGE FILE

```

7 DO 42 I=1,200
42 WRITE(82'I) (IDUM(J),J=1,12)
WRITE(82'1) INIT
WRITE(LUN,306)
306 FORMAT(5X,'****KINETIC DATA STORAGE FILE CLEARED****',
S/)
GO TO 100
8 CONTINUE
9 CONTINUE

```

II-A-9

DM001

... (CONT'D)

100 CALL RESET
CALL VIAQ
END

```

C *****
C *
C *
C *
C *
C *
C *
C *
C *
C *
C *
C *****

```

```

SUBROUTINE CHROM (CR,COMP,N)
DIMENSION COMP(7),CR(6,3),ATTEN(3),CHSN2(2,3),CSON2(2)
DATA CHSN2/0.06201,0.5824,0.02324,0.71151,0.02236
S,0.79005/
DATA CSON2/-0.10977,1.00671/
DATA ATTEN/-14.,9.8,10.3/
XN=N
READ(82'1) ILN30,ATTEN(2)
DO 1 J=1,3
CR(6,J)=0.
DO 1 I=1,N
1 CR(6,J)=CR(6,J)+CR(I,J)*((21.-2.*ATTEN(J))/XN
IF(9.6-ATTEN(2))3,4,5
3 M1=1
GO TO 6
4 M1=2
GO TO 6
5 M1=3
6 HNRAC=CHSN2(1,M1)/100.+CHSN2(2,M1)*CR(6,2)/CR(6,1)
SNRAC=CSON2(1)/100.+CSON2(2)*CR(6,3)/CR(6,1)
COMP(1)=1./(1.+HNRAC+SNRAC)
COMP(2)=1.-COMP(1)-SNRAC*COMP(1)
COMP(3)=1.-COMP(1)-HNRAC*COMP(1)
RETURN
END

```

```

C *****
C *
C *          BALAN
C *
C * BALAN CALCULATES THE MATERIAL BALANCE ACROSS THE
C * RECYCLE REACTOR AND FROM THIS OBTAINS REACTION RATE
C * AND PARTIAL PRESSURES. THIS INFORMATION IS STORED
C * ON A DISK FILE FOR LATER RECOVERY.
C *
C *****

```

```

SUBROUTINE BALAN (PRESS,FDCOM,PRCOM,RTEMP,ILN30)
DIMENSION PRCOM(7),FDCOM(7),BAL(2,7),PRESS(3),V(3)
DATA V/22403.60,22144.24,21889.30/
WC=1.
DO 10 J=1,3
10 BAL(1,J)=FDCOM(J)*PRESS(3)/V(J)*28317.016
BAL(2,1)=BAL(1,1)
BAL(2,2)=BAL(2,1)*(PRCOM(2)*V(1)/PRCOM(1)/V(2))
BAL(2,3)=BAL(2,1)*(PRCOM(3)*V(1)/PRCOM(1)/V(3))
BAL(2,4)=(2.*(BAL(1,3)-BAL(2,3))+BAL(1,2)-BAL(2,2))/2.
BAL(2,5)=BAL(1,2)+BAL(1,3)-BAL(2,2)-BAL(2,3)
RTEMP=RTEMP+273.
PRS=PRESS(2)/760.*BAL(2,5)/8.
22 CALL FREM(PRS,RTEMP,XS)
PRS1=PRESS(2)/760.*BAL(2,5)/XS
IF(ABS((PRS-PRS1)/PRS1)-0.005) 20,20,21
21 PRS=PRS1
GO TO 22
20 BAL(2,5)=BAL(2,5)/XS
BAL(2,6)=BAL(1,2)-BAL(2,2)-BAL(2,4)
RXH2S=(BAL(1,2)-BAL(2,2))/WC
RXSO2=(BAL(1,3)-BAL(2,3))/WC
FDRAT=BAL(1,2)/BAL(1,3)
H2SCN=(BAL(1,2)-BAL(2,2))/BAL(1,2)*100.
SO2CN=(BAL(1,3)-BAL(2,3))/BAL(1,3)*100.
PRRAT=BAL(2,2)/BAL(2,3)
PRESS(3)=PRESS(3)*28317.016
TOT=0.
DO 12 J=1,5
FDCOM(J)=FDCOM(J)*100.
12 TOT=TOT+BAL(2,J)
DO 13 J=1,5
13 PRCOM(J)=BAL(2,J)*PRESS(2)/TOT
RTEMP=RTEMP-273.
WRITE(82,ILN30) PRESS(3),RXH2S,RXSO2,RTEMP,PRESS(2)
S,FDRAT
ILN30=ILN30+1
WRITE(82,ILN30) PRRAT,H2SCN,SO2CN
DO 100 J=1,6
ILN30=ILN30+1
100 WRITE(82,ILN30) FDCOM(J),PRCOM(J),BAL(1,J),BAL(2,J)

```

II-A-12

BALAN

... (CONT'D)

RETURN
END

```

*****
*
*               SUBROUTINE FREM
*
* THIS SUBROUTINE AND ASSOCIATED SUBROUTINES GSET,
* GAUSS, FREN AND NEZE ARE USED FOR DETERMINING THE
* AVERAGE MOLECULAR WEIGHT OF SULFUR AT THE TEMPER-
* ATURE AND PRESSURE OF THE EXPERIMENTAL RUN. THESE
* SUBROUTINES WILL NOT BE LISTED HERE SINCE THEY
* ALREADY APPEAR IN APPENDIX B OF PART I.
*
*****

```

```

SUBROUTINE FREM(PRESS,T,XS)
END

```

```

C *****
C *
C *                               DM002
C *
C * DM002 IS A DISK RESIDENT PROCESS CORELOAD WHICH IS *
C * QUEUED BY PICO5. IS PURPOSE IS TO SUPERVISE THE *
C * GAS CHROMATOGRAPH PEAK AREA DETECTION ROUTINES. *
C * THE PEAK AREAS ARE TRANSFERRED TO FILE 81 FROM *
C * WHICH THEY ARE LATER RECOVERED BY DM001 FOR DATA *
C * REDUCTION. *
C *
C *****

```

```

EXTERNAL DMGC
DIMENSION LPID(2),IDUM(7),LPHEX(2)
DATA LPID/0109,0119/
DATA IDUM/7*0/
DATA LPHEX/20109,Z0119/
DEFINE FILE 81(30,7,U,IDM)
DEFINE FILE 82(200,12,U,KDM)
LUN=9
INIT=2
CALL BTNSW(0,N1)
CALL BTNSW(1,N2)
CALL BTNSW(2,N3)
N=4*(N1-1)+2*(N2-1)+N3
GO TO(1,1,1,2,3,4,5,6),N
1 READ(81'1) ICOUN,IFINC
WRITE(81'1) IFINC)N
IFINC=IFINC+1
WRITE(81'1) ICOUN,IFINC
WRITE(LUN,53) N
53 FORMAT(/,5X,'***** CHROMATOGRAM LABELLED',I2,' *****')
GO TO 7
2 DO 10 I=1,30
10 WRITE(81'I) (IDUM(J),J=1,7)
WRITE(81'1) INIT,INIT
WRITE(LUN,54)
54 FORMAT(/,5X,'***** GC FILE INITIALIZED *****')
GO TO 7
3 ATT=9.8
GO TO 8
4 ATT=9.6
GO TO 8
5 ATT=9.4
8 READ(82'1) ILN30
WRITE(82'1) ILN30,ATT
WRITE(LUN,55) ATT
55 FORMAT(/,5X,'***** H2S ATTENUATION =',F4.1,' *****')
GO TO 7
6 CALL DOUT1(10,9,1)
CALL TIME (IHR,IMIN,ISEC)

```

DM002 ...(CONT'D)

```
CALL RSLP(LPHEX(2),K)
DO 11 I=1,2
11 CALL OPER(LPID(I))
CALL DEFER
CALL QUEUE (DMGC,5,0,9,4500)
12 CALL TIME(JHR,JMIN,JSEC)
ITIME=3600*(JHR-IHR)+60*(JMIN-IMIN)+JSEC-ISEC
IF (15-ITIME) 13,13,12
13 CALL DOUT1(10,9,0)
WRITE(LUN,51)
51 FORMAT(/,10X'*** GC NOW BEING SCANNED ***')
7 CONTINUE
CALL RESET
CALL VIAQ
END
```



```

*****
*
*                               DMGC
*
*   DMGC IS A DISK RESIDENT PROCESS CORELOAD WHICH IS
*   QUEUED BY COMMAND FROM DM002. ITS PURPOSE IS TO
*   SUPERVISE THE GAS CHROMATOGRAPH PEAK AREA DETECTION
*   AND DETERMINATION SUBROUTINES. THE PEAK AREAS ARE
*   TRANSFERRED TO DISK FILE 81 FROM WHICH THEY ARE
*   LATER RECOVERED BY DM001 FOR KINETIC DATA PROCESS-
*   ING AND REDUCTION.
*
*****
```

```

INTEGER RECSZ,DKIN,DKOUT,ERR1,ERR2
DIMENSION LPID(2),LPHEX(2),IDATA(500),START(5),END(5)
$ ,NTIME(3),ARA

```

```
1(3)
DEFINE FILE 81(30,7,U,IDM)
DEFINE FILE 83(64,320,U,IDO)
DEFINE FILE 84(2,320,U,JDO)
DATA LPHEX/Z0109,Z0119/
DATA LPID/0109,0119/
DATA END/102.,240.,430.,0.,0./
DATA START/55.,102.,170.,0.,0./
LPDI=LPHEX(2)
NOPTS=450
RECSZ=320
NRECS=2
DKIN=83
DKOUT=84
LUN=9
NUMBR=3
CALL NONOP(LPID(2))
CALL NONOP(LPID(1))
```

C EXTRACT DATA FROM BUFFER USING GBDAT

```

CALL NIGBD (LPDI,NOPTS,RECSZ,NRECS,DKIN,DKOUT,NTIME
S,ERR1,ERR2)
WRITE (LUN,23) ERR1,ERR2
23 FORMAT (20X,'ERR1 =',I6/20X,'ERR2 =',I6////)

```

C ZERO ACCUMULATION RECORD

```

CALL RSLP(LPHEX(2),K)
IF (ERR2-10) 2,2,7
2 WRITE (LUN,3)
3 FORMAT (10X,'***** NUMBER OF DATA LESS THAN 10 **
S*****'//)
GO TO 8
7 CONTINUE

```

DMGC ... (CONT'D)

```
READ(84'1) (IDATA(J),J=1,320)
READ(84'2) (IDATA(J),J=321,450)
CALL PKARA (START,END,IDATA,NOPTS,NUMBR,ARA)
READ(81'1) ICOUN
IDUMY=0
WRITE(81'1) ICOUN, IDUMY, ARA
ICOUN=ICOUN+1
WRITE(81'1) ICOUN
8 CONTINUE
CALL VIAQ
END
```

```

C *****
C *
C *
C *
C *
C *
C *
C *
C *
C *****

SUBROUTINE PKARA (START,END,Y,NPTS,NUMBR,ARA)
  INTEGER Y(1)
  DIMENSION AREA(5),START(1),END(1),BCARA(5),ARA(3)
  S,NG(3)
  COMMON IEND(5),NPEAK,ISTRT(5),NAPEX(5),BSAR(5)
  H=1.
  LUN=9
  NPEAK=0
  CALL PKFND (Y,NPTS,NCOND)

C   IS THERE ANY PEAK FOUND BY SUBROUTINE LIUPK
      IF (NPEAK) 250,250,1

C   NO PEAK WERE FOUND

250 WRITE(LUN,251) NPEAK
251 FORMAT(5X,'** NO PEAKS FOUND IN DATA, NPEAK=',I5,' **'
  $///)
      GO TO 8
1 CONTINUE
      IF (NCOND) 33,33,34

C   END OF DATA DURING PEAK ELUTION

34 WRITE (LUN,35)
35 FORMAT (15X,'*--* END OF DATA DURING PEAK ELUTION *--'
  $-* '///)
33 CONTINUE

C   SOME PEAKS HAD BEEN FOUND

      DO 120 K=1,NPEAK
      AREA(K)=0.

C   APEX IS REQUIRED FOR 1ST AND 2ND PEAKS

      IF (K-2) 4,4,5
5 L=IEND(K)-ISTRT(K)
      IAPFL=3
      AR1=0.
      X=FLOAT(L)/2.

```

PKARA ... (CONT'D)

L=L/2

C CHECK NO. OF INTERVALS EVEN OR ODD

IF (X-L) 22,22,21

C ODD NUMBER OF INTERVALS ADD ONE INTERVAL TO PEAK

21 IEND(K)=IEND(K)+1

22 IBGN=ISTRT(K)+1

JEND=IEND(K)-1

GO TO 20

4 ISTR=ISTRT(K)

L=IEND(K)-ISTRT(K)

CALL APEX (L,Y,APARA,ISTR,IFL,IBF)

L=IFL-ISTRT(K)

IAPFL=0

JEND=IFL

IBGN=ISTRT(K)

GO TO 6

16 L=IEND(K)-IBF

IBGN=IBF

JEND=IEND(K)

C CHECK IF NUMBER INTERVALS EVEN OR ODD

6 X=FLOAT(L)/2.

L=L/2

IF(X-L)20,20,10

C ODD NUMBER OF INTERVALS ADD ONE INTERVAL TO PEAK

10 IF(IAPFL) 12,12,11

11 JEND=IEND(K)-1

GO TO 20

12 IBGN=ISTRT(K)+1

C SIMPSONS RULE INTEGRATION

20 JJEND=JEND-2

DO 40 I=IBGN,JJEND,2

40 AREA(K)=AREA(K)+Y(I)+4.*Y(I+1)+Y(I+2)

AREA(K)=AREA(K)*H/3.

IF (K-2) 126,126,127

126 CONTINUE

IF (IAPFL) 14,14,15

14 CONTINUE

AR1=AREA(K)

AREA(K)=0.

IAPFL=1

PKARA ...(CONT'D)

```
      GO TO 16
15  CONTINUE
      AR2=AREA(K)
      AR3=AR1+AR2+APARA
C    BASE-LINE CORRECTED AREA

      BCARA(K)=AR3-BSAR(K)
      CONST=BCARA(K)/FLOAT(NAPEX(K))
      GO TO 120
127 CONTINUE

C    BASE-LINE CORRECTED AREA

      BCARA(K)=AREA(K)-BSAR(K)
      CONST=BCARA(K)/FLOAT(NAPEX(K))
120 CONTINUE

C    CHECK IF NO. OF PEAKS FOUND = NO. SPECIFIED

      IF (NUMBR-NPEAK) 122,125,122
122 CONTINUE
      WRITE (LUN,90)
90  FORMAT (15X,'*-*-* NUMBER OF PEAKS FOUND DIFF. FROM
      $ SPECIFIED *-*-
      1*'/)
125 CONTINUE
8   CONTINUE
      RETURN
      END
```

```

C *****
C *
C *
C *
C *
C *
C *
C *
C *
C *
C *
C *****
C
C SUBROUTINE PKFND (Y,NPTS,NCOND)
C   INTEGER Y(1)
C   DIMENSION NEN(5),NST(5)
C   COMMON IEND(5),NPEAK,ISTR(5),NAPEX(5),BSAR(5)
C   DATA DBST,DBEND,ITEST/3.0,1.0,3/
C   DATA DRV1,DRV1A,ICFST,ICFED,NGHG/0.,0.,0,0,0/
C   NPEAK=0
C   H=1.
C   NCOND=0
C   LUN=9
C   BSAR(1)=0.
C   BSAR(2)=0.
C   BSAR(3)=0.
C   BSAR(4)=0.
C   BSAR(5)=0.
C   NDATA=NPTS-4
C   DO 200 I=3,NDATA
C     DRV1B=DRV1
C
C     COMPUTE FIRST DERIVATIVE AT Y(I)
C
C     DRV1=DRV1A
C
C     COMPUTE FIRST DERIVATIVE AT Y(I+1)
C     SEVEN POINT LEAST SQUARES ESTIMATE OF FIRST DERIVATIVE
C
C     
$$DRV1A = 3. * (Y(I+4) - Y(I-2)) + 2. * (Y(I+3) - Y(I-1)) +$$

C     
$$1Y(I+2) - Y(I)$$

C     DRV1A=DRV1A/(28.*H)
C
C     IS PEAK IN PROGRESS
C
C     IF(NCOND)10,10,40
C
C     PEAK IS NOT PROGRESS
C     CHECK FIRST DERIVATIVE FOR PEAK START
C
C     IF(DRV1-DBST) 200,20,20
C
C     CONFIRM PEAK START ITES TIMES

```

PKFND ... (CONT'D)

```
20   ICFST=ICFST+1
25   IF(ICFST-ITEST)200,30,30

C     PEAK HAS STARTED

30   NCOND=1

C     INCREMENT PEAK COUNTER

      NPEAK=NPEAK+1
      IF (NPEAK-5) 300,300,301
300  CONTINUE

C     SAVE INDEX OF STARTING POINT

      ISTRT(NPEAK)=I-ITEST+1
      IIST=ISTRT(NPEAK)
      NST(NPEAK)=Y(IIST)
      ICFST=0
      GO TO 200

C     CHECK FOR PEAK END
C     HAS FIRST DERIVATIVE GONE +VE TO -VE

40   IF(NGHG)50,50,70
50   IF(DRV1)60,200,200

C     FIRST DERIVATIVE HAS GONE +VE TO -VE

60   NGHG=1

C     SAVE INDEX OF PEAK HEIGHT

      IF (Y(I)-Y(I-1)) 41,45,45
41   NAPEX(NPEAK)=Y(I-1)
      IMAX=I-1
      GO TO 70
45   NAPEX(NPEAK)=Y(I)
      IMAX=I

C     CHECK FOR PEAK END

70   IF(DRV1+DBEND)200,80,80

C     CONFIRM PEAK END

80   ICFED=ICFED+1

C     CHECK FOR START OF NEW PEAK
```

PKFND ... (CONT'D)

```

      IF (DRV1-DBST) 77,75,75
75    ICFST=ICFST+1
      GO TO 78
77    ICFST=0
78    IF (ICFED-ITEST) 200,87,87

C     PEAK END
C     SAVE INDEX OF END POINT

      87 IEND(NPEAK)=I
        NEN(NPEAK)=Y(I)
        NFRNT=NAPEX(NPEAK)-NST(NPEAK)
        NBK=NAPEX(NPEAK)-NEN(NPEAK)
        L=IEND(NPEAK)-ISTR(NPEAK)

C     CHECK IF THE DETECTED PEAK IS NOISE

      IF (L-10) 33,33,22
33    NPEAK=NPEAK-1
      GO TO 37
22    CONTINUE

C     CHECK IF THE DETECTED PEAK IS BASELINE DRIFT

      IF (NFRNT-500) 31,31,38
38    IF (NBK-500) 31,31,35

C     YES      DECREASE PEAK COUNTER

31    NPEAK=NPEAK-1
      GO TO 37
35    CONTINUE
      IF (NPEAK) 202,202,201
201   CONTINUE
      BSAR(NPEAK)=(FLOAT(NEN(NPEAK)+NST(NPEAK)))
      S*(FLOAT(IEND(NPEAK)-ISTR
      1T(NPEAK)))/2.

C     CHECK FOR IMMEDIATE START OF NEW PEAK

37    CONTINUE
      IF (ICFST) 88,88,25
88    ICFED=0
      NCOND=0
      NGHG=0
      ICFST=0
200   CONTINUE
      GO TO 400
202   CONTINUE
      WRITE (LUN,203)

```


PKFND ... (CONT'D)

```
203 FORMAT (10X,'***** NPEAK=0 *****'///)
    GO TO 400
301 CONTINUE
    WRITE (LUN,302) NPEAK
302 FORMAT (10X,'NPEAK =',I5///)
400 CONTINUE
    RETURN
    END
```

```

C *****
C *
C *
C *
C *
C *
C *
C *
C *
C *****

```

APEX

```

* APEX IS USED TO ANALYTICALLY CALCULATE THE AREA OF *
* THE APEX OF SHARP PEAKS. *

```

```

SUBROUTINE APEX (NPTS,Y,APARA,ISTR,IFL,IBF)
  INTEGER Y(1)
  DIMENSION SM(8),X(11)
  DATA X/0.,1.,2.,3.,4.,5.,6.,7.,8.,9.,10./
  DO 20 I=1,8
20 SM(I)=0.
  M=3
  ISTRT=ISTR+1
  NPT=NPTS+ISTR
  DO 1 I=ISTR,NPT
  DER2=Y(I)-Y(I-1)
  DER3=Y(I+1)-Y(I)
  IF (DER3) 1,1,2
2 IF (DER3-DER2) 3,3,1
3 DER4=Y(I+2)-Y(I+1)
  IF (DER4) 5,1,1
5 IF (DER4+DER2-2.*DER3) 6,6,7
6 IBF=I+1
  IFL=I
  GO TO 8
7 IFL=I+1
  IBF=I+2
  GO TO 8
1 CONTINUE
8 DO 9 I=1,M
  J=I+M
  J1=IFL-I+1
  J2=IFL-M+I
  J3=IBF+I-1
  SM(1)=SM(1)+X(I)
  SM(2)=SM(2)+Y(J1)
  SM(3)=SM(3)+X(I)*Y(J2)
  SM(4)=SM(4)+X(J)
  SM(5)=SM(5)+Y(J3)
  SM(6)=SM(6)+X(J)*Y(J3)
  SM(7)=SM(7)+X(I)**2
  SM(8)=SM(8)+X(J)**2
9 CONTINUE
  A1F=(M*SM(3)-SM(1)*SM(2))/(M*SM(7)-SM(1)**2)
  A1B=(M*SM(6)-SM(4)*SM(5))/(M*SM(8)-SM(4)**2)
  A0F=(SM(7)*SM(2)-SM(3)*SM(1))/(M*SM(7)-SM(1)**2)
  A0B=(SM(8)*SM(5)-SM(6)*SM(4))/(M*SM(8)-SM(4)**2)
  APARA=(A0F-A0B)**2/(2.*(A1B-A1F))-X(M)*(A0F+X(M)*A1F

```

APEX

...(CONT'D)

```
$/2.)+X(M+1)*(A  
UOB+X(M+1)*A1B/2.)  
RETURN  
END
```

```

C *****
C *
C *
C *
C * THE PURPOSE OF DM006 IS TO EXTRACT PROCESSED FROM *
C * FILES AND WRITE IT OUT ON THE LINE PRINTER OR CARDS*
C * FOR FUTURE MACHINE REPRODUCTION.
C *
C *****

```

```

      DEFINE FILE 80(9,100,U,IPLAC)
      DEFINE FILE 82(200,12,U,KDM)
      DIMENSION COL1(8),ICOL2(8),COL3(8),COL4(8),COL5(8)
      S,COL6(8),NRUN(8)
      DIMENSION FDCOM(7),PRCOM(7),BAL(2,7),PRESS(3),SNAM(2
      S,3)
      DATA SNAM/'FEED',' ','PROD','UCT ','DELE','TED '/
      LUN=6
      ILN30=2
      IPLAC=2
      READ(80,1) NEXT,NRNS
      READ(5,1) NCOPY
10  READ(5,1) (NRUN(J),J=1,NRNS)
      1 FORMAT(10I5)
      READ(5,4) WC
      4 FORMAT(5F10.5)
      DO 2 I=1,NRNS
      READ(80,IPLAC) (COL1(J),ICOL2(J),COL3(J),COL4(J)
      S,COL5(J),COL6(J),
      1J=1,8),NWORD
      READ (5,1) NDUM
      WRITE(5,7) NRUN(I)
      WRITE(5,6) (COL1(J),ICOL2(J),COL3(J),COL4(J)
      S,COL5(J),COL6(J),
      1J=1,8)
      6 FORMAT(F10.5,I5,4F10.5)
      WRITE(5,7) NWORD
      7 FORMAT(I5)
      DO 8 K=1,NCOPY
      WRITE(6,3)
      3 FORMAT('1')
      WRITE(6,9) NRUN(I)
      9 FORMAT(////,25X,'H2S/SO2 PROJECT-RUN NUMBER',I3)
      WRITE(LUN,21)
21  FORMAT(///,13X,'REACTOR DATA          LOOP RECORD DATA
      S EXPRESSED IN PE
      1RCENT'//)
      WRITE(LUN,22)
22  FORMAT(10X,'TEMPERATURES (DEG C) RECORD AVERAGE
      S MAXIMUM MINIMUM ST
      1D DEV'/31X,'NUMBER      RDG      RDG      RDG'//)
      WRITE(6,23) (COL1(J),ICOL2(J),COL3(J),COL4(J)

```

DM006 ... (CONT'D)

```

$ ,COL5(J),COL6(J),
1J=1,5)
23 FORMAT(11X,'REACTOR BED 'F6.1,2X,I4,3(2X,F6.2),E9.2//
1      ,11X,'REACTOR WALL 'F6.1,2X,I4,3(2X,F6.2),E9.2//
1      ,11X,'FLUIDIZED BED'F6.1,2X,I4,3(2X,F6.2),E9.2//
1      ,11X,'GAS CHROM. 'F6.1,2X,I4,3(2X,F6.2),E9.2//
1      ,11X,'REACTOR FEED 'F6.1,2X,I4,3(2X,F6.2),E9.2//
$      )
      WRITE(6,24)      (COL1(J),ICOL2(J),COL3(J),COL4(J)
$ ,COL5(J),COL6(J),
1J=6,8)
24 FORMAT(10X,'ABSOLUTE PRESSURE (MM HG) '//11X,'REACTOR
$ FEED 'F6.1,2
1X,I4,3(2X,F6.2),E9.2//11X,'CATALYST BED 'F6.1,2X,I4
$ ,3(2X,F6.2),E9
1.2///10X,'FD RATE (SCFH) ',F7.3,1X,I4,3(2X,F6.2),E9.2)
      WRITE(LUN,36) NWORD
36 FORMAT(////,10X,'NUMBER OF DATA SAMPLES TAKEN WAS',I3
$ ,'.')
8 CONTINUE
      READ(82'ILN30) ICOUN
      ICOUN=ICOUN-2
      DO 12 ICHRO=1,ICOUN
      ILN30=ILN30+1
12 READ(82'ILN30) ICOL2(ICHRO),COL1(ICHRO),COL3(ICHRO)
$ ,COL4(ICHRO)
      ILN30=ILN30+1
      READ(82'ILN30) (FDCOM(L),L=1,3),(PRCOM(L),L=1,3)
      DO 16 K=1,NCOPY
      WRITE(6,3)
      WRITE(6,14) NRUN(I)
14 FORMAT(////,25X,'H2S/SO2 PROJECT-RUN NUMBER',I3)
      WRITE(6,15)
15 FORMAT(///,13X,'STREAM',12X,'COMPUTER INTEGRATED PEAK
$ AREAS'//10X,
1'DESCRIPTION',10X,'N2',11X,'H2S',11X,'SO2'//)
      DO 17 L=1,ICOUN
      LK=ICOL2(L)
17 WRITE(6,18) (SNAM(J,LK), J=1,2),COL1(L),COL3(L)
$ ,COL4(L)
18 FORMAT(12X,2A4,6X,3(E11.5,3X)//)
      WRITE(6,35) (FDCOM(L),PRCOM(L),L=1,3)
35 FORMAT(///,15X,'MOLECULAR'      ,6X,'FEED MOLE',6X
$ , 'PRODUCT MOLE'
1,///17 X,'SPECIE',8X,'FRACTION',8X,'FRACTION'//18X,'N2'
$ ,10X,F6.4,11
2X,F6.4//18X,'H2S',9X,F6.4,11X,F6.4//18X,'SO2',9X,F6.4
$ ,11X,F6.4)
16 CONTINUE
      WRITE(5,7) ICOUN

```

DM006 ... (CONT'D)

```
DO 19 L=1, ICOUN
  LK=ICOL2(L)
19 WRITE(5,20) (SNAM(J,LK), J=1,2), COL1(L), COL3(L), COL4(L)
20 FORMAT(2A4,3(E11.5,3X))
  ILN30=ILN30+1
  READ(82, ILN30) PRESS(3), RXH2S, RXSO2, RTEMP, PRESS(2)
  $, FDRAT
  RXH2S=RXH2S/WC
  RXSO2=RXSO2/WC
  ILN30=ILN30+1
  READ(82, ILN30) PRRAT, H2SCN, SO2CN
  WRITE(5,26) (FDCOM(L), L=1,3), (PRCOM(L), L=1,3)
  WRITE(5,26) PRESS(3), RXH2S, RXSO2, RTEMP, PRESS(2), FDRAT
  WRITE(5,26) PRRAT, H2SCN, SO2CN
26 FORMAT(6F10.5)
  DO 30 JK=1,6
  ILN30=ILN30+1
  READ(82, ILN30) FDCOM(JK), PRCOM(JK), BAL(1,JK), BAL(2,JK)
30 WRITE(5,31) FDCOM(JK), PRCOM(JK), BAL(1,JK), BAL(2,JK)
31 FORMAT(4F10.5)
  KRUN=NRUN(I)
  DO 25 K=1, NCOPY
  CALL OUTPT(KRUN, RXH2S, RXSO2, RTEMP, PRESS, PRCOM, FDCOM
  $, FDRAT, PRRAT, BA
  1L, H2SCN, SO2CN)
25 CONTINUE
  ILN30=ILN30+1
  2 CONTINUE
  CALL EXIT
  END
```

C
C
C
C
C
C
C
C

```

*****
*
*                               OUTPT
*
* OUTPT HAS THE SOLE FUNCTION OF WRITING OUT THE
* CALCULATED RESULTS ON THE LINE PRINTER
*
*****

```

```

SUBROUTINE OUTPT (NRUN,RXH2S,RXS02,RTEMP,PRESS,PRCOM
$ ,FDCOM,FDRAT,P
1RRAT,BAL,H2SCN,SO2CN)
  DIMENSION PRESS(3),PRCOM(7),FDCOM(7),BAL(2,7)
  WRITE(6,5)
5  FORMAT('1')
  WRITE(6,1) NRUN
1  FORMAT(////10X,'RUN NUMBER',I3, /37X,'UNITS'//18X
$ , 'MASS.....'
1  ..GRAM'//18X,'PRESSURE.....MILLIMETERS OF MERCURY' /
$ /18X,'TEMPER
1  ATURE.....DEGREES KELVIN'//18X,'TIME.....HOUR' /
$ /18X,'COMPOS
1  ITION.....MOLE PERCENT'//18X,'VOLUME.....STANDARD
$ CUBIC CENTI
1  METER'//18X,'REACTION RATE...GM MOLES/(HR-GM OF
$ CATALYST)'//)
  WRITE(6,3) PRESS(3)
3  FORMAT(10X,'VOLUMETRIC FEED RATE MEASURED BY D/P CELL'
$ ,11X,F9.1/)
  WRITE(6,2) RXH2S,RXS02,RTEMP,PRESS(2)
2  FORMAT(10X,'REACTION RATE OF H2S',F7.4,5X , 'REACTION
$ RATE OF S02
1  'F7.4//10X,'REACTION TEMPERATURE',F7.2,5X , 'REACTION
$ PRESSURE
1  'F7.1/)
  WRITE(6,6) FDRAT,PRRAT,H2SCN,SO2CN
6  FORMAT(10X,'FEED H2S/SO2 RATIO ' ,F7.4,5X , 'PRODUCT
$ H2S/SO2 RATIO
10',F7.4//10X,'CONVERSION OF H2S ' ,F7.2,5X
$ , 'CONVERSION OF S02
1  ' ,F7.2,///)
  WRITE(6,4) (FDCOM(J),PRCOM(J),BAL(1,J),BAL(2,J) ,J=1
$ ,6)
4  FORMAT(10X,'MOLECULAR',5X,'FEED',6X,'PARTIAL PRESSURE'
$ ,4X,'MATERIA
1  L BALANCE'//11X,'SPECIE',4X'COMPOSITION',4X,'IN
$ REACTOR',8X,'FEED
1  PRODUCT'//13X,'N2 ' ,7X,F6.2,9X,F6.1,9X,F7.3,3X
$ ,F7.3//13X,'H2S'
1  ,7X,F6.2,9X,F6.1,9X,F7.3,3X,F7.3//13X,'SO2',7X,F6.2,9X
$ ,F6.1,9X,F7.
13,3X,F7.3//13X,'H2O',7X,F6.2,9X,F6.1,9X,F7.3,3X,F7.3/

```

II-A-31

OUTPT ... (CONT'D)

```
$/13X,'SX ',7X  
1,F6.2,9X,F6.1,9X,2(F7.3,3X)//13X'H2'8X,F6.2,9X,F6.1,9X  
$,2(F7.3,3X))  
RETURN  
END
```